

Repurposed Battery Energy Storage System for use in applications of Renewable Energy Generation

By

Dexter M. T. J. Williams

A Thesis submitted to the Faculty of Graduate Studies of

The University of Manitoba

In partial fulfilment of the requirements of the degree of

MASTER OF SCIENCE

Department of Electrical and Computer Engineering

University of Manitoba

Winnipeg

Copyright © 2012 by Dexter M. T. J. Williams

Abstract

Electric and hybrid electric vehicles' batteries not only have great potential for alleviating the world's gasoline consumption problem, but may also stand poised to secure the world's renewable energy generation. Electric and hybrid electric vehicles' batteries that have reached the end of their cycle life in vehicles may still have the capacity to be repurposed into stationary utility energy storage. However, the phenomenon known as battery aging must be given careful consideration in the construction of a repurposed battery energy storage system. The battery aging phenomenon reduces the battery's nominal voltage, capacity and current rating, while increasing its internal resistance. These factors were taken into consideration for the development of the Repurposed Battery Energy Storage System (RBESS). The system utilizes a method called Multi-Level Interlaced Pulse Charging (MLIPC) which was developed for the RBESS to manage the battery's voltage, current, and energy to extend the useful cycle life of the batteries. The repurposed battery energy storage system has been modeled in PSCAD/EMTDC and tested in a constructed hardware implementation of the system.

Acknowledgments

The author wishes to acknowledge the thesis Advisor Dr. Airuddha M. Gole for his guidance and mentoring throughout the thesis and Masters of Science program.

The author would like to acknowledge the Manitoba HVDC Research Center a Division of Manitoba Hydro International for providing sponsorship and facilities for the development and implementation of the thesis.

In addition the author would like to thank the staff of the Manitoba HVDC Research Center a Division of Manitoba Hydro International for their support in the development of the thesis project.

The author would like to acknowledge the contributions of Mitacs program to this thesis.

The author would like to acknowledge the support and advice of the Professors and the Support Staff of the Power System Group.

Dedication

This thesis is dedicated to my parents, who taught me to strive for excellence, and to my godparents, to all my family and to my friends who have continuously supported me in my goals.

Table of Contents

Abstract	ii
Acknowledgments	iii
Dedication	iv
Table of Contents	v
List of Tables	ix
List of Figures	x
List of Acronyms	xiv
List of Symbols	xv
Chapter 1: Introduction	1
1.1 Background	1
1.2 Motivation for This Research.....	2
1.3 The Objective of the Thesis	4
1.4 A Brief Description of the Repurposed Battery Energy Storage System	5
Chapter 2: Renewable Energy Systems and Battery Energy Storage System Analysis and Review	8
2.1 Renewable Energy Generation.....	8
2.2 Battery Energy Storage	10
2.2.1 Batteries	10
2.2.2 Battery Aging	12
2.3 Battery Types	13
2.3.1 Lead Acid Batteries	13
2.3.2 Nickel Cadmium Batteries.....	15
2.3.3 Nickel Metal Hydride Batteries.....	16
2.3.4 Lithium Ion Batteries.....	17
2.3.5 Battery Comparison.....	18
2.4 Battery Modes of Operation.....	20
2.4.1 Battery Charging	20
2.4.2 Battery Discharging.....	23
2.5 Battery Energy Storage System.....	23
2.5.1 Battery Energy Storage System Grid Interconnection	23
2.5.2 Battery Energy Storage System Application	24
2.5.3 Battery Energy Storage System in Use	25

2.5.4 Repurposed Battery Energy Storage System.....	25
2.6 Key Contributions of the Repurposed Battery Energy Storage System (RBESS)..	27
2.7 Chapter summary	27
Chapter 3: The Design of the Repurposed Battery Energy Storage System.....	28
3.1 General Battery Energy Storage System Structure	28
3.2 The Repurposed Battery Energy Storage System Design.....	30
3.3 The RBESS's Battery Bank System	33
3.3.1 RBESS: Charge Block Unit Controls.....	37
3.3.2 RBESS: Battery Bank Protection	47
3.4 RBESS: Charge Converter System	48
3.4.1 RBESS: Converter System Controls	53
3.4.2 RBESS: Converter System Primary Controls	53
3.4.3 RBESS: Converter System protection.....	67
3.5 Chapter summary	68
Chapter 4: RBESS Simulation Model and Hardware Implementation	69
4.1 RBESS Simulation and Hardware Implementation Overview	70
4.1.1 RBESS Battery Bank Batteries	75
4.1.2 RBESS Bus.....	79
4.1.3 RBESS Simulation and Hardware Converters	80
4.1.4 RBESS Simulation and Hardware Pre-charge units.....	84
4.1.5 RBESS Simulation Model's and Hardware Implementation's Charge Converter controls	85
4.1.6 Charge Converter Hardware Implementation's control interface	87
4.2 RBESS Simulation Model and Hardware Implementation of the Battery Bank	91
4.2.1 RBESS Simulation and Hardware Charge Block Units	91
4.2.2 RBESS Simulation Model's and Hardware Implementation's Charge Block Unit Controls	92
4.2.3 Hardware Implementation's Charge Block Unit Control Interface.....	92
4.3 RBESS Hardware Implementation Communication.....	94
4.3.1 RBESS Hardware Implementation's Control Board Communication	94
4.3.2 RBESS Hardware Implementation's Computer Communication	95
4.4 RBESS Simulation Model Human Machine Interface.....	95
4.5 RBESS Hardware Implementation Human Machine Interface.....	96
4.5.1 RBESS Hardware Implementation's Hardware Interface	96
4.5.2 RBESS Hardware Implementation's Graphic User Interface (GUI).....	100

4.5.3 RBESS implementation issues	107
4.6 Chapter summary	109
Chapter 5: RBESS Test and Performance Analysis.....	110
5.1 The Bus Voltage Regulation Test	110
5.1.1 The RBESS Simulation Model’s Discharge Bus Voltage Regulation Test ...	111
5.1.2 The RBESS Simulation Model’s Charge Bus Voltage Regulation Test.....	113
5.1.3 The RBESS Hardware Implementation’s Discharge Bus Voltage Regulation Test	116
5.1.4 The RBESS Hardware Implementation’s Charge Bus Voltage Regulation Test	118
5.1.5 The RBESS Bus Voltage Regulation Test Overview.....	121
5.2 Battery Balance Test	121
5.2.1 The RBESS Simulation Model’s Discharge Battery Balance Test	122
5.2.2 The RBESS Simulation Model’s Charge Battery Balance Test.....	123
5.2.3 The RBESS Hardware Implementation’s Discharge Battery Balance Test ...	124
5.2.4 The RBESS Hardware Implementation’s Charge Battery Balance Test.....	125
5.2.5 The RBESS Battery Balance Test Overview	126
5.3 Battery Pack Balance Test.....	127
5.3.1 The RBESS Simulation Model’s Discharge Battery Pack Balance Test	127
5.3.2 The RBESS Simulation Model’s Charge Battery Pack Balance Test	128
5.3.3 The RBESS Hardware Implementation’s Discharge Battery Pack Balance Test	129
5.3.4 The RBESS Hardware Implementation’s Charge Battery Pack Balance Test	131
5.3.5 The RBESS Battery Pack Balance Test Overview.....	133
5.4 Battery Pack Pulse Test.....	133
5.4.1 The RBESS Hardware Implementation’s 100 ms Battery Pack Charging Pulse Test	133
5.4.2 The RBESS Hardware Implementation’s 1000 ms Battery Pack Charging Pulse Test	135
5.4.3 The RBESS Hardware Implementation’s Battery Pack Charging Non-Pulse Test	137
5.4.4 The RBESS Hardware Implementation’s Battery Pack Charging Pulse Test Analysis	139
5.4.5 The RBESS Hardware Implementation’s 100 ms Battery Pack Discharge Pulse Test	140
5.4.6 The RBESS Hardware Implementation’s 1000 ms Battery Pack Discharge Pulse Test.....	142

5.4.7 The RBESS Hardware Implementation’s Battery Pack Discharge Non Pulse Test	143
5.4.8 The RBESS Hardware Implementation’s Battery Pack Discharging Pulse Test Analysis	145
5.4.9 The RBESS Hardware Implementation’s Battery Pack Pulse Test Overview	146
5.5 Chapter summary	147
Chapter 6: Conclusions and Recommendations	148
6.1 Conclusion.....	148
6.2 Recommendations for Future Work.....	151
References.....	153
Appendix A Schematics.....	157
Appendix B Battery Profiling System.....	183

List of Tables

Table 2.1: Advantages and disadvantages of lead acid battery plate types [18].....	15
Table 2.2: The advantages and disadvantages of nickel cadmium batteries [18].....	16
Table 2.3: The advantages and disadvantages of NiMH batteries [6] [19].	17
Table 2.4: The advantages and disadvantages of Lithium batteries [6] [19] [20].	18
Table 2.5: list of four batteries' characteristics [18][17] [6].....	19
Table 2.6: Battery preferred charging strategies and full charge identify factor [6].	20
Table 3.1: The inputs table for the RBESS charge converter system's primary converter controls (<i>Note: subscript "R" means reference value</i>).....	56
Table 4.1: Parameters for the PSCAD/EMTDC simulation's battery model.	78
Table 4.2: Step down and up stage one and two converter parameters.	83
Table 4.3: RBESS charge converter switch control interface.....	97
Table 4.4: RBESS charge converter display page indexes.	98
Table 4.5: RBESS battery bank switch control interface.	99
Table 4.6: RBESS charge converter display page indexes.	99
Table 4.7: RBESS charge converter data logging format.....	102
Table 4.8: RBESS battery bank data logging format.....	103
Table 5.1: Battery pack 100 ms pulse charging test set 1.	135
Table 5.2: Battery pack 100 ms pulse charging test set 2.....	135
Table 5.3: Battery pack 1000 ms pulse charging test set 1.....	136
Table 5.4: Battery pack 1000 ms pulse charging test set 2.....	137
Table 5.5: Battery pack non pulse charging test set 1.....	138
Table 5.6: Battery pack non pulse charging test set 2.....	138
Table 5.7: Pulse test converter efficiency during charge.....	140
Table 5.8: Battery pack 100 ms pulse discharging test set 1.	141
Table 5.9: Battery pack 100 ms pulse discharging test set 2.	141
Table 5.10: Battery pack 1000 ms pulse discharging test set 1.	143
Table 5.11: Battery pack 1000 ms pulse discharging test set 2.	143
Table 5.12: Battery pack non pulse discharging test set 1.....	144
Table 5.13: Battery pack non pulse discharging test set 2.....	144
Table 5.14: Pulse test converter efficiency during discharge.	146
Table B.1: RBESS charge converter switch control interface.....	185
Table B.2: RBESS charge converter display page indexes.	185
Table B.3: RBESS charge converter data logging format.	186

List of Figures

Figure 1-1: RBESS full scale model single line diagram.	6
Figure 3-1: General BESS Structure.....	29
Figure 3-2: The Repurposed Battery Energy Storage System (RBESS) connected to the power grid via the DC to AC converter interface.	32
Figure 3-3: The RBESS’s battery bank.	33
Figure 3-4: The schematic layout of the “Charge block unit” used to control the pulsed charge exchanged with a battery.	34
Figure 3-5: Multi-level battery pack control.....	38
Figure 3-6: The MLIPC controller flowchart.	40
Figure 3-7: Load queue flow chart subroutine for charge block unit.	41
Figure 3-8: Pulse controls running subroutine for charge block units.....	42
Figure 3-9: Pulse period update subroutine for the pulse controls running subroutine.	44
Figure 3-10: Reflex period control subroutine for the pulse controls running subroutine.	45
Figure 3-11: Stacking level check subroutine for the pulse control running subroutine..	46
Figure 3-12: Empty Queue flowchart subroutine for MLIPC controller.....	47
Figure 3-13: The Charge Converter system.....	48
Figure 3-14: Stage one DC to DC converter for Charge Converter system.	49
Figure 3-15: Stage two DC to DC converter for Charge Converter system.	50
Figure 3-16: Buck converter control.....	55
Figure 3-17: Boost converter control. (<i>Note: “Non-controlled Measured” is the “Controlled Measured” complement on the opposite end of the converter</i>).....	55
Figure 3-18: Overall secondary control for RBESS charge converter system.	59
Figure 3-19: Load queue flow chart subroutine.....	60
Figure 3-20: Energize queue flow chart subroutine.....	61
Figure 3-21: Activate converter flow chart subroutine.....	62
Figure 3-22: System running flowchart subroutine.	63
Figure 3-23: Current set point calculator.	65
Figure 3-24: De-energize flow chart subroutine.....	66
Figure 3-25: Empty Queue flowchart subroutine.	67
Figure 4-1: Block layout of the simulated and implemented RBESS.	70
Figure 4-2: Hardware implementation of the RBESS prototype.....	71
Figure 4-3: Hardware implementation of the RBESS completed.....	72
Figure 4-4: PSCAD/EMTDC model of the RBESS.	73
Figure 4-5: Cerebot 32MX4 development board.....	74
Figure 4-6: K2 Energy Constructed battery pack.....	76
Figure 4-7: Battery management system.	77
Figure 4-8: PSCAD/EMTDC developed Battery model.	79
Figure 4-9: Simulation model and hardware implementation of the stage one converters.	83
Figure 4-10: Simulation model and hardware implementation of the stage two converters.	83

Figure 4-11: Simulation model and hardware implementation of the power grid interface pre-charge and contactor system.....	84
Figure 4-12: Simulation model and hardware implementation of the battery pack interface pre-charge and contactor system.....	85
Figure 4-13: PSCAD/EMTDC primary control step down stage implmentation.....	86
Figure 4-14: PSCAD/EMTDC primary control step down stage implmentation.....	86
Figure 4-15: PSCAD/EMTDC primary control step up stage implmentation.....	87
Figure 4-16: Converter MOSFET’s interface driver board.	89
Figure 4-17: Power grid relay’s interface driver board.	90
Figure 4-18: Battery pack relay’s interface driver board.....	90
Figure 4-19: Simulation model and hardware implementation of a charge block unit. ...	91
Figure 4-20: Charge block unit’s interface driver board.	93
Figure 4-21: RBESS simulation model’s HMI.....	96
Figure 4-22: Hardware interface elements.....	97
Figure 4-23: GUI file menu.	100
Figure 4-24: GUI Status bar.....	100
Figure 4-25: Serial port tab of GUI.....	101
Figure 4-26: Serial data tab of GUI.	103
Figure 4-27: Fault data tab of GUI.	103
Figure 4-28: System control tab GUI of charge converter.	104
Figure 4-29: System control tab GUI of battery bank.	105
Figure 4-30: Control tab GUI of charge converter.	106
Figure 4-31: Control tab GUI of battery bank.	107
Figure 4-32: Hardware physical layout.....	109
Figure 5-1: RBESS simulation model’s discharge bus voltage regulation test’s bus voltages and battery pack current.	112
Figure 5-2: RBESS simulation model’s discharge bus voltage regulation test’s battery pack’s batteries’ voltages and currents.	113
Figure 5-3: RBESS simulation model’s charge bus voltage regulation test’s bus voltages and battery pack current.....	114
Figure 5-4: RBESS simulation model’s charge bus voltage regulation test’s battery pack’s batteries’ voltages and currents.	115
Figure 5-5: RBESS hardware implementation’s discharge bus voltage regulation test’s bus voltages and battery pack current.....	117
Figure 5-6: RBESS hardware implementation’s discharge bus voltage regulation test’s battery pack’s batteries’ voltages and currents.	118
Figure 5-7: RBESS hardware implementation’s charge bus voltage regulation test’s bus voltages and battery pack current.	120
Figure 5-8: RBESS hardware implementation’s charge bus voltage regulation test’s battery pack’s batteries’ voltages and currents.	120
Figure 5-9: The RBESS simulation model’s discharge battery balancing test.....	122
Figure 5-10: The RBESS simulation model’s charge battery balancing test.....	123
Figure 5-11: The RBESS hardware implementation’s discharge battery balancing test.....	125
Figure 5-12: The RBESS hardware implementation’s charge battery balancing test. ...	126
Figure 5-13: The RBESS simulation model’s battery pack discharge balancing test. ...	128
Figure 5-14: The RBESS simulation model’s battery pack charge balancing test.	129

Figure 5-15: The RBESS hardware implementation’s battery pack discharge balancing test.....	131
Figure 5-16: The RBESS hardware implementation’s battery pack charge balancing test.....	132
Figure A-1: Repurposed Battery Energy Storage System Schematic 1 of 25.....	158
Figure A-2: Repurposed Battery Energy Storage System Schematic 2 of 25.....	159
Figure A-3: Repurposed Battery Energy Storage System Schematic 3 of 25.....	160
Figure A-4: Repurposed Battery Energy Storage System Schematic 4 of 25.....	161
Figure A-5: Repurposed Battery Energy Storage System Schematic 5 of 25.....	162
Figure A-6: Repurposed Battery Energy Storage System Schematic 6 of 25.....	163
Figure A-7: Repurposed Battery Energy Storage System Schematic 7 of 25.....	164
Figure A-8: Repurposed Battery Energy Storage System Schematic 8 of 25.....	165
Figure A-9: Repurposed Battery Energy Storage System Schematic 9 of 25.....	166
Figure A-10: Repurposed Battery Energy Storage System Schematic 10 of 25.....	167
Figure A-11: Repurposed Battery Energy Storage System Schematic 11 of 25.....	168
Figure A-12: Repurposed Battery Energy Storage System Schematic 12 of 25.....	169
Figure A-13: Repurposed Battery Energy Storage System Schematic 13 of 25.....	170
Figure A-14: Repurposed Battery Energy Storage System Schematic 14 of 25.....	171
Figure A-15: Repurposed Battery Energy Storage System Schematic 15 of 25.....	172
Figure A-16: Repurposed Battery Energy Storage System Schematic 16 of 25.....	173
Figure A-17: Repurposed Battery Energy Storage System Schematic 17 of 25.....	174
Figure A-18: Repurposed Battery Energy Storage System Schematic 18 of 25.....	175
Figure A-19: Repurposed Battery Energy Storage System Schematic 19 of 25.....	176
Figure A-20: Repurposed Battery Energy Storage System Schematic 20 of 25.....	177
Figure A-21: Repurposed Battery Energy Storage System Schematic 21 of 25.....	178
Figure A-22: Repurposed Battery Energy Storage System Schematic 22 of 25.....	179
Figure A-23: Repurposed Battery Energy Storage System Schematic 23 of 25.....	180
Figure A-24: Repurposed Battery Energy Storage System Schematic 24 of 25.....	181
Figure A-25: Repurposed Battery Energy Storage System Schematic 25 of 25.....	182
Figure B-1: Battery profiling system board.....	183
Figure B-2: Serial port tab of GUI.....	186
Figure B-3: The USB-6008 DAC GUI interface.....	187
Figure B-4: the battery profiling system GUI’s converter control tab.....	188
Figure B-5: K2 Battery charging open circuit test.....	189
Figure B-6: K2 Battery discharging open circuit test.....	190
Figure B-7: K2 Battery open circuit voltage SOC characteristic.....	190
Figure B-8: Battery profiler system schematic 1 of 17.....	191
Figure B-9: Battery profiler system schematic 2 of 17.....	192
Figure B-10: Battery profiler system schematic 3 of 17.....	193
Figure B-11: Battery profiler system schematic 4 of 17.....	194
Figure B-12: Battery profiler system schematic 5 of 17.....	195
Figure B-13: Battery profiler system schematic 6 of 17.....	196
Figure B-14: Battery profiler system schematic 7 of 17.....	197
Figure B-15: Battery profiler system schematic 8 of 17.....	198
Figure B-16: Battery profiler system schematic 9 of 17.....	199
Figure B-17: Battery profiler system schematic 10 of 17.....	200

Figure B-18: Battery profiler system schematic 11 of 17.....	201
Figure B-19: Battery profiler system schematic 12 of 17.....	202
Figure B-20: Battery profiler system schematic 13 of 17.....	203
Figure B-21: Battery profiler system schematic 14 of 17.....	204
Figure B-22: Battery profiler system schematic 15 of 17.....	205
Figure B-23: Battery profiler system schematic 16 of 17.....	206
Figure B-24: Battery profiler system schematic 17 of 17.....	207

List of Acronyms

A	-	Amps
AC	-	Alternating Current
AGM	-	Absorbed Glass Mats
Ah	-	Amp hours
BESS	-	Battery Energy Storage System
BMS	-	Battery Management System
DC	-	Direct Current
DOD	-	Depth of Discharge
EV	-	Electric Vehicles
F	-	Farads
GUI	-	Graphic User Interface
H	-	Henries
IGBT	-	Insulated Gate Bipolar Transistor
MLIPC	-	Multi-Level Interlaced Pulsed Charge
MOSFET	-	Metal–Oxide–Semiconductor Field-Effect Transistor
MOV	-	Metal Oxide Varistor
NiCd	-	Nickel Cadmium
NiMH	-	Nickel Metal Hydride
OC	-	Open Circuit
PHEV	-	Plug-in Hybrid Electric Vehicles
PWM	-	Pulse Width Modulation
RBESS	-	Repurpose Battery Energy Storage System
SOC	-	State Of Charge
SVC	-	Static VAR compensator
SPI	-	Serial Peripheral Interface
USB	-	Universal Serial Bus
V	-	Volts
W	-	Watts
Wh	-	Watt hours

List of Symbols

A	- Exponential curve fitting parameter multiplier
B	- Exponential curve fitting parameter polynomial multiplier
$Capacity_{Nominal}$	- Battery's nominal capacity
$Capacity_{Remaining}$	- Battery's remaining capacity
$C_{Battery}$	- Battery's nominal capacity
C_{Boost}	- Capacitor for boost
C_{Buck}	- Capacitor for buck
$Count_{Limit}$	- Number of converters to be over current limits.
C_{Out}	- Capacitor
CSV	- Comma Separated Value
DOD	- Depth to Discharge
DOD_{AVE}	- Depth to Discharge average
$Dutycycle_{Boost}$	- W Duty cycle of boost converter
$Dutycycle_{Buck}$	- Duty cycle of buck converter
f_{Boost}	- Frequency of boost converter
f_{Buck}	- Frequency of buck converter
i	- Instantaneous current
I	- Current set point
IC	- Integrated Circuit
I_d_{Boost}	- Inductor current during boost
I_d_{Buck}	- Inductor current during buck
I_R	- Current reference
K	- Polarization factor of battery
L_{Boost}	- Inductor for boost
L_{Buck}	- Inductor for buck
$L_{Scale\ Factor}$	- Inductor scaling factor
P	- Power out
P_{Curr}	- Current power of converter
P_{set}	- Power level set for converter stage
$Ratio_{Diff}$	- Remainder of ratio limits
$Ratio_{Limit}$	- Max current ratio limit of converter
$Ratio_{temp}$	- Current ratio limit of converter
$R_{Internal}$	- Battery's internal resistance
$R_{Overvoltage}$	- resistance of the connected plates
SOC	- State of Charge

$SOCAVE$	- State of Charge average
$Stack$	- Staking multiplier for batteries
$StackMultiplier$	- Stack multiplier value
t	- Time
$T_{Cycle\ Period}$	- Time for all battery pulse periods in a pack
$T_{Pulse\ Period}$	- Time of battery pulse period
$V_{battery}$	- Battery's voltage
$V_d\ Boost$	- Voltage out for boost converter
$V_d\ Buck$	- Voltage out for buck converter
V_{in}	- Voltage in on high side
V_{low}	- Voltage on low side expected
$V_{Nominal}$	- Battery's nominal voltage
V_{Out}	- Voltage out on low side
V_R	- Voltage Reference

Chapter 1: Introduction

This chapter discusses the drawbacks of present transportation and energy generation technologies and how these technologies can be integrated to improve their performance. The successful integration of these technologies requires the development of a new energy storage system. The main focus of this thesis is the design and development of a Repurposed Battery Energy Storage System (RBESS).

1.1 Background

Climate change is a growing concern of today's society. Many individuals believe that the excessive amounts of greenhouse gases that are being introduced into the environment are responsible for the climate change phenomenon. The burning of fossil fuels is held to be the leading culprit of the greenhouse gasses [1]. Society burns excessive amounts of fossil fuels to drive the transportation and power generation industries. The burning of fossil fuels is detrimentally contributing to the climate change problem. However, society's concerns about climate change and the rising cost of fossil fuels has forced society to begin searching for a more sustainable method of producing energy for the transportation and power generation industries [2] [3]. One outcome of this search is the introduction of electric vehicles (pure electric vehicles (EV) and plug in hybrid electric vehicles (PHEV)).

Electric vehicles are rapidly growing in popularity [2][4]. Electric vehicles are powered by high energy batteries, which drive the motors that propel the vehicles. These special batteries are not like traditional vehicle batteries, which were used mainly to start

the vehicle. Traditional vehicle batteries have a relatively low capacity in comparison with the batteries being introduced for the electric vehicle. Since, these electric vehicle batteries require regular charging, they depend on the availability of energy from a dependable power system to provide the required energy to charge the batteries. However, in order to prevent the transfer of the excessive burning of fossil fuel to produce energy from one industry to another, the power industry has begun expanding and incorporating renewable energy generation into the energy system.

The production of renewable energy is a fast growing industry. Renewable energy can be harvested from many sources. Some of the sources of renewable energy are the sun, the wind, the river flow, the sea tides and current [5]. Unlike, traditional energy generation systems which burn oil, coal or gas, that produce green house gasses during the production of energy, the harvesting of renewable energy from sources like the ones listed above do not produce the same level of green house gasses.

1.2 Motivation for This Research

Although the development of electric vehicles and the production of renewable energy are rapidly growing industries they are not without their own disadvantage. For instance, the electric vehicle battery can only be used in an electric vehicle for a limited time before the battery's performance starts to degrade, owing to aging, and must be replaced. Furthermore, the reliability of the renewable energy system depends on the availability of the renewable energy source. This poses a problem because the renewable energy source may not always be present. This loss of the renewable energy source can hinder the power system's ability to dispatch the energy needed to support the load [3]. However, dispatchability of renewable energy systems can be obtained by providing an

energy storage system to compensate for the weakness in the renewable energy system. The renewable energy system's dispatchability is greatly improved by the introduction of an energy storage system [3] [5].

The solution to these two problems is an opportunity for the two industries (transportation and the power generation) to cooperate in the development of a symbiotic relationship between the two. For instance, the aged batteries which are being removed from electric vehicles may still have the capacity to store and deliver energy to meet the needs of a different application. These aged electric vehicle batteries that have been removed from the electric vehicles can be repurposed to form a stationary energy storage system. This new storage system can be used to support the energy storage needs of the renewable energy generation system. In essence, this will produce a true synthesis between the two industries. The renewable energy system will produce energy for the charging of the batteries used in the electric vehicles, and the repurposed aged electric vehicle batteries will become an energy storage system which will support the renewable energy generation system.

However, the development of a repurposed electric vehicle battery energy storage system must give close consideration to factors which affect the capacity of the batteries to be used in the new energy storage system. The aged electric vehicle batteries will be at different stages of their cycle life since they have been subject to different driving conditions before they were removed from the electric vehicle. Battery aging is a common phenomenon in batteries [6] [7]. Battery aging tends to affect key characteristics of the battery. These characteristics are the battery's capacity, voltage and internal resistance [6] [7]. Therefore, any energy storage system developed around these aged

electric vehicle batteries must carefully consider the impact of these factors in the development of the energy storage system.

1.3 The Objective of the Thesis

In order to address the issues discussed in the previous section this thesis investigates techniques for efficiently charging repurposed electric vehicle batteries. In particular the following items are addressed:

- An investigation of how the battery aging phenomenon affects the repurposing of used electric vehicle batteries;
- An investigation of charging methods to determine the optimal charging strategy for the battery energy storage system;
- An investigation of discharging methods to determine the optimal discharge strategy for the battery energy storage system;
- The modeling of a battery energy storage system (Repurposed Battery Energy Storage System (RBESS) platform)
- The construction of the RBESS platform;
- Experimentation and analysis of discharging batteries under the constructed RBESS platform;
- Experimentation and analysis of charging batteries under the constructed RBESS platform.

1.4 A Brief Description of the Repurposed Battery Energy Storage

System

The RBESS is a multi-stage converter system that branches from a single converter in the first stage to multiple converters in the second stage. The converters in the second stage are connected to their own battery pack in the battery bank. This provides the converters with a more direct means of control over the batteries in the battery bank. This situation makes it easier for the converters to control the energy of the batteries because it is easier to control the charging and the balancing of a small system of batteries than to control one large system of batteries. The Multi-Level Interlaced Pulse Charging (MLIPC) system controls the batteries in each battery pack. The MLIPC system is used to combat the battery aging problem that is evident in the end of cycle life of electric vehicle batteries. The MLIPC scheme utilizes pulse charging, virtually paralleling of batteries and battery interleaving (interlacing) [8] [9] [10] [11] [12] [13] in order to reduce the stresses on the aged batteries and to prolong the remaining life of the batteries.

A full scale implementation of the RBESS would be rated for a capacity of 1000 KWh at 250 KW and the grid interface bus would be rated for 1000 V. This was done to allow sufficient overhead to convert the DC voltage to an AC distribution voltage of 600 V AC (*Standard in Canada*). The DC collector bus would be rated at 550 V to enable equal distribution of the work done in the two stages. Finally, the battery pack bus would be rated at 400 V to support the maximum charge voltage of a 300 V battery pack. The RBESS's battery bank would consist of 10 battery packs and there would be four batteries in each battery pack. Each battery would have a capacity of 25 KWh and a

current rating (discharge and charge) of 30 A. Approximately 28 batteries would be needed to meet the system’s power specification. This would allow a margin for pulsing of the batteries. The second stage of converters would require 10 converters to accommodate the 10 battery packs in the battery bank.

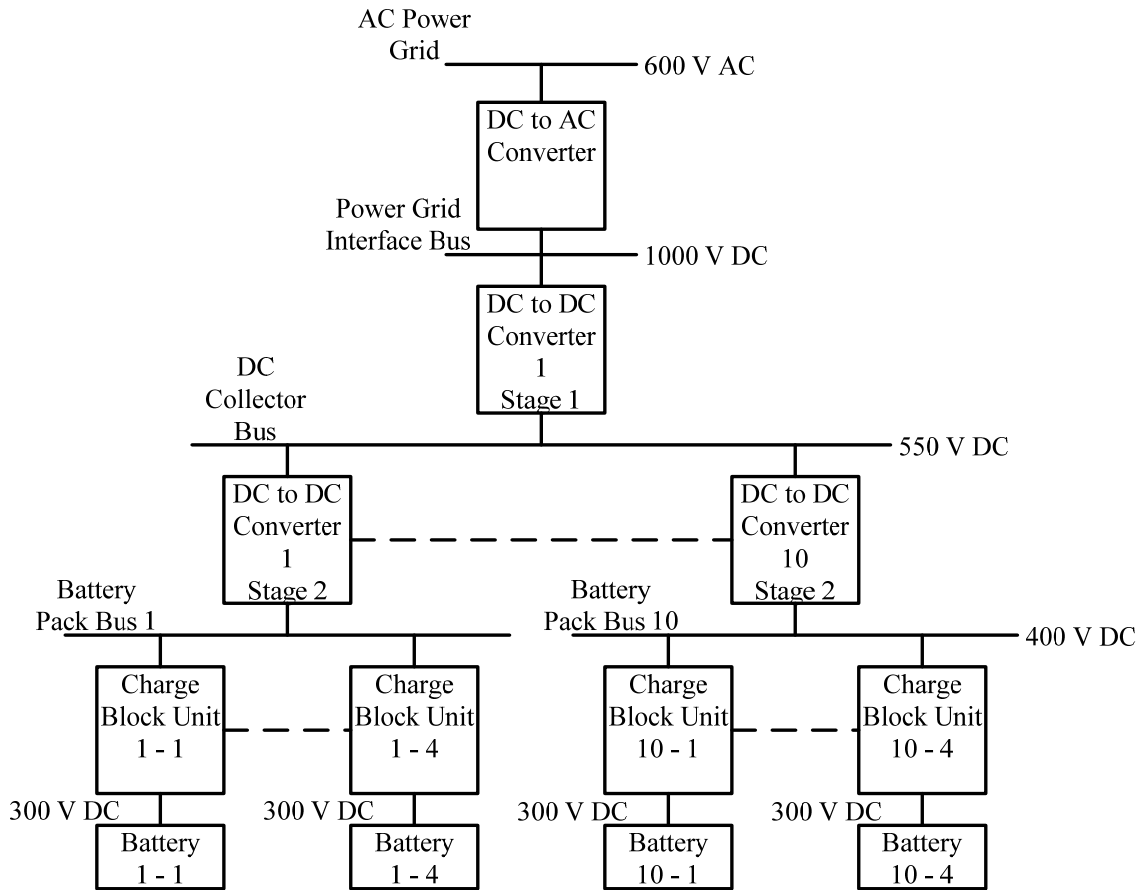


Figure 1-1: RBESS full scale model single line diagram.

The RBESS has been developed and tested in the software simulator PSCAD/EMTDC to verify the functionality of the RBESS. In addition, a reduced scaled hardware implementation of the simulated software model was constructed to further the test and to verify the capabilities of the RBESS in a real word model.

The following chapters take an in-depth look at the development of the RBESS. “Chapter 2: Renewable Energy Systems and Battery Energy Storage System Analysis and Review,” will look at renewable energy systems and battery energy storage systems and why battery energy storage systems are needed for renewable energy generation. “Chapter 3: The Design of the Repurposed Battery Energy Storage System,” will discuss the design of the Repurposed Battery Energy Storage System. “Chapter 4: RBESS Simulation Model and Hardware Implementation,” examines the simulation model of the RBESS used to design and confirm the operation of the RBESS and the hardware implementation constructed from the simulation model used to verify the RBESS operation. “Chapter 5: RBESS Test and Performance Analysis,” discusses the results of the tests conducted on the RBESS used to confirm the operation of the RBESS. “Chapter 6: Conclusions and Recommendations,” summarizes the discussion of the RBESS and gives recommendations for further research in to the development of the RBESS.

Chapter 2: Renewable Energy Systems and Battery Energy Storage System Analysis and Review

This chapter takes a detailed look at renewable energy systems and battery energy storage systems. Specifically, this chapter explores the dispatchability of renewable energy systems and how it can be improved with the introduction of a battery energy storage system. Furthermore, this chapter takes an in-depth look at the batteries and their operation and use in a battery energy storage system and the performance of the battery energy storage system itself. This sequence of analyses leads to the development of a repurposed battery energy storage system.

2.1 Renewable Energy Generation

Renewable energy generation is the key to the development of a clean energy system. Renewable energy can be generated from a wide variety of resources. These resources includes biomass, wind, water and solar. Renewable energy resources are quite readily available around the world. However, there are the problems of quantity and persistence of the renewable energy resource [5].

Renewable energy resources can be broken into two categories of energy availability. The first category of a renewable energy resource is called a dispatchable renewable energy resource. A dispatchable renewable energy resource is a renewable energy resource whose generation can be controlled to meet the load demand by

changing the amount of the resource used [3]. For example, biomass systems utilize the burning of biomass material to produce energy. Thus, by controlling the amount of the biomass material that is burnt in the process, the energy produced from this resource can be made dispatchable to meet the demand of the load.

The second category of a renewable energy resource is called a non-dispatchable renewable energy resource. A non-dispatchable renewable energy resource is a renewable energy resource whose generation cannot be controlled to meet the load demand is due to an inability to control the resource itself [3]. For instance, wind power can be harnessed in almost any part of the world but the ability to constantly control the wind speed levels needed to produce the energy required to meet the load demands is an impossible goal. In addition, the energy available from the sun is available around the world but solar energy is usually only available for part of the day or it can be blocked by cloud cover which will prevent conversion of solar energy to meet the load demand.

It is virtually impossible to correlate the availability of the non-dispatchable renewable resource with the demand of the load without an auxiliary support system to mitigate the resources' instability [3]. Energy storage systems are convenient ways to store energy to improve dispatchability of the renewable energy. Energy storage systems can be used for storing the energy during periods of high availability for use in the periods of low energy generation to support the load. Two types of energy storage systems are mechanical and electrochemical storage [14]. Mechanical storage systems use machines like the fly wheels (short term storage) or pumped hydro (long term storage) to store energy [14]. In electrochemical storage, the energy is stored in a chemical reaction to be released at a later time. Fuel cells and batteries are examples of

electrochemical storage systems that can be used for short-to long-term energy storage [14]. However, the battery energy storage systems are by far one of the most prevalent energy storage system used to support renewable energy generation.

2.2 Battery Energy Storage

The main kinds of batteries found in the power industry and the electric vehicle industry are lead acid and, Nickel Cadmium (NiCd) in the power industry and, Nickel Metal Hydride (NiMH) and lithium batteries in the electric vehicle industry. These batteries have unique compositions and these unique compositions provide the system with the ability to charge and discharge the batteries and to determine the cycle life of the batteries. However, since no two batteries are identical, care must be taken to provide a balanced charge to all of the batteries in the battery bank to prevent failure or damage.

2.2.1 Batteries

There are two main types of batteries, primary batteries and secondary batteries. The primary battery is a battery whose capacity cannot be replenished after it has been depleted. The secondary battery is a battery whose capacity can be replenished after it has been depleted. The secondary battery can be replenished by applying a charge to the battery to replenish it. The construction and chemical makeup of the battery determine whether the battery will be a primary or secondary battery.

Generally, all batteries share the same basic structure except for some variations which are due to different technologies and chemistries. All batteries are made up of several electrochemical cells connected in a series/parallel combination. The basic electrochemical cells consist of two electrodes (anode and cathode) suspended in an

electrolyte. Generally, during the discharge process the anode ionizes and the ions are collected by the cathode and this causes electrons to migration from the cathode to the anode in the external circuit. The process is reversed during the charging process and this causes electrons to flow from anode to cathode [7].

The main factors that affect battery characteristics are the chemical makeup of the electrodes and the electrolyte used in the cell. In addition, the designs and the separation of the electrodes also help to determine the capacity and longevity of a cell [7]. These cell characteristics determine the battery's voltage, current capability, internal resistance, cycle life and capacity [7].

The battery's internal resistance opposes the current flow from the battery. The internal resistance of the battery is due to ionic and electrical characteristics of the battery cells components and terminals [15][6].

The capacity of a battery can be measured by what is known as the battery's State of Charge (SOC) or Depth of Discharge (DOD). The SOC is the ratio between the current capacity of the battery and the nominal capacity of the battery equation (2.1) [6] [16]. Conversely, the DOD is the ratio of the capacity used from the battery to the nominal capacity of the battery equation (2.2) [6] [16]. In addition, the capacity of a battery can be determined by Open Circuit Voltage (OCV) of the battery. When the battery chemistry is allowed to rest and reach a no load equilibrium state, the OCV of the battery is proportional to the capacity remaining in the battery. Based on this knowledge characteristic curves can be developed that relates the OCV to the battery's capacity [16].

$$SOC = \frac{Capacity_{Remaining}}{Capacity_{Nominal}} = 1 - DOD \quad (2.1)$$

$$DOD = \frac{Capacity_{Nominal} - Capacity_{Remaining}}{Capacity_{Nominal}} = 1 - SOC \quad (2.2)$$

Other important parameters of a battery are the self discharger rate, the gassing rate, temperature of operation and the cycle life [6] [7][16]. The self discharger rate of a battery is the rate at which the capacity is naturally loss by the battery owing to natural chemical reactions in the cell [6]. Battery gassing is the lost of reactive electrolyte materials owing to gaseous air bubble produced by reaction in charging and discharging [6]. The temperature of operation is also important since the temperature of the battery can affect the capacity of the battery by increasing or decreasing losses in the cells. The cycle life of a battery is the number of charge and discharge cycles a battery may go through before the end of life of the battery (loss of useable capacity) [17].

2.2.2 Battery Aging

Battery aging is a phenomenon that is characteristic of all batteries. The battery aging phenomenon causes permanent capacity loss in the battery. As a result of this capacity loss a battery will exhibit lower voltages and current capabilities, while at the same time increasing its internal resistance [6][15]. During operation (charge or discharge cycles) or storage, the battery will experience a permanent loss of capacity. This is due to chemical reactions in the battery which over time reduce the recombination ability of ions in the battery cells [6][15]. The formation of crystals in the cell structure over the

battery's life reduces the battery capacity in lead acid, NiCd and NiMH batteries [15]. Similarly, in Lithium ion batteries a film which builds up on the electrode is the factor that reduces ion mobility in the battery [15].

In order to integrate, the aged batteries into the repurposed battery energy storage system, the battery's capacity, charge and discharge current ratings and voltage ratings must be known. This information is incorporated into the battery's charging controls as will be discussed in Section 3.3.1. Battery capacity is a key factor in the battery repurposing process. The battery repurposing process must effectively utilize the remaining battery capacity for the new application. For instance, the energy loss incurred during the conversion process can be reduced by improving the efficiency of the new application's converters.

2.3 Battery Types

2.3.1 Lead Acid Batteries

There are several different models of lead acid batteries. Two examples are vented (flooded) batteries and valve regulated/sealed (gel cell and Absorbed Glass Mats (AGM)) batteries. The liquid electrolyte is exposed in vented batteries. This allows the electrolyte to evaporate from the battery. Therefore, the battery will require top ups for maintenance. The electrolyte can be refilled in a vented battery. Vented batteries will generally have a higher capacity than sealed batteries as permanent loss of electrolyte, owing to venting is not an issue as vented batteries can be refilled and therefore, vented batteries can have a higher electrolyte levels [17].

The electrolyte is completely enclosed in a case in a valve regulated lead acid battery. This prevents evaporation and the need for maintenance of the battery. The valve reduces the excessive pressure which builds up in the battery. The valve also vents the excessive pressure to the outside of the battery. However, the venting process of the battery can lead to permanent capacity loss, since the venting process vents electrolyte from the sealed battery and the electrolyte cannot be refilled [17]. Also, the electrolyte is lower in sealed types batteries in order to reduce the chance of pressure build up [17].

The electrodes in the lead acid battery are important components because they help to determine the characteristics of the batteries. Thick electrodes allow a greater depth of discharge of the cells, but the cells can handle less current. On the other hand, thin electrodes can support higher currents, but can only support a shallow discharge. In addition, the material used to separate the electrodes help to determine the internal resistance of the battery [17].

Since lead is too soft of a material to be used directly in a battery, therefore it must be doped with another material to create a suitable alloy for the electrodes. The two main types of dopes used in lead acid cells are antimony and calcium. The material used to dope the lead can affect the battery's self discharger rates, depth of discharge, state of charge and gassing. The advantages and disadvantages of the two doping materials are shown in Table 2.1.

Table 2.1: Advantages and disadvantages of lead acid battery plate types [18].

Battery type	Lead acid antimony	Lead acid calcium
Advantages	<ul style="list-style-type: none"> • Increases lead strength • Can accept/deliver larger currents • Discharged from 50% to 80% of its capacity • Capacity 1000 Ah or greater 	<ul style="list-style-type: none"> • Increases lead strength • Reduces gassing and water loss • Low maintenance required • Low self-discharge rate • Capacity 80-1000 Ah
Disadvantages	<ul style="list-style-type: none"> • High self-discharge rates • Early gases during recharge • High recharge gassing rates • High maintenance required 	<ul style="list-style-type: none"> • Poor charge acceptance for deep depth of discharge • Battery life reduced if discharged more than 15% to 20% DOD • Shedding of active materials

Furthermore, an effect known as sulfation is a problem for lead acid batteries. The sulfation effect is a growth of sulfate crystals on the electrodes. Sulfation occurs when lead acid battery capacity is left at a low level for a period of time. Depending on the growth of the crystals, a portion of the sulphate crystals can be reversed by a slow charge or pulse charge [17].

Generally, lead antimony batteries are used in energy storage systems for storing renewable energy [18]. Lead antimony batteries are used because they have a high discharge capacity. These batteries can either be vented or sealed. Sealed or vented batteries are selected based on the accessibility of the batteries for maintenance.

2.3.2 Nickel Cadmium Batteries

Similarly, Nickel Cadmium (NiCd) batteries can be vented or valve regulated. The NiCd batteries also have several advantages and disadvantages.

Table 2.2 lists the advantages and disadvantages of the NiCd batteries [17].

Table 2.2: The advantages and disadvantages of nickel cadmium batteries [18].

Battery type	Advantages	Disadvantages
Nickel Cadmium	<ul style="list-style-type: none"> • Long life • Low maintenance • Deep discharged without damage • Performance less affected by temperature deviations • Voltage regulation not as important • Excellent charge retention • High capacity at low temperatures 	<ul style="list-style-type: none"> • High self discharge rates • High cost per Ah • Displays a memory effect of battery history

The main problem of the NiCd battery is the memory effect of the battery chemistry. The chemical makeup of the NiCd battery creates the phenomena known as the “memory effect.” The memory effect prevents a battery from becoming fully discharged after several shallow discharge and charge cycles. This shallow cycle changes the structure of the active materials in the cell and these changes lead to the formation of crystals in the cells. These crystals cause the memory effect in the cell. This memory effect can be partially reversed by reconditioning the battery and this can be achieved by fully discharging and recharging the battery [17] [6].

2.3.3 Nickel Metal Hydride Batteries

Nickel Metal Hydride (NiMH) batteries are an advanced type of nickel based batteries. NiMH batteries were developed in an effort to reduce some of the problems associated with NiCd batteries [6]. The main benefits of NiMH batteries are that hydrogen instead of toxic cadmium is used in the construction of the batteries and that the

hydrogen reduces the impact of the memory effect on the batteries [6]. Table 2.3 lists the advantages and disadvantages of the NiMH technology.

Table 2.3: The advantages and disadvantages of NiMH batteries [6] [19].

Battery type	Advantages	Disadvantages
Nickel Metal Hydride	<ul style="list-style-type: none"> • Low internal resistance • High efficiency • High energy density • Sealed • Good cycle life 	<ul style="list-style-type: none"> • High self discharge • Displays a memory effect of battery history • Cells can reverse polarity in a string (can occur when a cell is fully discharged before others) • Cost between NiCd and Lithium ion

2.3.4 Lithium Ion Batteries

Lithium ion batteries can be divided into two subdivisions. These subdivisions are liquid electrolyte based batteries and polymer based batteries. The liquid electrolyte based batteries use a special material that is soaked in the electrolyte compound between the electrodes to produce a medium for ionic travel [6] [15]. On the other hand, the polymer based batteries use the polymer as the separator and the transport medium. The main benefit of the polymer based batteries is that the cells are safer and less susceptible to fire than the cells of the liquid electrolyte based lithium batteries [6] [15]. This fact is due to the construction of the cell. However, the cells of the polymer based lithium batteries have a lower capacity capability than those of the liquid electrolyte lithium batteries [6] [15]. Table 2.4 lists the general advantage and disadvantages of the lithium ion technology over other batteries.

Table 2.4: The advantages and disadvantages of Lithium batteries [6] [19] [20].

Battery type	Advantages	Disadvantages
Lithium ion	<ul style="list-style-type: none"> • High specific energy • High energy density • Low self-discharge • Long cycle life • No maintenance • No memory effect • Wide operating temperature • Fairly high rate capability • Possibility of miniaturization • Very thin form factors 	<ul style="list-style-type: none"> • Relatively high initial cost • Need of a protection circuit (overcharge, over discharge) • Excessive temperature rise • Degradation at high temperature • Lower power than NiCd or NiMH, especially at low temperatures.

2.3.5 Battery Comparison

The four battery technology characteristics discussed in the previous section are provided in Table 2.5. Table 2.5 is a detailed list of the characteristics of the lead acid and the NiCd batteries found in stationary energy storage systems and the characteristics of the NiMH and lithium ion batteries found in electric vehicles. The review of these four batteries' characteristics indicated that lithium ion batteries are by far the best batteries (technology) in terms of the capacity for energy storage. Therefore, the repurposing of electric vehicle batteries for stationary energy storage can be a useful undertaking. Especially since at the end of the batteries' cycle life in electric vehicle there is approximately up to 80% of the capacity remaining in the battery [6].

Table 2.5: list of four batteries' characteristics [18][17] [6].

Battery	Lead-acid	NiCd	NiMH	Lithium ion
Type	Medium rate, deep discharge, lead-calcium grid	Medium rate, cycle service, vented pocket plate	EV and HEV general	EV general
Nominal discharge cut-off voltage	1.75 V per cell	1.0 V per cell	1.0 V per cell	2.5-3.0 V per cell
Nominal voltage	2.45 V per cell, varies with state of charge	1.25 V per cell, fairly constant with SOC	1.4 V per cell fairly constant with SOC	4.2V per cell, sloped with SOC
Capacity against temperature (% of rated capacity)	70% at 32°F 20% at -20°F	90% at 32°F 65% at -20°F	100% at 32°F 60% at -20°F	-
Nominal energy efficiency	70-80%	60-70%	90% >	95%
Nominal cycle life	1,000-1,500 @80% DOD	1,500-2,000 @80% DOD	600-1200 @80% DOD	3000 @100% DOD
Nominal calendar life without cycling	10-20 years	24 years	5-10 years	5-10 years
Energy density	6-13 Wh lb ⁻¹	9-10 Wh lb ⁻¹	28-43 Wh lb ⁻¹	45-72 Wh lb ⁻¹
Internal resistance	0.6-3.0 mΩ/100 Ah	0.2-1.5 mΩ/100 Ah	-	-
Charge control	Sensitive to long overcharging	Can accept 5-10% overcharge	Sensitive to overcharging and undercharging	Very Sensitive to overcharging and undercharging
Self discharge rate	2-5% per month	5-20% per month	15-25% per month	2-10% per month
Required maintenance	Water replacement; charge equalization; protection against freezing and temperature extremes	Water replacement; occasional full discharge	Occasional full discharge	None

2.4 Battery Modes of Operation

2.4.1 Battery Charging

There are three main battery charging process. The first is current controlled charging, the second is voltage controlled charging, and the third is pulse charging [6][15]. However, there is also a fourth battery charging process and this forth process is a hybridization of the three above processes [6]. In addition, one of the following factors can be used to determine whether a battery is fully charged: the battery voltage, the specific gravity of the electrolyte, the pressure of the battery under charge or the temperature of the battery under charge [6]. Table 2.6 lists the preferred charging strategy and identifier for four battery types.

Table 2.6: Battery preferred charging strategies and full charge identify factor [6].

Battery type	Charging strategy	Charge identifier
Lead acid	Constant current , Constant voltage	specific gravity or voltage
NiCd	Constant current	Pressure or temperature
NiMH	Constant current	Pressure or temperature
Lithium Ion	Constant current , Constant voltage	Voltage

2.4.1.1 Battery Current Charging

There are three methods of charging a battery under the current controlled charging mode [21]. First, a battery can be charged at a single current level to restore the battery's capacity [6] [21]. However, it is difficult to fully charge such a battery because the high current imposed on the battery will give false readings of the battery's capacity. The alternative to this single level control is a method which uses a multi stage current

charging method in which the battery is started at high current level and then is stepped down to a lower current level to return more of the battery's capacity [6] [21]. The last alternative is a tapered current charging in which the current input to the battery changes proportionally with the battery capacity or voltage [21] [17][15].

2.4.1.2 Battery Voltage Charging

The voltage controlled charging system has two ways of charging the battery. The first method is a single level voltage system and the second method is a multi level voltage system. The single level voltage charging system applies a continuous high voltage to the battery until the battery becomes fully charge [6] [21].

The first stage of the multi level voltage system is a high voltage level being applied to the battery. This rapidly returns approximately 80% of the battery's capacity. The secondary stage of the multi level voltage system is a secondary voltage level applied to the battery at the nominal battery voltage level to maintain and to top up the battery [6] [21]. The problem with voltage charging is the possible negative impact of high currents injected at the beginning of the charging process. The negative impact is due to high potential difference between the battery and the applied voltage [6] [15] [21].

2.4.1.3 Battery Pulsed Charging

Pulse charging is a method that uses pulses to charge to the battery. Pulsed charging can either be voltage or current controlled based [8] [9] . The key problem with the continuous battery charging methods, by either continuous voltage or current charging, are the stresses developed by the battery [6], such as increased heat, polarization and other factors that reduce the battery's ability to accept charge [15]. The

key benefit of the pulse charging scheme is the reduction of stress on the battery. The introduction of a rest period between the pulses of the battery can alleviate the stresses, give time for the battery to recover and reduce the polarization on the battery and therefore improve the charge acceptance capability of the battery [22].

Reflex charging is an advanced form of the pulse charging scheme [23]. Reflex charging extends the pulse charging scheme by introducing a short discharge pulse to the pulse charging scheme. The reflex charging pulse helps with the diffusion of ions within the electrodes [23].

2.4.1.4 Battery Hybridized Charging

Combining the above three methods, leads to an approach that can maximize the benefits obtained from each of the three methods [6] [15] [21]. This approach is referred to as a, “hybridized,” approach to battery charging. The first stage of the hybridization method uses constant current charging to return the bulk of the battery’s capacity. This eliminates the current spike caused by pure voltage charging. The second stage of the process uses voltage controlled charging. This traditionally occurs after 80% of the battery’s capacity has been returned by current controlled charging. This mode eliminates the problem of fully charging a battery since the current used to charge the battery in this mode will slowly taper off to zero as the battery voltage reaches the applied charge voltage. Finally, either a low voltage pulse charge or constant voltage at the nominal battery voltage (open circuit fully charged battery voltage) is used to maintain the battery’s capacity [24]. Whether the final stage is implemented will depend on the charger. This thesis developed and implemented a hybridized approach to battery

charging utilizing a pulsed constant current charging scheme followed by a pulsed constant voltage charging scheme.

2.4.2 Battery Discharging

There are two ways by which a battery can be discharged. These are by a constant discharge and by an intermittent discharge [6]. Constant discharging is similar to constant charging, in that they both increase the stress on the battery. The increased stress is due to the fact that continuous power is drawn from the battery increases the battery's temperature and the stress on the battery. However, this stress can be reduced by intermittently discharging the battery. When a battery is intermittently discharged the battery recovers its voltage. The recovery reduces polarization of the battery and this can enable more energy to be extracted from the battery rather than it being lost in the discharge [7][15]. This thesis developed and implemented a pulsed discharging scheme to take advantage of the benefits associated with intermittent discharging of a battery.

2.5 Battery Energy Storage System

2.5.1 Battery Energy Storage System Grid Interconnection

Battery energy storage systems can be integrated in the grid in two ways. These ways are the aggregated and distributed connections [25]. An aggregated connection occurs when the energy storage facility is connected at a single point on the system to provide support for the entire renewable energy facility. An aggregated battery energy storage system is a larger and more expensive facility than the distributed facility. The converters must be rated at a higher level to operate on the grid and to provide larger amounts of energy for grid support [25].

A distributed connection occurs when multiple energy storage systems are connected to the network to support local generation facilities [25]. Distributed energy storage systems are usually less expensive than aggregated facilities. This is due to the fact that lower rating converters are needed to support smaller generation systems [25]. Distributed generation energy storage systems can either be shunt (parallel) connected to the generator on either the AC bus or DC bus (if available) or in series with the dc bus, if available in the generator's converter.

A review of the aggregated and the distributed energy storage systems indicates that the aggregated and the distributed energy storage systems have similar capabilities for compensating for voltage and frequency disturbances in the systems [25].

2.5.2 Battery Energy Storage System Application

There are three main areas of power system support from energy storage systems. These are power quality, bridging power and energy management [26]. Power quality applications fall into the domain of short term system support. This entails the supply, for a short time, of high power to compensate for distortions in the voltage, current or power. An example of the need for a power quality support application is the reduction of voltage sag in the system caused by lightning or debris [26].

Bridging power falls under the regime of medium power and energy for support lasting several minutes. One possible application of bridging power is for brownout ride through where the power is lost and the energy storage system would provide the power needed to sustain the system until the power is restored or capacity is depleted [26].

Energy management support is the most energy demanding of the power system support regimes since the duration of the support can last for several hours. One possible application of energy management is load leveling. In this situation energy available from the source and the energy storage systems are balanced to provide the load with sufficient energy to meet the demand and maintain the capacity of the energy storage system [26]. An example of this situation is seen in a renewable energy generation where the availability of the renewable source is unpredictable (ex: wind, solar), and the energy storage system is used to level out or evenly distribute the energy generated by the renewable system.

2.5.3 Battery Energy Storage System in Use

Battery energy storage systems are highly adaptable to supporting the renewable energy systems. The lead acid and nickel cadmium batteries have proven in many applications to be suitable energy storage elements. Two examples, of battery energy storage system are the Chino, California USA 10 MWh lead acid battery facility [27] and the Fairbanks, Alaska, USA 26 MWh nickel cadmium facility [27]. Both energy storage systems are grid tied for energy support. The Alaska facility also is currently the largest battery energy storage facility in the world [28] .

2.5.4 Repurposed Battery Energy Storage System

The RBESS which is developed in this thesis utilizes three strategies to improve the efficiency of the energy being exchanged with the batteries. The three strategies are pulse charge exchanges with the system, virtually paralleling of batteries and pulse interleaving or interlacing.

The pulse charge exchange as was discussed earlier is a mechanism used to reduce stresses on the battery [8] [9] [13]. Pulsing of the battery produces a rest period in the energy exchange with the battery chemistry. The rest period relaxes and returns the battery to a lower energy state. Pulsing also has the effect of reducing the polarization on the battery and reducing temperature of the battery. Therefore, pulsing creates a more efficient means of exchanging energy with the battery.

Virtually paralleling is a technique that is used to isolate one battery from another battery in a parallel system of batteries [11] [12]. The benefit of using the virtually paralleling technique is that batteries no longer waste energy in an attempt to balance one another. This allows the full capacity of the battery to be exchanged with the power system and not waste capacity in unwanted balancing.

The final technique used in this system is interlacing of pulse [10] [13]. Traditionally, the pulsed technique would result in discontinuous operation of the system, and that pulsing would reduce the system's performance. However, interleaving or interlacing pulses form a continuous signal from the external networks point of view. The process, of interlacing battery pulses determines the particular battery that will exchange energy in a given pulse period. This prevents a discontinuous mode of operation in the DC to DC converter and improves the efficiency of the converter system.

The combination of the three techniques forms the basis of the controls that regulate the batteries in the RBESS. These techniques are used in the RBESS to better utilize the battery capacity and this mitigates the battery aging effects on the electric vehicle batteries. Therefore, the RBESS has the capacity to operate in a manner that will

regulate the aged electric vehicle batteries and support the generation of renewable energy.

2.6 Key Contributions of the Repurposed Battery Energy Storage System (RBESS)

Two key components of a clean energy society are the development of sustainable transportation and energy generation system. This thesis designs and builds a Repurposed Battery Energy Storage System, which is the foundation needed to expand the usefulness of aged electric vehicle batteries past their expected cycle life. The Repurposed Battery Energy Storage System bolsters the dispatchability of renewable energy systems. The Repurposed Battery Energy Storage System's multistage converter system's design and controls, and the battery bank's design and controls can play a major role in the development of society's sustainable energy future (See "Chapter 3: The Design of the Repurposed Battery Energy Storage System" for detailed)

2.7 Chapter summary

This chapter explored the limitations of renewable energy resources and battery energy storage technology. Renewable energy can either be dispatchable (biomass) or non-dispatchable (solar) and if the renewable energy resources is non-dispatchable then energy storage is needed to properly utilize the resource. There are many, types of batteries that can be used in construction of a battery energy storage system. However, battery aging must be considered in construction of a repurposed battery energy storage system. Thus, the RBESS utilizes pulse charging, virtually parallel batteries and battery interlacing to mitigate the battery aging phenomenon.

Chapter 3: The Design of the Repurposed Battery Energy Storage System

This chapter describes the development of the Repurposed Battery Energy Storage System (RBESS). The chapter investigates various types of Battery Energy Storage System (BESS) designs, in order to select the most appropriate design strategy. Then through the modeling of the BESS an appropriate control strategy for the RBESS is developed to maximizing the efficiency of the selected approach. In addition, a suitable presentation strategy is also developed. A discussion of the simulation model and constructed system's performance is discussed in the next chapters.

3.1 General Battery Energy Storage System Structure

Several BESS designs are possible, and the selection of a particular design determines how the BESS is connected to the batteries and to the power system. Furthermore, the arrangement of the batteries in the BESS is critical to the system's performance. One weak battery can degrade the performance of the BESS. A weaker battery may draw energy from the stronger batteries to maintain itself, and such a drawing is essentially wasting the energy that could be used in the energy exchanged with the external system.

Typically a BESS consists of several battery strings connected to a converter (see Figure 3-1). The battery string consists of several batteries connected, in series and/or in parallel combinations, to make up the desired voltage, current rating and capacity

required for the BESS. Each of these strings of batteries can be connected either to a singular converter or to multiple converters.

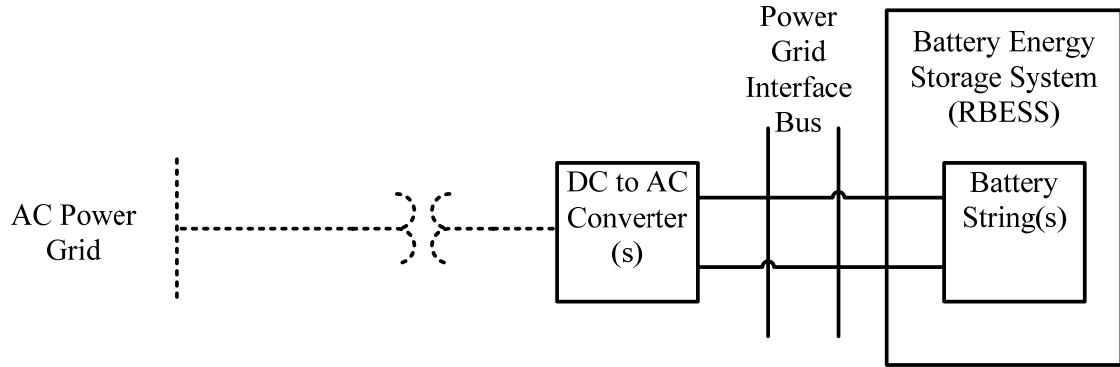


Figure 3-1: General BESS Structure.

The, selection of the battery arrangement is critical to the design of the BESS. When batteries are connected in series the voltage required to meet the systems requirement can easily be met. However, failure of a battery (short circuit) will result in the failure of the string and the loss of the total capacity afforded by the string [29]. Even when protection methods are implemented to protect the other batteries in the string, the use of the string cannot be reinstated until the battery is replaced or fault is cleared from the string. In addition, the high voltage of the series connected batteries makes it significantly more dangerous to work with than with a lower voltage paralleled connected battery strings.

When the battery strings consist of batteries connected in parallel combinations an additional step up/step down conversion is needed to raise or lower the voltage to the voltage required for the system. However, the parallel combination system is safer to work with because its battery string voltages are lower. In addition, the loss of a battery is

not too critical in a parallel combination system because there are multiple current paths rather than one series path.

The decision to use a singular converter or multi converter system in a BESS is critical to the system's performance. A singular converter system usually has simpler controls than multi converter system because the former does not require the coordination of the multiple converters. However, in the singular converter system the loss of the singular converter would mean the loss of the entire BESS where as in the multi converter system, the loss of a converter would simply causes the system to operate at reduced capacity. Furthermore, the cost and rating of each of the converters in a multi converters system is less than in a singular converter system.

All together, both battery string architectures (series battery string and parallel battery string) and both converter configurations (single converter and multiple converters) have their benefits and drawbacks. However, parallel batteries and multiple converters appear to provide greatest benefits to the design. Specifically, the parallel battery pack and multiple converters provide higher reliability and safety for the BESS. Thus, the RBESS utilizes these approaches in its design.

3.2 The Repurposed Battery Energy Storage System Design

The RBESS is a system that was design to control and monitor the charge exchanged with used electric vehicle batteries that have been repurposed for stationary applications on the power grid. Figure 3-2 depicts the RBESS connected to the power grid via an AC to DC converter which converts the DC voltage from the RBESS to a usable AC voltage for the power grid and vice versa. The selection of the AC to DC

converter system is based on the power rating of the RBESS and the system's grid application of the RBESS.

The RBESS monitors the batteries in the system to determine the dispatchability of the energy from or to the RBESS. The RBESS monitors the voltage and the current at the power grid interface, while also monitoring the SOCs, the voltages and the currents of each of the individual batteries to determine the dispatchability of each battery pack.

The RBESS can be broken into two main systems. These systems are the battery bank system and the charge converter system which are depicted in Figure 3-2. The battery bank manages the balancing of the batteries in each of the battery packs in the battery bank. The charge converter system regulates the voltage and the current exchanged with the power grid to maintain the battery bank.

The RBESS battery bank system consists of multiple networks of batteries that are connected in parallel. The RBESS battery bank system can be broken down into a system of multiple battery packs as is seen in Figure 3-3. Each battery pack is connected to its own converter in the RBESS charge converter system via its own battery pack bus. (The converters in the RBESS converter system will be discussed in the next section 3.4.)

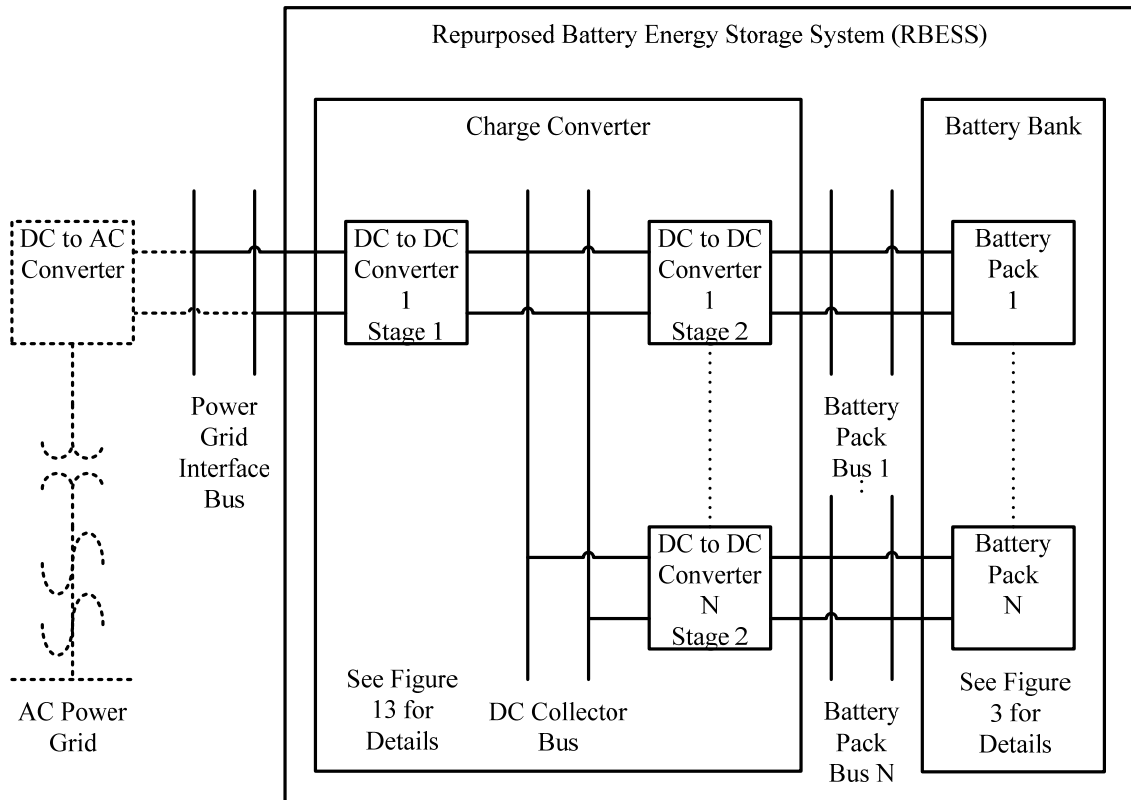


Figure 3-2: The Repurposed Battery Energy Storage System (RBESS) connected to the power grid via the DC to AC converter interface.

3.3 The RBESS's Battery Bank System

Each battery pack in the RBESS battery bank is made up of several charge block units (Figure 3-3). Each charge block unit is connected to the battery pack's battery pack bus on one side of the charge block unit and the other end of the charge block unit is connected to its own battery (Figure 3-3). Consequently, every charge block unit connected in a battery pack forms a parallel network of batteries in a battery pack.

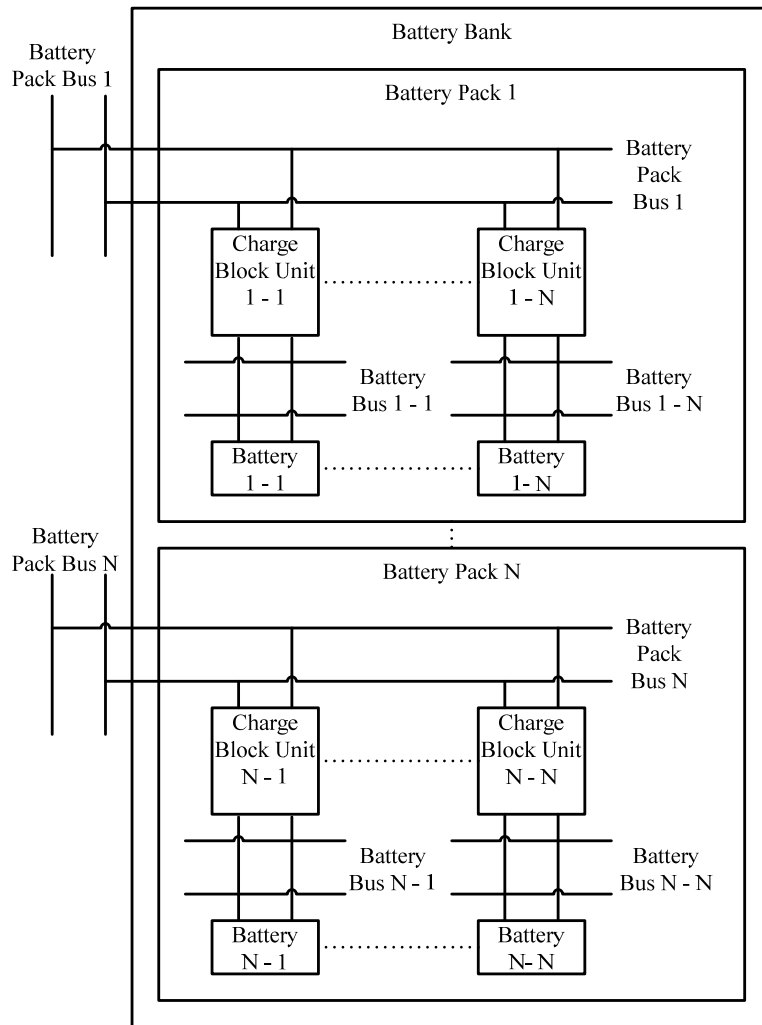


Figure 3-3: The RBESS's battery bank.

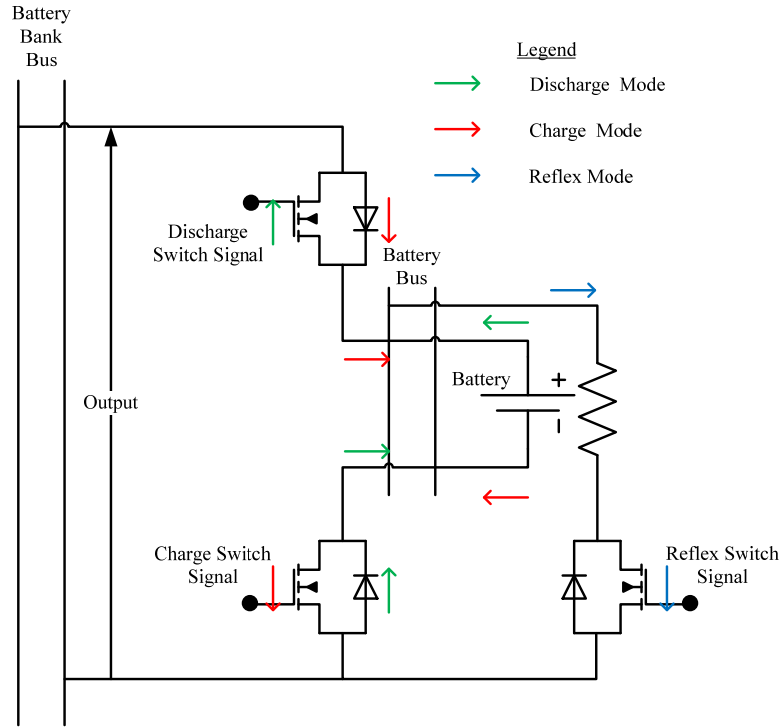


Figure 3-4: The schematic layout of the “Charge block unit” used to control the pulsed charge exchanged with a battery.

The charge block unit is a switching cell that controls the flow of charge and discharging pulses into and out of a battery. The charge block unit contains three switches with anti parallel diodes. Two of the switches are placed in the negative and positive paths of the battery terminal as is seen in Figure 3-4. The drain of the MOSFET switches and the cathode of the anti parallel diodes are connected to the battery terminals (Figure 3-4). Pulsed charge control of the batteries is accomplished by a process in which the switch in the negative terminal path is pulsed while the switch in the positive terminal path is left in the off state. This process allows current to flow from the converter through the diode into the battery and then through the switch. Furthermore, to allow for pulsed discharge control of the batteries, the switch in the positive terminal path

is pulsed while the switch in the negative terminal path is left in the off state. This process allows current to flow through the diode then through the battery, then through the switch and then out into the converter. When both switches are in the off state, current is prevented from flowing, by the anti parallel diodes in the terminal conduction paths.

The type of arrangement used in the charge block unit substantively reduces the number of power electronic elements used in the bidirectional controls of the charge block unit. An anti parallel diode is commonly found in power electronic switches like power MOSFETS and IGBT modules. Therefore, if the two switches are to be paralleled in opposite conduction directions and isolated on either side of the battery terminals there should be at least one uncontrolled current path owing to the presence of the anti parallel diode in the module. This situation would require that an additional diode be placed in series with the switch whose diode was conducting in order to prevent the uncontrolled flow of current.

Furthermore, the charge block unit arrangement selected reduces the complexity of the interface controller needed for the bidirectional control of the charge block unit. For instance, if the two switches were in series on the positive side of the battery a more complex interface control circuit would be required. The additional complexities of the controls would be due to the fact that the switches were not referenced to ground.

In addition, the charge block unit arrangement selected minimizes the potential difference between the battery's negative terminals and ground. For example, if the two switches were in series on the negative terminal of the battery, the voltage drop on both

the MOSFET and diodes would be greater than the voltage drop on just one of the elements.

However, the charge block unit switch arrangement used poses a problem for correct measurement of the battery voltage. Firstly, since the battery's negative terminal is connected to the ground via the switch, the battery is floating over the system's ground. Secondly, since the impedance to the ground changes when the switch is conducting, or when the diode is conducting, or when both the diode and switch are not conducting, the use of direct single ended or differential measurements are not suitable because the ground reference of the battery terminal changes. This problem is solved by taking a differential measurement of the battery via two tapped high resistance resistors with one resistor tied to either terminal of the battery on one side of the resistors, and by tying the other end of the resistors to ground, and by feeding the taps of the resistors into the differential amplifier. These adjustments will enable the differential measurement circuit and the battery to have a common ground point through the high resistance resistors for measurement.

In addition, the charge block unit has the capability of reflex charging of a battery [23]. The series resistor and the switch connected to the battery bus terminals (Figure 3-4) of the charge block unit create a path for current to flow that momentarily discharges the battery. As mention in section 2.4.1.3, this "Reflex charging," improves the electrode formation in lead acid batteries resulting in an increased battery performance and life.

3.3.1 RBESS: Charge Block Unit Controls

The Multi-Level Interlaced Pulsed Charge (MLIPC) controller was developed in order to control the charge block units. The MLIPC is based on the three techniques, battery pulse charging [8] [9], battery interlining [10] [13] and virtual battery paralleling [11] [12] which were discussed in the previous chapter. A MLIPC controller is used to control one battery pack in a battery bank. Thus, each battery pack is controlled by its own MLIPC controller.

The MLIPC controller works by sending control signals to the charge block units which determine the number of batteries participating in the charge exchange. The control signals determine how long (pulse period) the charge block needs to participate in the charge exchange in order to balance the batteries in a battery pack. The MLIPC controller controls the charge exchange by sequentially triggering the charge block units to pulse for their given pulse period, as is seen in column one of Figure 3-5. Therefore, the entire charge block units' pulses are interlaced together, thereby producing a charge exchange path with continuous voltage and current flow. The continuity provided by interlacing the charge block units eliminates the dead band periods between pulses that have occurred in traditional pulse charging scheme. The continuity improves the performance of the system and no time is wasted in an idle state.
















Battery Number	Control Signals		
	Single Level	Double Level	Triple Level
1			
2			
3			
4			
All			

Figure 3-5: Multi-level battery pack control.

In addition, the MLIPC controller can compensate for changes in the demand for the power exchange. The MLIPC controller, by overlapping the pulse periods of the charge block units parallels the charge block units' operation and thereby allowing the pack to increase its current exchange capacity. Therefore, the battery packs can exchange more energy with the converter by paralleling the charge block units than can be obtained from a single charge block unit's battery. Thus, the multi-level stacking feature of the MLIPC controller allows it to change the battery packs' current rating dynamically which in turn leads to an efficient utilization of the energy being exchanged with the battery pack.

$$T_{Pulse_Period}(x) = \frac{SOC(x)^2}{\sum_{n=1}^N SOC(n)^2} \times T_{Cycle_Period} \quad (3.1)$$

Another benefit of the MLIPC controller is the fact that it uses a variable Pulse Width Modulation (PWM) scheme to assist in the balancing of the batteries. The active

pulse period of a charge block unit is based on a percentage of a selected period that requires all charge block units to be activated. During discharge, equation (3.1) is used to determine the duration of the period in which the charge block unit will participate in the discharge of energy. From equation (3.1), it can be observed that charge block units whose batteries have higher SOC will participate longer in the discharge than those with lower SOC. Consequently, the batteries with higher SOC will discharge more energy with the converter system because they are active longer. However, over time the SOC of all the batteries in the battery pack will become equal because higher SOC batteries will exchange more energy than lower SOC batteries thereby allowing the battery SOC to converge to the same value. When using aged batteries it is likely that each will have a different charge capacity. As mentioned in section 2.2.2, it is important to know the aged batteries parameters. Once batteries parameters are known, the batteries capacity (SOC) range can be mapped in to the 0% to 100% scale, enabling it to be put into this charging scheme.

Likewise, during charging of the batteries, equation (3.2) is used to determine the duration of the period in which the charge block unit will participate in the charging of the battery. It can be seen from equation (3.2) that charge block units whose batteries have a higher DOD will be charged longer than those with lower DOD. Therefore, the batteries with higher DOD will be charged longer because they are active longer. However, over time the DOD of all the batteries in the battery pack will become equal because higher DOD batteries will be charged more than lower DOD batteries thereby allowing the battery DOD to converge to a common value.

$$T_{Pulse_Period}(x) = \frac{DOD(x)^2}{\sum_{n=1}^N DOD(n)^2} \times T_{Cycle_Period} \quad (3.2)$$

Overall, the flow of the MLIPC controller occurs as is depicted in Figure 3-6. The MLIPC controller first starts by calculating the Open Circuit voltage (OCV) of each battery in the battery pack. Then once the system is enabled the MLIPC controller runs the load queue subroutine.



Figure 3-6: The MLIPC controller flowchart.

The load queue subroutine in Figure 3-6 is further detailed in Figure 3-7. The load queue subroutine pushes all enabled charge block units into the online queue of charge block units and all disabled charge block units into the offline queue of charge block units.

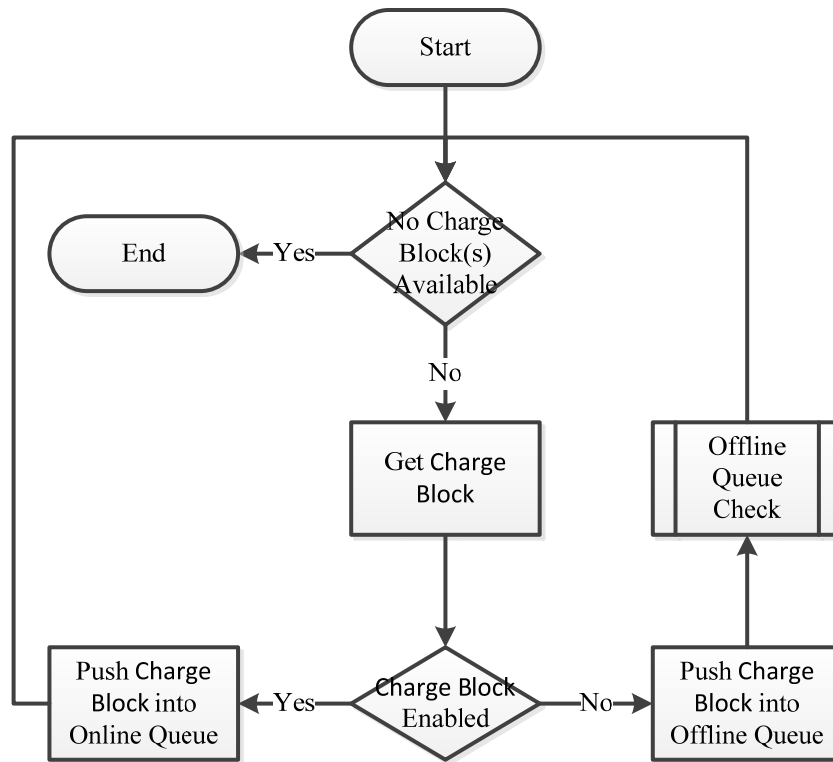


Figure 3-7: Load queue flow chart subroutine for charge block unit.

When a charge block unit is pushed into the offline queue, the unit remains in the offline queue until the unit is re-enabled. Another, subroutine in the MLIPC controller periodically checks the top of the offline queue to determine whether the charge block unit has been enabled. This subroutine is run every 10 seconds to check the offline queue. The charge block unit at the top of the queue is moved to the bottom of the queue if the charge block unit is disabled. On the other hand, if the charge block unit is found to be

enabled the unit is removed from the top of the offline queue and pushed into the bottom of the online queue such that it can then be used.

The flowchart in Figure 3-6 shows that all charge block units in the battery pack are activated for a set time period in order to share the energy needed to pre-charge the converters before the main pulse controls are activated. The full control subroutine is illustrated in the flowchart depicted in Figure 3-8.

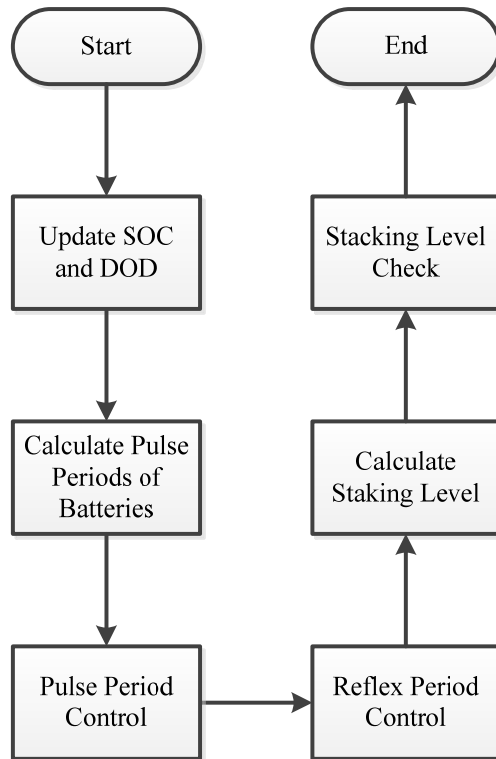


Figure 3-8: Pulse controls running subroutine for charge block units.

The pulse controls running subroutine (Figure 3-8) first updates the SOC of all batteries in the battery pack. The update involves integrating the current exchange with

the battery to determine the capacity gained or lost in the charge exchange and adding the result to the current known capacity of the battery and then calculating the SOC (DOD). After the SOC update, the pulse period of the charge block units is determined by using equations (3.1) or (3.2). The equation chosen depends on the mode of operation (discharge or charge).

The pulse controls running subroutine executes the pulse period update subroutine. The pulse period update subroutine shown in Figure 3-9 simply loops through all active charge block units in the active queue to determine whether their pulse periods are finished. If the pulse periods are finished the charge block units are pushed into the online queue. However, if the charge block units' reflex controls are enabled, then the charge block units are moved into the reflex queue and the charge block unit's reflex system is activated. The reflex system activates the reflex switch in the charge block units in order to discharge part of the energy in the battery to improve diffusion capability of ions in the cells.

The pulse controls running subroutine operates the reflex period control subroutine seen in Figure 3-10. The reflex period control subroutine moves all charge block units into the online queue if the reflex period of the charge block units are over. Otherwise the charge block units are left in the reflex queue for the next test step.

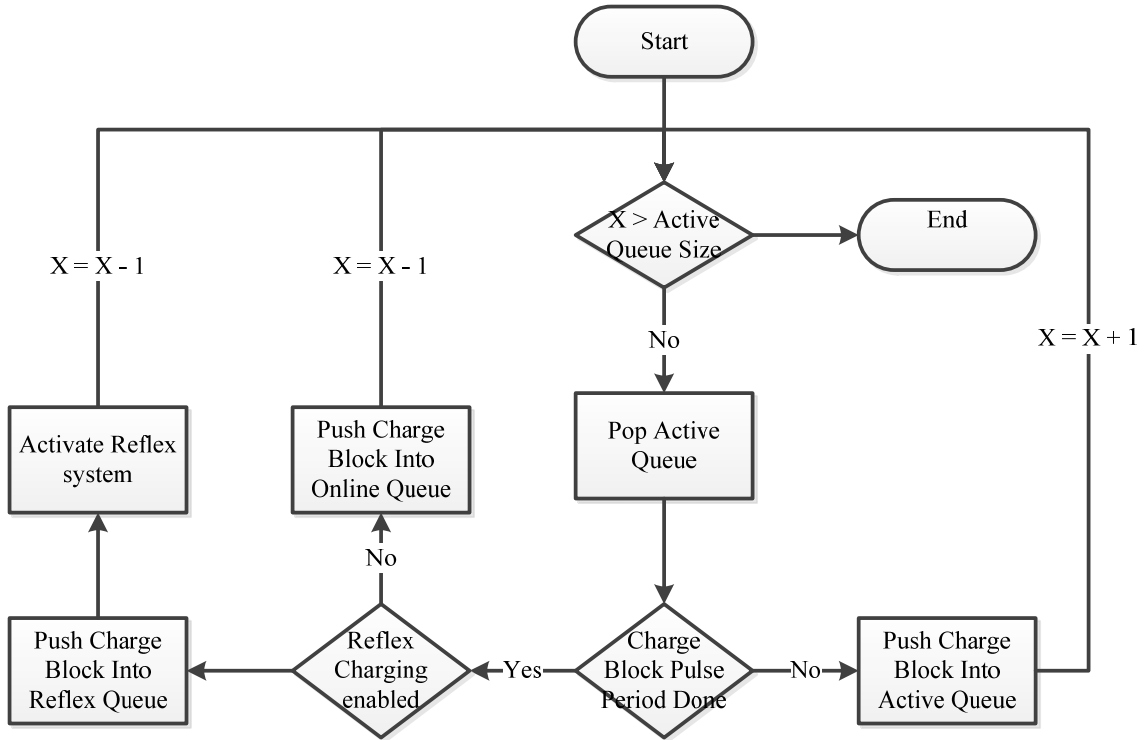


Figure 3-9: Pulse period update subroutine for the pulse controls running subroutine.

After the reflex controls have been checked, the pulse controls running subroutine calculates the stacking level of the multi-level control. The pulse controls running subroutine counts the number of batteries that are drawing current over or under the stack change setpoints. If all of the batteries are found to be either over or under their stack change setpoints, the stacking level is accordingly increased or decreased by one level to change the rating of the battery pack. Furthermore, the stacking value selected is multiplied by the stack multiplier required by the the charge converter(See next section for stack multiplier). Finally, the pulse controls running subroutine runs the stacking level check subroutine. As is depicted in Figure 3-11, this subroutine simply loops to add more

batteries to the stack if there is a deficiency in the currently stacked battery levels. At this stage the pulse controls running subroutine is ended.

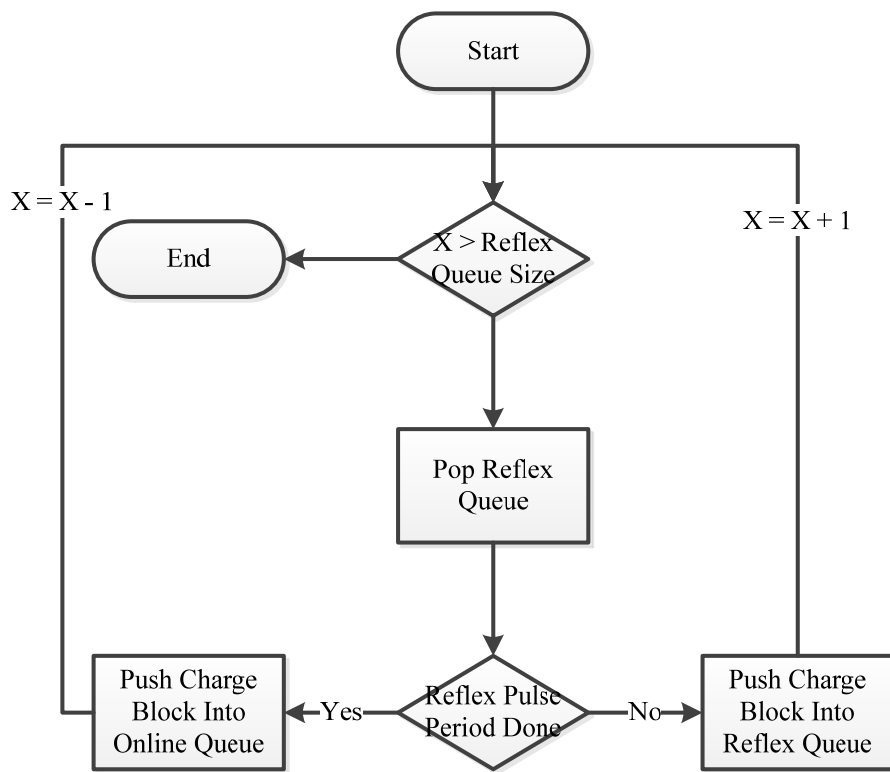


Figure 3-10: Reflex period control subroutine for the pulse controls running subroutine.

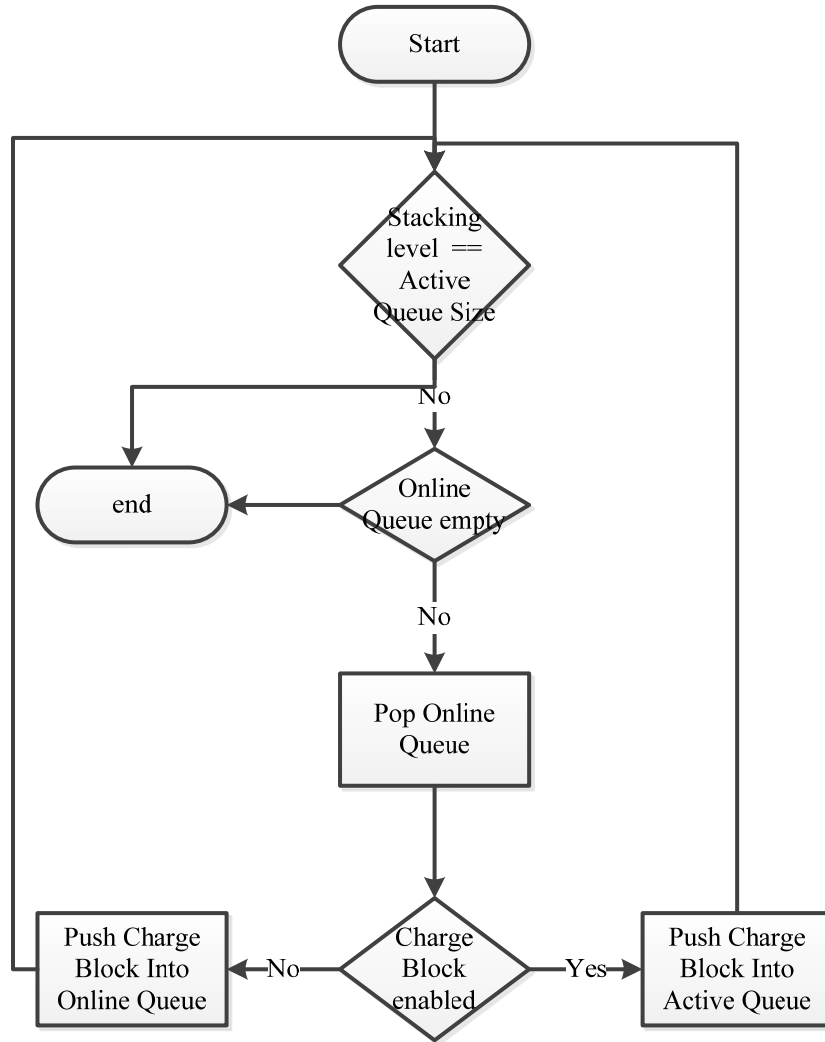


Figure 3-11: Stacking level check subroutine for the pulse control running subroutine

Once the pulse control running subroutine is completed, the MLIPC controller checks to see if the system is disabled. If the system is not disabled the pulse control running subroutine is re-ran. Otherwise, the empty queue subroutine is ran (Figure 3-12). The empty queue subroutine reinitializes the memory of the MLIPC controller.

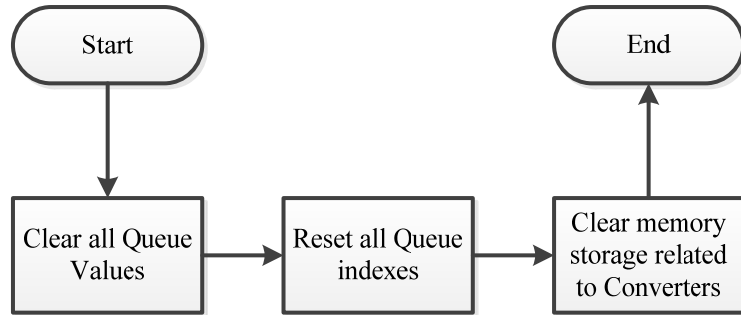


Figure 3-12: Empty Queue flowchart subroutine for MLIPC controller.

Given the description of the RBESS battery bank’s MLIPC controller, it is possible for a battery bank of 1 to N battery packs to be maintained by N MLIPC controllers. In addition, the charge converter together with the added stack multiplier factor can balance the entire battery bank. The charge converter is described in the next section.

3.3.2 RBESS: Battery Bank Protection

The RBESS battery bank has the ability to detect faults in the system. This ability protects the system. The RBESS battery bank monitors each charge block unit’s current and voltage and the DOD of the battery. If during normal operation of the system the voltage of the charge block unit goes more than 5.0% over or under the desired voltage set point limits, for a sustained period of time, the system will disable charge block unit and set the fault flag for the event. If during normal operation of the system the current of the charge block unit goes more than 5.0% over the desired current set point limit, for a sustained period of time, the system will disable charge block unit and set the fault flag for the event. If the DOD of the battery goes out of the range (10% to 90%) the system

will disable the charge block unit and set the fault flag for the event. These, protection mechanisms were put in place to protect the batteries from damage.

3.4 RBESS: Charge Converter System

The RBESS charge converter system can be further sub divided into two stages. The first stage of the system provides an interface between power grid and the second stage converters, and the second stage of the system provides an interface between the first stage converter and the battery packs of the battery bank (Figure 3-13). The RBESS charge converter system is further detailed in Section 4.1.3 and Appendix A.

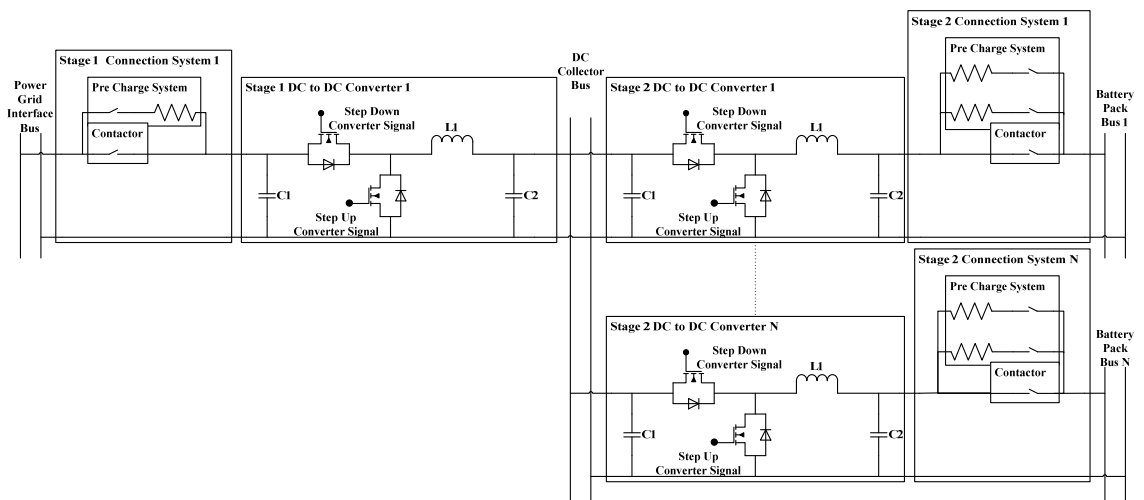


Figure 3-13: The Charge Converter system.

The first stage of the RBESS charge converter system consists of a single DC to DC converter which regulates the voltage and current between the power grid interface bus and the DC collector bus (Figure 3-14). The first stage converter of the RBESS converter system is connected to the power grid interface bus via a pre-charge relay and resistor combination, which is paralleled to a contractor (Figure 3-14). The pre-charge

relay and resistor combination are used to energize the system during the start-up of the system. The contactor is used during the regular operation of the RBESS system after the pre-charge phase of the system is completed.

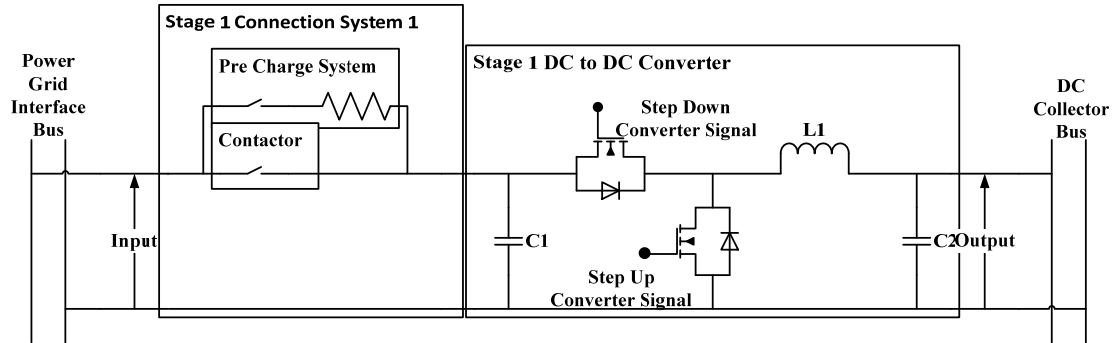


Figure 3-14: Stage one DC to DC converter for Charge Converter system.

The second stage of the RBESS converter system consists of multiple DC to DC converters each of which are connected on one end to the DC collector bus and on the other end to one of the battery pack buses (Figure 3-15). Each battery pack bus is connected to one of the battery packs in the battery bank. In addition, the pre-charge system and the contactor are connected between each of the stage two converters and their corresponding battery bank bus (Figure 3-15). The pre-charge system consists of two relay and resistor combinations which are used for energizing the system. One of the relay and resistor combinations is used for energizing the system during charging mode operations and the other relay and resistor combination is used for energizing the system during discharge mode of operations. The contactor is used for the regular operation of

the RBESS system after the pre-charge phase of the system is completed. This collection of multiple DC to DC converters in the second RBESS converter system stage allows batteries of multiple chemistry and voltages to be interfaced into the same system.

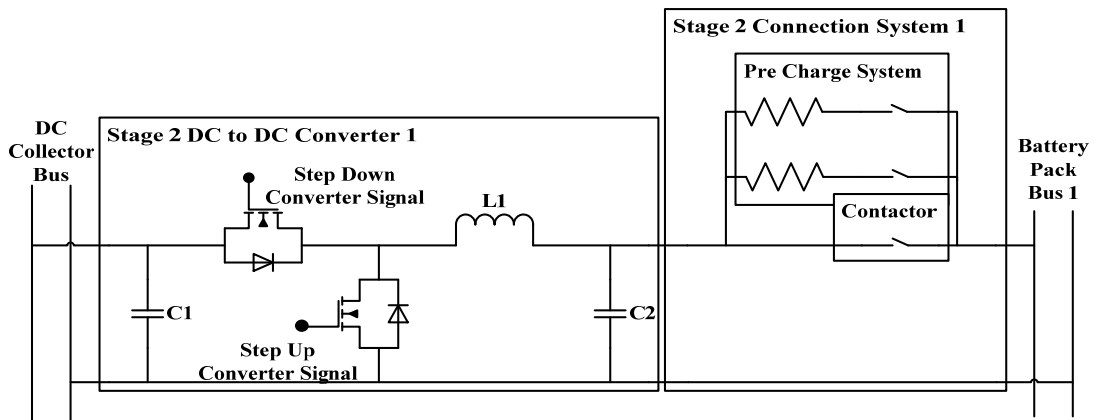


Figure 3-15: Stage two DC to DC converter for Charge Converter system.

Typically batteries of multiple chemistry and voltages are not connected into the same battery bank system because these different types of batteries require different charging and discharging regimes. The difference in their charging and discharging regimes prevents them from being directly intermix in a system. However, the DC to DC converters in the secondary stage of the RBESS converter system provides an interface which accommodates this mixture of multiple battery types. This accommodation is possible because all of the different battery packs are isolated behind the second stage DC to DC converters.

All of the converters in both stages of the RBESS converter system utilize a DC to DC step down converter (Buck converter) to regulate the voltage and current to charge

the batteries. In Addition, the DC to DC step down converter is designed to operate as a step up converter (Boost converter). This is achieved by adding an anti parallel diode and a switch to the switch and diode of the conventional DC to DC step down converter (Figure 3-14 and Figure 3-15) [30] [31]. The addition of the anti parallel diode and switch enables the converter to be used to regulate the voltage and current that discharges the batteries [30] [31]. The arrangement of switch and diode produces a bidirectional converter system with the capability to control the flow of energy in the RBESS charge converter system.

The RBESS charge converter system consists of two stages of converters connected to a common bus. This fact produces a system of back to back converters. Since, converters are connected in back to back fashion, the impedance seen from the interface bus is critical to the operation of the converter network [32] [33]. Therefore, the output impedance of the first stage converter must be equal to or greater than the second stage converter. This is necessary to prevent the introduction of unwanted resonance in a unidirectional converter. Such unwanted resonance could cause instability in the system. However, in a bi-directional converter, it is ideal for the impedance of the two stages to be matched to prevent unwanted resonance in one or both directions.

However, in a system such as the RBESS charge converter system, in which multiple converters are connected to the converter bus, it is far more difficult to balance the impedance of the buses for an unknown quantity of converters [33]. However, there are several methods that can be used to reduce or mitigate the resonance problem.

The first method is a specific system, designed with a set number of converters that will force the impedance of the converters to be equal. This method will prevent the resonance problem from occurring. However, this method will limit the size of the system, will prevent further expansion of the system and will require all converters be connected to the system for correct operation. In addition, the tolerance of the converter components can vary and the matching of the components may prove to be extremely difficult. Furthermore, as converter components age the impedances of the converters will change and the system will become unstable.

The second method uses additional reactor controlled devices, such as switched capacitors, to provide additional control of impedance and to reduce the impedance mismatch between the converters. This method will allow the size of the system to be expanded or contracted by controlling the additional reactors on the bus. However, the additional reactor controlled devices will introduce an additional cost to the system in terms of the cost of the devices themselves and the cost of the controls for the devices.

In the third method, the resonance of the converters is dampened out or eliminated by the converters' controls. This method will allow the system to contract or expand. Of course, this will depend on the level of sophistication of the controls. This method will not require additional hardware. Therefore, it will be cheaper than the previous method. Thus, the RBESS charge converter system uses this method of control to eliminate the resonance problem in the system.

3.4.1 RBESS: Converter System Controls

The RBESS converter system's control contains two levels of control. The controls of the two stages in the RBESS converter system are independent of each other. The primary level of control in the RBESS charge converter system is the control of the PWM duty cycle which runs the switching DC to DC converters. The secondary level of control in the RBESS converter system sets the control modes and power level of the converters to control the system and balance the battery packs. The, secondary level of control in the RBESS charge converter system also selects which one of the converter will be operating and determines the number of converters that will be operating in a given stage.

3.4.2 RBESS: Converter System Primary Controls

The primary controls of the converters in the RBESS charge converter system are all identical to each other. Each converter's control system has two modes of operation. These modes are the step up and step down modes of control which are used to discharge and charge the batteries. Each one of the converter control modes contains two sub control modules which are used for voltage control and for current control. These sub control modules facilitate proper bus voltage control and current flow of the system and also provide the means whereby different charging strategies can be implemented for different battery chemistries.

All sub control modules use the same control topology. Sub control modules contain two main parts. These are a steady state response control and a feed forward error response control [31]. The steady state response and the error response control are summed and passed through a limiter to limit the duty cycle between 0% and 100%

(Figure 3-16 and Figure 3-17). The steady state response control consists of a ratio converter which is used for converting the desired step up or step down voltage or current to its corresponding duty cycle value. The input to the steady state controls is the desired value for the system added to the feedback loop value. The feedback loop consists of the difference between the filtered and non-filtered measured value (Figure 3-16 and Figure 3-17). The feedback loop is used to reduce the steady state ripple [30] [31] . Furthermore, the addition of this difference component to the desired steady state value helps to reduce the resonance problem previously discussed. Table 3.1 indicates the input for this half of the converter module.

The feed forward loop helps to compensate for transient in the system. The feed forward loop consists of a gain controller in series with a PI controller. This controller unit is used to reduce the error between the desired value and the actual value of the converter. The input to the feed forward transient response control is the difference between the desired value and the actual value of the system to be controlled (Figure 3-16 and Figure 3-17). Table 3.1 indicates the input for this half of the converter.

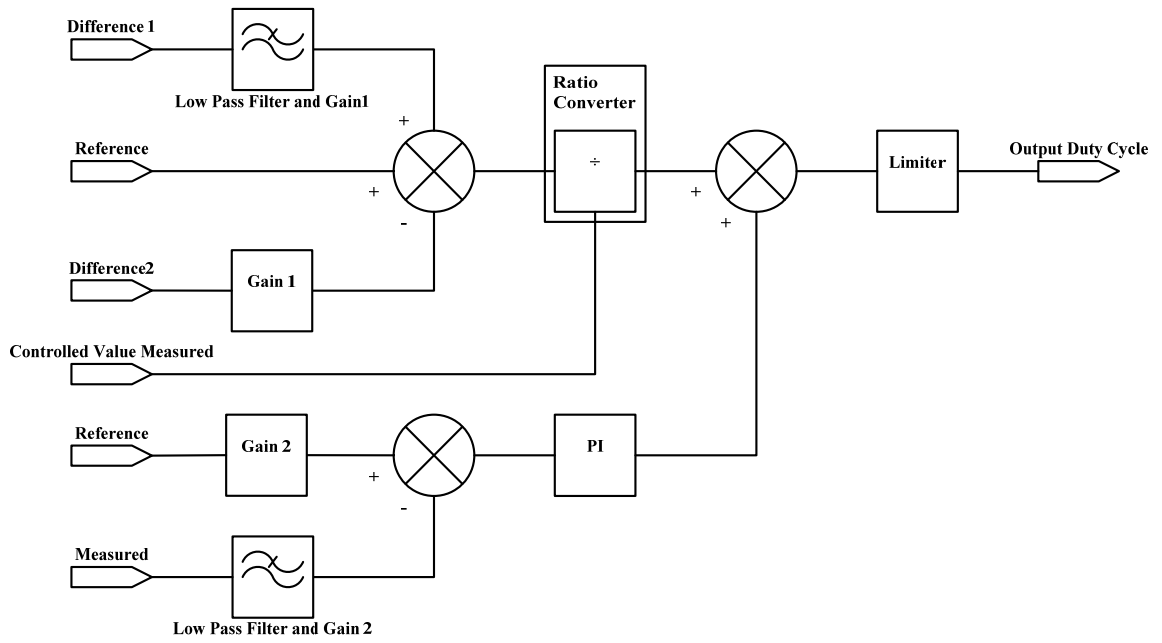


Figure 3-16: Buck converter control.

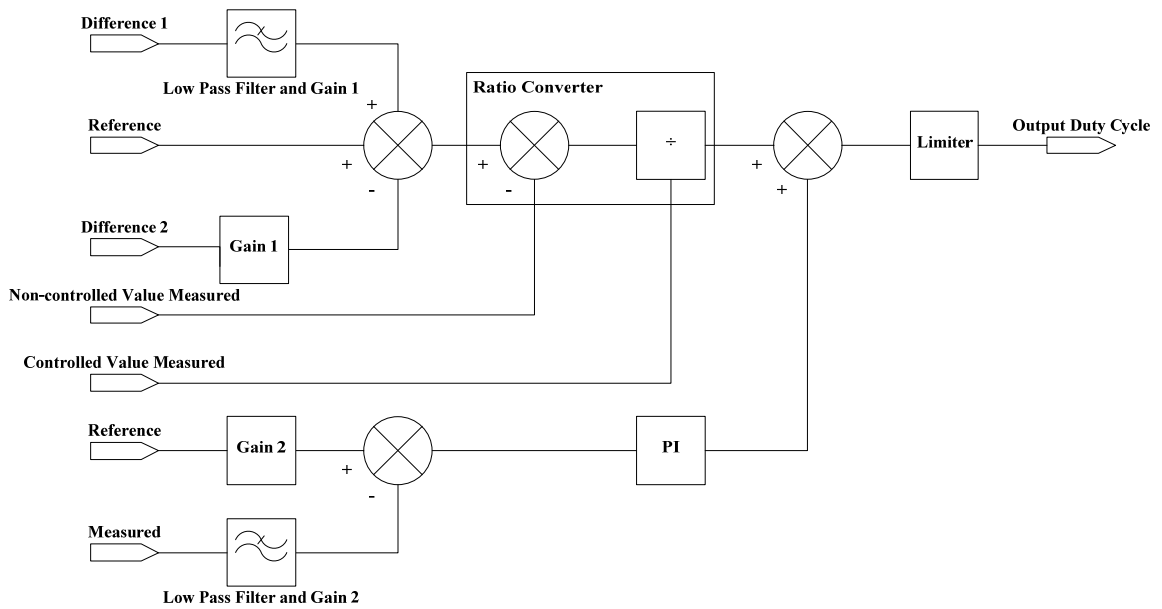


Figure 3-17: Boost converter control. (Note: “Non-controlled Measured” is the “Controlled Measured” complement on the opposite end of the converter)

Table 3.1: The inputs table for the RBESS charge converter system’s primary converter controls (Note: subscript “R” means reference value)

Controls		Steady State Control			Transient Response Control	
Mode	Sub mode	Reference	Difference		Reference	Measured
			1	2		
Step up	Voltage	$V_R(\text{Output})$	$V(\text{Output})$	$V(\text{Output})$	$V_R(\text{Output})$	$V(\text{Output})$
	Current	$I_R(\text{Input})$	$I(\text{Input})$	$I(\text{Input})$	$I_R(\text{Input})$	$I(\text{Input})$
Step Down	Voltage	$V_R(\text{Output})$	$V(\text{Output})$	$V(\text{Output})$	$V_R(\text{Output})$	$V(\text{Output})$
	Current	$I_R(\text{Input})$	$I(\text{Input})$	$I(\text{Input})$	$I_R(\text{Input})$	$I(\text{Input})$

An additional limiter is placed in series with the output voltage and current modules. The limits of the voltage control module are from 0% duty cycle to the current duty cycle of the current control module. Conversely, the limits of the current control module are 0% duty cycle to the current duty cycle of the voltage control module. The limiting is used to prevent the system from exceeding its desired power setting. The output of the limiters is connected to a selector, which is used to select either current or voltage mode control in the desired step up or down mode.

3.4.2.1 RBESS: Charge Converter System Secondary Controls

The secondary controls of the RBESS charge converter’s two stage converter systems are also independently controlled by their own secondary level controller. The secondary level controller is the master controller for all converters in a given stage of the system. The secondary level controller determines whether the converters, should be in step up or step down, voltage or current control mode, the amount of voltage or current they should produce to meet the demands of the system and which and how many controllers should participate in the charge exchange.

Multiple converters connected to the same bus in the same mode and set point may create a condition in which the converters end up in a struggle to control the bus. The power struggle may lead to oscillations in the system or may cause the system to go unstable. The struggle stems from each converter's attempt to control the bus to its desired set point. Errors in the measurements and hardware tolerances prevent the converters from reaching the same set point. Therefore, the RBESS converter system's secondary control mitigates this problem by using master slave architecture to control both the voltage on the bus and power delivered.

The master slave architecture works by having only one converter in the stage to act as the master controller of the voltage of the bus. The remaining converters in a given stage are then operated in a current control mode to inject sufficient current into the bus to meet the required power demand. This means that the master converter controls the bus voltage and delivers the remaining current to meet the desired power demand. Therefore, the converters of the bus are never in contention and will therefore remain stable.

Figure 3-18 depicts the overall secondary control of the RBESS converter system. Once the system is enabled the system loads the queues with the appropriate converters. Then the controller energizes a converter when the system is started. Once the converter is energized, it is then activated and allowed to operate normally. If the system is stopped or disabled the converter is de-energized and then disabled until the process is restarted.

The load queue subroutine in Figure 3-18 is further detailed in Figure 3-19. The load queue subroutine pushes all enabled battery packs into the online queue of converter and all disabled converter into offline queue of converters.

When a converter is pushed into the offline queue, the converter remains in the offline queue until the converter is re-enabled. Another, subroutine in the second stage converter periodically checks the top of the offline queue to see whether the converter has been enabled every 10 seconds. If the converter is disabled, the converter at the top of the queue is moved to the bottom of the queue. On the other hand, if the converter is found to be enabled, the converter is removed from the top of the offline queue and is pushed into the bottom of the online queue such that it can be used.

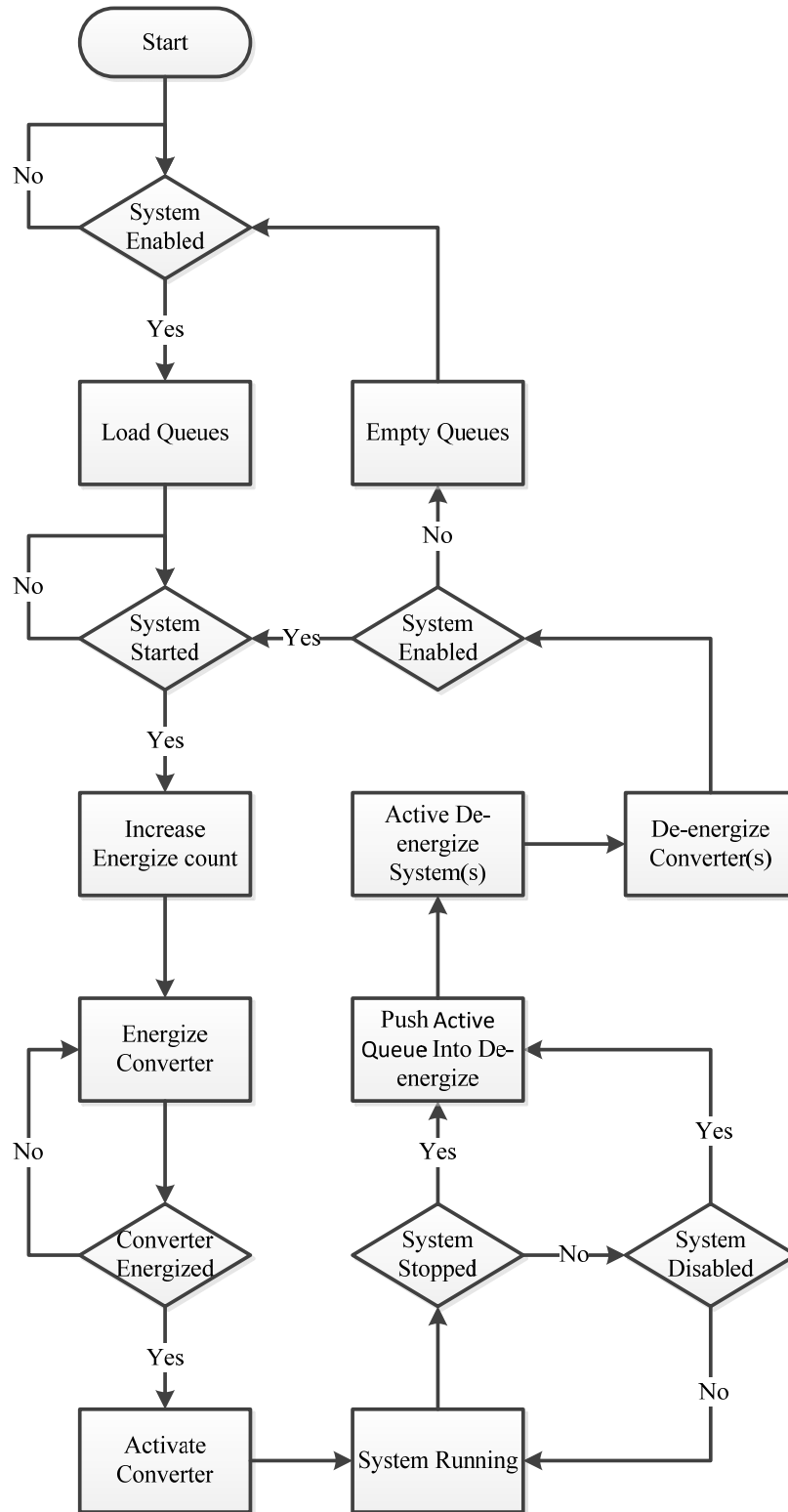


Figure 3-18: Overall secondary control for RBESS charge converter system.

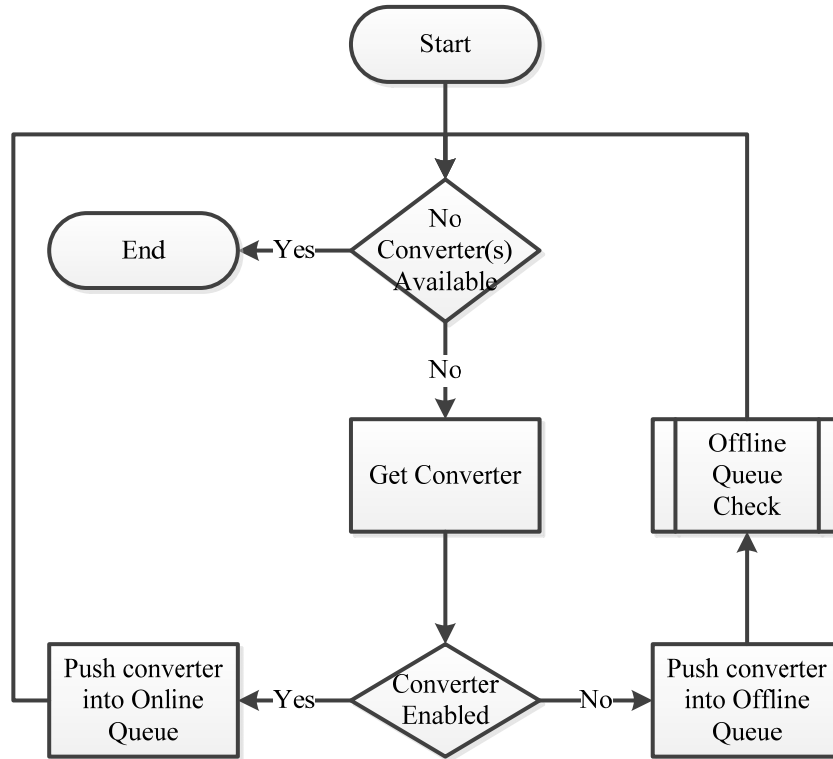


Figure 3-19: Load queue flow chart subroutine.

The energize subroutine seen in Figure 3-20 energizes the required number of converters. When the system is starting a single converter is selected for running but when the system is running the number of converter to be energized is determined by how many packs are needed to meet the required power demand. The subroutine first loads the required number of enabled converters into the energize queue and activates their pre-charge system. Secondly, the pre-charge system closes the appropriate relays to allow the capacitors in the system to become ready to reduce the inrush current when the converters' primary controls are activated. When converters are in the pre charge stage, their associated battery pack stacking level is set to maximum. This is done to prevent

any one battery from taking the brunt of the inrush charge. On the other hand, disabled converters are pushed into the offline queue.

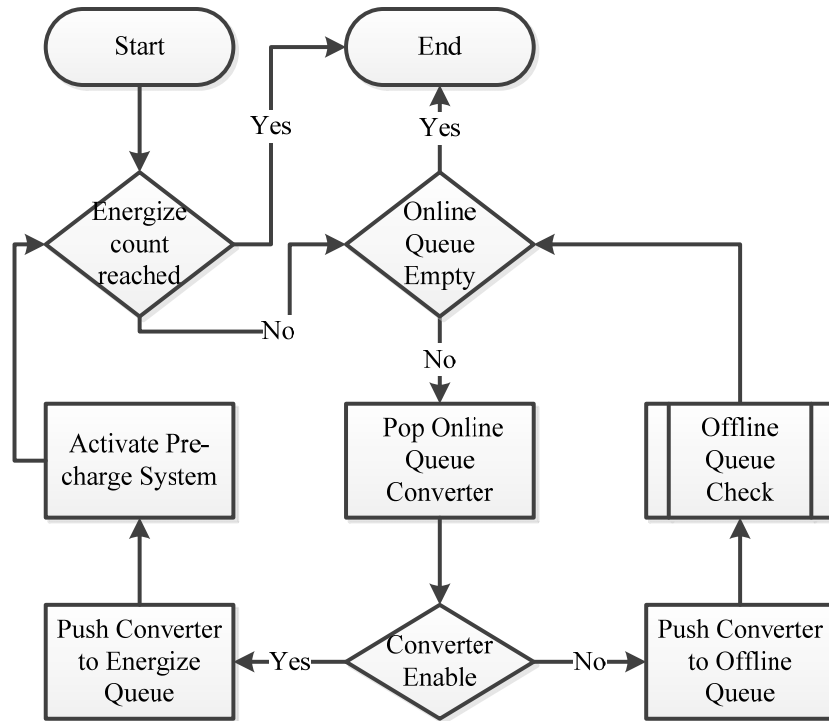


Figure 3-20: Energize queue flow chart subroutine.

As is seen from Figure 3-21, the activated subroutine loads all the energized converters that are enabled into the active queue, and activates the converters' primary converter controls. The converters that are not enabled are pushed into the de-energized queue and the de-energize system is activated.

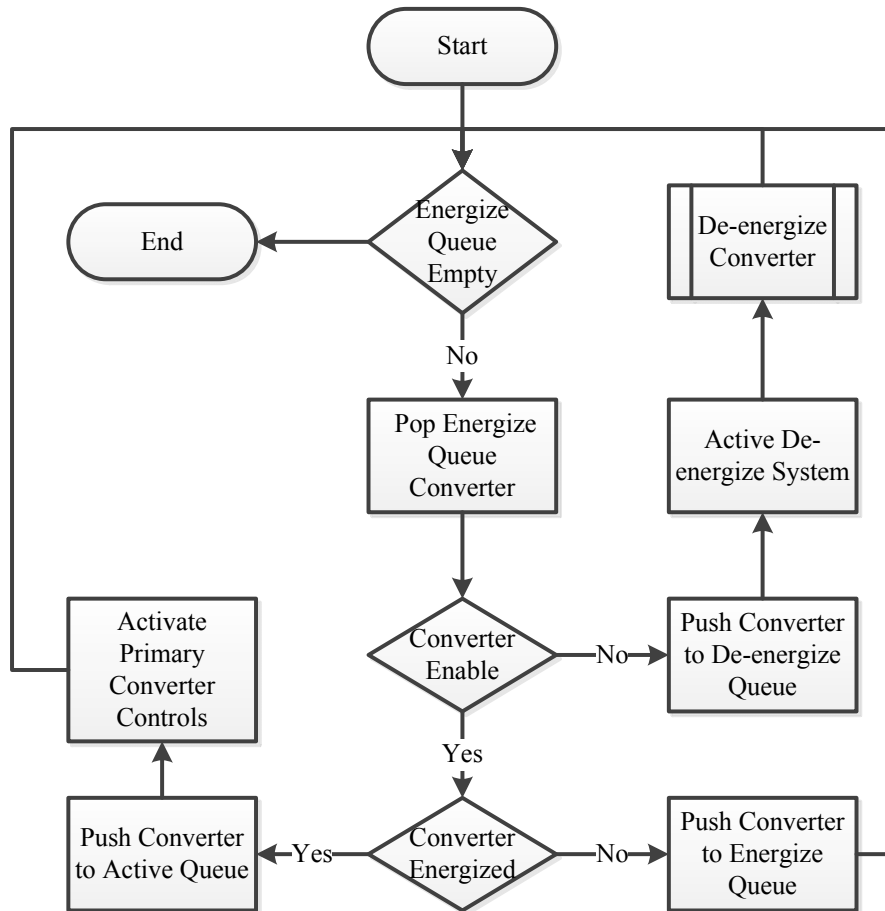


Figure 3-21: Activate converter flow chart subroutine.

As is seen in Figure 3-22, the main operations of the controls are looked after when the system enters the system running subroutine. The subroutine first verifies that the system is enabled and is running and that there are converters in the active queue to be controlled. Secondly, it tests to determine whether there are converters in the energized queue or de-energized queue and takes the appropriate action to energize or de-energize the converters.

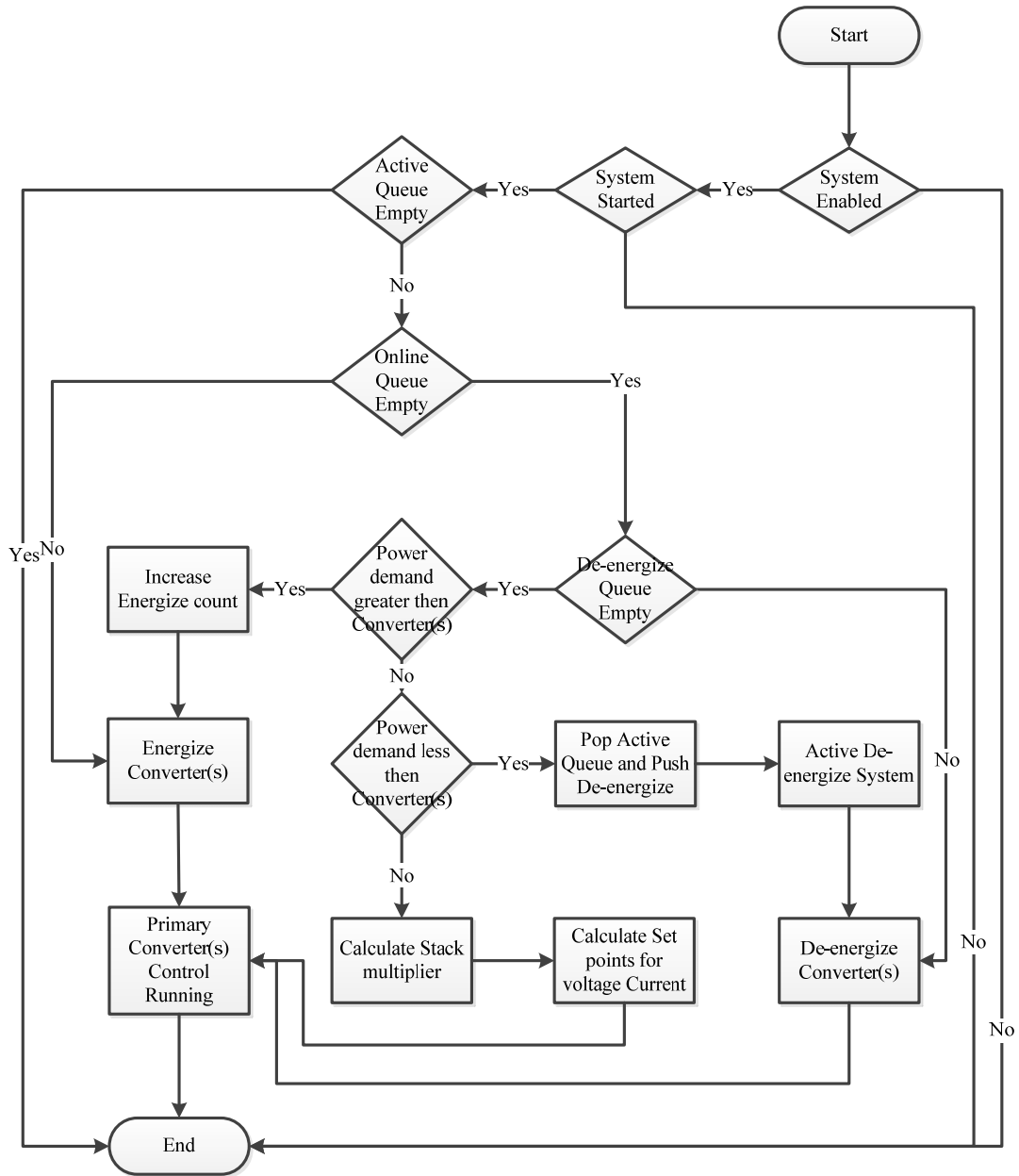


Figure 3-22: System running flowchart subroutine.

Thirdly, the system running subroutine checks to determine whether the converters are drawing current over or under the converters' set points, and takes the

appropriate action to increase or decrease the number of active converters. Fourthly, the system determines whether to send a stacking multiplier to each converter's battery pack. The stacking multiplier is sent when the charge converter wants to balance unbalanced battery packs. Fifthly, the system uses equation (3.3) for discharging and equation (3.4) for charging, to select the stack multiplier and to send it to the battery pack. The multiplier increases the number of batteries in a pack, and this enables the pack to produce or absorb more current without increasing the work done by any one battery. Sixthly, the system follows the procedure seen in Figure 3-23 to calculate the current draw required for both the input and output of each active converter. Finally, the system gives the set points to the appropriate converters to take appropriate action to control their bus current.

$$Stack_{Multiplier}(x) = \frac{SOC_{AVE}(x) - MAX(SOC_{AVE})}{0.1\%} \quad (3.3)$$

$$Stack_{Multiplier}(x) = \frac{DOD_{AVE}(x) - MIN(DOD_{AVE})}{0.1\%} \quad (3.4)$$

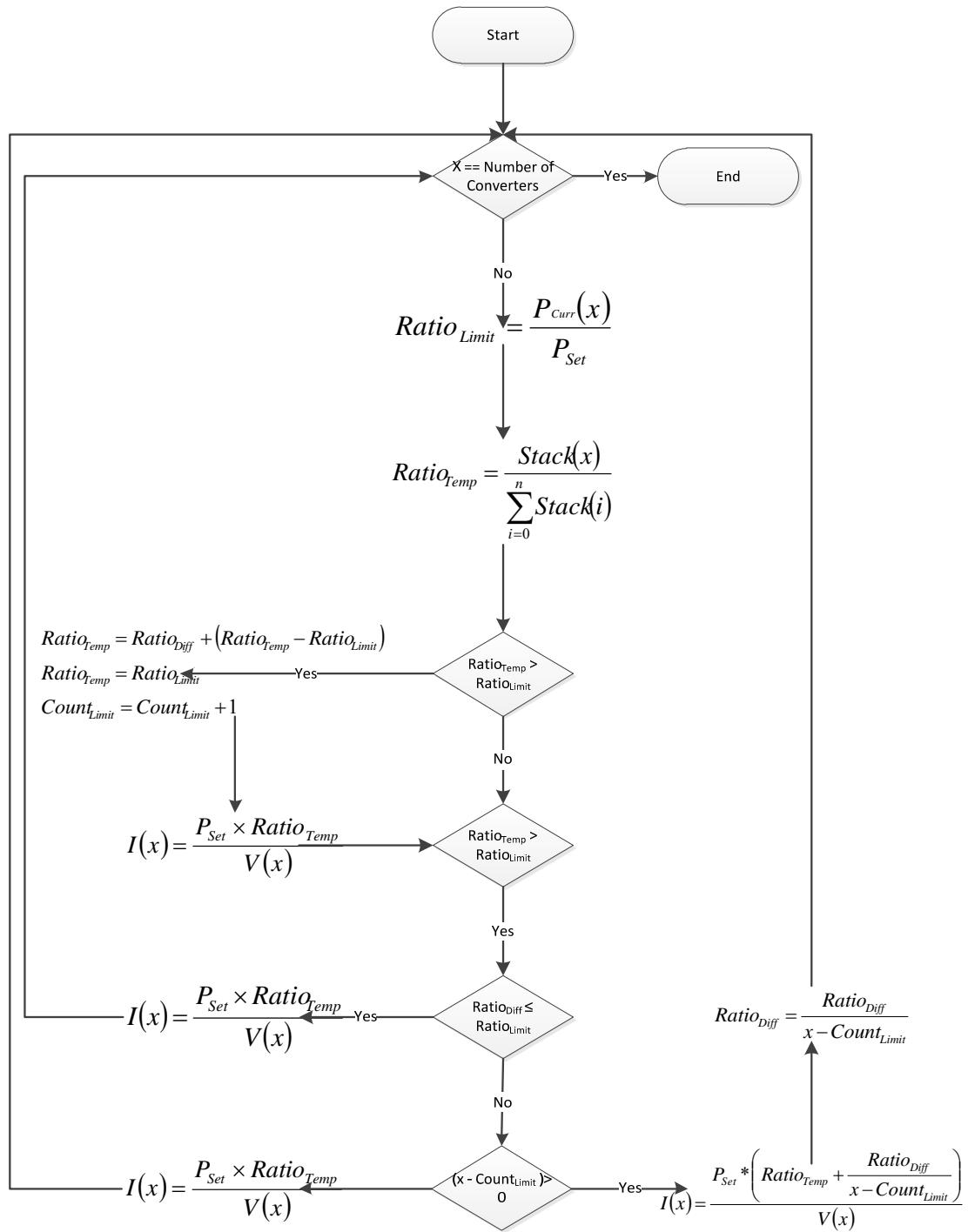


Figure 3-23: Current set point calculator.

In accordance with the flow of Figure 3-18 the secondary controls for the RBESS charge converter system, will push all active converters into the de-energized queue, if the system is stopped or disabled. The de-energized system of the converter is then activated and the converters are de-energized as seen in Figure 3-24. Once the converters are de-energized the converters are placed into the offline queue.

The de-energized system simply provides a means to discharge the energy stored in the reactive energy components of a converter. The reactive energy of the converter is allowed to flow back into the battery pack to reduce the loss of energy.

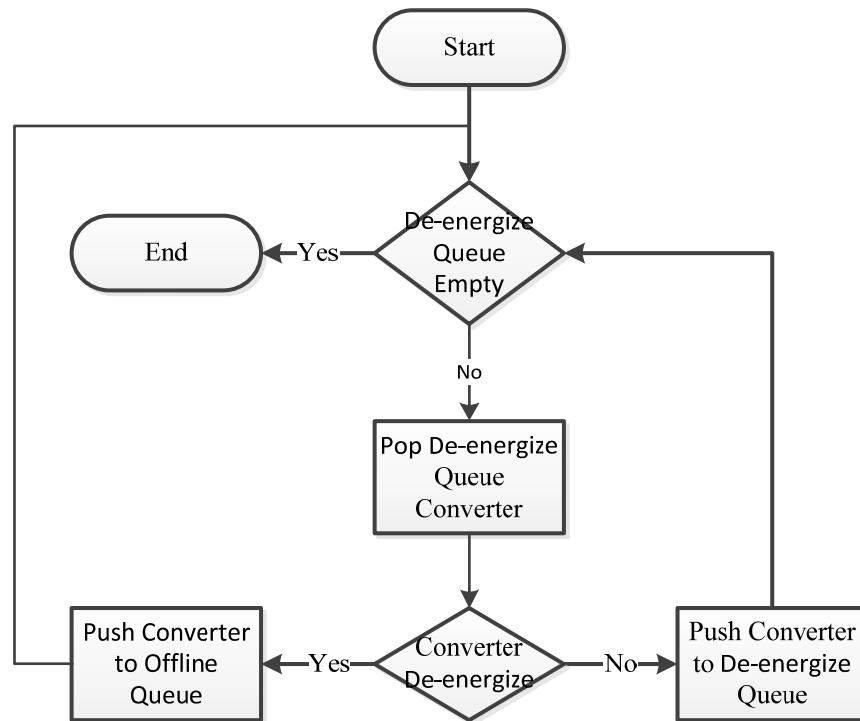


Figure 3-24: De-energize flow chart subroutine.

Finally, if the system remains disabled after it is de-energized then all queues of the system are emptied as is seen in Figure 3-25 of the empty queue flowchart subroutine.

Then the empty queue subroutine will reinitialize the memory for the secondary control system.

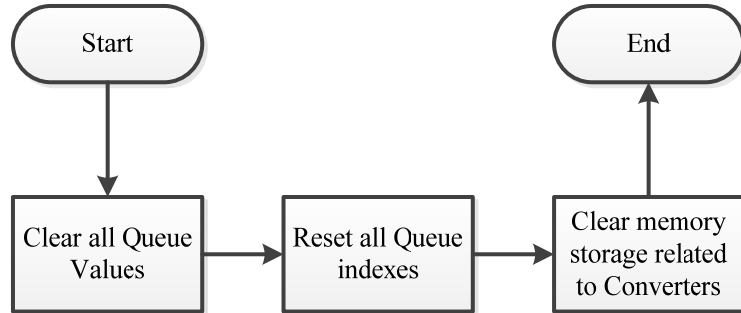


Figure 3-25: Empty Queue flowchart subroutine.

The RBESS converter system's secondary controller can maintain 1 to N converters. Therefore, secondary stage controller of the RBESS charge converter system is capable of controlling multiple converters in the second stage of the RBESS converter system or the single converter of the first stage of the RBESS converter system.

3.4.3 RBESS: Converter System protection

The RBESS converter system also has the capability to detect faults and this capacity protects the system. The RBESS converter system monitors each converter's current and voltage on the input and the output side of the converter. The system will shut down and set the fault flag for the event, if during normal operation of the system the voltage of the converter goes more than 5.0% over or under the desired voltage for a sustained period of time. Similarly, the system will shut down and set the fault flag for the event, if during normal operation of the system the current of the converter goes more than 5.0% over the desired current for a sustained period of time.

3.5 Chapter summary

This chapter looked at the design, development and optimization of the RBESS's structure, controls and protection systems in order for the RBESS to be modeled and constructed (*See next Chapter 4: RBESS Simulation Model and Hardware*). The RBESS's battery bank is a multi battery pack system in which each battery pack is controlled by a MLIPC controller that manages the battery to improve battery performance. The RBESS's charge converter system contains two levels of cascaded converters with multiple converters in the second stage to control each battery pack. Each, converter stage has two levels of control. The first level is the direct control of the converter PWM scheme and the second level of control regulates which converters are participating in the charge exchange and their power rating.

Chapter 4: RBESS Simulation Model and Hardware Implementation

The RBESS was constructed both as a simulation model and as a hardware implementation. The RBESS simulation model is shown side by side with the RBESS hardware implementation. The simulation model was developed in order to design and to test the RBESS concept prior to it being constructed in hardware. The electromagnetic transient simulator PSCAD/EMTDC was used to model and to design RBESS. The PSCAD/EMTDC simulator was used in the design of the circuit and in the development of the control strategies discussed in the previous chapter. The hardware implementation of the RBESS was later constructed based on the design of the RBESS created in PSCAD/EMTDC. Furthermore, the controls used in the PSCAD/EMTDC RBESS model was used directly in the embedded boards used to control the hardware implementation of the RBESS.

A block diagram of the RBESS PSCAD/EMTDC simulation model and hardware implementation structure is shown in Figure 4-1. The RBESS simulation model and hardware implementation contains three batteries in a battery pack. There are two battery packs in the battery bank. Two secondary stage converters from the charge converter are connected to each battery pack in the battery bank. In the charge converter the two secondary stage converters are connected to one primary stage converter; the primary stage converter is connected to a passive DC load for discharging and DC source for charging.

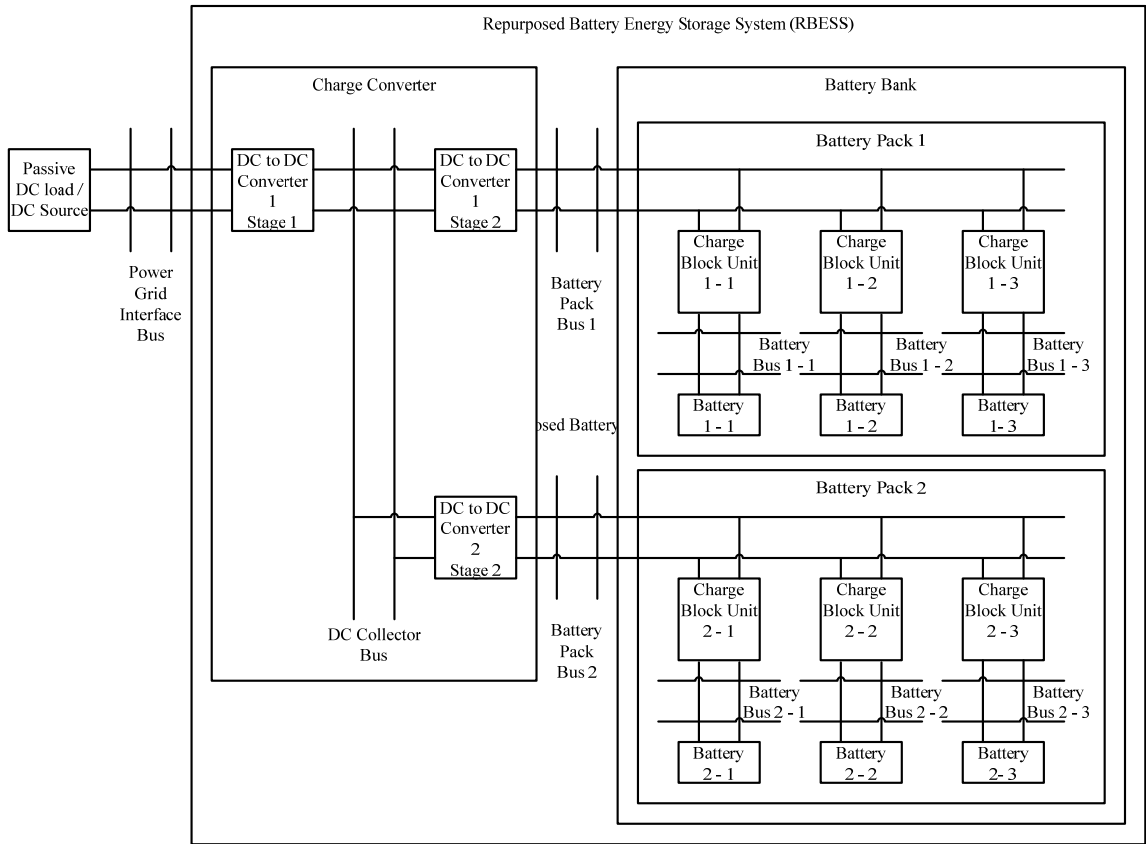


Figure 4-1: Block layout of the simulated and implemented RBESS.

4.1 RBESS Simulation and Hardware Implementation Overview

The RBESS was designed using simulation and then implemented in hardware. The hardware implementation as originally tested in prototype form is shown in Figure 4-2. The final implementation is shown in Figure 4-3. The circuit as simulated is shown in Figure 4-4. The RBESS consists of two battery packs in the battery bank. Thus, the second stage of charge converter consisted of two converters to accommodate the two

battery packs. The RBESS hardware and simulation models were rated for 100 V at 400 W out (discharge) and 150W in (charge) with a capacity of 49.8 Wh.

The controls for the RBESS were divided into two parts, one to control the charge converter and one to control the battery bank. The details of the individual control blocks were described in Chapter 3:. The charge converter controller sends messages to the battery bank indicating whether the stage two converters are enabled or energized, the mode of operation and the stacking value. While the battery bank controller sends to the charge converter information about the average SOC of each battery pack. The communication of these two control systems allows the RBESS to operate and manage the batteries in the battery bank.

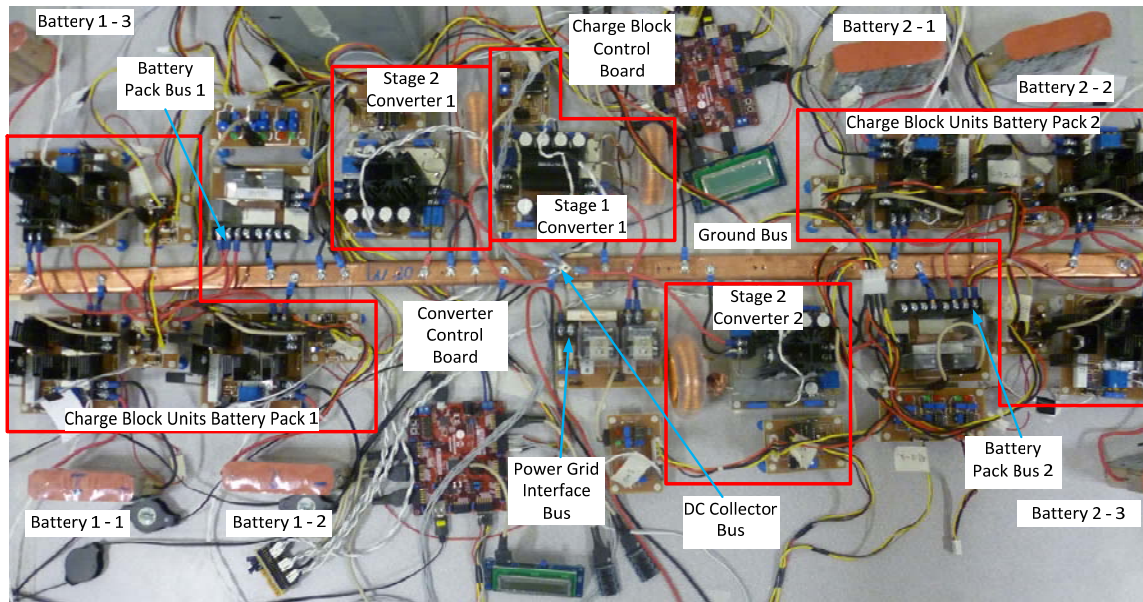


Figure 4-2: Hardware implementation of the RBESS prototype.

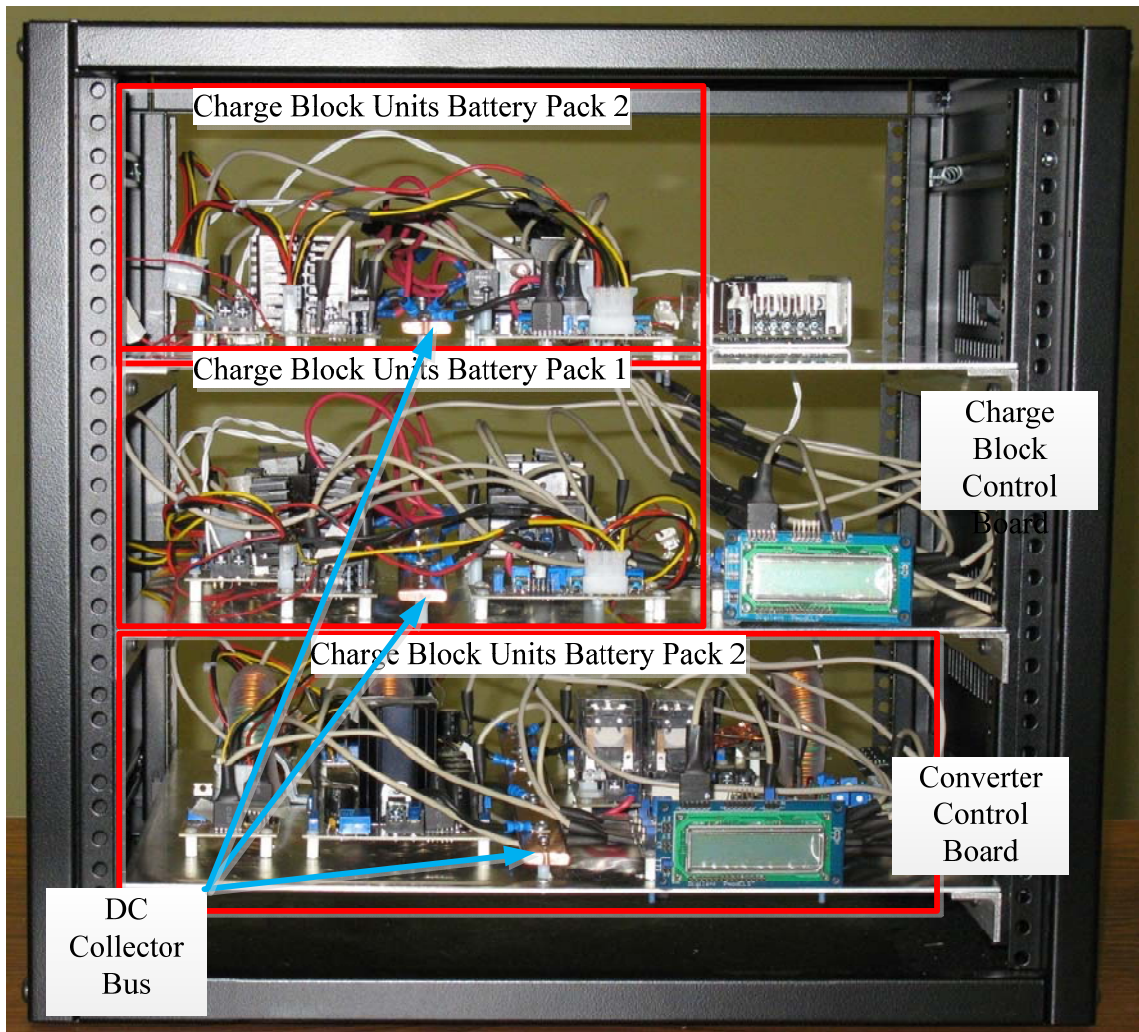


Figure 4-3: Hardware implementation of the RBESS completed.

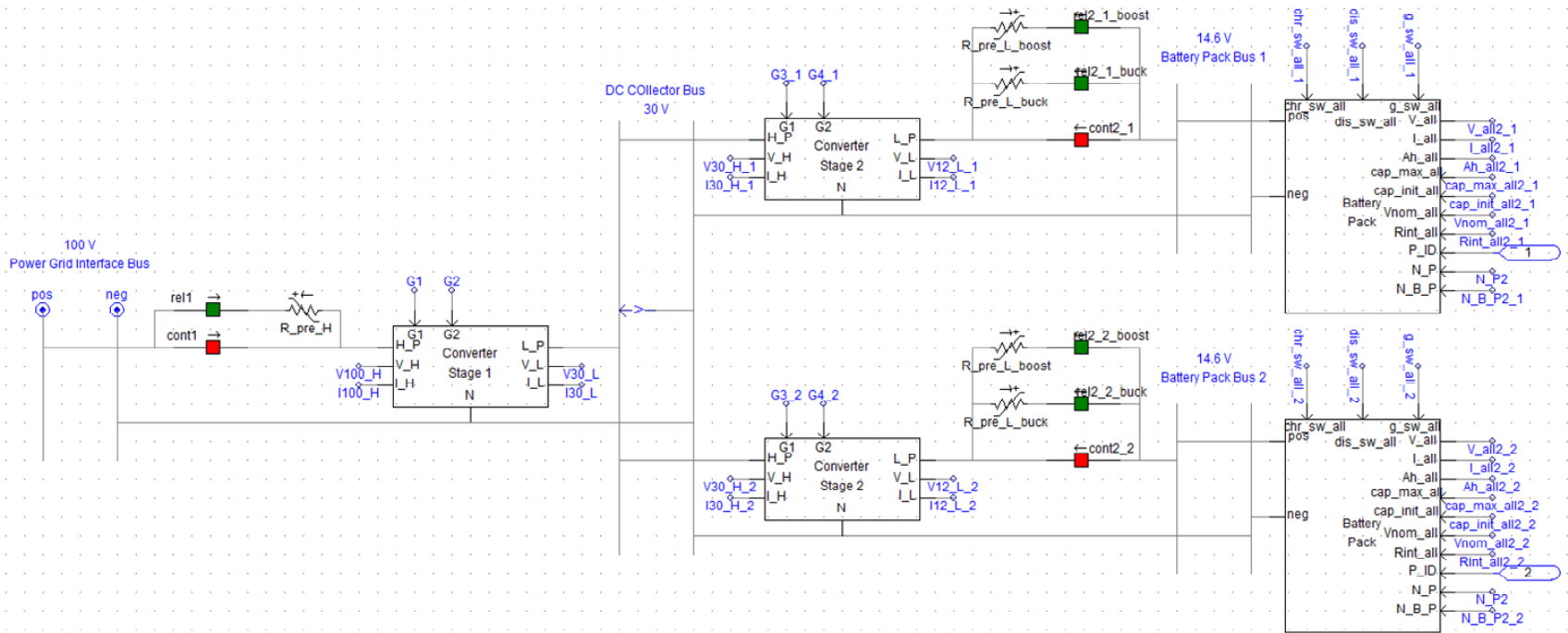


Figure 4-4: PSCAD/EMTDC model of the RBESS.

Each of the control systems for the hardware implementation of the RBESS, was implemented on Cerebot 32MX4 development board (Figure 4-5) [34] running Microchip PIC32 32-bit MIPS processor PIC32MX460F512L [35]. The Cerebot 32MX4 development board provided eight 12-pin and 1 6-pin peripheral ports (Pmod) for analog and digital I/O. In addition, the Pmod ports have the capacity to be connected to peripheral devices such as an LCD, switches, rotary dial and more. Furthermore, the Cerebot 32MX4 development board provided the 16 Analog to Digital (A/D) converts and USB ports. The Cerebot 32M7 development board also has the capability to produce PWM wave forms up to 5 I/O pins.



Figure 4-5: Cerebot 32MX4 development board.

4.1.1 RBESS Battery Bank Batteries

The batteries used in these models were constructed for this project by K2 Energy. Each of the batteries were made up of four K2 Energy cells in series. The cells that were used are the K2 Energy lithium cell model 26650P [36]. These cells are rated for 3.2 V nominal under load, with a capacity of 2.6 Ah (8.3 Wh). The cell's maximum charge voltage is 3.65 V and the maximum charge current is 2.6 A. The cell's maximum discharge voltage is 2.5 V and its maximum discharge current is 10 A. The batteries produced from these cells are rated at 12.8 V nominal under load, with a capacity of 2.6 Ah (8.3 Wh). The battery's maximum charge voltage is 14.6 V and their maximum charge current is 2.6 A. The battery's maximum discharge voltage is 10.0 V and its maximum discharge current is 10 A.

A battery test system was developed to profile and to estimate the SOC of the battery (*See Appendix B for details on the test system and profile tests*). The battery profiler system is used to determine the open circuit characteristic of the battery. The use of the battery profiler was based on the information obtained from the manufacture which indicated that the battery's open circuit could be obtained after 15 to 20 minutes of rest after charge or discharge. Once the open circuit voltage is obtained, the initial capacity of the battery can be estimated when the battery is started from a rest period greater than 20 minutes. Therefore, to determine the capacity of the battery during operation the charge extracted or absorbed (current) is measured and used to decrease or increase the capacity (SOC) of the battery. The capacity measurement is achieved by integration of the instantaneous current measurers being added to the current battery capacity.



Figure 4-6: K2 Energy Constructed battery pack.

Each battery is equipped with a Battery Management System (BMS) (Figure 4-7). The BMS was purchased from K2 Energy as part of the specially constructed batteries. The BMS consists of several battery management boards, each of which is connected in parallel to a battery cell. The battery management board consists of a network of series resistors and MOSFETs. The MOSFET on the battery management board is connected across the battery cell. Once the voltage across the cell exceeds 3.581 V the MOSFET turns on and drains current through the series resistor to burn off energy from the cell. The MOSFET turns off when the voltage across the cell drops below 3.411 V. This operation essentially balances all cells in a battery. In addition, there is an LED that indicates the state of the battery management board when it is active or inactive.

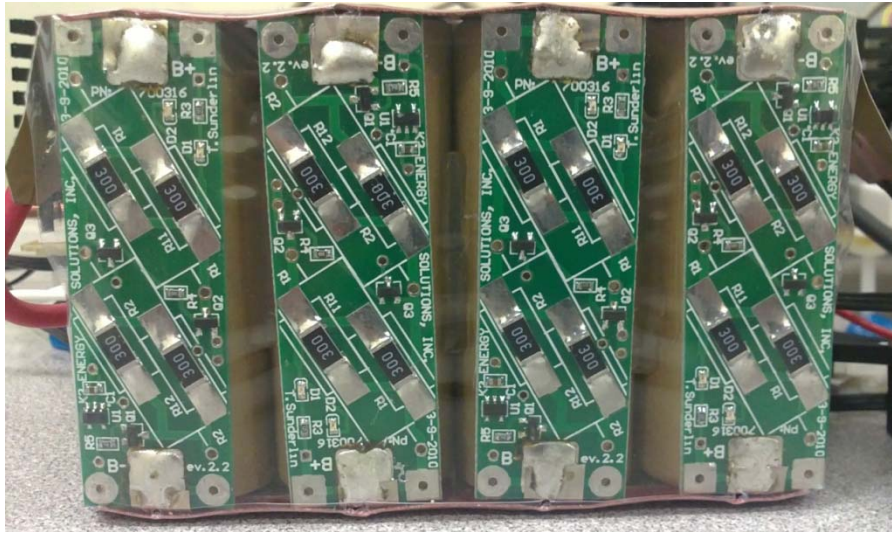


Figure 4-7: Battery management system.

Six of the specially constructed batteries purchased from K2 Energy were used to construct the battery bank for the RBESS. The six batteries are divided into two groups to form two battery packs for the battery bank. Each battery pack in the battery bank is rated for 12.8 V nominal under load, with a capacity of 7.8 Ah (24.9 Wh), and the entire battery bank capacity is rated for 15.6 Ah (49.8 Wh).

The maximum power output of a discharging battery is 100 W. This assessment is based on the battery's maximum discharge parameters. There are three batteries in a battery pack, and at most two of them will be used for the proper operation of the pulse controls. Therefore, the maximum power that the system can achieve at a nearly completely discharged state is 400 W. Furthermore, the maximum power input of a charging battery is 37.96 W. This is based on the maximum charge parameters of the battery. Similar to the battery's discharge rating, the maximum power charge rating is 151.84 W or approximately 150 W.

4.1.1.1 RBESS simulation's battery model

The battery simulation model chosen for this project is shown in Figure 4-8. The Thevenin battery model [37] and the Shepherd battery equations [38] were used in the construction of the PSCAD/EMTDC battery model for the RBESS. In Figure 4-8, $R_{Internal}$ is the battery's internal resistance, $C_{Battery}$ represents the battery capacitance which accounts for the mass transport effects in the battery and the $R_{Overvoltage}$ represents the resistance of the connected plates [39]. The internal voltage of the battery $V_{Battery}$ is given by equation (4.1) which is based on the capacity change of the battery. The K in equation (4.1) is a constant describing the polarization of the battery and the constant values A and B are curve fitting parameters of the battery's exponential region [38] of operation. $Capacity_{Nominal}$ is the nominal capacity of the battery.

The aging phenomenon of the battery is represented by increasing $R_{Internal}$ and reducing the battery's $Capacity_{Nominal}$.

Table 4.1: Parameters for the PSCAD/EMTDC simulation's battery model.

Parameter	Value
$R_{Internal}$	36 mΩ
$R_{Overvoltage}$	259.733 mΩ
$C_{Battery}$	1732.546 F
K	0.03
A	0.36
B	150
$Capacity_{Nominal}$	2.6 Ah

$$V_{Battery} = V_{Nominal} - K \left(\frac{Capacity_{Nominal}}{Capacity_{Nominal} - \int i(t) dt} \right) + A e^{-B \times \frac{\int i(t) dt}{Capacity_{Nominal}}} \quad (4.1)$$

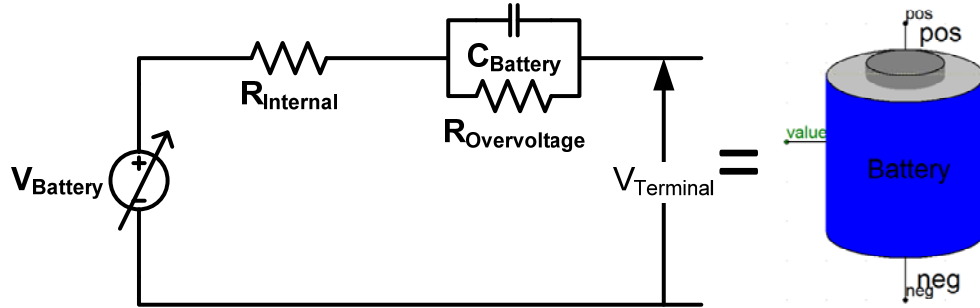


Figure 4-8: PSCAD/EMTDC developed Battery model.

4.1.2 RBESS Bus

The models of the RBESS are designed to mimic a full scale implementation of the RBESS. Thus, the RBESS models are designed to be one tenth of voltage rating of the full scale implementation of the RBESS. Therefore, in a full scale implementation of the RBESS the power grid interface bus would be rated at 1 kV, while the RBESS models' power grid interface bus would be rated at 100 V.

The rating of the DC collector bus of a full scale implementation of the RBESS would be based on the batteries' voltage. This should prevent any one stage from becoming over burdened from performing the operations required for step up or step down of the voltage or current. Hence, the step up or step down ratio of both stages is approximately the same. For example, if the battery was rated for nominally 300 V then the collector bus should be rated at 550 V to split the work done by the two stages of converters. Therefore, the RBESS models' DC collector bus is rated at 30 V. This splits the work done by the two stages of the RBESS converters.

The battery pack bus of a full scale implementation of the RBESS rate would be based on the batteries, max charge voltage. Thus, a 300 V battery with a MAX charge voltage of 350 V would be rated for 350 V. As such the RBESS 12 V batteries are rated for a charge voltage of up to 14.6 V and therefore the bus is rated at a voltage 14.6 V.

RBESS Simulation Model's and Hardware Implementation's Charge Converter

4.1.3 RBESS Simulation and Hardware Converters

The frequency of the converters in the two stages had to be selected before constructing the models of the RBESS. The frequency of operation of the converters is important as it helps to determine the size of components and ripple levels of the converters. Thus, the correct selection of the frequency is important when operating cascaded converters, since one stage depends on the operation of the previous stage. Therefore, the frequency of operation of cascaded converters should be decreased as more converters are added. The frequency of cascaded converters should decrease to ensure that the input to the next stage appears to be continuous from the prospective of the next stage. However, in this system bidirectional power flow was required and this indicated that there was the need to change the frequency. This choice would have been easy to accomplish in the simulation model, but might have proven to be problematic in the hardware implementation owing to delays in the physical implementation for the transition. Thus, a fixed frequency was chosen with stage one operating at 4000 Hz and stage two operating at 6000 Hz. The selection of the 4000 Hz for stage one and the 6000 Hz for stage two was based on the results of the PSCAD/EMTDC simulations which had shown the RBESS to operating in both modes as expected.

The power grid interface bus, the DC collector bus and the battery pack bus were chosen as 100 V, 30 V and 14.6 V respectively. This means that the stage 1 converter must step up or down the voltage by a factor of approximately three times or by one third to maintain the desired bus voltages. Furthermore, the stage two converters, in the best case, must step up or down the voltage by a factor of approximately two times or by one half to maintain the desired bus voltages. Similarly, in the worst case the converters must step up or down the voltage by a factor of approximately 3 times or by one third to maintain the desired bus voltages.

At nominal voltage and maximum current the system can output 512 W or approximately 500 W. Thus, the system was designed to meet the nominal maximum output power of 500 W. Equations (4.2), (4.3) and (4.4) were used to calculate the step up parameters for the two stages of converters in the RBESS charge converter. Equations (4.5), (4.6) and (4.7) were used to calculate the step down parameters for the two stages of converters in the RBESS charge converter.

The inductor scale factor was used to increase the inductance value. This scaling factor moved the converters' region of operation away from the boundary of the discontinuous current conduction mode. Furthermore, the ripple percentage of the current and voltage ripple was adjusted to below 2.5% in order to obtain suitable parameters for the construction of the hardware implementation. The results from these six equations and the selected values for the converters are illustrated in Table 4.2. The chosen DC collector bus capacitor was the larger of the two possible capacitors. This was done to ensure proper ripple reduction in the boost stage of the RBESS. The implementation of

both models can be seen in Figure 4-9 and Figure 4-10. The schematics of the hardware implementation are available in Appendix A.

$$DutyCycle_{Buck} = \frac{V_{Out}}{V_{In}} \quad (4.2)$$

$$C_{Out} = C_{Buck} = \frac{(1 - DutyCycle_{Buck})}{8 \times L_{Buck} \times V_{d_Buck} \times f_{Buck}^2} \quad (4.3)$$

$$L_{Buck} = \left(\frac{1 - DutyCycle_{Buck}}{I_{d_Buck} \times f_{Buck}} \times \frac{V_{Low}^2}{P} \right) \times L_{Scale_Factor} \quad (4.4)$$

$$DutyCycle_{Boost} = \frac{V_{Out} - V_{In}}{V_{Out}} \quad (4.5)$$

$$C_{Out} = C_{Boost} = \frac{DutyCycle_{Boost}}{\frac{V_{Low}^2}{P} \times V_{d_Boost} \times f_{Boost}} \quad (4.6)$$

$$L_{Boost} = \left(\frac{\frac{V_{Low}^2}{P} \times DutyCycle_{Boost} \times (1 - DutyCycle_{Buck})^2}{I_{d_Boost} \times f_{Boost}} \right) \times L_{Scale_Factor} \quad (4.7)$$

Table 4.2: Step down and up stage one and two converter parameters.

Mode	Primary			Secondary		
	Power grid interface bus Capacitor (μF)	Middle Inductor (mH)	DC collector bus Capacitor (μF)	Middle Inductor (mH)	Battery pack bus Capacitor (μF)	
Step Down	-	3.3	47.946	-	24.521	
Step Up	680	3.3	-	1200	-	
Selected	680	3.3	1200	3.3	24.521	

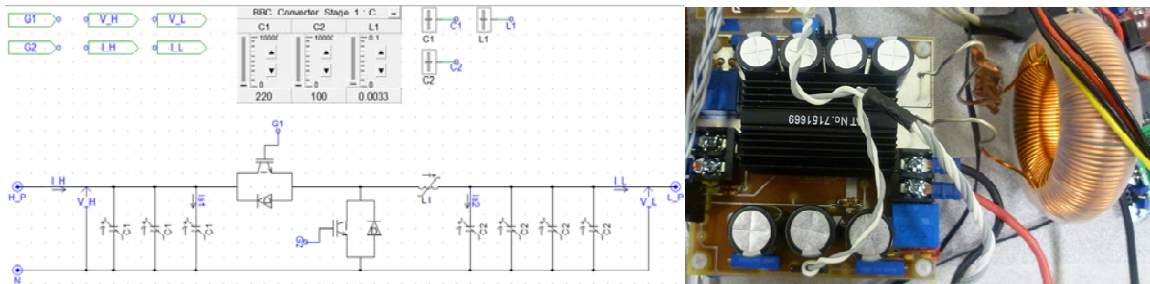


Figure 4-9: Simulation model and hardware implementation of the stage one converters.

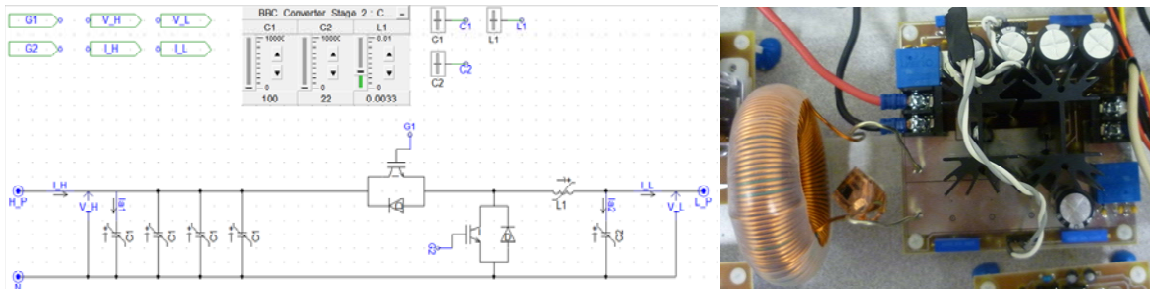


Figure 4-10: Simulation model and hardware implementation of the stage two converters.

4.1.4 RBESS Simulation and Hardware Pre-charge units

The pre-charge system on the power grid interface bus consists of a main relay contactor and a paralleled series relay resistor combination (Figure 4-11) (*See Appendix A for schematics of the circuit*). The main contactor and pre-charge relay operation, follows the process discussed in the previous chapter, when pre-charging the RBESS from the power grid interface. The main contactor and relay are rated to operate at 100 V and 5 A to accommodate the operation of the converters.

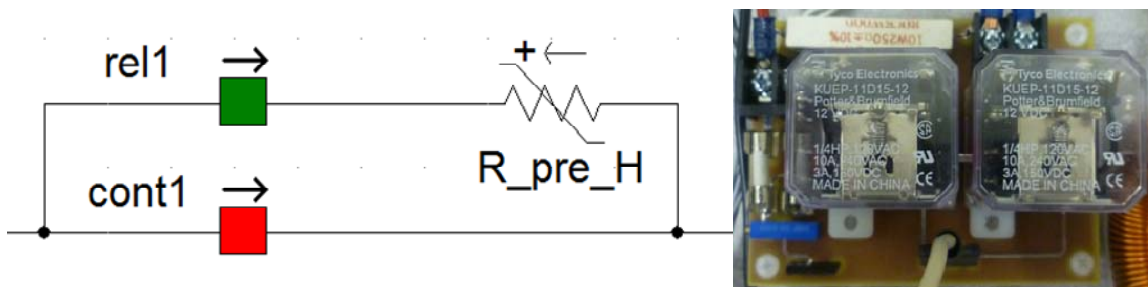


Figure 4-11: Simulation model and hardware implementation of the power grid interface pre-charge and contactor system.

The pre-charge system on the battery pack interface bus consists of a main relay contactor and two paralleled series relay resistor combination (Figure 4-12) (*See Appendix A for schematics of the circuit*). The main contactor and step down pre-charge relay operation, follows the process discussed in the previous chapter, when pre-charging the RBESS from the power grid interface. When pre-charging the RBESS from the

battery pack interface the main contactor and step up pre-charge relay operation, follows the process discussed in the previous chapter. The main contactor and relay are rated to operate at 20 V and 35 A to accommodate the operation of the converters and a range of different battery packs.

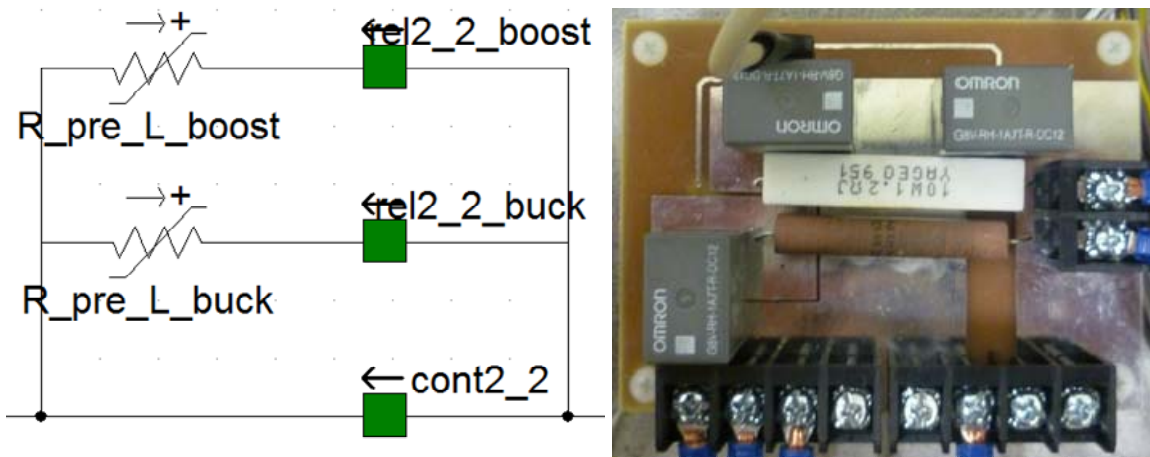


Figure 4-12: Simulation model and hardware implementation of the battery pack interface pre-charge and contactor system.

4.1.5 RBESS Simulation Model's and Hardware Implementation's Charge Converter controls

The controls for the RBESS charge converter described in the previous chapter were implemented in the PSCAD/EMTDC simulator. The PSCAD/EMTDC control blocks (Figure 4-13) were used to construct and optimize the primary controls of the RBESS charge converter. The primary controls were implemented in C function code

4.1.6 Charge Converter Hardware Implementation's control interface

The interface circuitry was required to allow for the Cerebot 32MX4 development board to control the converter hardware and pre-charge relay hardware. The interface circuitry was required because the development board's I/O did not have the required voltage or current to drive the circuitry of the charge converter system. The same interface circuitry was used to drive both stages of the charge converter system. The constructed hardware for the converter interface driver can be seen in Figure 4-16 and the schematic is in Appendix A.

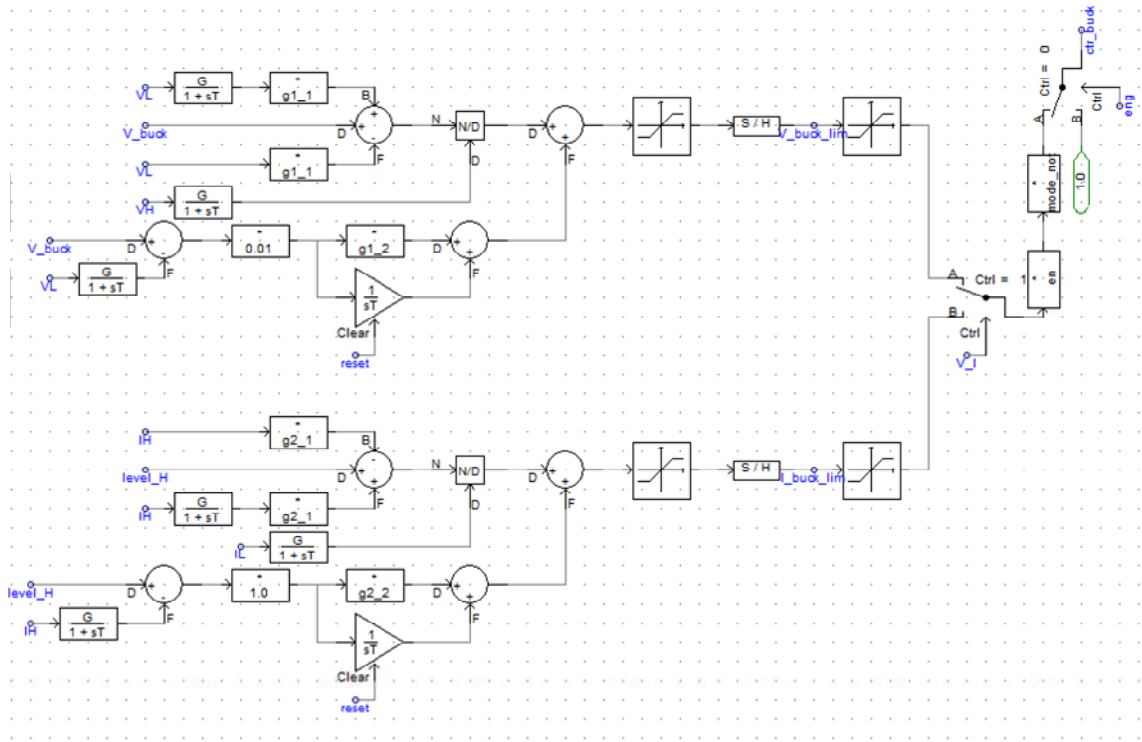


Figure 4-15: PSCAD/EMTDC primary control step up stage implementation.

The converter interface driver was developed around the Fairchild Semiconductor high and low side MOSFET driver IC FAN7392N [40]. This driver IC has a feature that is capable of independently controlling both the high and low side driver circuits and enabling or disabling the input. The FAN7392N featured an external “Bootstrap” [41] circuit that provided the voltage needed to drive the gate of the high side MOSFET.

The high side MOSFET is the MOSFET where none of the terminals are grounded but are floating above ground at sum potential. The gate and source voltage must be referenced to the source to properly turn on the MOSFET. The bootstrap circuit charges up a capacitor through a diode when the MOSFET’s source terminal is grounded and the driver uses the charge in the capacitor to drive the MOSFET when the MOSFET’s source terminal is no longer grounded. This circuitry requires that the MOSFET’s source terminal be grounded at some point in order to charge the capacitor to drive the gate.

However, during tests of the converter, it was found that there was insufficient time to charge the capacitor to drive the MOSFET. Therefore, the bootstrap circuit was replaced with an isolated DC to DC module which is able to maintain the voltage required to drive the high side gate. The isolated DC to DC module has the ability to reference the isolated side of the DC to DC module to the source of the MOSFET without shorting the circuit. Therefore, a continuous voltage that can be used to drive the MOSFET at the required rate was always present.

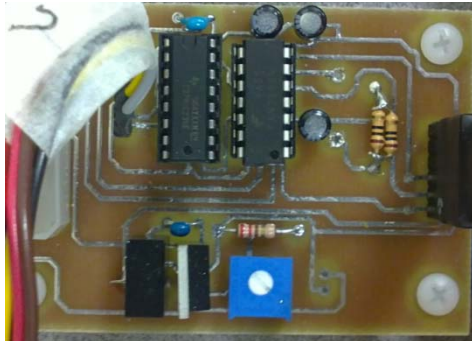


Figure 4-16: Converter MOSFET's interface driver board.

A PWM was used to drive each of the control interface boards. A de-multiplex circuit (See Appendix A) was developed, in such a manner, that based on the currently selected mode of control, the PWM would be directed to the correct input of the MOSFET driver IC.

The same interface circuitry was used to drive both the power grid relays and the battery pack relays for the pre-charge systems. The constructed hardware for the relay interface drivers is shown in Figure 4-17 and Figure 4-18 and the schematic are in Appendix A. The converter interface driver was developed around the STMicroelectronics relay driver IC TDE1767DP. Each relay in both pre-charge systems used its own relay driver IC to drive the relay. This driver IC is an op amp based IC that drives the output to the positive rail value of the IC when the input from the development board exceeds the threshold voltage of the circuit.

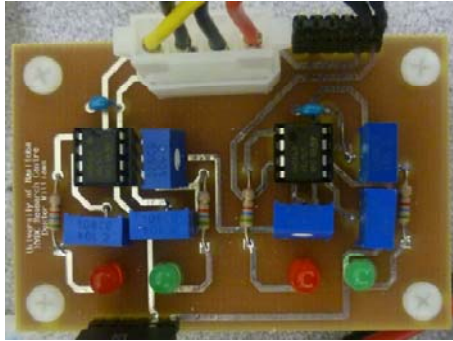


Figure 4-17: Power grid relay's interface driver board.

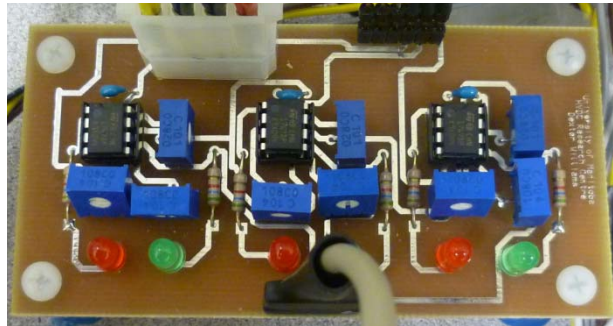


Figure 4-18: Battery pack relay's interface driver board.

4.2 RBESS Simulation Model and Hardware Implementation of the Battery Bank

4.2.1 RBESS Simulation and Hardware Charge Block Units

The charge block units were constructed for both simulated model and hardware Implementation are seen in Figure 4-19. The schematics of the hardware charge block unit can be found in Appendix A. As was mentioned in the previous chapter, the voltage measurement of the battery was measured off two pull down resistors that were tapped and fed into a differential amplifier. This measurement system was implemented to eliminate the floating ground reference for the battery, which originally caused unstable (unreliable) voltage readings.

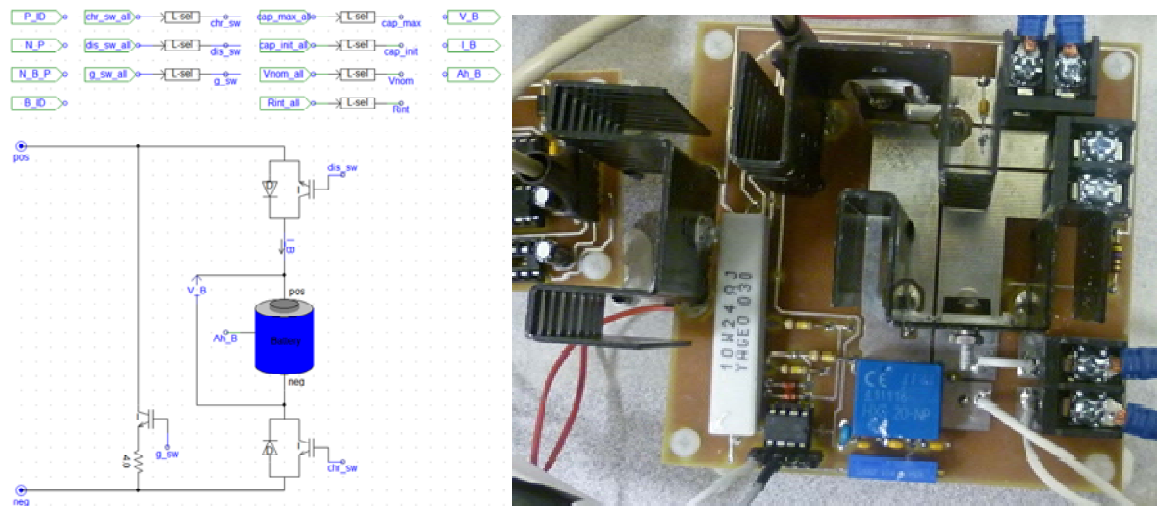


Figure 4-19: Simulation model and hardware implementation of a charge block unit.

4.2.2 RBESS Simulation Model's and Hardware Implementation's Charge Block Unit Controls

The controls for the RBESS charge block unit described in the previous chapter were implemented in the PSCAD/EMTDC simulator. Then, the controls were implemented in a C function which is based on the previously described control concept. The PSCAD/EMTDC to C interface was used to integrate the C functions PSCAD/EMTDC. This allowed the C code function to run in PSCAD/EMTDC as modules. Thus, the C functions were verified in PSCAD/EMTDC before the C functions were integrated into the hardware controls. The C functions were then integrated into an embedded program for the second embedded development board, which was used to control the RBESS charge block units in the battery bank hardware.

4.2.3 Hardware Implementation's Charge Block Unit Control Interface

An interface circuitry was used to drive the MOSFETs of the charge block unit board. The constructed hardware for the charge block unit MOSFET drivers can be seen in Figure 4-20 and the schematics are in Appendix A. The unit's interface driver was developed around the Texas Instruments MOSFET driver IC UCC37322P [42]. This MOSFET driver IC was configurable to operate on either high or low side MOSFET driver. Thus, three of these MOSFET drivers IC were required, with one configured as a high side driver to drive the discharge MOSFET of the charge block unit. The other two MOSFET drivers IC were configured as low side drivers to drive the charge and reflex MOSFETs. The high side MOSFET driver IC utilizes a charge pump and bootstrap circuit to produce the voltage required to turn on the MOSFET on the high side [42] (positive terminal) of the battery. However, unlike the pure bootstrap circuit initially used

for the charge converter's interface, this MOSFET driver IC does not require a low period to charge the gate capacitor, because the charge pump charges the capacitor in conjunction with the bootstrap to maintain the gate capacitor. Therefore, this circuit can keep the gate on the high side on indefinitely.

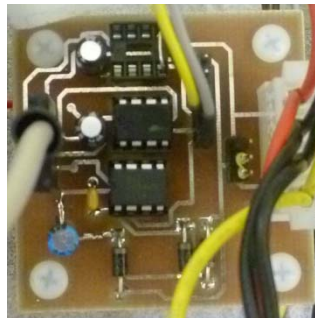


Figure 4-20: Charge block unit's interface driver board.

However, parallelism of the three driver circuits causes an unwanted current path to form. This, unwanted current path did not affect the normal operations of the circuit. During a fault, in which the battery fuses are blown, the capacitor of the bootstrap circuit would cause the source terminal of the MOSFET to switch from positive to negative. The switch would occur because the charge on the capacitor would have caused the MOSFET IC driver pin to exceed its limit and to blow both the MOSFET and MOSFET driver IC. A Metal Oxide Varistor (MOV) was placed across the MOSFET to provide a short circuit path for the MOSFET. This process is intended to prevent future damage of the circuit.

4.3 RBESS Hardware Implementation Communication

The RBESS hardware implementation required two communication interfaces. The first interface was intended to communicate information between the two development boards. The second of two communication interfaces of the RBESS hardware implementation was via USB to a computer for data logging and control.

4.3.1 RBESS Hardware Implementation's Control Board Communication

The RBESS hardware implementation uses the Cerebot 32MX4 development board's SPI communication port to transfer data between the boards [43]. SPI communication is a serial communication standard that uses master and slave architecture to simultaneously communicate data to and from the master and slave over two individual lines. The charge converter control board executes an SPI communication once every cycle, to exchange the latest information between the two boards. This communication initiates an interrupt service routine to service the SPI communication on the battery bank's development board.

The charge converter board sends message to the battery bank board to indicate which of the stage two converters are enabled, whether the associated battery pack is in the energize mode, whether all the batteries are participating in the charge exchange, the mode of operation of the converter and the requested stack multiplier needed to balance battery packs.

The battery bank board sends messages, about the average SOC of each battery packs to the charge converter control board which is responsible for maintaining the

battery packs. In addition, the SPI communication is used to synchronize the real time clock of the two development boards at the start-up of the boards.

4.3.2 RBESS Hardware Implementation's Computer Communication

The RBESS hardware implementation uses the Cerebot 32MX4 development board's USB port for data logging of the measured signals and the control of the RBESS hardware. The Microchip USB to Serial Demo kit's [44] framework was used to construct a method for sending data from the development board to the PC for data login and for messages from the computer to the development board for control of the RBESS. The USB to Serial framework allows the USB port to act as a virtual RS-232 serial port. The computer recognizes the communication from the development board as a standard RS-232 serial port and can use the RS-232 communication protocol to communicate with the board.

4.4 RBESS Simulation Model Human Machine Interface

The RBESS simulation model uses standard PSCAD/EMTDC control blocks for the Human Machine Interface (HMI) of the RBESS simulation model. The RBESS simulation model uses a series of PSCAD/EMTDC sliders, switches and pots to control the RBESS. These controls allow the user to enable or to disable a converter's battery pack's charge block units. Furthermore, the user can control the voltage, the current and the frequency set points of the converters. Most importantly, the user can control the power and mode of operation of the RBESS.

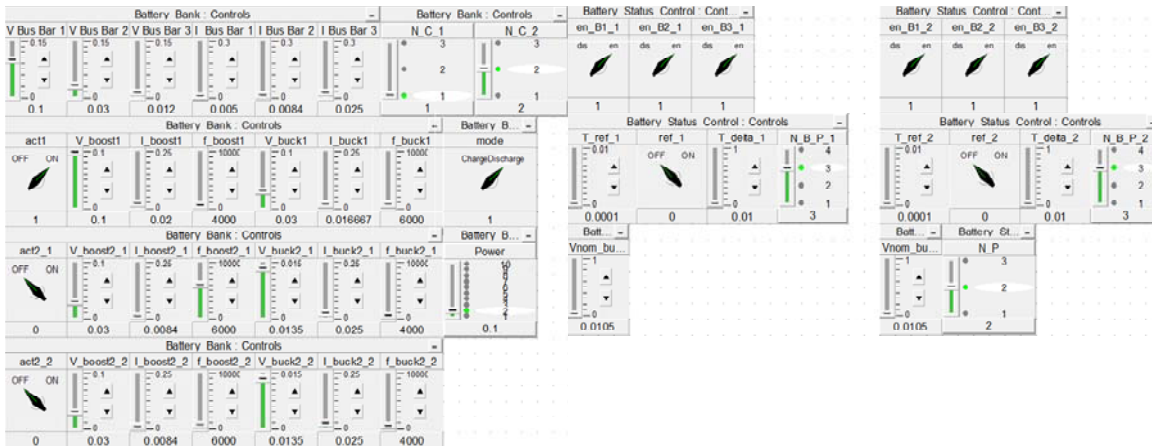


Figure 4-21: RBESS simulation model’s HMI.

4.5 RBESS Hardware Implementation Human Machine Interface

The RBESS hardware implementation has two HMIs which it uses to control the operation of the RBESS. The first HMI is the direct hardware interface and the second is a computer based Graphic User Interface (GUI).

4.5.1 RBESS Hardware Implementation’s Hardware Interface

The hardware HMI of the RBESS hardware implementation consists of one LCD, eight slide switches, two push button switches and one rotary dial (Figure 4-22). The charge controller development board utilizes all four hardware elements. The slides switches are used to enable the RBESS, to select the mode of operation and to enable the converters (see control operations in Table 4.3). The push button switches work in conjunction with the LCD to scroll through the different pages of the LCD (see Table 4.4 for description of pages). Furthermore, the push button switches can also be used to start or stop or reset the RBESS charge converter’s controls when they are on the associated

LCD page and the rotary dial can be used to increase or decrease the power, when the LCD display is on the 13th page of the LCD.

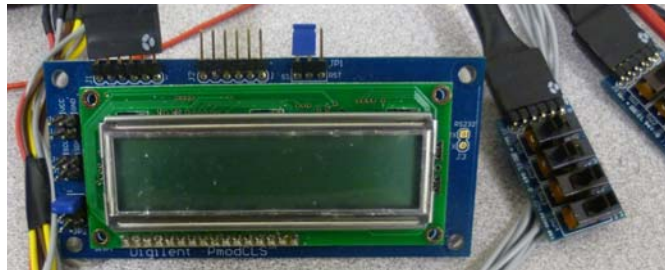


Figure 4-22: Hardware interface elements.

Table 4.3: RBESS charge converter switch control interface.

Slide switch	Operation (0/1)
0	Disable/Enable RBESS
1	Step down/Step up RBESS control mode
2	Disable/Enable Stage 1 converter 1
3	Disable/Enable Stage 2 converter 1
4	Disable/Enable Stage 2 converter 1
5-7	Not used

Table 4.4: RBESS charge converter display page indexes.

Page index	Page Display
0	Start RBESS
1	Stop RBESS
2	Reset RBESS controls
3	Average depth of discharge for both battery packs, Transmitted Control signals and Current Time
4	Stage 1 Converter 1 High and low side voltage and current
5	Stage 2 Converter 1 High and low side voltage and current
6	Stage 2 Converter 1 High and low side voltage and current
7	Stage 1 Converter 1 Step down mode: Low side voltage set point, duty cycle, actual voltage Step up mode: High side voltage set point, duty cycle, actual voltage
8	Stage 2 Converter 1 Step down mode: Low side voltage set point, duty cycle, actual voltage Step up mode: High side voltage set point, duty cycle, actual voltage
9	Stage 2 Converter 2 Step down mode: Low side voltage set point, duty cycle, actual voltage Step up mode: High side voltage set point, duty cycle, actual voltage
10	Stage 1 Converter 1 Step down mode: Low side current set point, duty cycle, actual current Step up mode: High side current set point, duty cycle, actual current
11	Stage 2 Converter 1 Step down mode: Low side current set point, duty cycle, actual current Step up mode: High side current set point, duty cycle, actual current
12	Stage 2 Converter 2 Step down mode: Low side current set point, duty cycle, actual current Step up mode: High side current set point, duty cycle, actual current
13	Current power set point, Power high side Stage 1 Converter 1, Stage 2 Converter 1 enabled and Stage 2 Converter 2 enabled: Power low side Stage 2 Converter 1, Power low side Stage 2 Converter 2 Stage 2 Converter 1 enabled and Stage 2 Converter 2 disabled: Power high side Stage 2 Converter 1, Power low side Stage 2 Converter 1 Stage 2 Converter 1 disabled and Stage 2 Converter 2 enabled: Power high side Stage 2 Converter 2, Power low side Stage 2 Converter 2

The charge controller development board utilizes LCD, slide switches and push button switches. The slides switches are use to enable each charge control unit, or to enable reflex charging on the battery pack (see control operations in Table 4.5). The push

button switches work in conjunction with the LCD to scroll through the different pages of the LCD (see Table 4.6 for description of the pages). Furthermore, the push button switches can also be used to reset the RBESS battery bank's controls when it is on the reset page of the LCD. The rotary dial is used to increase or decrease the power when the LCD display is on the 13th page of the LCD.

Table 4.5: RBESS battery bank switch control interface.

Slide switch	Operation (0/1)
0	Disable/Enable reflex charging for battery pack 1
1	Disable/Enable charge block unit 0 battery pack 1
2	Disable/Enable charge block unit 1 battery pack 1
3	Disable/Enable charge block unit 2 battery pack 1
4	Disable/Enable reflex charging for battery pack 2
5	Disable/Enable charge block unit 0 battery pack 2
6	Disable/Enable charge block unit 1 battery pack 2
7	Disable/Enable charge block unit 2 battery pack 2

Table 4.6: RBESS charge converter display page indexes.

Page index	Page Display
0	Start RBESS
1	Stop RBESS
2	Reset RBESS controls
3	Average depth of discharge for both battery packs, Transmitted Control signals and Current Time
4	Battery pack 1 battery 0 voltage and current Battery pack 1 battery 1 voltage and current
5	Battery pack 1 battery 2 voltage and current Battery pack 2 battery 0 voltage and current
6	Battery pack 2 battery 1 voltage and current Battery pack 2 battery 2 voltage and current
7	Battery pack 1 battery 0 DOD, Battery pack 1 battery 1 DOD, Battery pack 1 battery 2 DOD, Battery pack 1 average DOD,
8	Battery pack 2 battery 0 DOD, Battery pack 2 battery 1 DOD, Battery pack 2 battery 2 DOD, Battery pack 2 average DOD,

4.5.2 RBESS Hardware Implementation's Graphic User Interface (GUI)

The two GUIs were created for the RBESS, one for the charge converter board and the other for the battery bank board. Both GUIs use the USB to serial communication interface to send and receive data. Both of the GUIs' interfaces are the same except for the design under the system control and control tabs.

The file menu (Figure 4-23) present in both menus allows all control settings of each board to be saved and loaded back. The control settings are stored in a CSV file that contains all the controls current set points and activity. The status bare (Figure 4-24) of the GUI displays the current time of the board. In addition, the GUI status bar displays a progress bar that indicates which data is being transferred between the GUI and the development board.

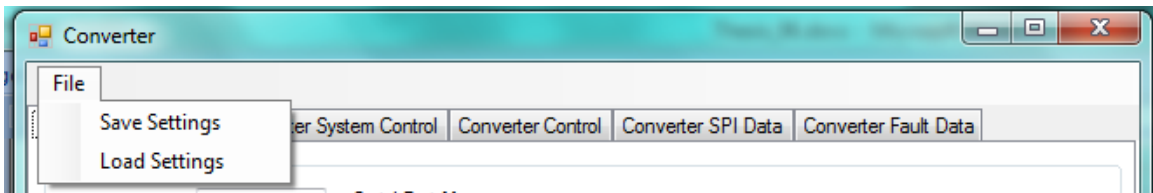


Figure 4-23: GUI file menu.



Figure 4-24: GUI Status bar.

The serial port tab in each of the GUIs is used to initiate serial communication with the board. When the serial port tab is activated it automatically detects any available serial port, and a user can use the interface to connect or to disconnect from a port. All connections and errors are logged in the text box on the serial port tab. The serial port tab also has the ability to start and to stop the logging of data being sent from the development board. The logged data is stored in a Comma Separated Value (CSV) file that can be used for analysis of the system's operation. (See Table 4.7 and Table 4.8 for data logging format). Furthermore, Table 4.8 shows the data logging format for both of battery packs that are being enabled. However, if only one of the battery packs is enabled then the other battery pack data will not be logged.

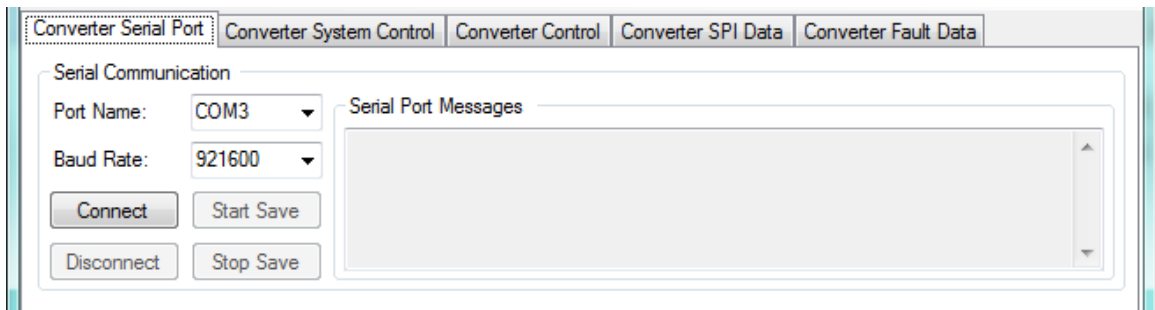


Figure 4-25: Serial port tab of GUI.

Table 4.7: RBESS charge converter data logging format.

Time		Stage 1 Converter 1 Voltage		Stage 2 Converter 1 Voltage		Stage 2 Converter 2 Voltage		Stage 1 Converter 1 Current	
Hours/ Minutes/ Seconds	Ticks	High side	Low side	High side	Low side	High side	Low side	High side	Low side
Stage 2 Converter 1 Current		Stage 2 Converter 2 Current		Average Depth of Discharge		Control signals			
High side	Low side	High side	Low side	Battery pack 1	Battery pack 2	Enable/Energize/Mode/Stack value			

The SPI data tab (Figure 4-26) is available in both GUIs. The SPI data tab displays the information communicated over the SPI communication channel. Specifically, it displays the average DOD for both battery packs and the control signal message sent.

The fault data tab (Figure 4-27) is present in both GUIs. In the fault data tab the fault ID is displayed in the ID box and the faults are decoded and displayed in the text box on the tab. All faults voltage and current on both sides of all converters, average depth of discharge, and start up and stopping are on the charge converter fault data tab. All faults voltage, current and DOD of each battery in the battery bank are on the battery bank fault data tab.

Table 4.8: RBESS battery bank data logging format.

Time		Battery pack 1 voltage			Battery pack 2 voltage		
Hours/ Minutes/ Seconds	Ticks	Battery 0	Battery 1	Battery 2	Battery 0	Battery 1	Battery 2
Battery pack 1 current			Battery pack 2 current				
Battery 0	Battery 1	Battery 2	Battery 0	Battery 1	Battery 2		
Battery pack 1 DOD			Battery pack 2 DOD			Average Depth of Discharge	
Battery 0	Battery 1	Battery 2	Battery 0	Battery 1	Battery 2	Battery pack 1	Battery pack 2
Charge block units switch control states and Control signals							
Battery pack 1 charge/ Battery pack 2 charge/ Battery pack 1 discharge/ Battery pack 2 discharge/ Enable/Energize/Mode/Stack value							

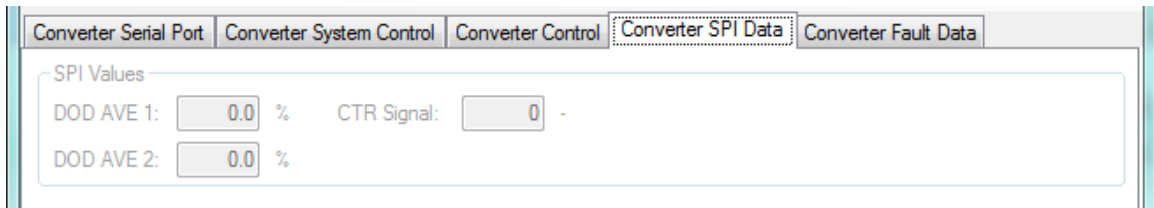


Figure 4-26: Serial data tab of GUI.



Figure 4-27: Fault data tab of GUI.

The charge converter system GUI system's control tab (Figure 4-28) replaces the control of the slide switches and push button switches. The charge converter system's control tab allows a user to enable or disable the RBESS, to start and to stop the system, and to enable or to disable the converters in either stage of the charge converter system.

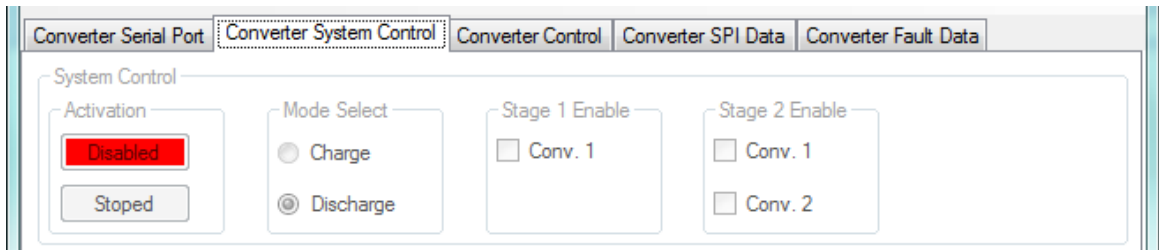


Figure 4-28: System control tab GUI of charge converter.

The battery bank system GUI system's control tab (Figure 4-29) replaces the control of the slide switches. The battery bank system's control tab allows a user to enable or to disable any battery's charge block unit in the battery bank and to enable or to disable the reflex operation of the battery pack.

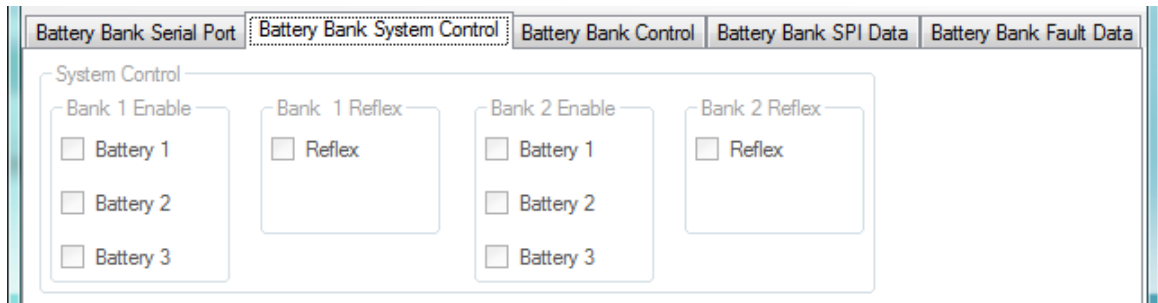


Figure 4-29: System control tab GUI of battery bank.

The charge converter system’s GUI system tab (Figure 4-30) provides online monitoring and control of the RBESS charge converter. The charge converter system’s GUI system tab displays all measured currents and voltages on the high and low sides of the converters. In addition, the charge converter system’s GUI system tab set points for the bus voltages can be changed as the power demand changes. Furthermore, the charge converter system GUI system’s tab primary converter controls can be tuned for each converter stage online.

The battery bank system GUI system’s tab (Figure 4-31) provides online monitoring and control of the RBESS battery bank. The battery bank system’s GUI system tab displays the voltage, the current, the SOC and the DOD for each battery in the battery bank. Finally, the battery bank system’s GUI tab shows the total activation period of the battery pack.

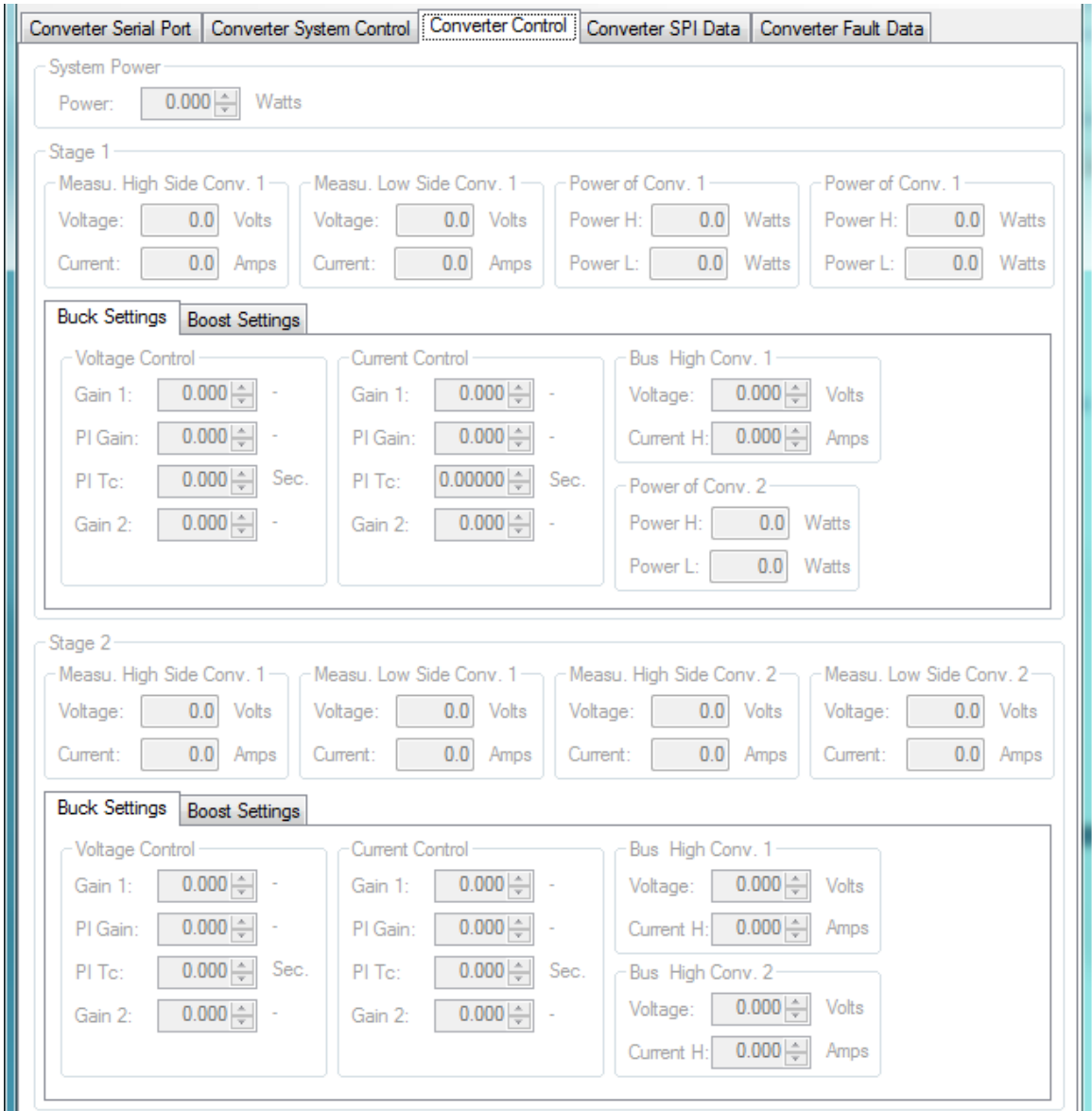


Figure 4-30: Control tab GUI of charge converter.

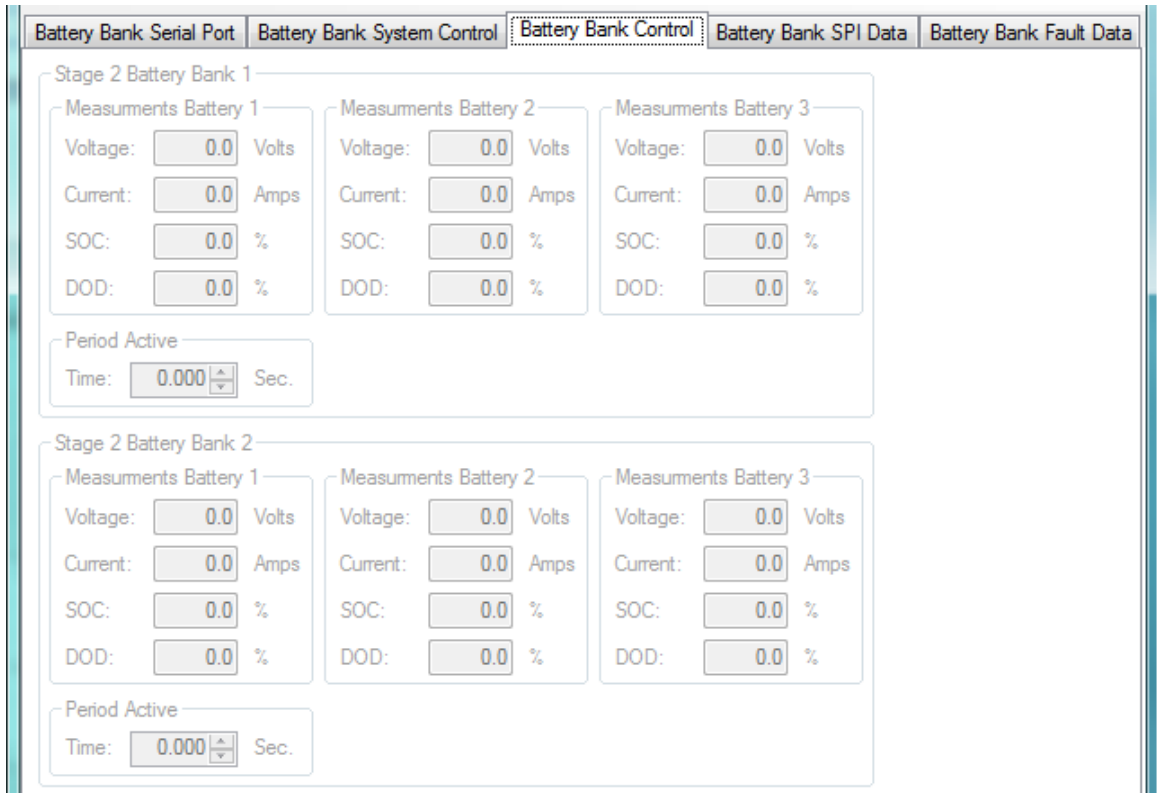


Figure 4-31: Control tab GUI of battery bank.

4.5.3 RBESS implementation issues

4.5.3.1 Switch Selection

The switching technology for the converters was selected for the development of the RBESS. MOSFETs and IGBTs are currently the most widely used switching technologies in switch mode converters. The switching technology helps to determine the system's losses and capabilities. Since the RBESS operates on a voltage range from 10 V to 100 V and at powers up to 500 W and on switching frequencies of up to 6000 Hz, the selection of the MOSFET switching technology is the better choice. MOSFETs operating

at the ratings listed above have less loss and therefore, have the better chance of improving converter efficiency [45] [46].

4.5.3.2 System grounding

One of the major implementation issues with the RBESS was the problem of improper measurement of the currents and the voltages. The voltage and the current on different component circuit boards were found to be wrong. The error was due to different ground potentials between the component boards and the control boards. A review of (Figure 4-32) the original RBESS layout indicated that if the control board was connected to any one of the three grounds bus bars the physical distance to all board would be different, and that difference in distances would cause different losses in the measurements and that would provide false values. In addition, it was found that even on single component board measurements from one side to the other side were also wrong. Therefore, it was determined that converters' switching was introducing noise into the measurements and that a bad ground plain on the component boards was allowing the propagation of noise in the circuit.

The grounding problem was solved by placing all the boards as close as possible to the same ground. Therefore, a single ground bus bar was constructed and the grounds on both sides of the component boards were tied to the bus bar. As such, the common coupling point for all of the grounds eliminated the distance problem, the noise problem and the measurement problem. This will allow the system to measure accurate values.

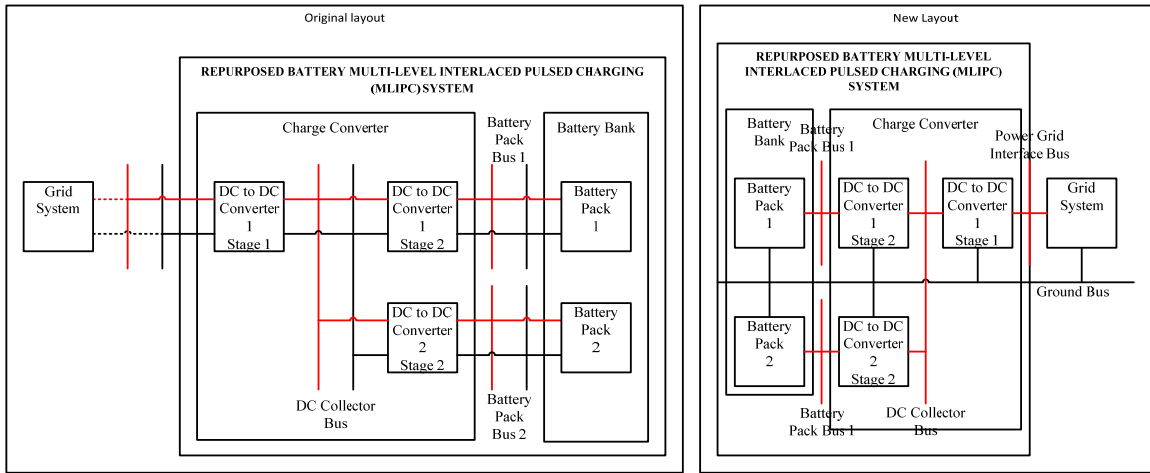


Figure 4-32: Hardware physical layout.

4.6 Chapter summary

This chapter looked at the construction of the RBESS models in the simulator PSCAD/EMTDC and in hardware. The RBESS simulation model was used in the design and development of the RBESS for construction of the hardware implementation of the system. A 400 W hardware implementation of the RBESS was constructed with both a hardware and software interface for control and data logging. The main problem resolved in the RBESS's hardware implementation's construction was the imbalanced ground causing false readings of the measurements. The problem was resolved by implementing a proper ground design to reduce losses and noise.

Chapter 5: RBESS Test and Performance

Analysis

The simulation model and hardware implementation of the RBESS were used to test the capabilities of the system. The following tests were performed to discover whether the system was able to operate correctly: the bus voltage maintainability test; the battery balancing test; and the battery pack balancing test. In addition, the system was tested to determine the effect of pulse charging in the RBESS. The hardware implementation of the RBESS is built for use on a 100 V bus (See Power Grid Interface Bus in Figure 4-1). However, since a 100 V supply was not available a 65 V supply was used. The 65 V supply is still within the operating region of the RBESS platform during the charge tests. Since a passive DC load was used, a discharge testing at the full 100 V was possible.

5.1 The Bus Voltage Regulation Test

The system must be capable of controlling the bus voltages at multiple power levels to confirm the RBESS' capability to maintain the bus. Thus, during the test the RBESS was made to step through a variety of power outputs. This was done to discover whether the RBESS would be capable of maintaining the bus voltages for the desired power demand. The structure of the RBESS is shown in Figure 4-1 of Chapter 4: RBESS Simulation Model and Hardware Implementation.

5.1.1 The RBESS Simulation Model's Discharge Bus Voltage Regulation Test

The discharge mode's bus voltage regulation test requires that the RBESS be stepped through a range of powers. This was required to determine whether the RBESS is capable of maintaining the bus voltages as the power demand is changed. In the test the RBESS was stepped up and down through powers ranging from 50 W to 300 W in increments of 50 W. Figure 5-1 (a and b) shows the bus voltages and battery pack currents wave forms respectively during the discharge bus voltage regulation tests in the RBESS simulation. The results showed that as the total current draw from the battery packs were increased in magnitude, during the incremental power changes. The buses referred to are buses labelled power grid interface bus, the DC collector bus, the battery bank bus one and the battery bank bus two in Figure 4-1. The voltages on the power grid interface bus, the DC collector bus and the battery bank buses were maintained around their respective voltages of 100 V, 30 V and 11.1 V. The results also showed the RBESS activated the second battery pack (At time = 1.1 seconds) to split the power demand among the battery packs (*See Chapter 3: The Design of the Repurposed Battery Energy Storage System for details on controller operation and design*). This reduced the stresses on the batteries of the first battery pack like the temperature of the battery and polarization of the battery.

Figure 5-2 (a and b) depicts a zoomed image of the voltage and current of the batteries in a battery pack during the discharge bus voltage regulation test. Note that the batteries are pulsed in the RBESS using the MLIPC system. The result showed that the pulsing of the batteries during the discharge bus voltage regulation tests maintained the current and voltage fairly constant at approximately -2.4 A and 11.08 V respectively (*See*

Chapter 3: The Design of the Repurposed Battery Energy Storage System for details on MLIPC system). From the perspective of the converters the current and voltage were kept constant, therefore it was concluded that the pulsing of the batteries had no negative effect on the operation of the converters.

Altogether, the results shown in Figure 5-1 and Figure 5-2 confirm the RBESS' ability to maintain the bus voltages in the discharge bus voltage regulation test. In addition, the results of the discharge bus voltage regulation proved that test the RBESS was also capable of handling multiple power levels and battery pack operational configurations.

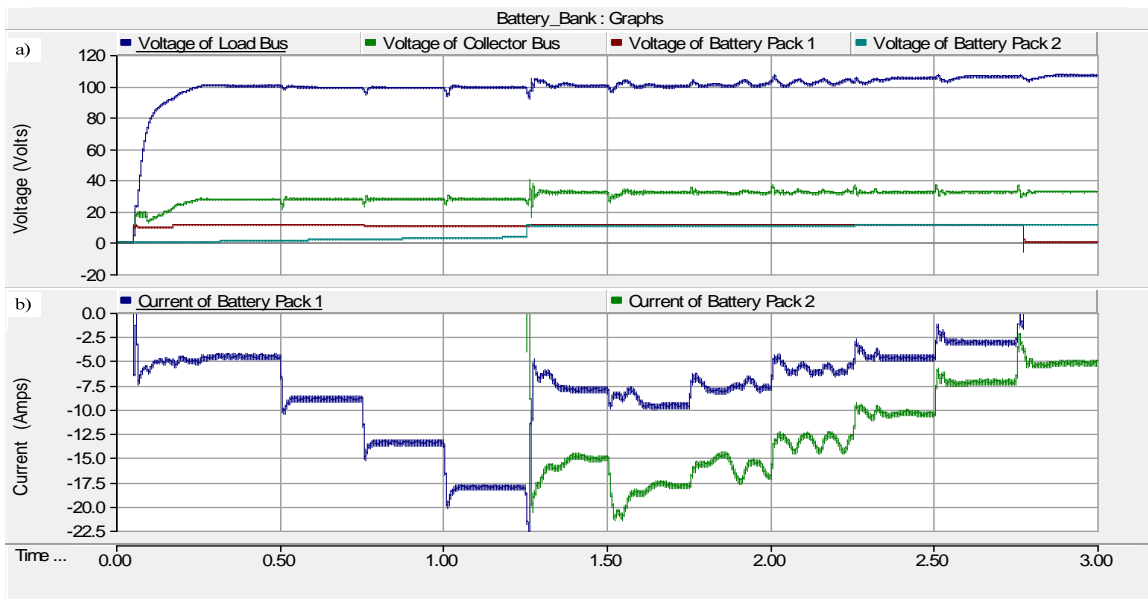


Figure 5-1: RBESS simulation model's discharge bus voltage regulation test's bus voltages and battery pack current.

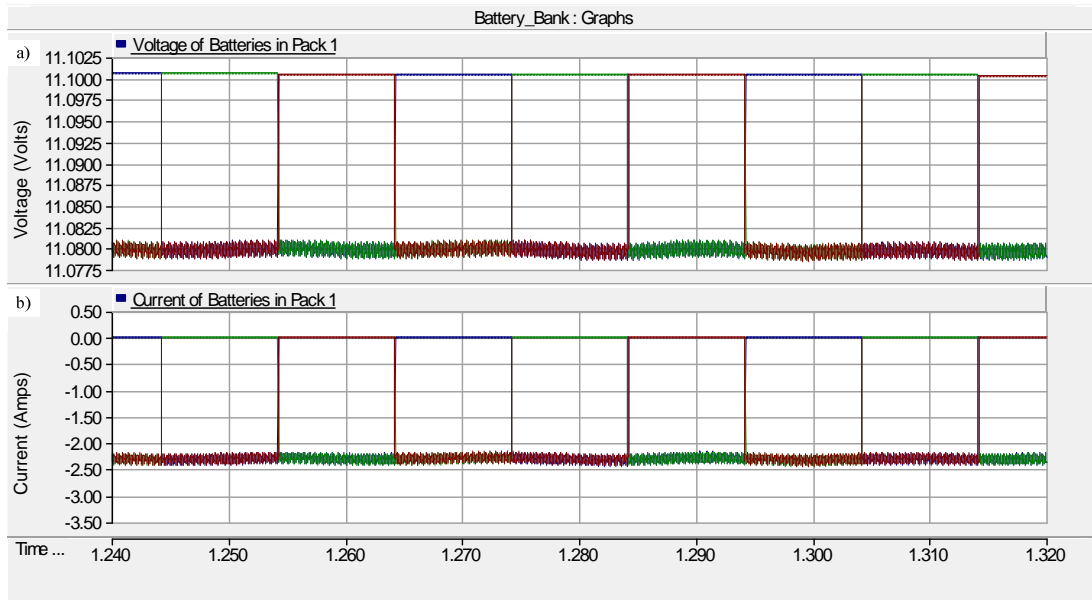


Figure 5-2: RBESS simulation model's discharge bus voltage regulation test's battery pack's batteries' voltages and currents.

5.1.2 The RBESS Simulation Model's Charge Bus Voltage Regulation Test

The charge mode's bus voltage regulation test required that the RBESS be stepped through a range of powers to determine whether the RBESS was capable of maintaining the bus voltages as the power demand was changed. In the test the RBESS was stepped up and down through powers ranging from 25 W to 150W in increments of 25 W. Figure 5-3 (a and b) shows the bus voltages and battery pack currents wave forms respectively during the charge bus voltage regulation tests in the RBESS simulation model. The results showed that as the total current draw from the battery packs were increased in magnitude, during the incremental power changes. The buses referred to are buses labelled power grid interface bus, the DC collector bus, the battery bank bus one and the battery bank bus two in Figure 4-1. The voltages on the power grid interface bus,

the DC collector bus and the battery bank buses are maintained around their respective voltages of 65 V, 30 V and 11.1 V. The results also showed that similar to the discharge process in 5.1.1, the RBESS activated the second battery pack (At time = 1.1 seconds) to split the power demand among the battery packs (*See Chapter 3: The Design of the Repurposed Battery Energy Storage System for details on controller operation and design*). This reduced the stresses on the batteries of the first battery pack like the temperature of the battery and polarization of the battery.

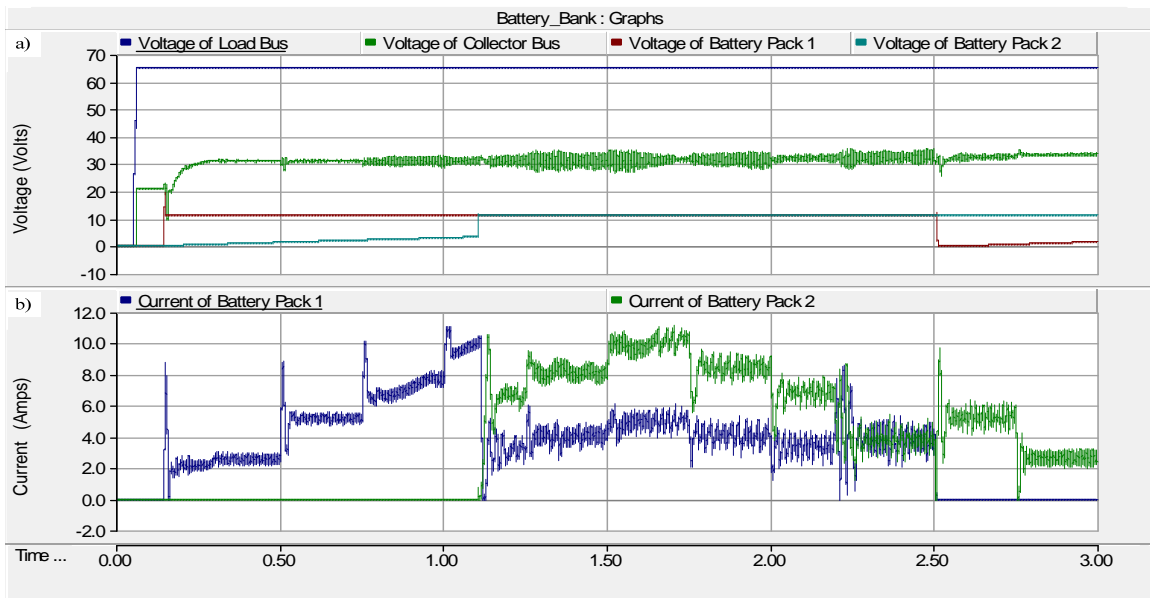


Figure 5-3: RBESS simulation model's charge bus voltage regulation test's bus voltages and battery pack current.

Figure 5-4 (a and b) depicts a zoomed image of the voltage and current of the batteries in a battery pack during the charge bus voltage regulation test. Note that the batteries are pulsed in the RBESS using the MLIPC system. The result showed that the pulsing of the batteries during the charge bus voltage regulation tests maintained the

current and voltage fairly constant at approximately 2.5 A and 11.125 V respectively (See Chapter 3: The Design of the Repurposed Battery Energy Storage System for details on MLIPC system). Similar to the discharge process in 5.1.1, from the perspective of the converters the current and voltage were constant, therefore it was concluded that the pulsing of the batteries had no negative effect on the operation of the converters.

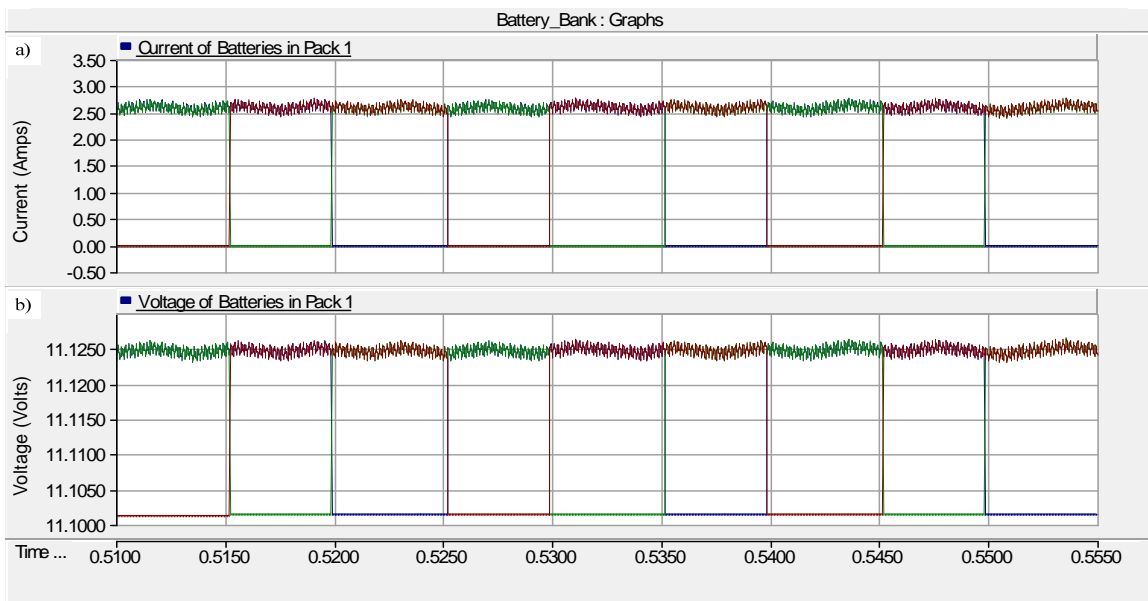


Figure 5-4: RBESS simulation model's charge bus voltage regulation test's battery pack's batteries' voltages and currents.

All together, the results shown in Figure 5-3 and Figure 5-4 confirmed the RBESS' ability to maintain the bus voltages in the charge bus voltage regulation test. In addition, the results of the discharge bus voltage regulation proved that test the RBESS was also capable of handling multiple power levels and battery pack operational configurations.

5.1.3 The RBESS Hardware Implementation's Discharge Bus Voltage

Regulation Test

The previous section described the simulation of the charge and discharge bus regulation process. This section and the following section discuss the performance of the physically implemented RBESS hardware.

The discharge mode's bus voltage regulation test required that the RBESS be stepped through a range of powers to determine whether the RBESS was capable of maintaining the bus voltages as the power demand was changed. In the test the RBESS was stepped up and down through powers ranging from 50 W to 300 W in increments of 25 W. Figure 5-5 (a and b) shows the bus voltages and battery pack currents wave forms respectively during the discharge bus voltage regulation tests on the RBESS hardware implementation. The results showed that as the total current draw from the battery packs were increased in magnitude, during the incremental power changes. The buses referred to are buses labelled power grid interface bus, the DC collector bus, the battery bank bus one and the battery bank bus two in Figure 4-1. The voltages on the power grid interface bus, the DC collector bus and the battery bank buses are maintained around their respective voltages of 100 V, 30 V and 11 V prior to the switching off of the system. The results also showed that similar to section 5.1.1 the RBESS activated the second battery pack at approximately time = 287.5 seconds to split the power demand among the battery packs (*See Chapter 3: The Design of the Repurposed Battery Energy Storage System for details on controller operation and design*). This reduced the stresses on the batteries of the first battery pack like the temperature of the battery and polarization of the battery.

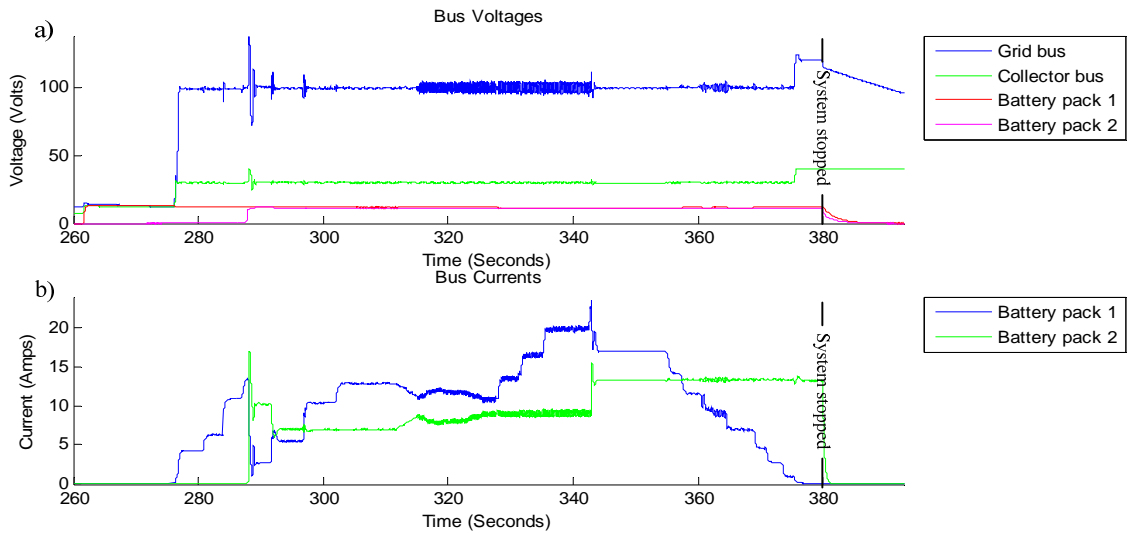


Figure 5-5: RBESS hardware implementation's discharge bus voltage regulation test's bus voltages and battery pack current.

Figure 5-6 (a and b) depicts a zoomed image of the current and voltage of the batteries in a battery pack during the discharge bus voltage regulation test. Note that the batteries are pulsed in the RBESS using the MLIPC system. The results show that pulsing of the batteries during the discharge bus voltage regulation tests maintained the current and voltage fairly constant at approximately 13.4 V and -2.0 A respectively (*See Chapter 3: The Design of the Repurposed Battery Energy Storage System for details on MLIPC system*). From the perspective of the converters the current and voltage were constant, therefore it was concluded that the pulsing of the batteries had no negative effect on the operation of the converters. The voltage on the battery pack bus in the hardware implementation (at 13.4 V) is greater than the simulation models voltage (at 11.1 V) because the hardware implementation's batteries had a greater capacity than the simulation model's batteries.

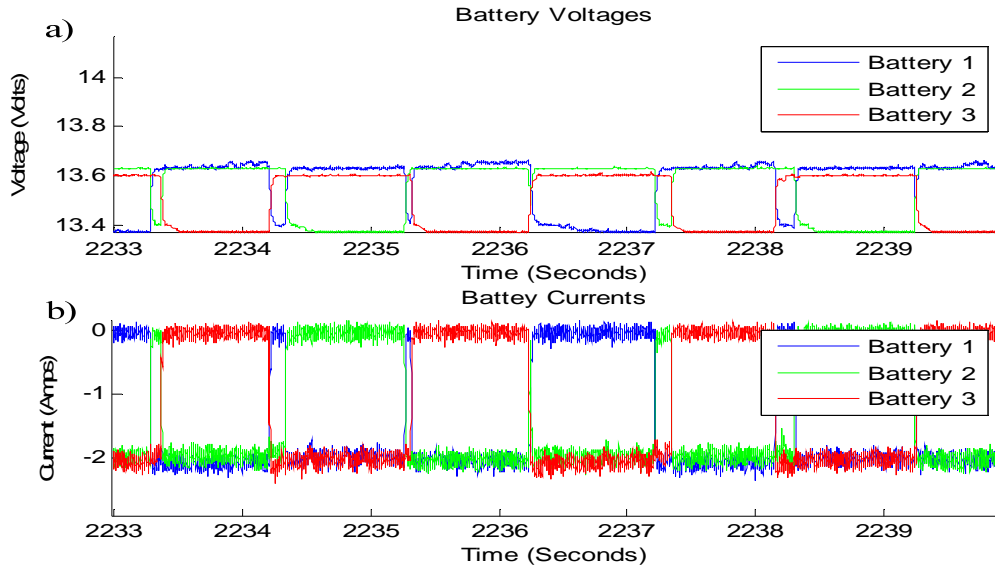


Figure 5-6: RBESS hardware implementation's discharge bus voltage regulation test's battery pack's batteries' voltages and currents.

All together, the results shown in Figure 5-5 and Figure 5-6 confirmed the RBESS' ability to maintain the bus voltages in the discharge bus voltage regulation test. In addition, the results of the discharge bus voltage regulation proved that test the RBESS was also capable of handling multiple power levels and battery pack operational configurations.

5.1.4 The RBESS Hardware Implementation's Charge Bus Voltage Regulation Test

The charge mode's bus voltage regulation test required that the RBESS be stepped through a range of powers to determine whether the RBESS was capable of maintaining the bus voltages as the power demand was changed. In the tests the RBESS was stepped up and down through powers ranging from 25 W to 150W in increments of

25 W. Figure 5-7 (a and b) shows the bus voltages and battery pack current wave forms respectively during the charge bus voltage regulation tests in the RBESS hardware implementation. The results showed that as the total current draw from the battery packs were increased in magnitude, during the incremental power changes. The buses referred to are buses labelled power grid interface bus, the DC collector bus, the battery bank bus one and the battery bank bus two in Figure 4-1. The voltages on the power grid interface bus, the DC collector bus and the battery bank buses are maintained around their respective voltages of 65 V, 30 V and 13V prior to the switching off of the system. The results also showed that similar to section 5.1.2 the RBESS activated the second battery pack at approximately time = 130 seconds to split the power demand among the battery packs (*See Chapter 3: The Design of the Repurposed Battery Energy Storage System for details on controller operation and design*). This reduced the stresses on the batteries of the first battery pack like the temperature of the battery and polarization of the battery.

Figure 5-8 (a and b) depicts a zoomed image of the current and voltage of the batteries in a battery pack during the charge bus voltage regulation test. Note that the batteries are pulsed in the RBESS using the MLIPC system. The result shows that pulsing of the batteries during the charge bus voltage regulation tests maintained the current and voltage fairly constant at approximately 13 V and 2.0 A respectively (*See Chapter 3: The Design of the Repurposed Battery Energy Storage System for details on MLIPC system*). From the perspective of the converters the current and voltage were constant, therefore it was concluded that the pulsing of the batteries had no negative effect on the operation of the converters. The voltage on the battery pack bus in the hardware implementation (at

13V) is greater than the simulation models voltage (at 11.1 V) because the hardware implementation's batteries had a greater capacity than the simulation model's batteries.

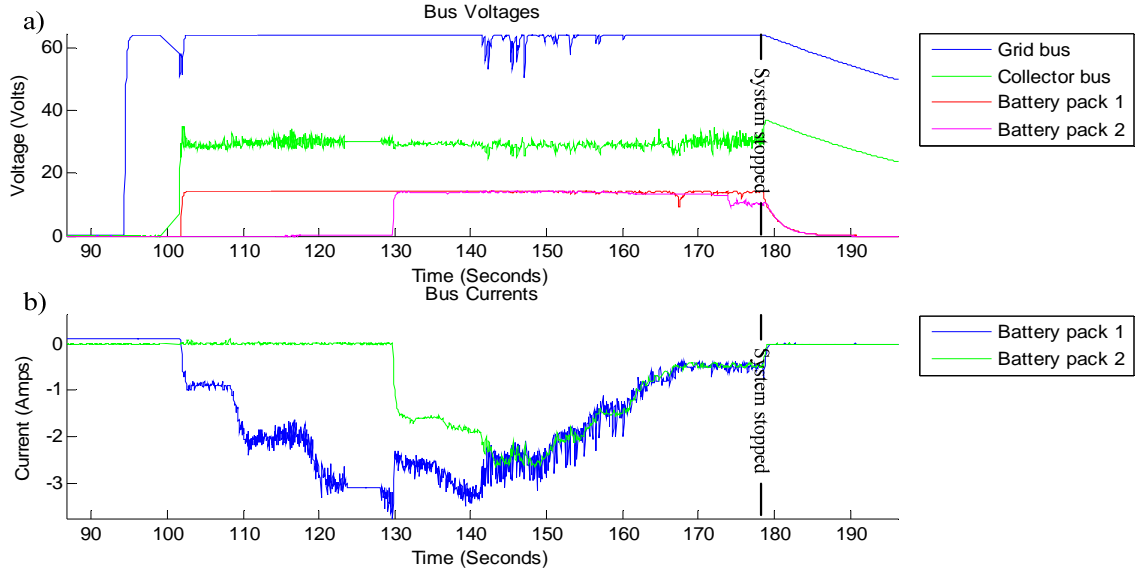


Figure 5-7: RBESS hardware implementation's charge bus voltage regulation test's bus voltages and battery pack current.

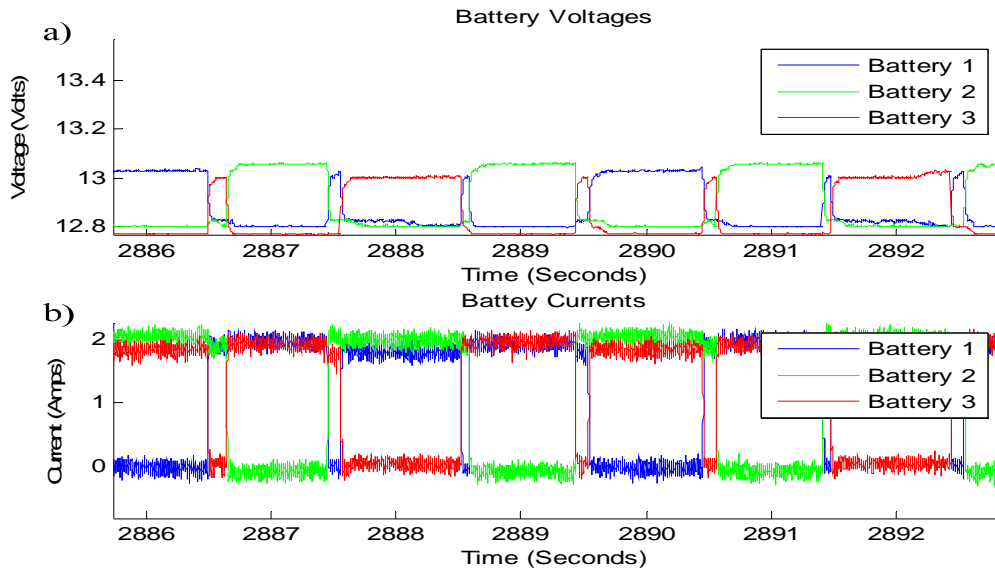


Figure 5-8: RBESS hardware implementation's charge bus voltage regulation test's battery pack's batteries' voltages and currents.

All together, the results shown in Figure 5-7 and Figure 5-8 confirmed the RBESS' ability to maintain the bus voltages in the charge bus voltage regulation test. In addition, the results of the discharge bus voltage regulation proved that test the RBESS was also capable of handling multiple power levels and battery pack operational configurations.

5.1.5 The RBESS Bus Voltage Regulation Test Overview

The results of the hardware implementation tests showed that the RBESS hardware implementation was capable of maintaining the bus voltages for a range of power levels. The tests also proved that the RBESS can operate at different power levels in both modes of operation for multiple configurations of the RBESS's battery packs. Thus, the RBESS simulation model was able to accurately predict the behaviour of the RBESS and hence proved to be a useful tool for the design and optimization of controls.

5.2 Battery Balance Test

Consider Figure 4-1, were the individual batteries are connected to form a battery pack. It is important to insure that all the batteries have the same Depth of Discharge (DOD). The charge and discharge systems must be able to manage the batteries' State of Charge (SOC) or it's opposite the DOD to maintain and regulate the capacity of the battery pack. The battery balance test of the RBESS was carried out to determine whether battery pulsing would prevent the balancing of the batteries. Battery balancing will occur naturally when batteries are paralleled on a bus.

5.2.1 The RBESS Simulation Model's Discharge Battery Balance Test

The purpose of the battery balancing algorithm in the RBESS controls is to balance the capacities (energy) in the batteries. Hence in this test, discharging of the batteries when they have different DOD was investigated. In the test the batteries' DODs differed from the lowest DOD by 5% and 10%. The battery pack was activated to exchange energy at the rate of 25 W. Then during the energy exchange, the power was increased from 25 W to 150 W. This was done to increase the rate of charge exchange and to expedite convergence of the batteries. Figure 5-9 shows the results of the RBESS simulation model's discharge battery balance test. The results have shown that under both power demands the battery pack's batteries' DOD converged approximately towards a common value. The results proved that the batteries in the RBESS can be balanced under the pulsing regime of the RBESS and under different power levels. (*Note: A 100% DOD means that the battery is full discharged*)

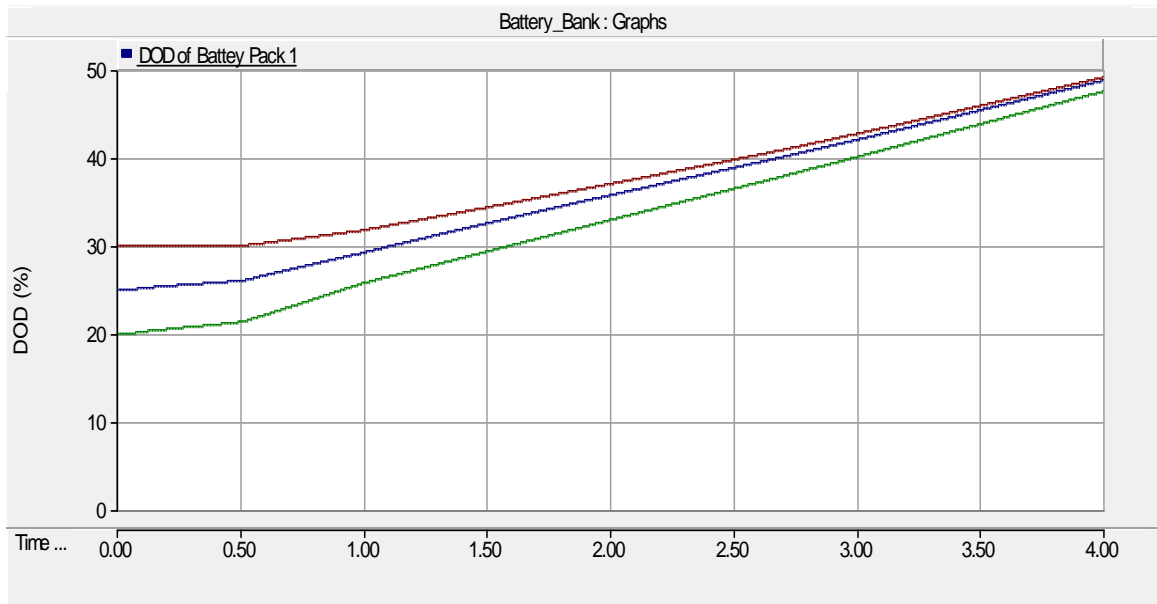


Figure 5-9: The RBESS simulation model's discharge battery balancing test.

5.2.2 The RBESS Simulation Model's Charge Battery Balance Test

Balancing the capacities of the batteries in the RBESS is conducted by the battery balancing algorithm. Hence in this test, charging of the batteries when they have different DOD was investigated. In the test case the batteries' DODs differed from the lowest DOD by 5% and 10%. The battery pack was activated to exchange energy at the rate of 25 W. Then during the energy exchange, the power was increased from 25 W to 150 W to increase the rate of charge exchange and to expedite convergence of the batteries. Figure 5-10 shows the results of the RBESS simulation model's charge battery balance test. The results have shown that under both power demands the battery pack's batteries' DOD converged approximately towards a common value. Thus the results proved that the batteries in the RBESS can be balanced under the pulsing regime of the RBESS and under different power levels.

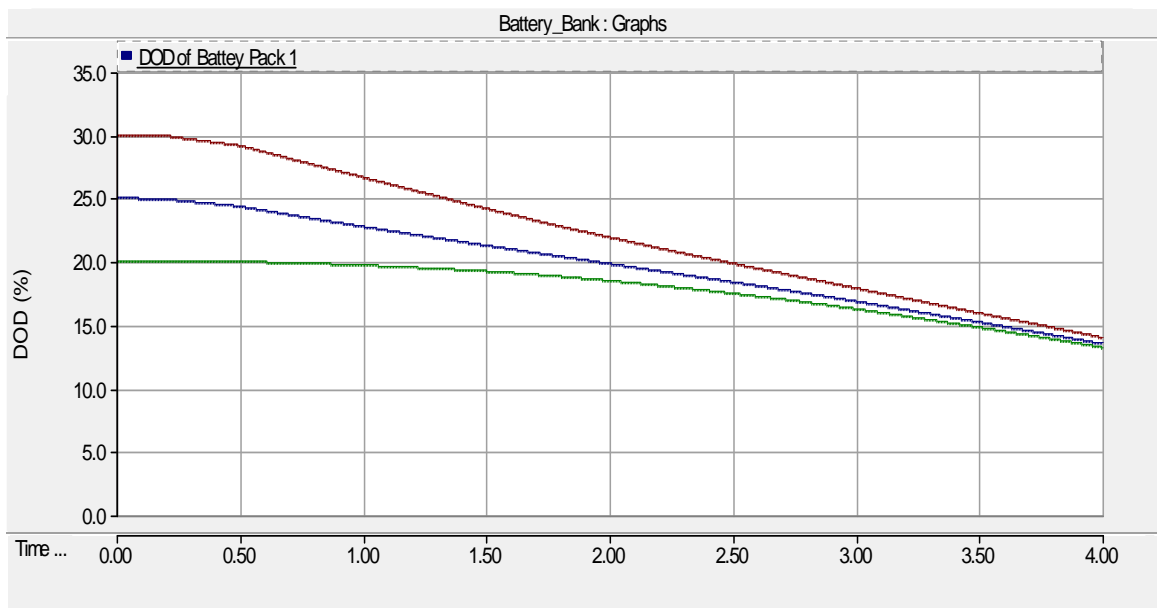


Figure 5-10: The RBESS simulation model's charge battery balancing test.

5.2.3 The RBESS Hardware Implementation's Discharge Battery Balance Test

In this section and the following section, the constructed RBESS was judged against the same tests as investigated by the RBESS simulation model in the two previous sections. Hence in this test, discharging of the batteries when they have different DOD was investigated on the RBESS hardware implementation. In the test the batteries' DODs differed from the lowest DOD by 5% and 10%. The battery pack was activated to exchange 25 W of power. Then, during the energy exchange, the power is increased from 25 W to 150 W to increase the rate of charge exchange and to expedite convergence of the batteries. Figure 5-11 shows the results of the RBESS hardware implementation's discharge battery balance test.

The similar to section 5.2.1 the results have shown that under both power demands the battery pack's batteries' DOD converged approximately towards a common value. Thus the results proved that the batteries in the RBESS can be balanced under the pulsing regime of the RBESS and under different power levels. The RBESS hardware implementation's battery discharge balance test was stopped once the batteries DOD had become equal while the RBESS simulation model was stopped at the end of the simulation time period. The DOD of the actual battery was measured by integrating the measured voltage times the measured current over time to determine what amount of the battery's capacity was used. This used capacity was then used to determine the capacity that still remained in the battery for calculation of equation (2.2).

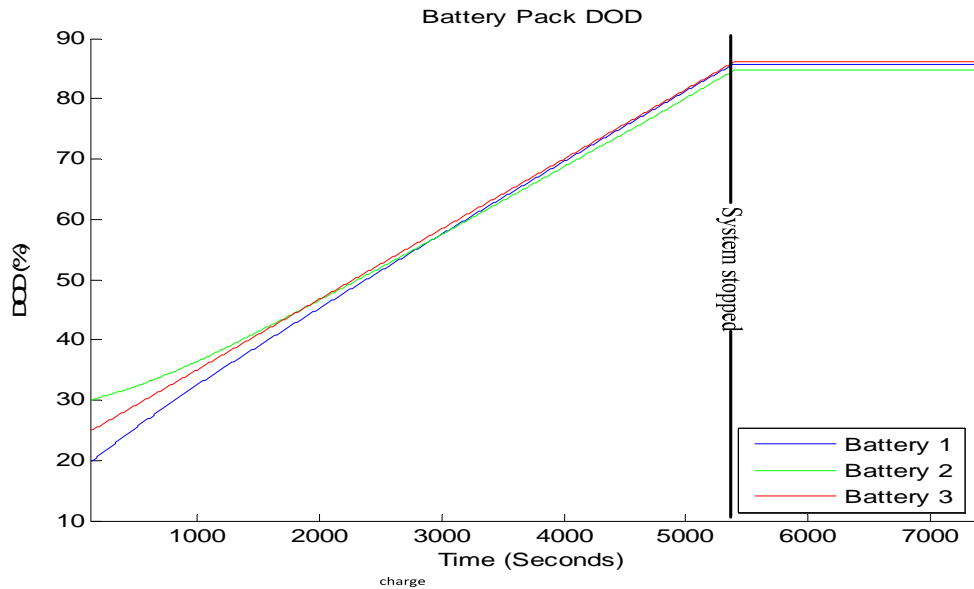


Figure 5-11: The RBESS hardware implementation’s discharge battery balancing test.

5.2.4 The RBESS Hardware Implementation’s Charge Battery Balance Test

Balancing the capacities of the batteries in the RBESS is conducted by the battery balancing algorithm. Hence in this test, charging of the batteries when they have different DOD was investigated. In the test the batteries’ DODs differed from the lowest DOD by 2.5% and 5%. The battery pack was activated to exchange 25 W of power. Then, during the energy exchange the power was increased from 25 W to 150 W to increase the rate of charge exchange and to expedite convergence of the batteries. Figure 5-12 shows the results of the RBESS simulation model’s charge battery balance test.

The similar to section 5.2.2 the results have shown that under both power demands the battery pack’s batteries’ DOD converged approximately towards a common

value. Thus the results proved that the batteries in the RBESS can be balanced under the pulsing regime of the RBESS and under different power levels. The RBESS hardware implementation's battery discharge balance test was stopped once the batteries DOD had become equal while the RBESS simulation model was stopped at the end of the simulation time period.

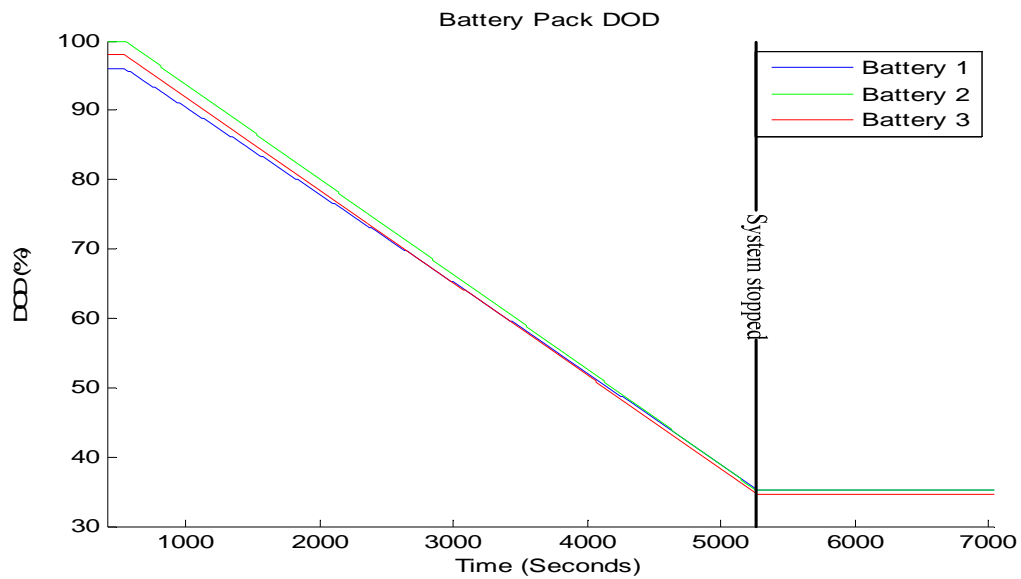


Figure 5-12: The RBESS hardware implementation's charge battery balancing test.

5.2.5 The RBESS Battery Balance Test Overview

The results of the hardware implementation tests proved that the RBESS hardware implementation was able to balance all the batteries in a given battery pack. Furthermore, the tests confirmed the assumption that the RBESS can actively balance the batteries in both the charging and discharging modes of operation. Thus, the RBESS

simulation model has shown that it can accurately predict the behaviour of the RBESS and thus making the simulation a valuable tool for the design and optimization of the RBESS.

5.3 Battery Pack Balance Test

The discussions in the previous sections 5.2 dealt with obtaining an equal DOD on all the batteries in a battery pack (See Figure 4-1). It is also important to ensure that each of the battery packs' DOD (Figure 4-1) are also balanced. Hence, the average DOD of the battery in any one pack should be equal to that of any other pack, to ensure the performance of the battery bank and the control of the battery bank's capacity.

5.3.1 The RBESS Simulation Model's Discharge Battery Pack Balance Test

Figure 5-13 is a demonstration of the RBESS simulation model's capacity to balance the battery packs of the battery bank during the discharge mode of operation. In the battery pack balancing test, both battery packs were initially started from the same DOD. Then, the first battery pack was brought online at 50 W and it was allowed to remain online until the battery pack's DOD had increased by 2%. At this point, the power was increased to 200 W. This power change caused the activation of the second battery pack. From Figure 5-13, it can be seen that the second battery pack was brought online at a higher current rating than the first battery pack. This was done to facilitate the balancing of the battery packs. Once the battery packs' DODs had become equal, the current draw would be equally distributed among the battery packs. The results of the test confirmed the RBESS simulation model's capacity to balance the battery packs during the discharge mode of operation.

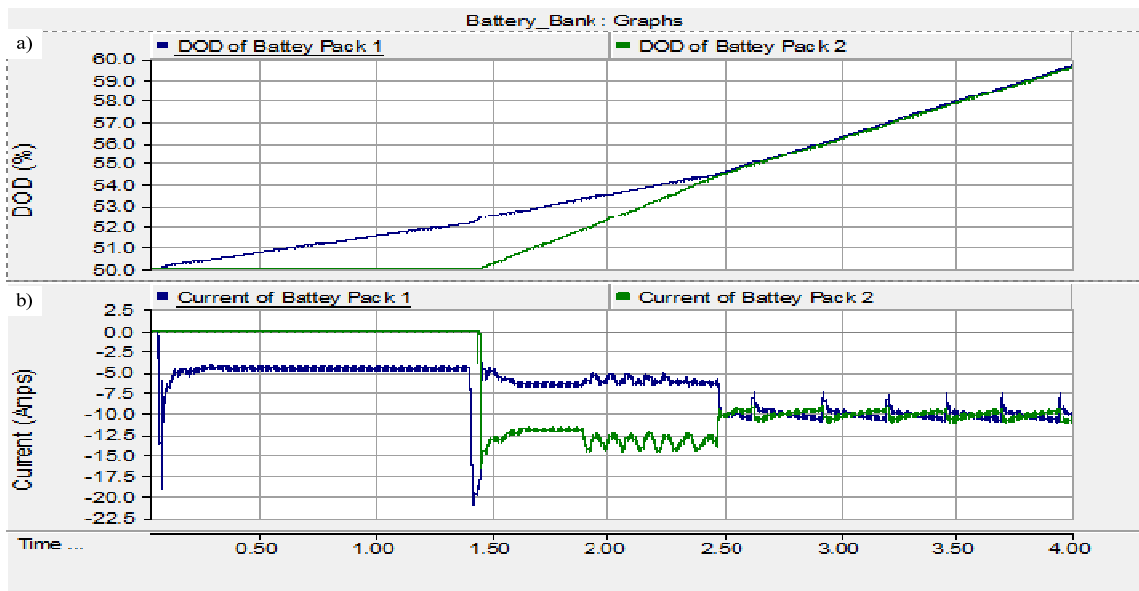


Figure 5-13: The RBESS simulation model's battery pack discharge balancing test.

5.3.2 The RBESS Simulation Model's Charge Battery Pack Balance Test

Figure 5-14 is an illustration of the RBESS simulation model's capacity to balance the battery packs of the battery bank during the charge mode of operation. Initially, the battery packs were held at the same DOD. The first battery pack was then brought online at 50 W and it was allowed to remain online until the battery pack's DOD had decreased by 2%. At his point, the power was increased to 150 W. This power change caused the activation of the second battery pack. From Figure 5-14, it can be seen that the second battery pack was brought online at a higher current rating than the first battery pack. This was done to facilitate the balancing of the battery packs. Once the battery packs' DODs had become equal, the current draw would be equally distributed

among the battery packs. Thus, the results of the test confirmed the RBESS simulation model’s capacity to balance the battery pack during the charge mode of operation.

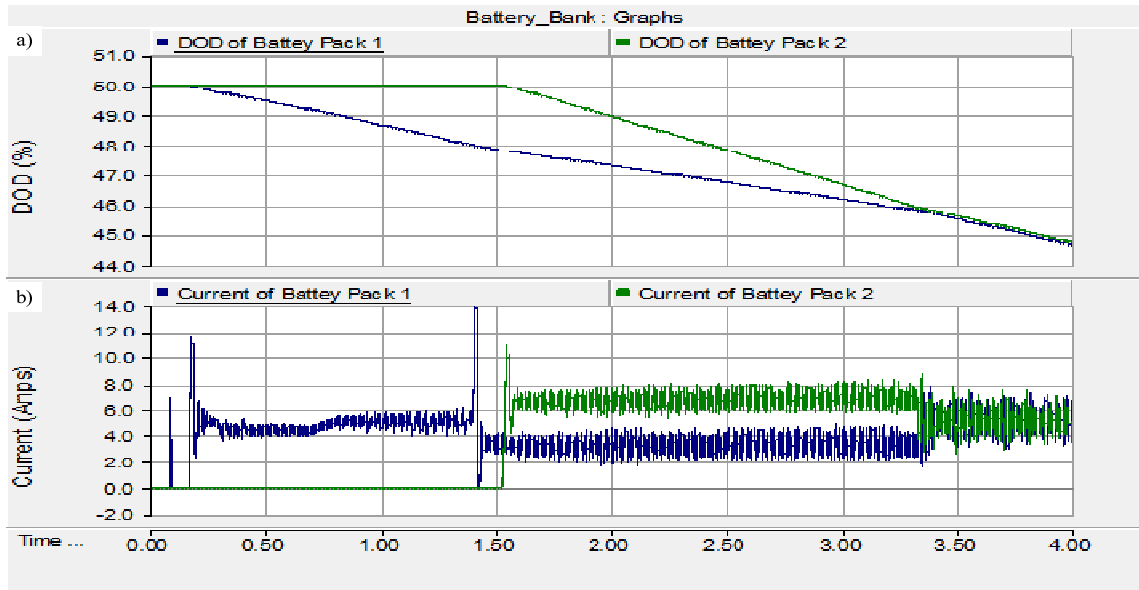


Figure 5-14: The RBESS simulation model’s battery pack charge balancing test.

5.3.3 The RBESS Hardware Implementation’s Discharge Battery Pack Balance Test

Figure 5-15 is a demonstration of the RBESS hardware implementation’s capacity to balance the battery packs of the battery bank during the discharge mode of operation. In the battery pack balancing test, both battery packs were initially started from the same DOD. Next, the first battery pack was brought online at 50 W and it was allowed to remain online until the battery pack’s DOD had increased by 2%. At this point, the power was increased to 100 W. This power change caused the activation of the second battery pack. From Figure 5-15, it can be seen that the second battery pack was brought online at a higher current rating than the first battery packs. This was done to

facilitate the balancing of the battery packs. Once the battery packs' DODs had become equal, the current draw would be equally distributed among the battery packs. Thus, the results of the test confirmed the RBESS hardware implementation's capacity to balance the battery pack during the discharge mode of operation.

The RBESS hardware implementation's battery pack discharge balance test was stopped once the batteries DOD had become equal while the RBESS simulation model was stopped at the end of the simulation time period. The RBESS hardware implementation's battery pack charge balance test was started from 0% DOD rather than 50% DOD as seen in RBESS simulation model owing to conveniences of the charge and discharge cycle.

The results obtained at this DOD will be similar at any DOD level owing to the nature of the controls (*See Chapter 3: The Design of the Repurposed Battery Energy Storage System for details on the control system*). The RBESS hardware implementation's battery pack charge balance test was stopped once the average battery packs' DOD had become equal for several seconds for comparison of results, while the RBESS simulation model was stopped at the end of the simulation time period.

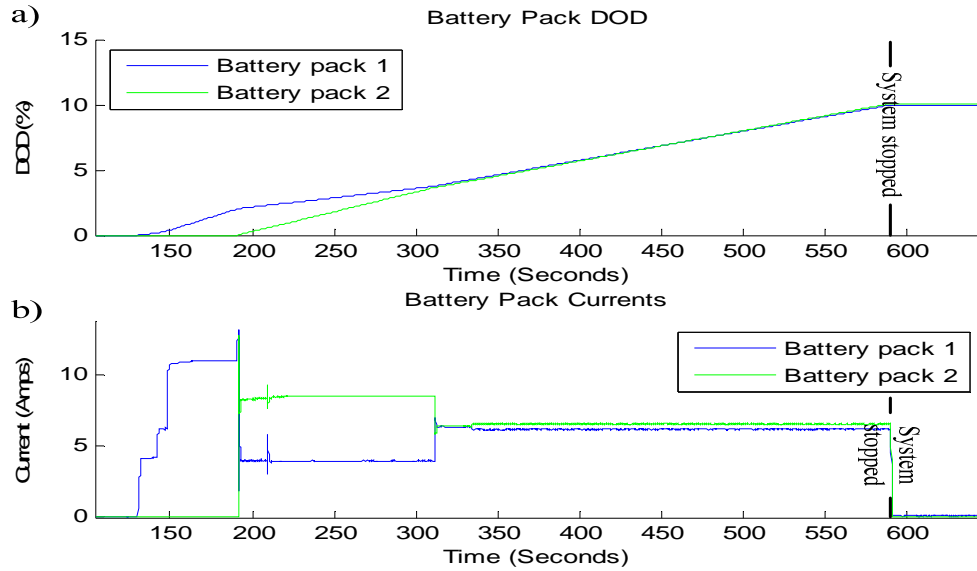


Figure 5-15: The RBESS hardware implementation’s battery pack discharge balancing test.

5.3.4 The RBESS Hardware Implementation’s Charge Battery Pack Balance Test

Figure 5-16 is an illustration of the RBESS hardware implementation’s capacity to balance the battery packs of the battery bank during the charge mode of operation. Initially, the battery packs were held at the same DOD. The first battery pack was then brought online at 50 W and it was allowed to remain online until the battery pack’s DOD had decreased by 2%. At this point, the power was increased to 150 W. This power change caused the activation of the second battery pack. From Figure 5-16 it can be seen that the second battery pack was brought online at a higher current rating than the first battery pack. This was done to facilitate balancing of the battery packs. Once the battery packs’ DODs had become equal, the current draw would be equally distributed among the battery packs. Thus, the results of the test confirmed the RBESS hardware implementation’s capacity to balance the battery pack during the charge mode of

operation. The RBESS hardware implementation's battery pack charge balance test was started from 10% DOD rather than 50% DOD as seen in RBESS simulation model owing to conveniences of the charge and discharge cycle.

The results obtained at this DOD will be similar at any DOD level owing to the nature of the controls (*See Chapter 3: The Design of the Repurposed Battery Energy Storage System for details on the control system*). The RBESS hardware implementation's battery pack charge balance test was stopped once the average battery packs' DOD had become equal for several seconds for comparison of results, while the RBESS simulation model was stopped at the end of the simulation time period.

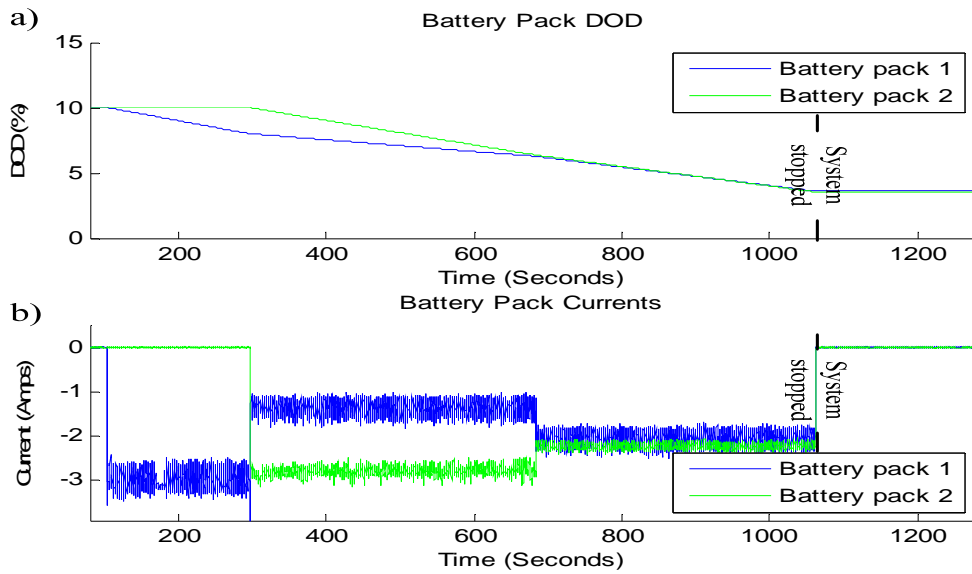


Figure 5-16: The RBESS hardware implementation's battery pack charge balancing test.

5.3.5 The RBESS Battery Pack Balance Test Overview

The results of the hardware implementation tests showed that the RBESS hardware implementation has capacity to balance all the battery packs in a given battery bank. The results also showed that the RBESS can actively balance the battery packs in both a charging and discharging modes of operation. Thus, the RBESS simulation model was able to accurately predict the behaviour of the RBESS and hence proved to be a useful tool for the design and optimization of controls.

5.4 Battery Pack Pulse Test

The final tests performed on the RBESS were the pulse width analysis tests of the battery pack's batteries. The tests were carried out to determine whether the pulse control of the charge block units would add any significant benefit to the operation of the RBESS. During the battery pulse tests, the power delivered and absorbed by the RBESS was kept constant at 50 W throughout both the charge and the discharge pulse modes. There was a minimum time lapsed, of three hours between each test, to allow the batteries' chemistry to relax and to prevent the results of one test from interfering with the next test. The tests in the following sections were conducted at 100 ms pulse periods, at 1000 ms pulses periods and during a non pulsed period (i.e. continue current from all batteries connected).

5.4.1 The RBESS Hardware Implementation's 100 ms Battery Pack Charging Pulse Test

During the 100 ms battery pack charge pulse tests, the batteries were charged from 20% SOC to 80% SOC (*Note: SOC is proportional to voltage of the battery. Thus, the batteries were stopped at set voltage that was proportional the selected SOC's*). At the

beginning of the tests, all batteries had approximately the same SOC. From Table 5.1 and Table 5.2 it can be seen that all the batteries' voltages were approximately the same verifying the fact that all the batteries' SOC were approximately equal to each other (The voltage of a battery is proportional to the SOC of a battery). The endpoint was chosen to prevent the battery's internal BMS from activating as the batteries were being charged. This BMS activation would cause invalidation of the results of the tests since the as energy put into the battery would be burned off by the battery's internal BMS in an effort to balance the cells of the battery (*See Section 4.1.1*). Therefore, energy meant to charge the battery would not be used to charge the battery. After the BMS is activated, it is not possible to tell how much energy is being fed into the batteries from charging or how much energy is being burned off by the BMS. Table 5.1 and Table 5.2 contain the results of the two 100 ms battery pack charge pulse tests performed.

Table 5.1 and Table 5.2 contain the open circuit voltage and temperature at the beginning of each of the tests, at the end of each of the tests and 30 minutes after each of the tests. A relaxation time of 30 minutes was allowed to give the battery's voltage sufficient time to recover and to provide a valid open circuit reading. The voltage measurements proved that the batteries were started and stopped at approximately the same SOC. Table 5.1 and Table 5.2 show the energy absorbed by each of the batteries in the battery pack and the total energy absorbed by the batteries in the battery pack. It was observed that each of the batteries, used in these tests exchanged about the same amount of energy. This observation confirmed the fact that the batteries exchanged the same amount of energy. A comparison of these tests with the other pulse tests will be done in Section 5.4.4.

Table 5.1: Battery pack 100 ms pulse charging test set 1.

Measurement	Voltage (Volts)			Temperature (°C)		
	<i>Battery 1</i>	<i>Battery 2</i>	<i>Battery 3</i>	<i>Battery 1</i>	<i>Battery 2</i>	<i>Battery 3</i>
Before	12.857	12.875	12.828	19.8	19.8	19.7
After	13.866	13.742	13.836	22.8	23.7	22.5
30 minutes After	13.348	13.343	13.316	21.5	22.4	22.4
Energy (Joules)	90878.1	90705.72	91775.08			
Total Energy (Joules)	273358.9					

Table 5.2: Battery pack 100 ms pulse charging test set 2.

Measurement	Voltage (Volts)			Temperature (°C)		
	<i>Battery 1</i>	<i>Battery 2</i>	<i>Battery 3</i>	<i>Battery 1</i>	<i>Battery 2</i>	<i>Battery 3</i>
Before	12.743	12.829	12.858	20.0	20.0	20.0
After	13.709	13.827	13.853	23.0	23.8	22.7
30 minutes After	13.37	13.343	13.343	21.7	22.1	21.5
Energy (Joules)	91450.09	91229.84	90558.68			
Total Energy (Joules)	273238.6					

5.4.2 The RBESS Hardware Implementation's 1000 ms Battery Pack Charging Pulse Test

During the 1000 ms battery pack charge pulse tests the batteries were charged from 20% SOC to 80% SOC. At the beginning of the tests, all batteries had approximately the same SOC. From Table 5.1 and Table 5.2 it can be seen that all the batteries' voltages were approximately the same verifying the fact that all the batteries' SOC were approximately equal to each other (The voltage of a battery is proportional to the SOC of a battery). The endpoint was chosen to prevent the battery's internal BMS from activating as the batteries were being charge. Such an activation would invalidate

the results of the tests. Table 5.3 and Table 5.4 contain the results of the two 1000 ms battery pack charge pulse tests performed.

Table 5.3 and Table 5.4 contain the open circuit voltage and temperature at the beginning of each of the tests, at the end of each of the tests and 30 minutes after each of the test. A relaxation time of 30 minutes was allowed to give the battery’s voltage sufficient time to recover and to provide a valid open circuit reading. The voltage measurements proved that the batteries were started and stopped at approximately the same SOC. Table 5.3 and Table 5.4 contain the energy absorbed by each of the batteries in the battery pack and the total energy absorbed by the batteries in the battery pack. It was observed that each of the batteries used in these tests exchanged about the same amount of energy. The observation confirmed the fact that the batteries exchanged the same amount of energy. A comparison of these tests with the other pulse tests will be done in Section 5.4.4.

Table 5.3: Battery pack 1000 ms pulse charging test set 1.

Measurement	Voltage (Volts)			Temperature (°C)		
	<i>Battery 1</i>	<i>Battery 2</i>	<i>Battery 3</i>	<i>Battery 1</i>	<i>Battery 2</i>	<i>Battery 3</i>
Before	12.688	12.855	12.83	20.6	20.6	20.6
After	13.626	13.873	13.858	22.8	23.6	23.1
30 minutes After	13.688	13.716	13.686	21.2	21.6	21.2
Energy (Joules)	99356.77	96661.88	92417.03			
Total Energy (Joules)	288435.7					

Table 5.4: Battery pack 1000 ms pulse charging test set 2.

Measurement	Voltage (Volts)			Temperature (°C)		
Parameter	<i>Battery 1</i>	<i>Battery 2</i>	<i>Battery 3</i>	<i>Battery 1</i>	<i>Battery 2</i>	<i>Battery 3</i>
Before	12.827	12.858	12.829	20.7	20.6	20.6
After	13.71	13.815	13.847	23.5	23.1	22.9
30 minutes After	13.344	13.342	13.313	21.9	21.4	21.3
Energy (Joules)	96381.72	95856.21	90552.48			
Total Energy (Joules)	282790.4					

5.4.3 The RBESS Hardware Implementation's Battery Pack Charging Non-Pulse Test

During the non pulse battery pack charge tests, the batteries were charged from 20% SOC to 80% SOC. At the beginning of the tests, all batteries had approximately the same SOC. From Table 5.1 and Table 5.2 it can be seen that all the batteries' voltages were approximately the same verifying the fact that all the batteries' SOC were approximately equal to each other (The voltage of a battery is proportional to the SOC of a battery). The endpoint was chosen to prevent the battery's internal BMS from activating while the batteries were being charged. Such an activation would invalidate the results of the tests. Table 5.5 and Table 5.6 contain the results of the two non pulse battery pack charge tests performed.

Table 5.5 and Table 5.6 contain the open circuit voltage and temperature at the beginning of each of the tests, at the end of each of the tests and 30 minutes after each of the tests. A relaxation time of 30 minutes was allowed to give the battery's voltage sufficient time to recover and to provide a valid open circuit reading. The voltage

measurements proved that the batteries were started and stopped at approximately the same SOC. Table 5.5 and Table 5.6 show the energy absorbed by each of the batteries in the battery pack and the total energy absorbed by the batteries in the battery pack. It was observed that each of the batteries used in the tests exchanged about the same amount of energy. This observation confirmed the fact that the batteries exchanged the same amount of energy. A comparison of these tests with the other pulse tests will be done in Section 5.4.4.

Table 5.5: Battery pack non pulse charging test set 1.

Measurement	Voltage (Volts)			Temperature (°C)		
Parameter	<i>Battery 1</i>	<i>Battery 2</i>	<i>Battery 3</i>	<i>Battery 1</i>	<i>Battery 2</i>	<i>Battery 3</i>
Before	12.715	12.742	12.715	20.7	20.6	20.7
After	13.942	13.889	13.887	23.7	23.9	23.8
30 minutes After	13.373	13.341	13.33	21.0	21.5	21.5
Energy (Joules)	94404.14	106529.8	109848.4			
Total Energy (Joules)	310782.4					

Table 5.6: Battery pack non pulse charging test set 2.

Measurement	Voltage (Volts)			Temperature (°C)		
Parameter	<i>Battery 1</i>	<i>Battery 2</i>	<i>Battery 3</i>	<i>Battery 1</i>	<i>Battery 2</i>	<i>Battery 3</i>
Before	12.802	12.746	12.744	20.7	20.6	20.7
After	13.938	13.902	13.886	23.3	23.7	23.9
30 minutes After	13.364	13.343	13.318	20.8	21.0	21.3
Energy (Joules)	96932.61	105158.7	107572.2			
Total Energy (Joules)	309663.5					

5.4.4 The RBESS Hardware Implementation's Battery Pack Charging Pulse Test Analysis

The results of the battery pack pulse charge tests are shown in Table 5.1, Table 5.2, Table 5.3, Table 5.4, Table 5.5 and Table 5.6. The tables show that the temperature changes on the batteries in all six tests were approximately the same. Therefore, temperature change factor can be ignored since the temperature change was approximately the same in each of the six tests. Furthermore, it was also observed from the review of the tables that the voltage of each of the batteries was approximately the same in each of the six tests. The results indicated that each of the batteries in the six tests was approximately at the same SOC at the beginning and at the end of each of the tests.

The energy absorbed by the batteries during the six tests is shown in Table 5.1, Table 5.2, Table 5.3, Table 5.4, Table 5.5 and Table 5.6. The results in the tables proved that the pulsed battery required less energy to charge the batteries to the same SOC as the non pulsed batteries. For example the non-pulsed battery test required 310782.4 Joules for charging the battery while the 100ms and 1000ms tests took only 273358.9 Joules and 288435.7 Joules respectively for charging the batteries. The tests confirmed the assumption that the pulse charging of the batteries was beneficial to the batteries in the RBESS. Table 5.7 lists the energy input into the RBESS and the energy absorbed by the batteries during the six battery pack pulse charge tests. In addition, Table 5.7 shows the conversion efficiency of the RBESS during the six battery pack pulse charge tests. The results of the six batteries pack pulse charge tests confirmed the assumption that pulse charging of the batteries improves the conversion efficiency of the RBESS charge converter. In addition, the results of the six RBESS charge converters tests revealed the

fact that finitely long pulse periods were more efficient than the shorter pulse periods. Hence, as a result of the tests the 1000 ms (1 second) pulse charge rate was selected.

Table 5.7: Pulse test converter efficiency during charge.

Pulse period	100ms		1000ms		No pulse	
	<i>1</i>	<i>2</i>	<i>1</i>	<i>2</i>	<i>1</i>	<i>2</i>
Energy into batteries (Joules)	273358.9	273238.6	288435.7	282790.4	310782.4	309663.5
Energy at Power grid interface (Joules)	369561.5	367706.4	372478.3	358374.2	438805.9	425856.5
Conversion efficiency (%)	73.9684	74.3089	77.4369	78.9093	70.8246	72.7154

5.4.5 The RBESS Hardware Implementation's 100 ms Battery Pack Discharge

Pulse Test

The tests in the previous section looked at pulse charging rates of the batteries in the RBESS, while this section looks at the pulse discharge rates of the batteries in the RBESS. During the 100 ms battery pack discharge pulse tests, the batteries were discharged from 100% SOC to 20% SOC. This was done to prevent the under discharging of the battery which could lead to the failure of the battery cells. Table 5.8 and Table 5.9 contain the results of the two 100 ms battery pack discharge pulse tests performed.

Table 5.8 and Table 5.9 contain the open circuit voltage and temperature at the beginning of each of the tests, at the end of each of the tests and 30 minutes after each of the test. A relaxation time of 30 minutes was allowed, to give the battery's voltage sufficient time to recover and to provide a valid open circuit reading. The voltage

measurements proved that the batteries were started and stopped at approximately the same SOC. Table 5.8 and Table 5.9 also show the energy dissipated by each of the batteries in the battery pack and the total energy dissipated by the batteries in the battery pack. It was also observed that the batteries used in each of the tests exchanged about the same amount of energy. This observation confirmed the fact that the batteries exchanged the same amount of energy. A comparison of the tests with the other pulse tests will be done in Section 5.4.8.

Table 5.8: Battery pack 100 ms pulse discharging test set 1.

Measurement	Voltage (Volts)			Temperature (°C)		
Parameter	Battery 1	Battery 2	Battery 3	Battery 1	Battery 2	Battery 3
Before	13.629	13.659	13.662	20.6	20.5	20.5
After	12.057	12.057	12.577	22.4	22.4	22.3
30 minutes After	12.649	12.831	12.816	21.2	21.3	21.0
Energy (Joules)	100076.9	97110.17	99835.58			
Total Energy (Joules)	297022.6					

Table 5.9: Battery pack 100 ms pulse discharging test set 2.

Measurement	Voltage (Volts)			Temperature (°C)		
Parameter	<i>Battery 1</i>	<i>Battery 2</i>	<i>Battery 3</i>	<i>Battery 1</i>	<i>Battery 2</i>	<i>Battery 3</i>
Before	13.628	13.63	13.657	20.7	20.7	20.7
After	12.227	11.983	12	23	23.4	23
30 minutes After	12.647	12.712	12.773	21.4	21.8	21.4
Energy (Joules)	96391.71	97629.12	97187.66			
Total Energy (Joules)	291208.5					

5.4.6 The RBESS Hardware Implementation's 1000 ms Battery Pack Discharge Pulse Test

During the 1000 ms battery pack discharge pulse tests, the batteries were discharged from 100% SOC to 20% SOC (*Note: SOC is proportional to voltage of the battery. Thus, the batteries were stopped at set voltage that was proportional the selected SOC*s). This was done to prevent the under discharging of the battery which could lead to failure of the battery cells. Table 5.10 and Table 5.11 contain the results of the two 1000 ms battery pack discharge pulse tests performed.

Table 5.10 and Table 5.11 show the open circuit voltage and the temperature at the beginning of each of the tests, at the end of each of the tests and 30 minutes after each of the tests. A relaxation time of 30 minutes was allowed to give the battery's voltage sufficient time to recover and to provide a valid open circuit reading. The voltage measurements proved that the batteries were started and stopped at approximately the same SOC. Table 5.10 and Table 5.11 show the energy dissipated by each of the batteries in the battery pack and the total energy dissipated by the batteries in the battery pack. It was observed that the batteries used in each of the tests exchanged about the same amount of energy. This observation confirmed the fact that the batteries exchanged the same amount of energy. A comparison of the tests with the other pulse tests will be done in Section 5.4.8.

Table 5.10: Battery pack 1000 ms pulse discharging test set 1.

Measurement	Voltage (Volts)			Temperature (°C)		
Parameter	<i>Battery 1</i>	<i>Battery 2</i>	<i>Battery 3</i>	<i>Battery 1</i>	<i>Battery 2</i>	<i>Battery 3</i>
Before	13.69	13.716	13.687	20.1	20.1	20.1
After	12.457	11.94	12.458	22.1	22.5	22.5
30 minutes After	12.814	12.857	12.801	21.0	21.6	20.9
Energy (Joules)	97382.04	93868	102566.7			
Total Energy (Joules)	293816.7					

Table 5.11: Battery pack 1000 ms pulse discharging test set 2.

Measurement	Voltage (Volts)			Temperature (°C)		
Parameter	<i>Battery 1</i>	<i>Battery 2</i>	<i>Battery 3</i>	<i>Battery 1</i>	<i>Battery 2</i>	<i>Battery 3</i>
Before	13.659	13.685	13.655	19.7	19.7	19.7
After	12.421	11.913	12.484	23.4	23.2	23.0
30 minutes After	12.784	12.846	12.802	20.7	20.7	20.7
Energy (Joules)	98973.89	94837.83	101415.1			
Test Energy (Joules)	295226.8					

5.4.7 The RBESS Hardware Implementation's Battery Pack Discharge Non Pulse Test

During the non pulse battery pack discharge tests, the batteries were discharged from 100% SOC to 20% SOC. This was done to prevent the under discharging of the battery which could lead to failure of the battery cells. Table 5.12 and Table 5.13 contain the results of the two non pulse battery pack discharge tests performed.

Table 5.12 and Table 5.13 show the open circuit voltage and temperature at the beginning of each of the tests, at the end of each of the tests and 30 minutes after each of the tests. A relaxation time of 30 minutes was allowed to give the battery's voltage sufficient time to recover and to provide a valid open circuit reading. The voltage

measurements prove that the batteries were started and stopped at approximately the same SOC. Table 5.12 and Table 5.13 show the energy dissipated by each of the batteries in the battery pack and the total energy dissipated by the batteries in the battery pack. It was observed that that each of the batteries used in the tests exchanged about the same amount of energy. This observation confirmed the fact that the batteries exchanged the same amount of energy. A comparison of the tests with the other pulse tests will be done in Section 5.4.8.

Table 5.12: Battery pack non pulse discharging test set 1.

Measurement	Voltage (Volts)			Temperature (°C)		
Parameter	<i>Battery 1</i>	<i>Battery 2</i>	<i>Battery 3</i>	<i>Battery 1</i>	<i>Battery 2</i>	<i>Battery 3</i>
Before	13.766	13.735	13.742	19.6	19.6	19.6
After	11.917	11.889	11.866	23.5	23.5	23.5
30 minutes After	12.6	12.541	12.57	21.7	21.7	21.2
Energy (Joules)	110369.2	108822.8	107129.1			
Total Energy (Joules)	326321.2					

Table 5.13: Battery pack non pulse discharging test set 2.

Measurement	Voltage (Volts)			Temperature (°C)		
Parameter	<i>Battery 1</i>	<i>Battery 2</i>	<i>Battery 3</i>	<i>Battery 1</i>	<i>Battery 2</i>	<i>Battery 3</i>
Before	13.685	13.685	13.686	19.8	19.8	19.8
After	11.943	11.906	11.886	22.5	23.0	22.5
30 minutes After	12.685	12.57	12.629	21.0	21.0	20.8
Energy (Joules)	108750.6	107351.5	107920.5			
Total Energy (Joules)	324022.5					

5.4.8 The RBESS Hardware Implementation's Battery Pack Discharging Pulse Test Analysis

The results of the battery pack pulse discharge tests are shown in Table 5.8, Table 5.9, Table 5.10, Table 5.11, Table 5.12 and Table 5.13. The tables show that the temperature change on the batteries in each of the six tests was approximately the same. Therefore, the effect of temperature change can be ignored since the temperature change was approximately the same in each of the six tests. Further, it was also observed that the voltages of the batteries were approximately the same for each of the six tests. The tests results indicated that each of the batteries in the six tests was at approximately the same SOC at the beginning and at the end of each of the tests.

The energy dissipated by the batteries during the six discharge tests are seen in Table 5.8, Table 5.9, Table 5.10, Table 5.11, Table 5.12 and Table 5.13. The tables revealed the fact that the pulsed batteries dispatched less energy to the load than the non pulsed batteries. For example, the non-pulsed battery test produced 326321.2 Joules for the discharging of the battery while the 100ms and 1000ms tests produced only 297022.6 Joules and 293816.7 Joules respectively for discharge of the batteries. The tests proved that the pulse discharging of the batteries was less beneficial than the continuous discharging of the batteries in the RBESS. Thus, as a result of the tests the non pulse discharge rate was selected. However, since the battery polarization effect is more prevalent at higher current discharge rates, pulse discharging may still prove to be beneficial at higher current discharge rates or longer pulse periods.

Table 5.14 lists the energy discharge from the RBESS and the energy dispatched by the batteries during the six battery pack pulse discharge tests. Table 5.14 also shows

the conversion efficiency of the RBESS during the six battery pack pulse discharge tests. The results of the six batteries pack pulse discharge tests, indicated that pulse discharging of the batteries improved the conversion efficiency of the RBESS charge converter.

Table 5.14: Pulse test converter efficiency during discharge.

Pulse period	100ms		1000ms		No pulse	
Test	<i>1</i>	<i>2</i>	<i>1</i>	<i>2</i>	<i>1</i>	<i>2</i>
Energy out of batteries (Joules)	297022.6	291208.5	293816.7	295226.8	326321.2	324022.5
Energy at Power grid interface (Joules)	177018.3	183389.1	177728.7	180535.2	183696.4	186461.8
Conversion efficiency (%)	59.5976	62.9752	60.4897	61.1514	56.2931	57.5459

5.4.9 The RBESS Hardware Implementation’s Battery Pack Pulse Test

Overview

The results from the RBESS hardware implementation’s six battery pack pulse tests proved that the RBESS would benefit from the pulse operation of the battery pack. In addition, the results also indicated that the batteries used in the discharge pulse tests may not benefit from the pulse discharge mode of operation. The latter discovery suggested that that one of the following two factors could have influenced the outcome. Firstly, the battery chemistry might not have been suited for pulse discharge and secondly, the batteries needed higher discharge rates or longer pulse periods to receive the full benefit of pulse discharging. However, further optimization of the pulse period should further improve the efficiency of the RBESS. As a result of the tests, 1000 ms pulse charging was selected for charging the batteries in the RBESS and non pulsed discharging was selected for discharging of the RBESS.

5.5 Chapter summary

This chapter looked at testing and verifying the capabilities of the RBESS. The RBESS tests were conducted to determine the capacity of the RBESS to maintain the bus voltages, to balance the batteries in a battery pack and to balance the battery packs in a battery bank. The results indicated that the RBESS can maintain the bus voltages, balance the batteries in the battery pack and balance the battery packs in the RBESS hardware implementation. The RBESS simulation model was useful in designing the approach for the controls and hardware implementation confirming that the design operated as intended. This design method demonstrated the validity of the software simulator based design approach. Furthermore, the slight differences in the results seen in the simulation and the hardware implementation can be attributed to hardware component tolerances and control tuning.

One additional test that was performed on the RBESS which was the analysis of the effect that battery pulsing had on the RBESS. The battery pack pulse tests, indicated that pulse discharging delivered less energy than non pulsed discharging, and that pulse charging delivered more energy than non pulse charging. Furthermore, the tests revealed that the RBESS' charge converter had higher conversion efficiency with pulsing than without pulsing. Thus, battery pulse charging has proven to be beneficial in the RBESS. However, further research is needed to determine the conditions under which pulse discharging of the batteries is beneficial to the RBESS. In conclusion, the tests allowed for selection of a pulse rate for charging and discharging the batteries. The test results indicated an increased performance for charging the batteries with 1000 ms pulse and discharging the batteries without pulsing.

Chapter 6: Conclusions and

Recommendations

6.1 Conclusion

This thesis developed a Repurposed Battery Energy Storage System (RBESS). The development took into account the special requirements of a used electric vehicle battery. Used electric vehicle batteries can have considerably different capacities and characteristics. The special design developed for RBESS makes possible the repurposing of used electric vehicle batteries for applications in power systems. Generally, repurposed batteries can be used to support non-dispatchable renewable energy systems in load leveling or peak shaving applications. The RBESS can become a key conduit between the retired vehicle batteries and the power grid. The RBESS has the capability to facilitate the exchange of energy between the repurposed batteries and the power system. The reapplication or the reuse of the used electric vehicle batteries will prolong the usefulness of electric vehicle batteries past their traditional cycle life.

The reapplication of used electric vehicle batteries must first overcome the problem of battery aging. The battery aging phenomenon reduces the capacity of the battery, the voltage, of the battery and increases the internal resistance of the battery.

The RBESS implements a MLIPC system to manage the repurposing process of used electric vehicle batteries. The MLIPC system utilizes the battery pulsing, interlacing of batteries and virtual paralleled batteries, techniques to repurpose the used electric vehicle batteries. The MLIPC system can dynamically change the ratings of the battery

pack. The rating changes better enable the battery pack batteries to utilize the energy required during the exchange process. Specifically, the MLIPC system controls the duration of the battery pulse and the number of battery pulses that are overlapped during the interlacing of the battery pulses. This controls the amount of current that each battery in the battery pack will exchange with the power system. The MLIPC system's process causes the battery pack's rating to change. The MLIPC also allows the charge block units to use varying pulse width to change the batteries.

However, since at this point the batteries' voltage is too low to be directly utilized on a power system, the RBESS' charge converter system was introduced. The RBESS charge converter system is constructed to form a cascaded two level bidirectional DC to DC converter system. The RBESS charge converter system has multiple converters present in the second stage of the cascaded converter system. The multiple converters are needed to regulate the battery packs in the battery bank. The multiple converters enable the RBESS's system to maintain the balancing of multiple battery packs in the battery bank. That balancing is possible because the battery packs are separated from each other by the second stage converter.

The RBESS simulation model was used for designing the RBESS and its control strategy. The RBESS hardware implementation was constructed based on the design of the RBESS simulation model. The RBESS hardware implementation was used to verify the capabilities of the RBESS and also to determine whether pulse charging was a useful exercise in the RBESS. The testing of the RBESS hardware implementation revealed that the RBESS was capable of managing the bus voltages, at multiple power levels and system configurations, to support energy exchange between the batteries and the power

system. Furthermore, the test also revealed that the RBESS was capable of balancing both the individual batteries in the battery pack and the individual battery packs in the battery bank.

The results of the battery pulsing tests revealed two facts about battery pulsing in the RBESS. The first fact revealed by the tests was that the discharge mode of operation, pulse discharging was not suitable for the power level and the pulse periods examined. The test results indicated that the energy dispatched in the pulsing process was less than the energy dispatched during the continuous process. However, since battery polarization reduces battery capacity and since polarization is more pronounced at higher current levels, therefore the battery pulsing could become useful at higher current ratings and longer pulse periods. The second fact that was revealed by the tests was that battery pulsing during the charging of the batteries was better for the RBESS than continuous charging. Pulse charging is better than continuous charging in the RBESS because continuous charging requires more energy than pulse charging to reach a given SOC in the battery. Overall, the tests of the RBESS indicated that pulse charging at 1000 ms and non pulsed discharging afforded the greatest performance of the RBESS during the tests.

In addition, the RBESS' charge converters tests revealed that there was increased conversion efficiency during pulsed operation than during continuous operation. Therefore, it was concluded that the RBESS should use pulse control to obtain maximum efficiency from the charge converter.

The several tests and analyses results proved that, the RBESS is a capable and viable system. Specifically, the RBESS can maintain control of the bus voltages. The

RBESS can balance the capacity of the batteries in battery packs and battery bank. Furthermore, it has been determined, that for the given power range of the RBESS model continuous discharge should be used for discharging batteries and pulsed charging should be used for charging batteries.

6.2 Recommendations for Future Work

The RBESS has proven that it is capable of performing specific control operations on the batteries. However, further research into the system will be valuable. For instance, the thesis has shown that pulse charging of the repurposed batteries improved the charge acceptance of the batteries and the efficiency of the RBESS charge converter system. However, further research is needed to determine what optimal pulse period for the batteries would improve the charge acceptance and efficiency of the used electric vehicle batteries, and the efficiency of the RBESS charge converter system. Further Information about the optimization of the battery's pulse period could lead to a reduction in the energy required to charge the battery, and to a better utilization of the used electric vehicle batteries' remaining capacity.

The thesis also concluded that pulse discharging was not suitable for the RBESS at the current levels provided during the experimental tests. Therefore, further explorations are required to determine what current levels and pulse periods would afford the greater benefits to the capacity of used electric vehicle batteries. Further research is necessary since the results of the tests also showed that while there was an increased performance from the RBESS charge converter system during the pulsed operation of the batteries there was no increase in the batteries' capacities. Thus, if pulsing could be used

to improve the capacity of used electric vehicle batteries an improved performance from the RBESS would also be obtained.

Therefore a commitment by the transportation and power generation industries to provide further research into the Repurposed Battery Energy Storage System's operation processes could prove to be beneficial to both the transportation and power generation industries.

References

- [1] B. Bose, "Global Warming: Energy, Environmental Pollution, and the Impact of Power Electronics," *Industrial Electronics Magazine, IEEE*, vol. 4, no. 1, pp. 6-17, March 2010.
- [2] V. Marano and G. Rizzoni, "Energy and economic evaluation of PHEVs and their interaction with renewable energy sources and the power grid," in *IEEE International Conference on Vehicular Electronics and Safety*, 22-24 Sept. 2008, pp. 84-89.
- [3] S.C. Smith, P.K. Sen, B. Kroposki, and K. Malmedal, "Renewable energy and energy storage systems in rural electrical power systems: Issues, challenges and application guidelines," in *Rural Electric Power Conference (REPC), 2010 IEEE*, 16-19 May 2010, pp. B4-B4-7.
- [4] A.S.O. Yu, L.L.C. Silva, C.L. Chu, P.T.S. Nascimento, and A.S. Camargo, "Electric vehicles: Struggles in creating a market," in *Technology Management in the Energy Smart World (PICMET), 2011 Proceedings of PICMET '11*, July 31 2011-Aug, pp. 1-13.
- [5] G. M. Masters, *Renewable and Efficient Electric Power Systems*. New Jersey, United States of America.: JOHN WILEY & SONS, INC., 2004.
- [6] T. Reddy. D. Linden, *Handbook of Batteries*, 3, Ed. New York, New York, United States of America: McGraw-Hill, 2002.
- [7] H. A. Kiehne, *Battery technology handbook*. Germany: CRC Press, 2003.
- [8] C. Y.Hsieh and C.Moo Wu, "A Multi-Mode Charging Circuit for Rechargeable Batteries," in *The 2005 International Power Electronics Conference*, 2005, pp. 1569-1574, [online]. <http://www.kyu.edu.tw/93/epaperv7/036.pdf>.
- [9] V. Srinivasan, G. Q. Wang, and C. Y. Wang, "Mathematical Modeling of Current-Interrupt and pulse Operation of Valve-Regulated Lead Acid Cells," *Journal of the Electrochemical Society*, pp. A316-A325, November 2003.
- [10] J.B. Wang and C.Y. Chuang, "A multiphase battery charger with pulse charging scheme," in *Industrial Electronics Society, 2005. IECON 2005. 31st Annual Conference of IEEE*, 6-6 Nov. 2005, p. 6.
- [11] D. Bertozzi and L. Benini, "Battery Lifetime Optimization for Energy-Aware Circuits," in *Low-Power Electronics DesignChapter*, Christian Piguet, Ed.: CRC Press, 2005, vol. VII, ch. 43, pp. 43-1-43-21.
- [12] K. Moo, N. Soon, and Y. Hsieh, "Parallel Operation of Battery Power Modules," *IEEE Transactions on Energy Conversion*, vol. 23, no. 2, pp. 701-707, June 2008.
- [13] Q. Wu, Q. Qiu, and M. Pedram, "An interleaved dual-battery power supply for battery-operated electronics," in *Design Automation Conference, 2000*.

Proceedings of the ASP-DAC 2000. Asia and South Pacific, 2000, pp. 387-390.

- [14] R. I. Hammerschlag and C. P. Schaber, "Energy Storage Technologies," in *Energy Management and Conservation Handbook*, D. Yogi. Goswami and Frank Kreith, Ed.: CRC Press, 2007, ch. 12, pp. 12-1–12-22.
- [15] T. R. Corompton, *Battery Refferance Book*, 3, Ed. Woburn: Reader Education and Professional Publishing Ltd, 2000.
- [16] C.S. Moo, K.S. Ng, Y.P. Chen, and Y.C. Hsieh, "State-of-Charge Estimation with Open-Circuit-Voltage for Lead-Acid Batteries," in *Power Conversion Conference - Nagoya, 2007. PCC '07*, 2-5 April 2007, pp. 758-762.
- [17] R. Dell, *Understanding batterie.:* Cambridge: Royal Society of Chemistry, 2001.
- [18] R. Foster, M. Ghassemi, and A. Cota, *Solar Energy Renewable Energy and the environment*. New Yor, New York, United States Of America: CRC Press, 2010.
- [19] G. Pistoia, *Battery Operated Devices and Systems - From Portable Electronics to Industrial Products.:* Elsevier , 2009.
- [20] M. Broussely and G. Pistoia, *Industrial Applications of Batteries - From Cars to Aerospace and Energy Storage.:* Elsevier, 2007.
- [21] E. Wehrle, "Charging Methods and Techniques:General Requirements and Selection of Chargers," in *Battery Technology Handbook.:* Expert Verlag, 2003.
- [22] L. Chen, "Design of Duty-Varied Voltage Pulse Charger for Improving Li-Ion Battery-Charging Response," *IEEE Transactions on Industrial Electronics*, vol. 56, no. 2, pp. 480-487, Feb. 2009.
- [23] Y.C. Hsieh, C.S. Moo, C.K. Wu, and J.C. Cheng, "A non-dissipative reflex charging circuit," in *Telecommunications Energy Conference*, 23 Oct. 2003, pp. 679-683.
- [24] N.H. Kutkut and D.M. Divan, "Dynamic equalization techniques for series battery stacks," in *Telecommunications Energy Conference*, 6-10 Oct 1996, pp. 514-521.
- [25] W. Li and G. Joos, "Performance Comparison of Aggregated and Distributed Energy Storage Systems in a Wind Farm For Wind Power Fluctuation Suppression," in *Power Engineering Society General Meeting 2007 IEEE*, 24-28 June 2007, pp. 1-6.
- [26] A. Oudalov, D. Chartouni, C. Ohler, and G. Linhofer, "Value Analysis of Battery Energy Storage Applications in Power Systems," in *Power Systems Conference and Exposition, 2006. PSCE '06. 2006 IEEE PES* , Oct. 29 2006-Nov. 1 2006, pp. 2206-2211.
- [27] EA Technology, "Review of Electrical Energy Storage Technologies and Systems and of their Potential for the UK," 2004.
- [28] ABB, "ABB Constructs World's Largest Battery Energy Storage System in

- Fairbanks," ABB, 2004.
- [29] IEEE, "IEEE Guide for the Protection of Stationary Battery Systems," IEEE, IEEE Standard IEEE Std 1375-1998, 1998.
 - [30] N. Mohan, T. M. Undeland, and W. P. Robbins, *Power Electronics Converters , Applications and design*, 3rd ed.: John Willey & Sons Inc., 2003.
 - [31] J. G. Kassakian, M. F. Schlecht, and G. C. Verghese, *Principle of Power Electronics*, 1st ed.: Addison-Wesley Publishing Company, 1991.
 - [32] H. Wang, J. Liu, and R. Wang, "Stability issue and corresponding design considerations in a system of cascaded bidirectional DC-DC Converters," in *Power Electronics Specialists Conference, 2008. PESC 2008. IEEE*, 15-19 June 2008, pp. 2813-2818.
 - [33] M. Dekker, "Multi-Converter Vehicular Dynamics and Control," in *Vehicular Electric Power Systems*: CRC Press, 2004, ch. 12.
 - [34] DigiLent, "Cerbot 32MX4 Board Reference Manual," Manual.
 - [35] Microchip, "PIC32MX3XX/4XX Family," Manual 2008.
 - [36] K2 Energy, HIGH CAPACITY LFP26650P POWER CELL DATA.
 - [37] A. Cruden, S. Gair, J.R. McDonald M. Dürr, "Dynamic model of a lead acid battery for use in a domestic fuel cell system," *Journal of Power Sources*, vol. 161, no. 2, pp. 1400-1411 2006, October 200.
 - [38] C. M. Shepherd, "Theoretical Design of primary and secondary Cells," US NAVAL Research Laboratory. , Washington , 405904, 1963.
 - [39] T. Hirai et al., "Automatic equivalent-circuit estimation system for lithium-ion battery," in *Universities Power Engineering Conference, 2008. UPEC 2008. 43rd International* , 1-4 Sept. 2008, pp. 1-5.
 - [40] Fairchild Semiconductor, "FAN7392 High-Current, High- and Low-Side, Gate-Drive IC," Fairchild Semiconductor Corporation, Datasheet 2010.
 - [41] Fairchild Semiconductor corporation, "AN-6076 Design and Application Guide of Bootstrap Circuit for High-Voltage Gate-Driver IC," Fairchild Semiconductor corporation, Application Note 2008.
 - [42] Texas Instruments Incorporated, "SINGLE9-A HIGH SPEED LOW-SIDEMOSFET DRIVER WITH ENABLE," Texas Instruments Incorporated, Datasheet JANUARY 2010.
 - [43] Microchip Technology Inc., "PIC32 Family Reference Manual, Sect. 23 Serial Peripheral Interface," Microchip Technology Inc., Reference Manual 2011.
 - [44] Microchiop. (2011) Microchiop: PIC32 USB Starter Kit II. [Online]. http://www.microchip.com/stellent/idcplg?IdcService=SS_GET_PAGE&nodeId=2615&dDocName=en535536

- [45] C. Blake and C. Bull, "IGBT or MOSFET: Choose Wisely," IRF,.
- [46] M. Kim, H. Bae, and B. Suh, "Comparison of IGBT and MOSFET Inverters in Low-Power BLDC Motor Drives," in *Power Electronics Specialists Conference, 2006. PESC '06. 37th IEEE*, 18-22 June 2006, pp. 1-4.

Appendix A Schematics

This appendix contains the schematics for the RBESS's charge converter and battery bank.

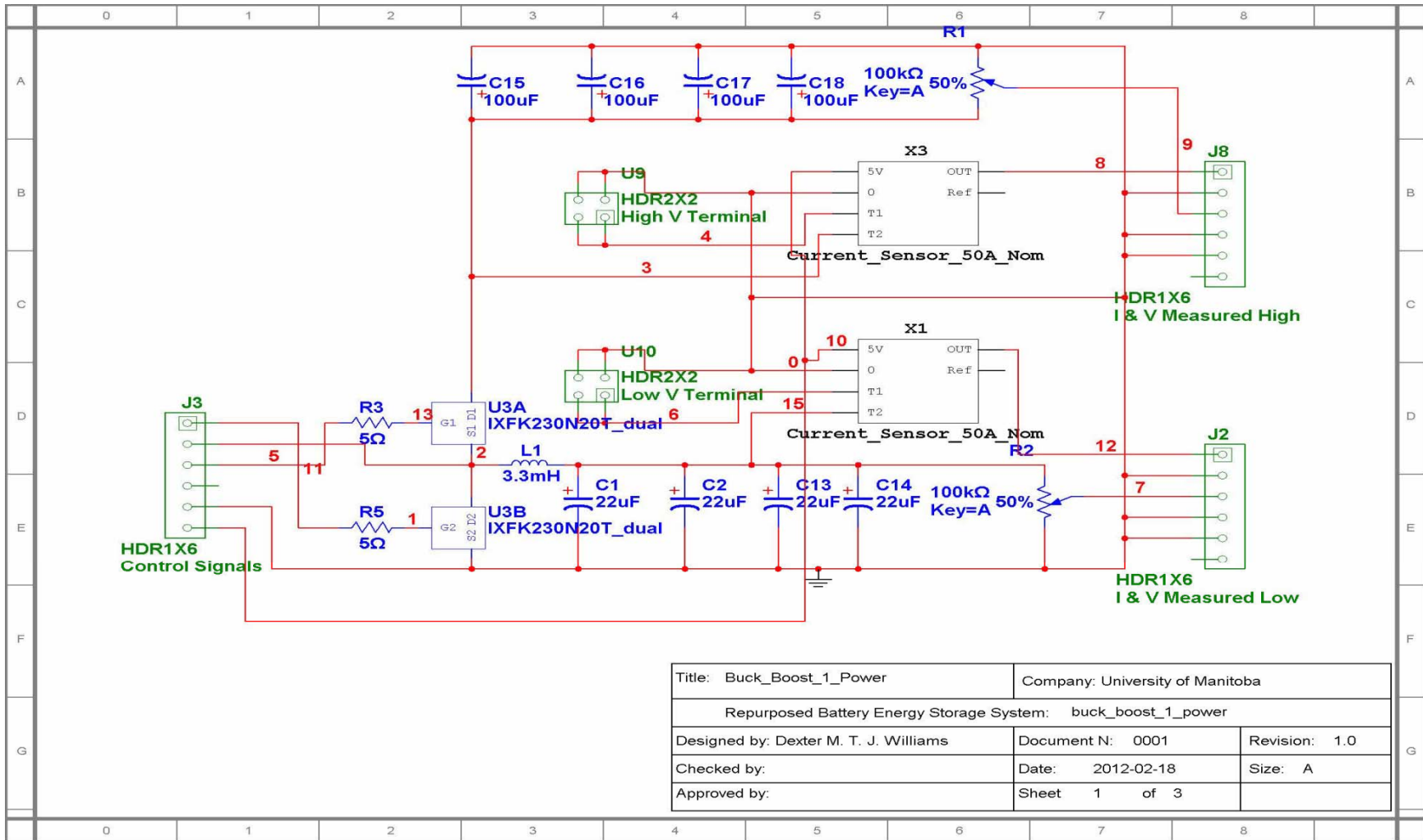


Figure A-1: Repurposed Battery Energy Storage System Schematic 1 of 25.

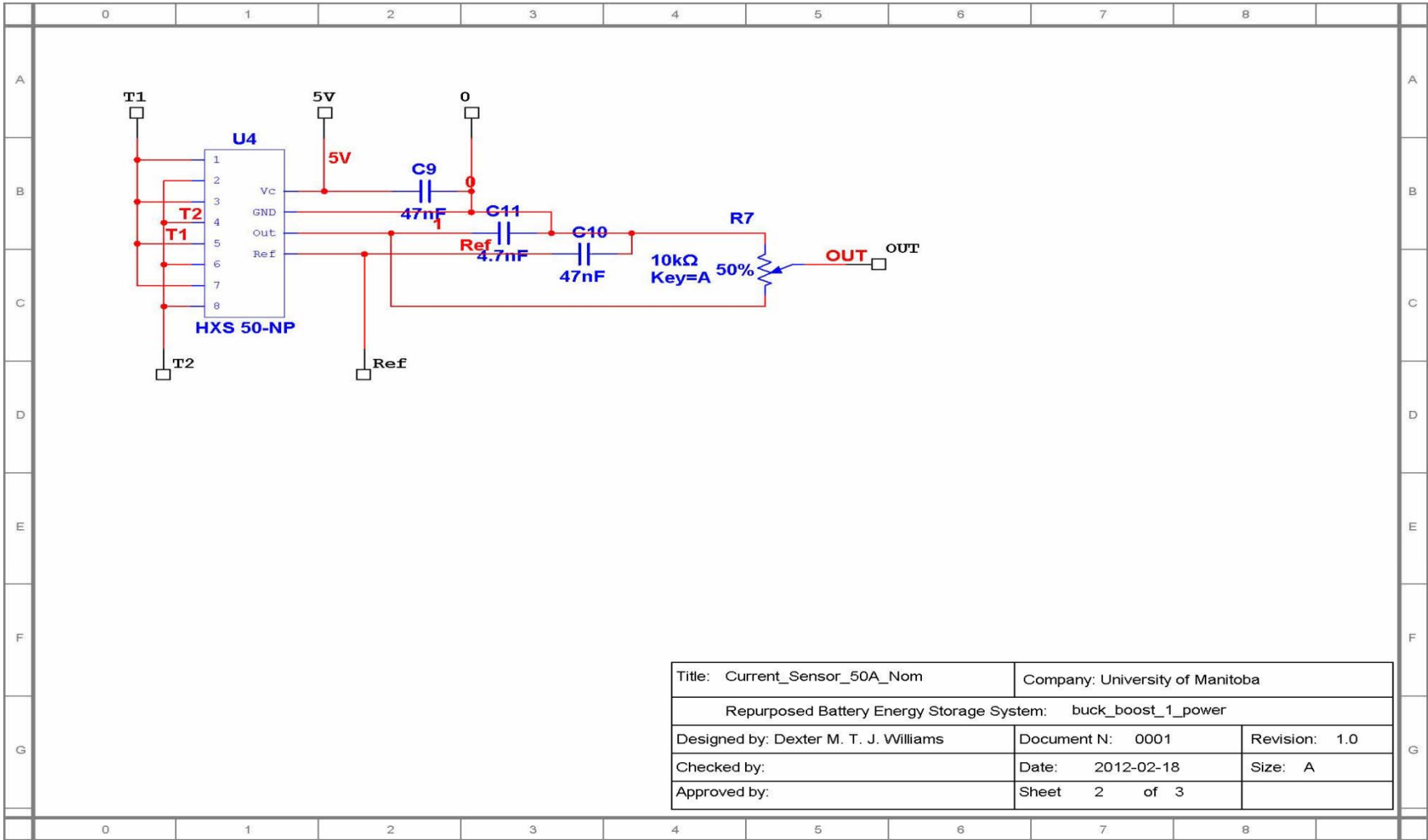


Figure A-2: Repurposed Battery Energy Storage System Schematic 2 of 25.

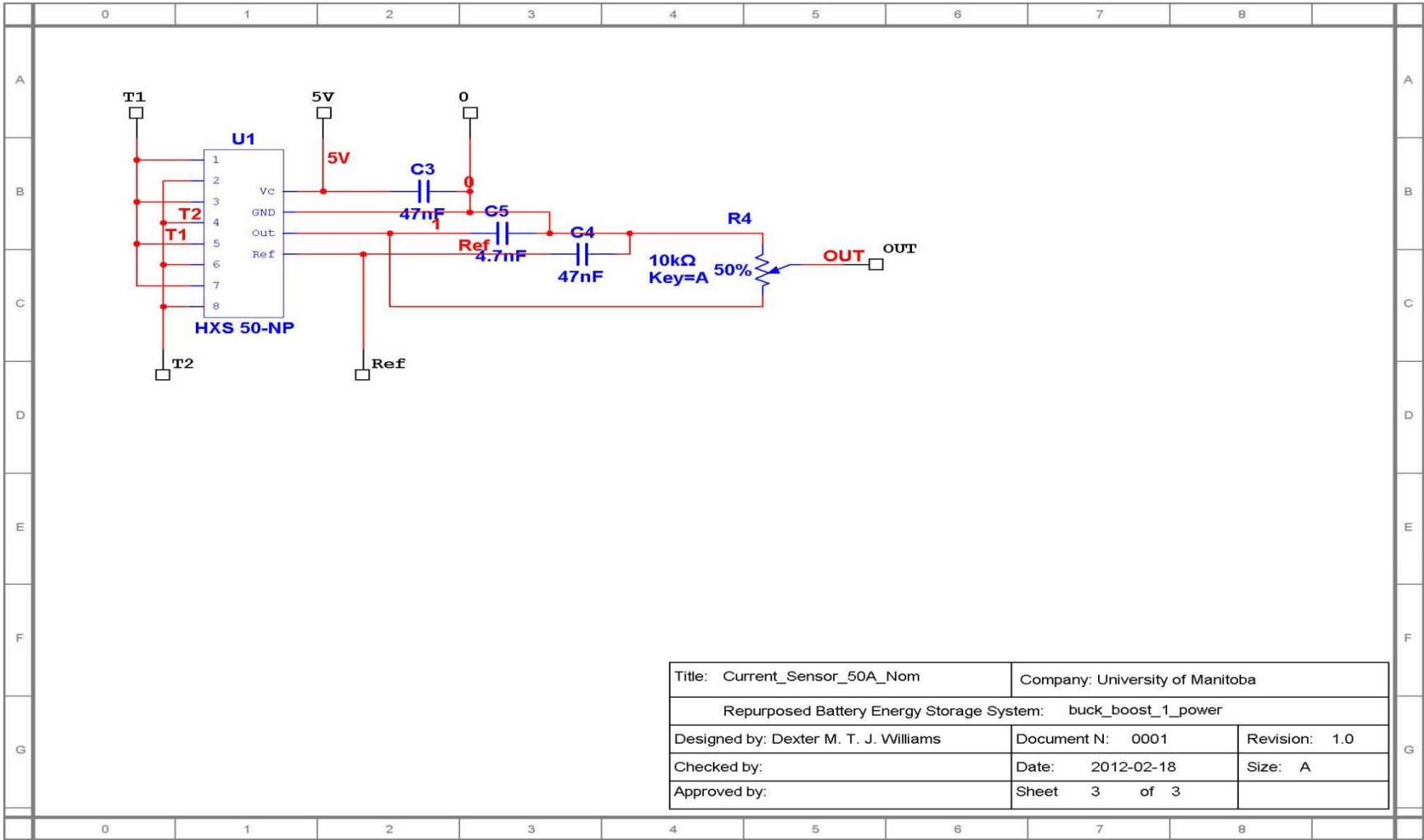


Figure A-3: Repurposed Battery Energy Storage System Schematic 3 of 25.

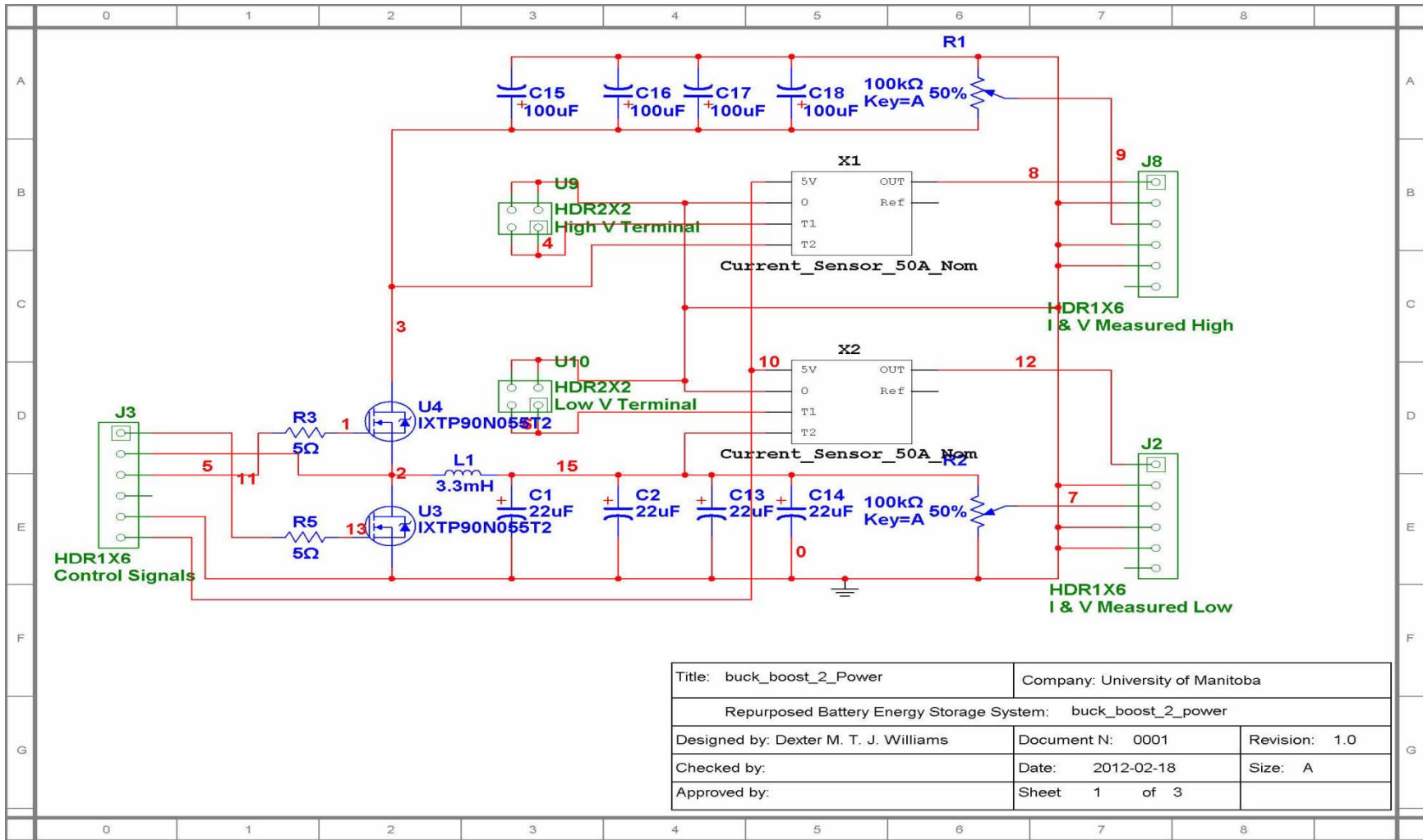


Figure A-4: Repurposed Battery Energy Storage System Schematic 4 of 25.

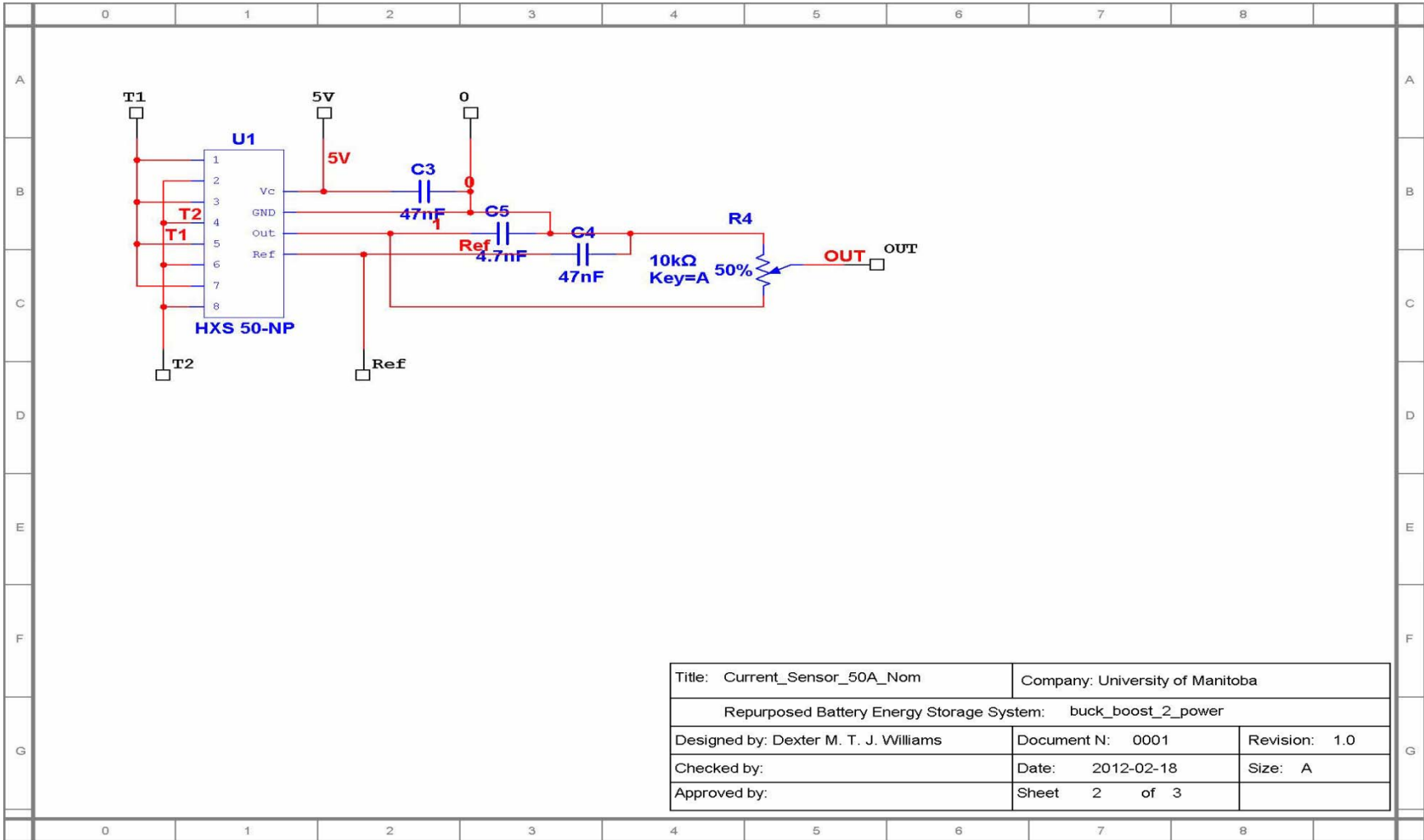


Figure A-5: Repurposed Battery Energy Storage System Schematic 5 of 25.

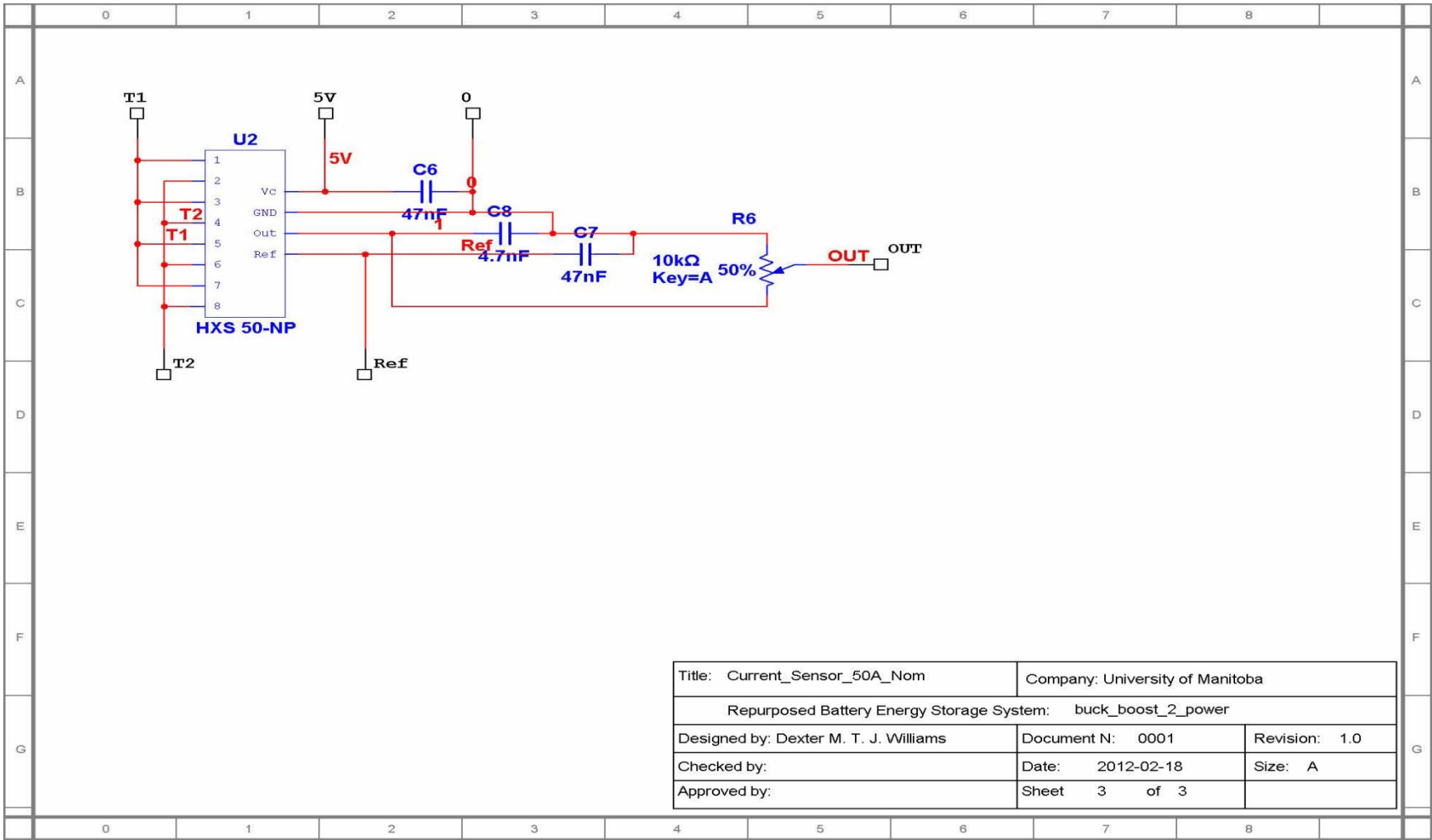


Figure A-6: Repurposed Battery Energy Storage System Schematic 6 of 25.

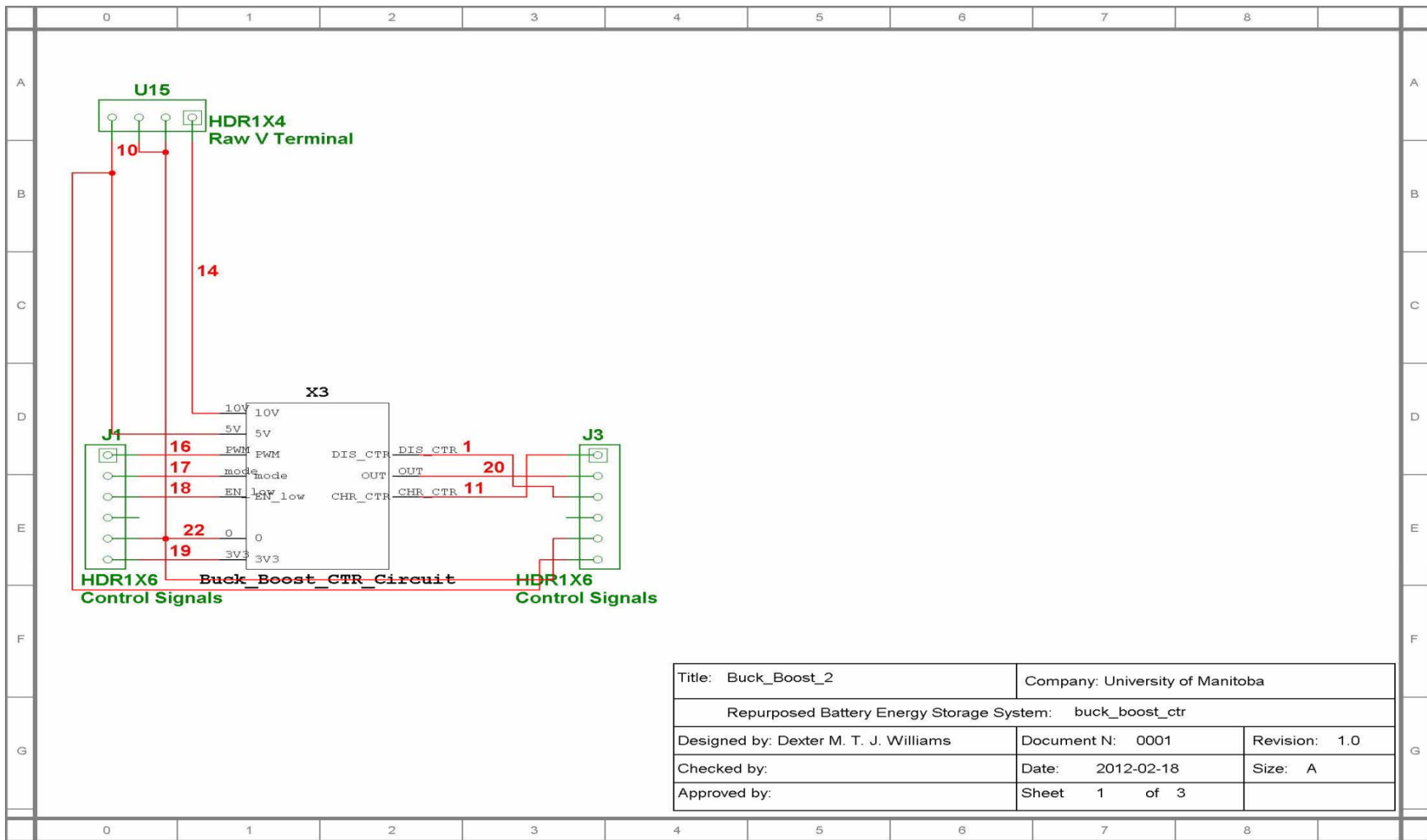


Figure A-7: Repurposed Battery Energy Storage System Schematic 7 of 25.

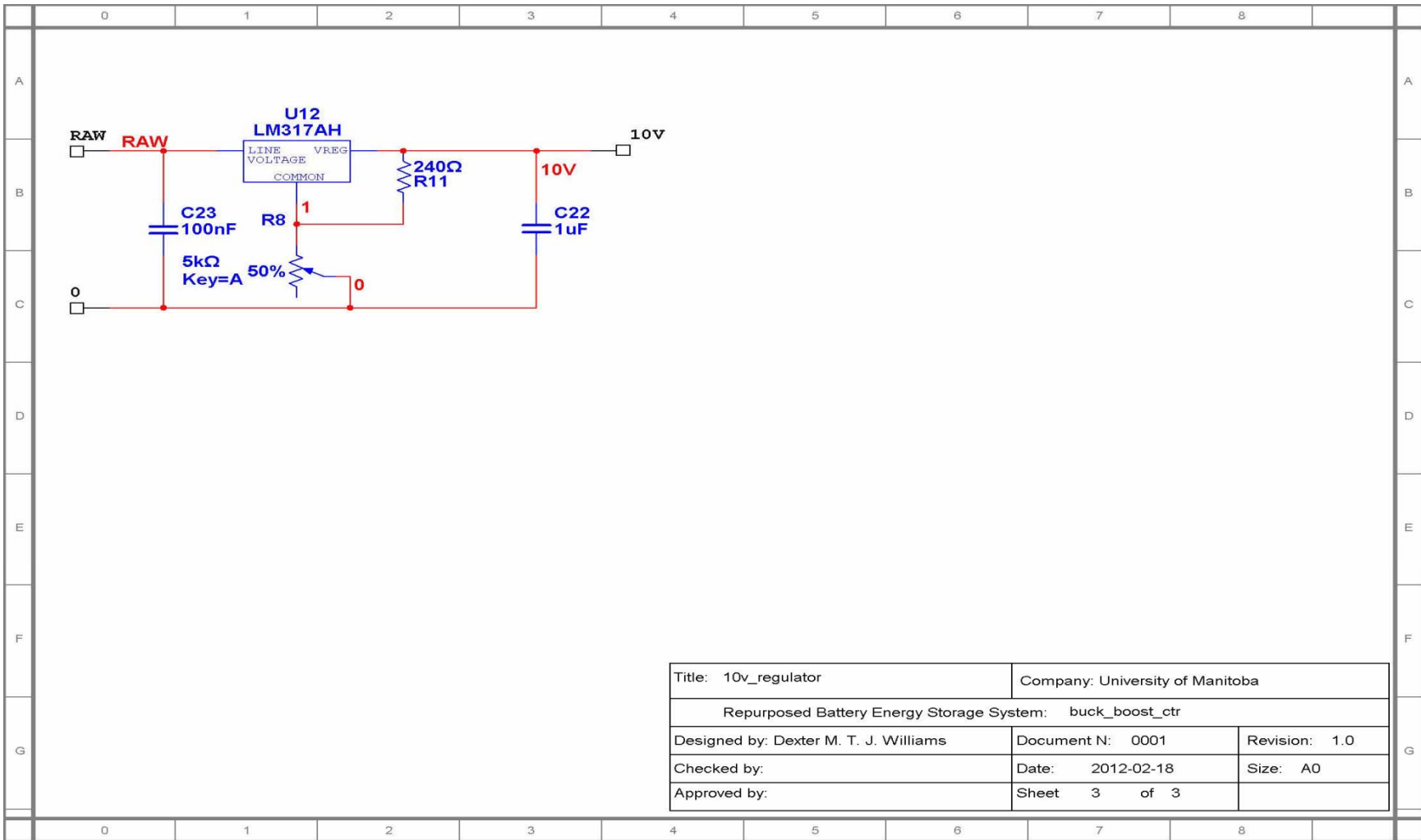


Figure A-9: Repurposed Battery Energy Storage System Schematic 9 of 25.

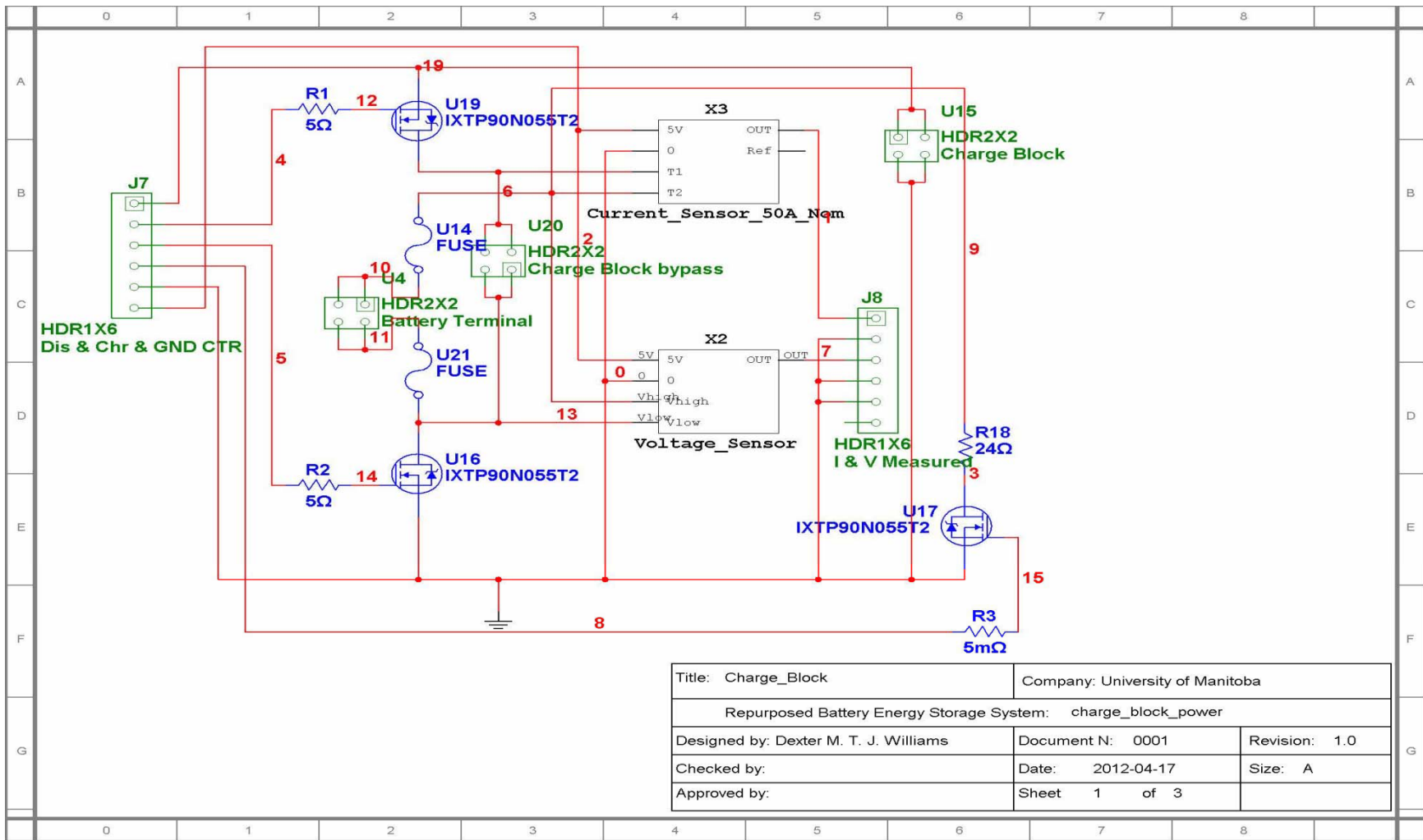


Figure A-10: Repurposed Battery Energy Storage System Schematic 10 of 25.

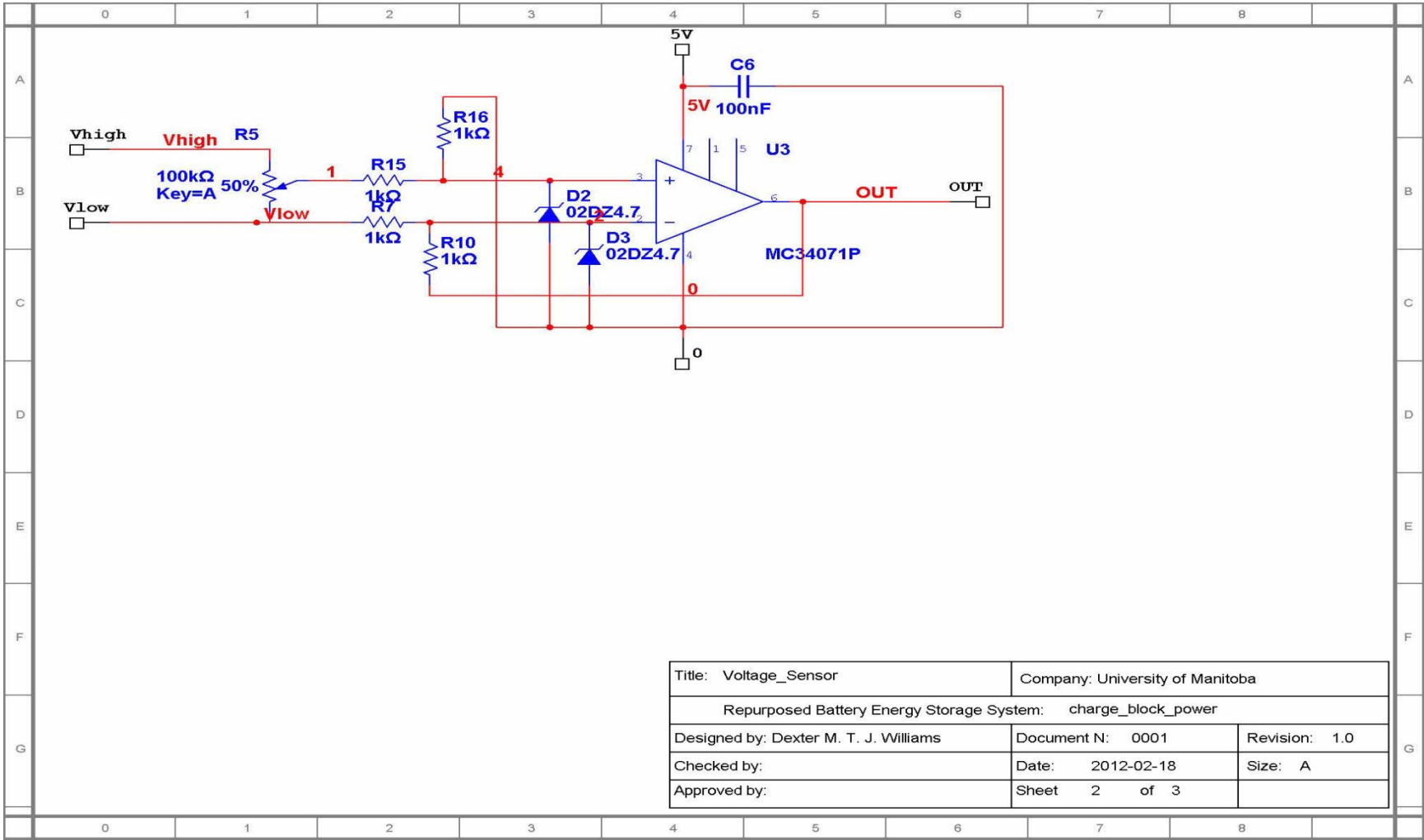


Figure A-11: Repurposed Battery Energy Storage System Schematic 11 of 25.

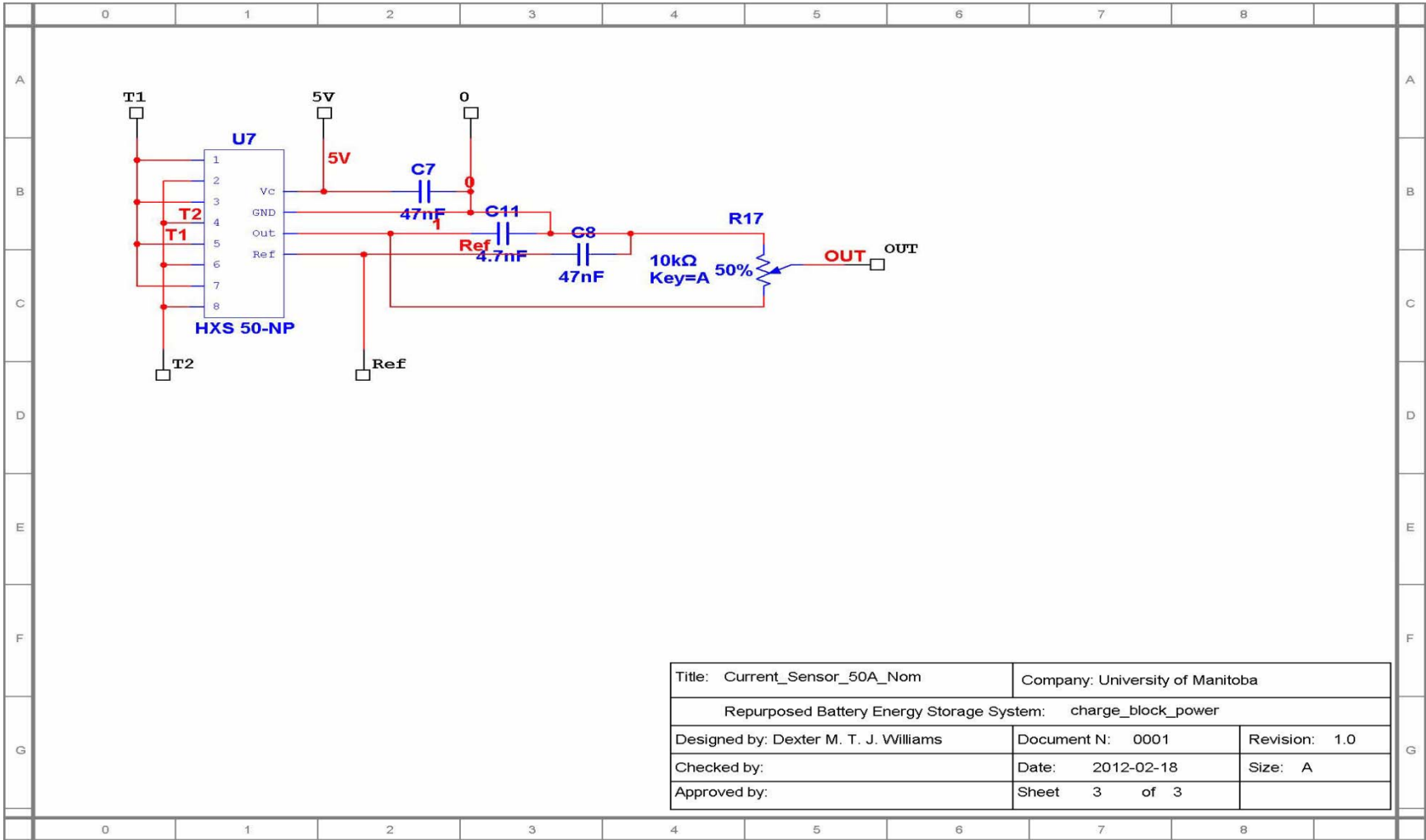


Figure A-12: Repurposed Battery Energy Storage System Schematic 12 of 25.

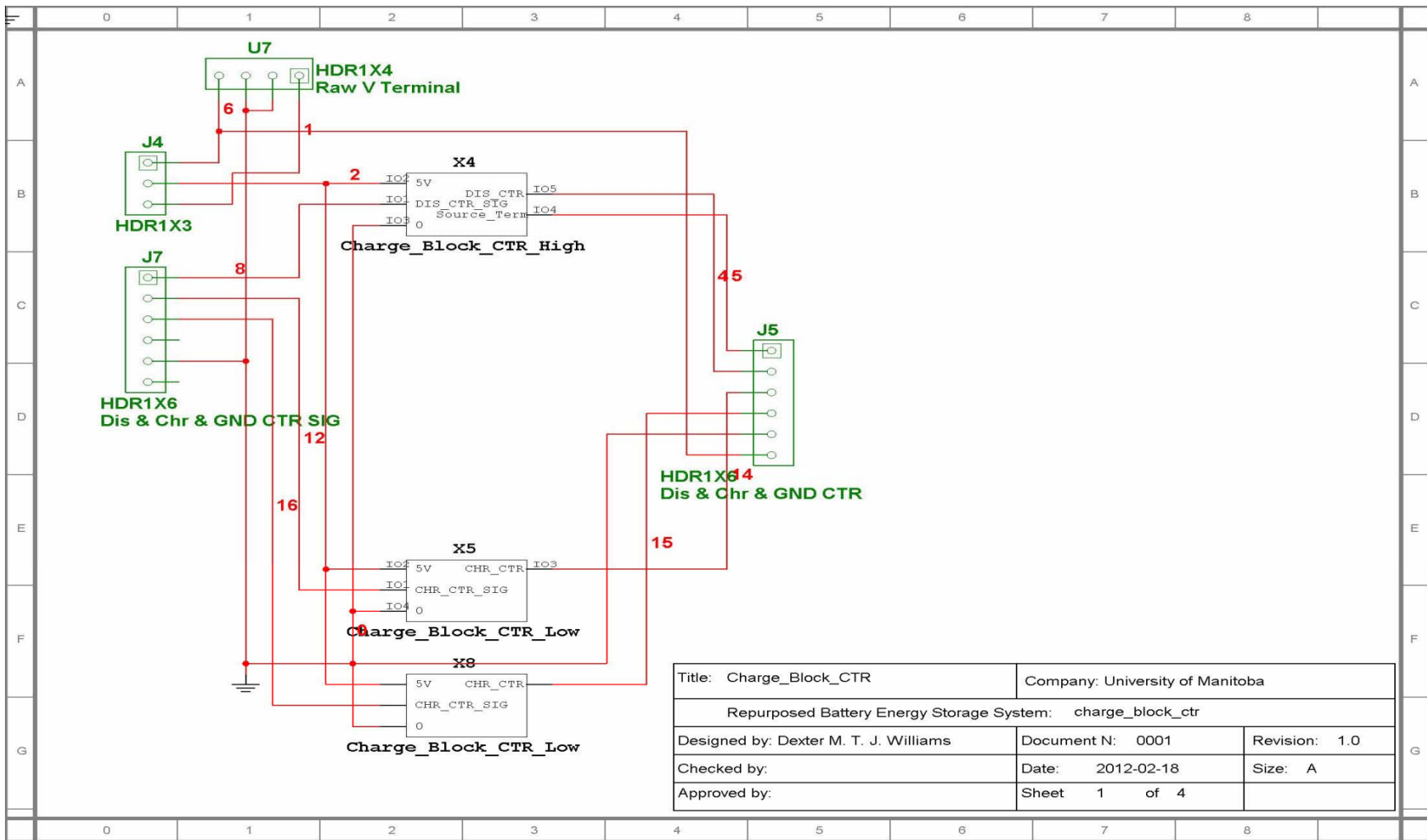


Figure A-13: Repurposed Battery Energy Storage System Schematic 13 of 25.

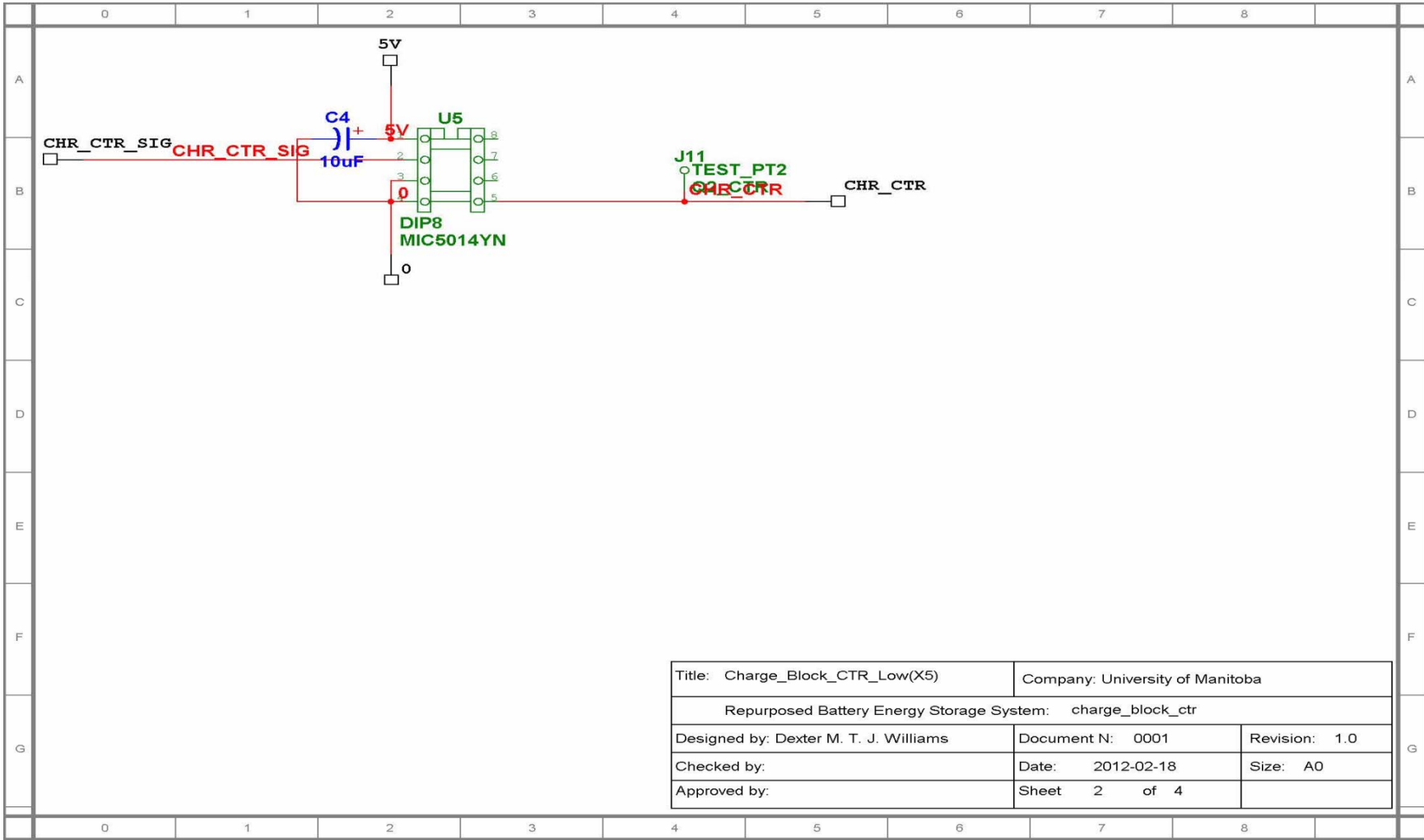


Figure A-14: Repurposed Battery Energy Storage System Schematic 14 of 25.

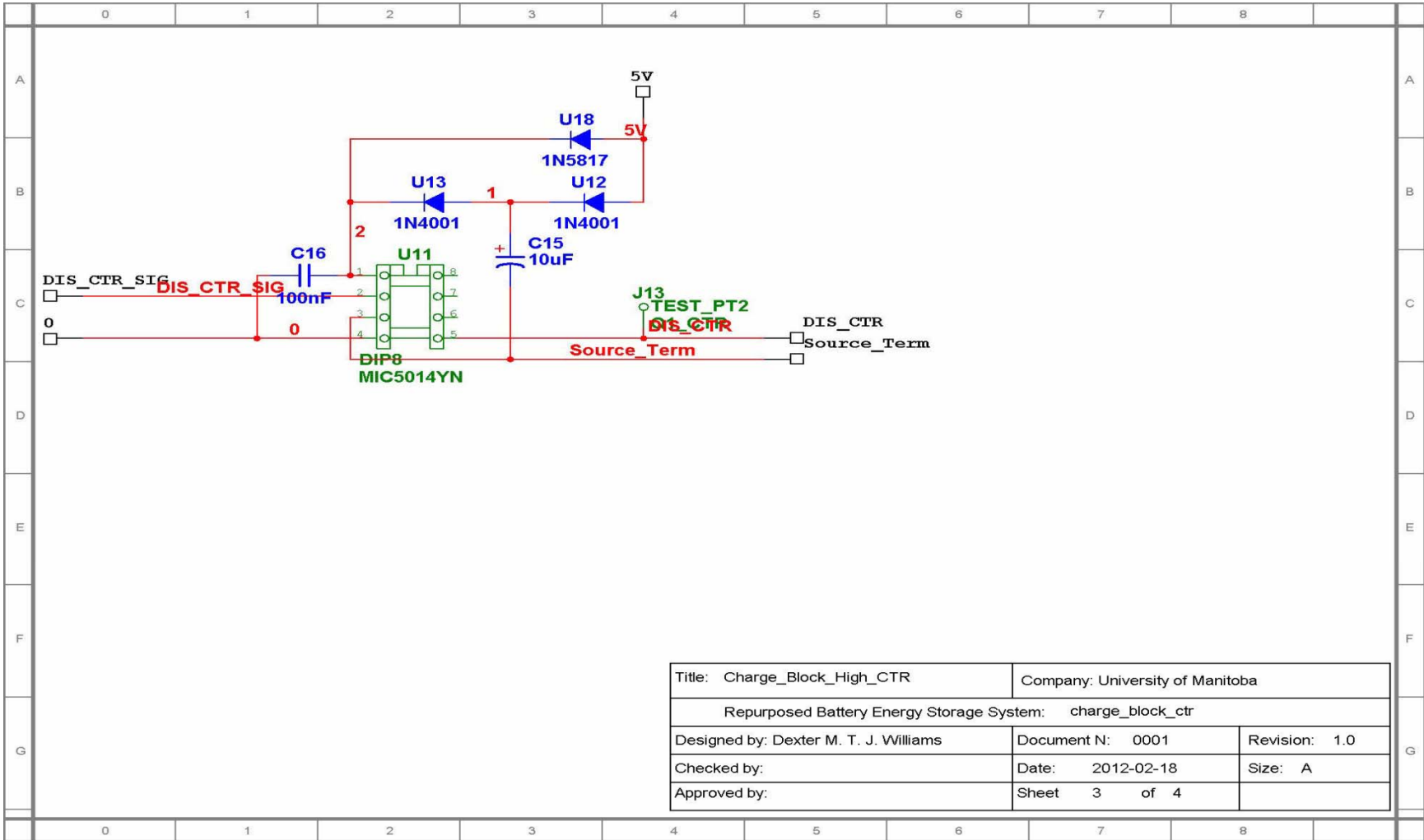


Figure A-15: Repurposed Battery Energy Storage System Schematic 15 of 25.

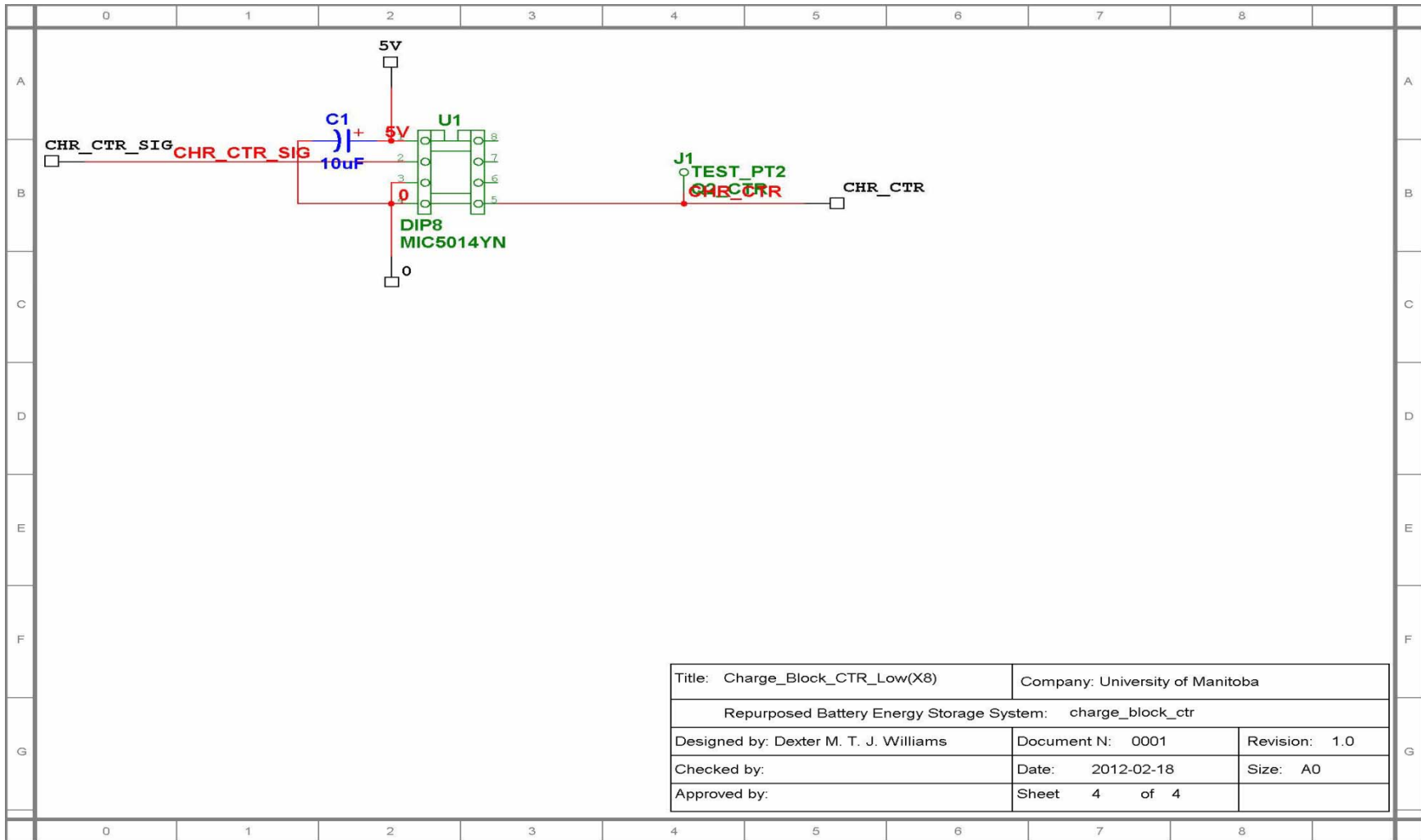


Figure A-16: Repurposed Battery Energy Storage System Schematic 16 of 25.

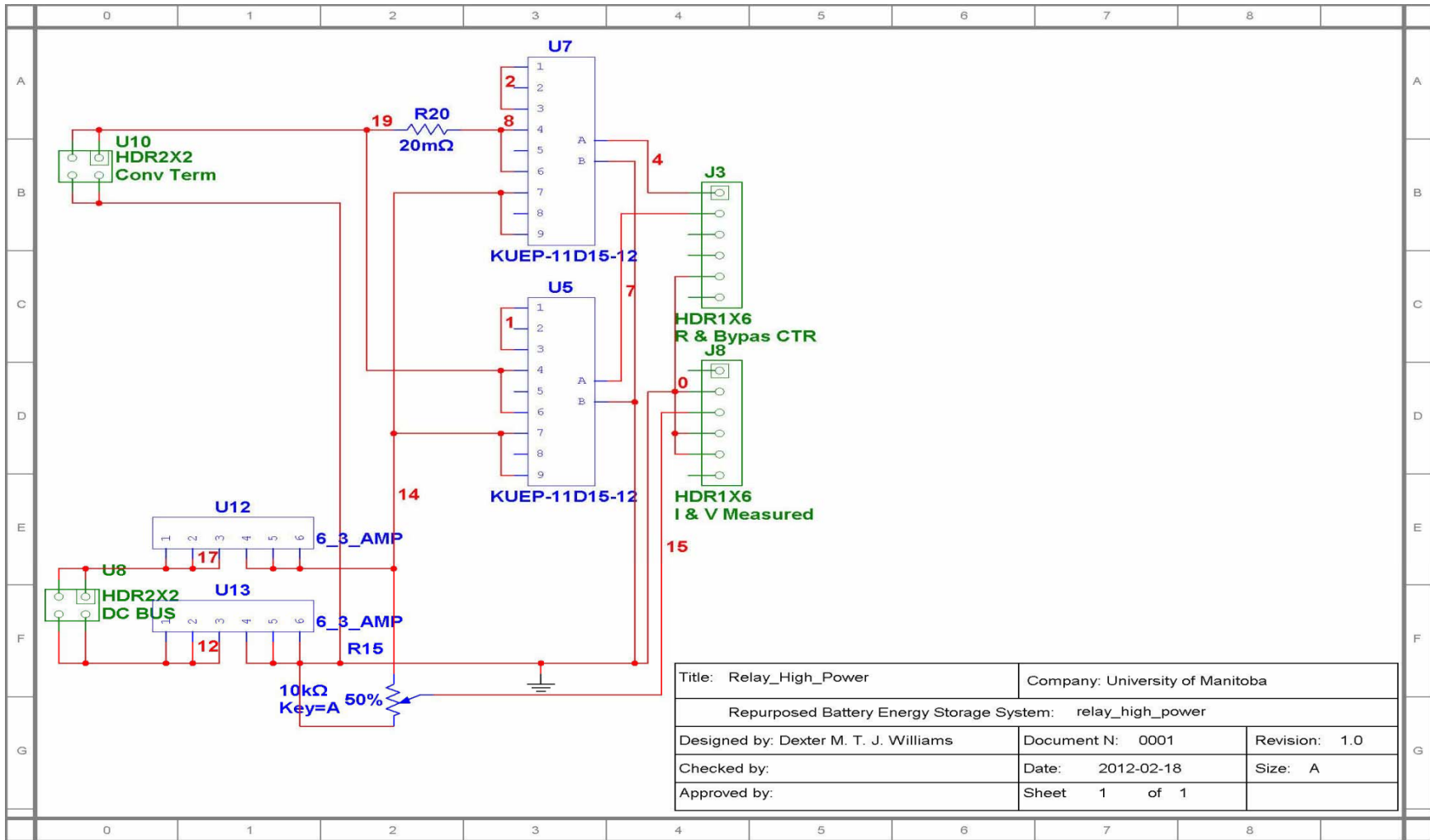


Figure A-17: Repurposed Battery Energy Storage System Schematic 17 of 25.

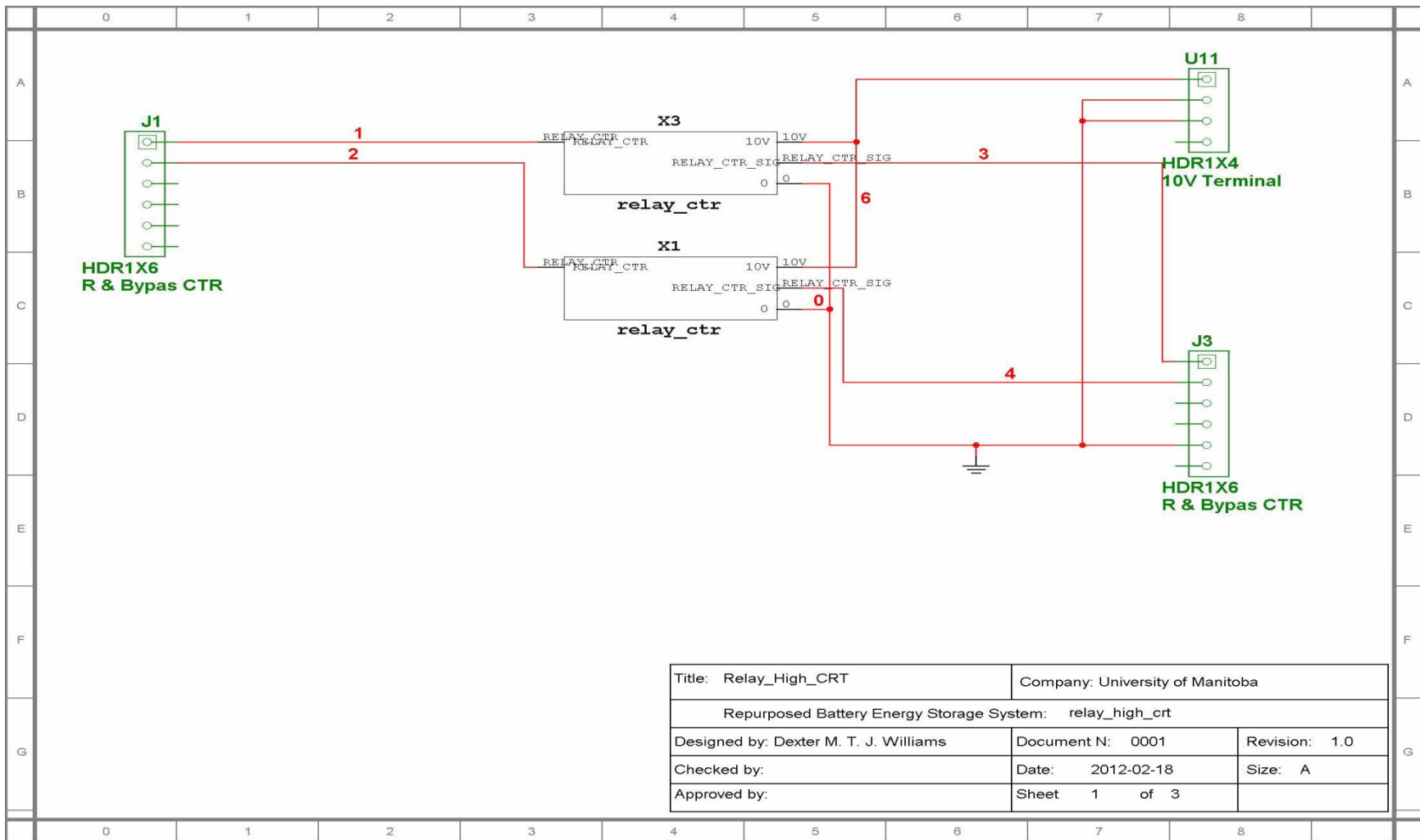


Figure A-18: Repurposed Battery Energy Storage System Schematic 18 of 25.

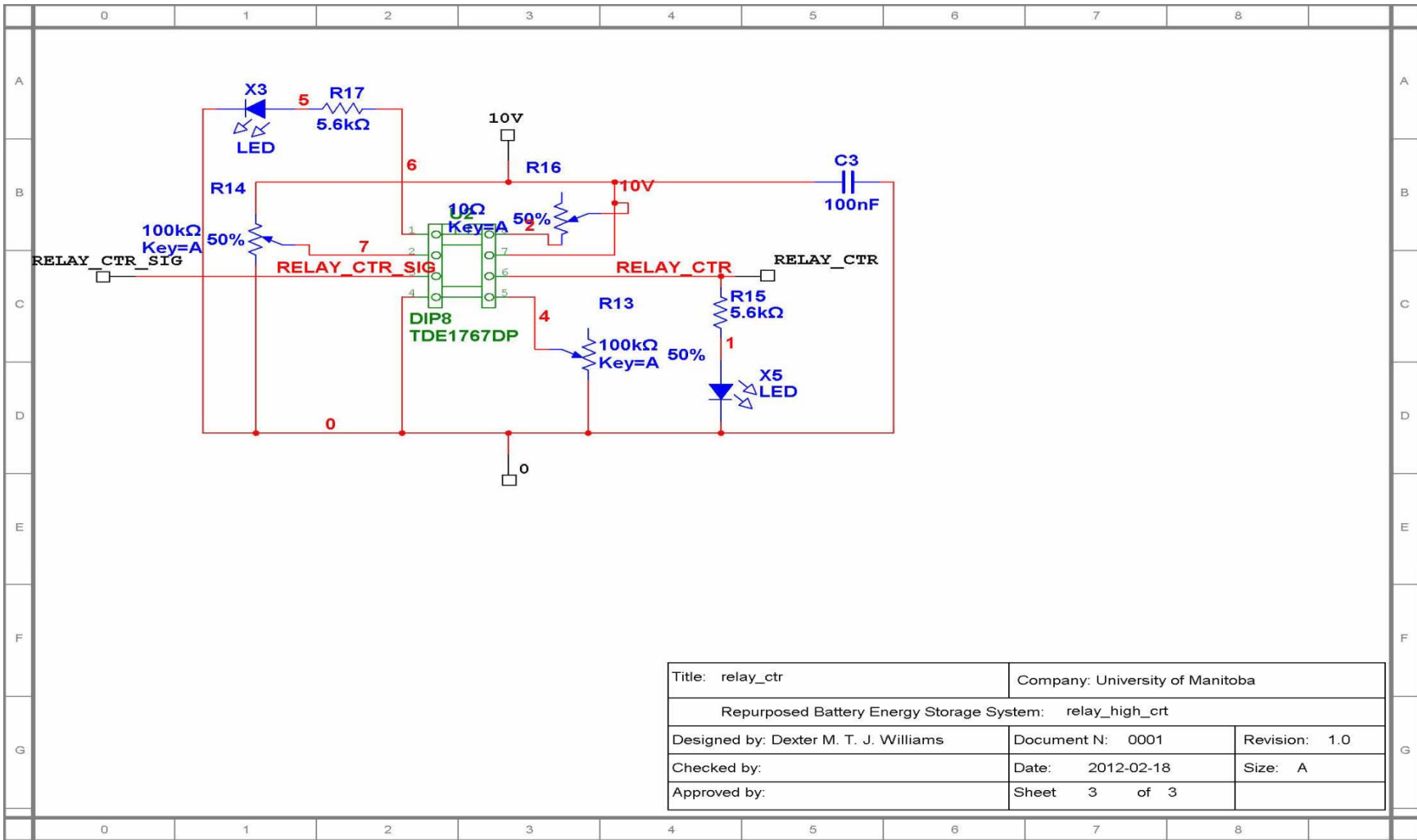
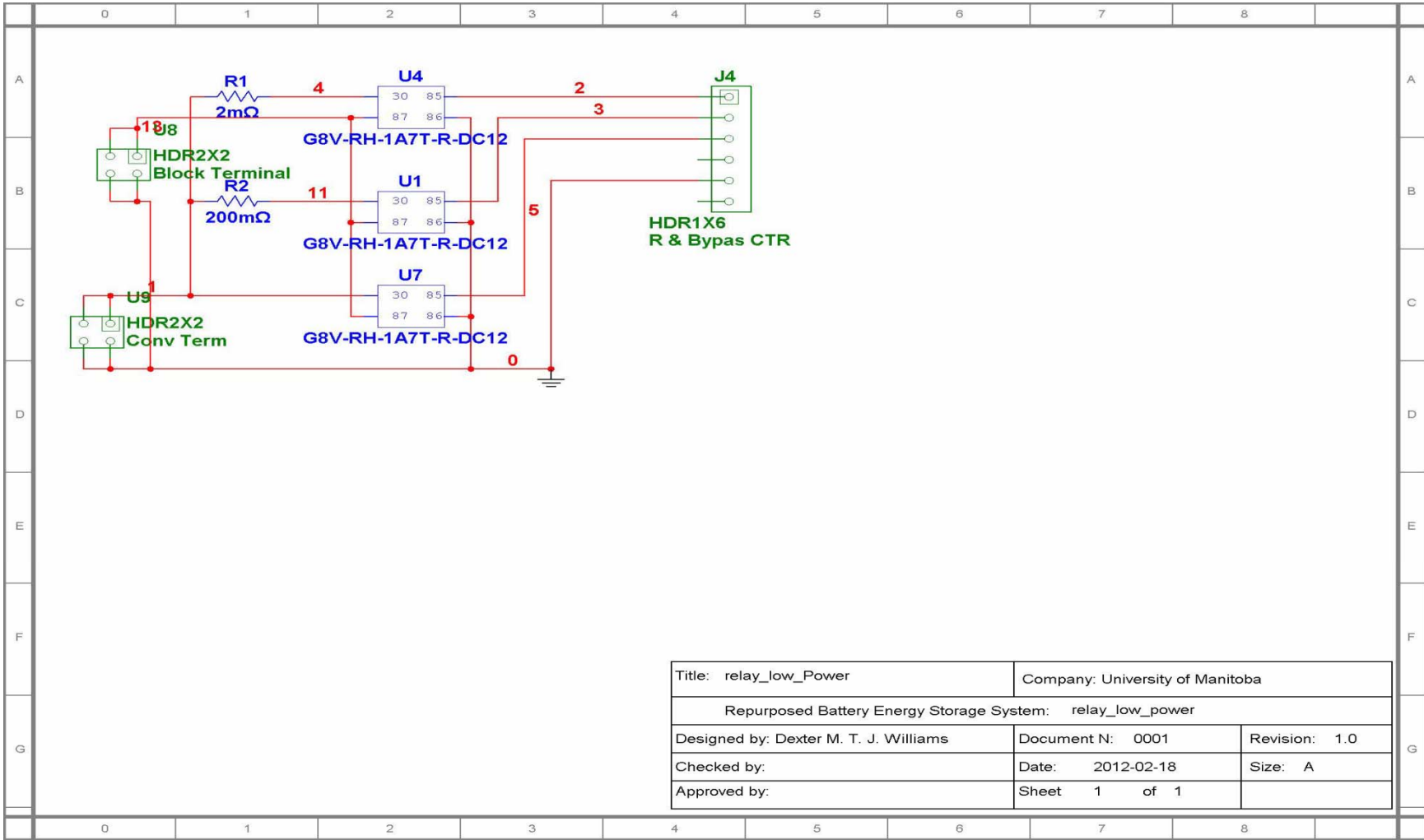


Figure A-20: Repurposed Battery Energy Storage System Schematic 20 of 25.



Title: relay_low_Power		Company: University of Manitoba	
Repurposed Battery Energy Storage System: relay_low_power			
Designed by: Dexter M. T. J. Williams		Document N: 0001	Revision: 1.0
Checked by:		Date: 2012-02-18	Size: A
Approved by:		Sheet 1 of 1	

Figure A-21: Repurposed Battery Energy Storage System Schematic 21 of 25.

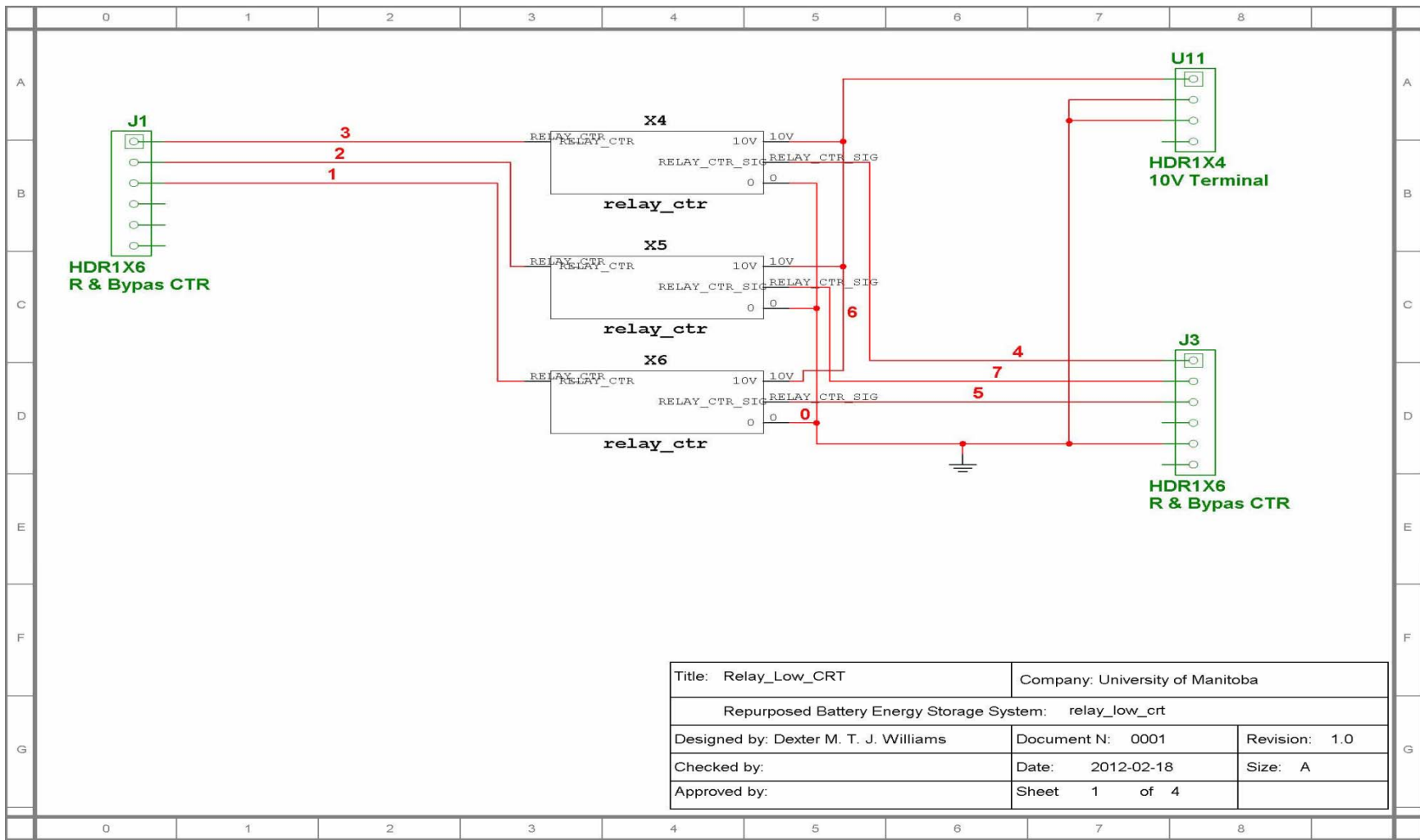


Figure A-22: Repurposed Battery Energy Storage System Schematic 22 of 25.

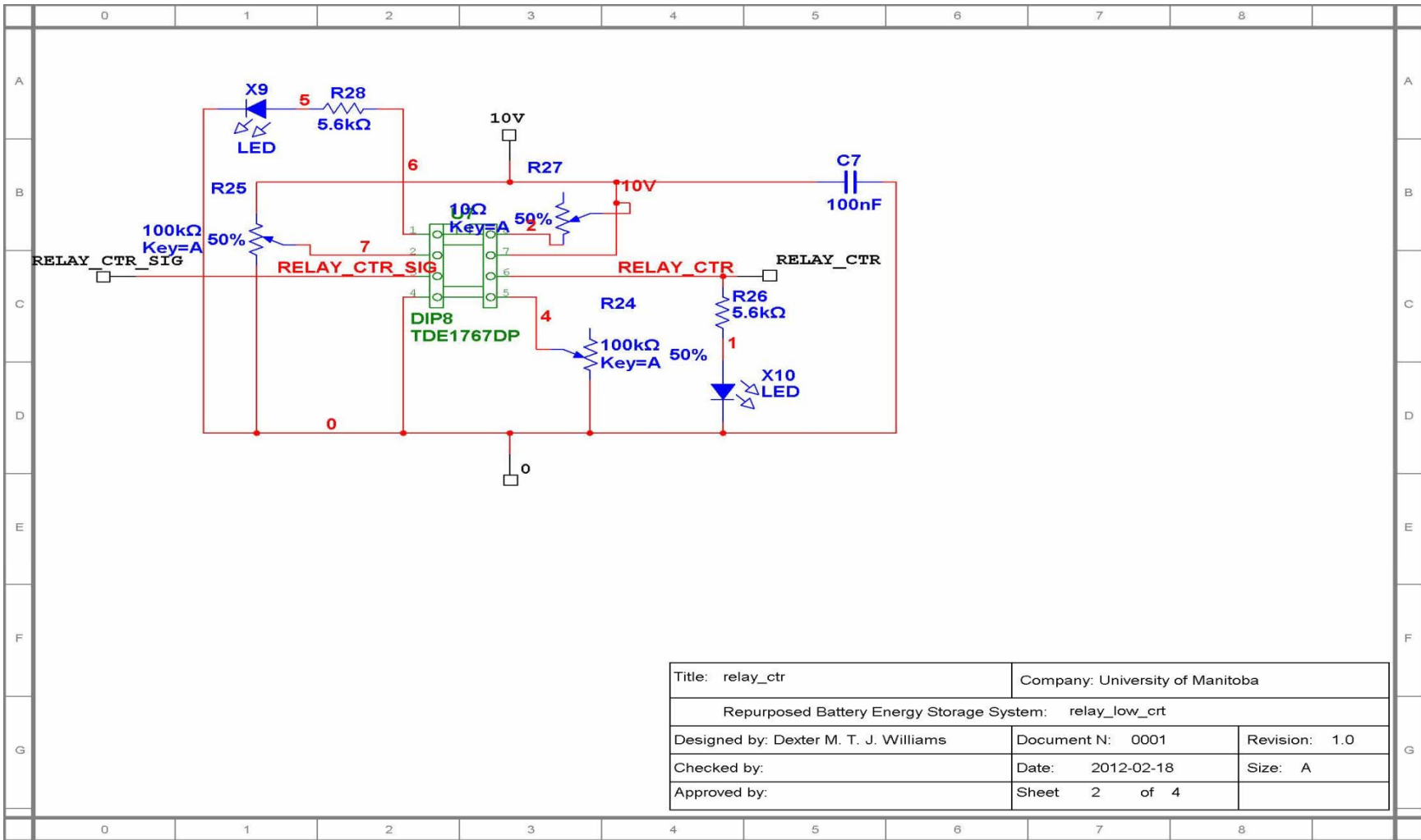


Figure A-23: Repurposed Battery Energy Storage System Schematic 23 of 25.

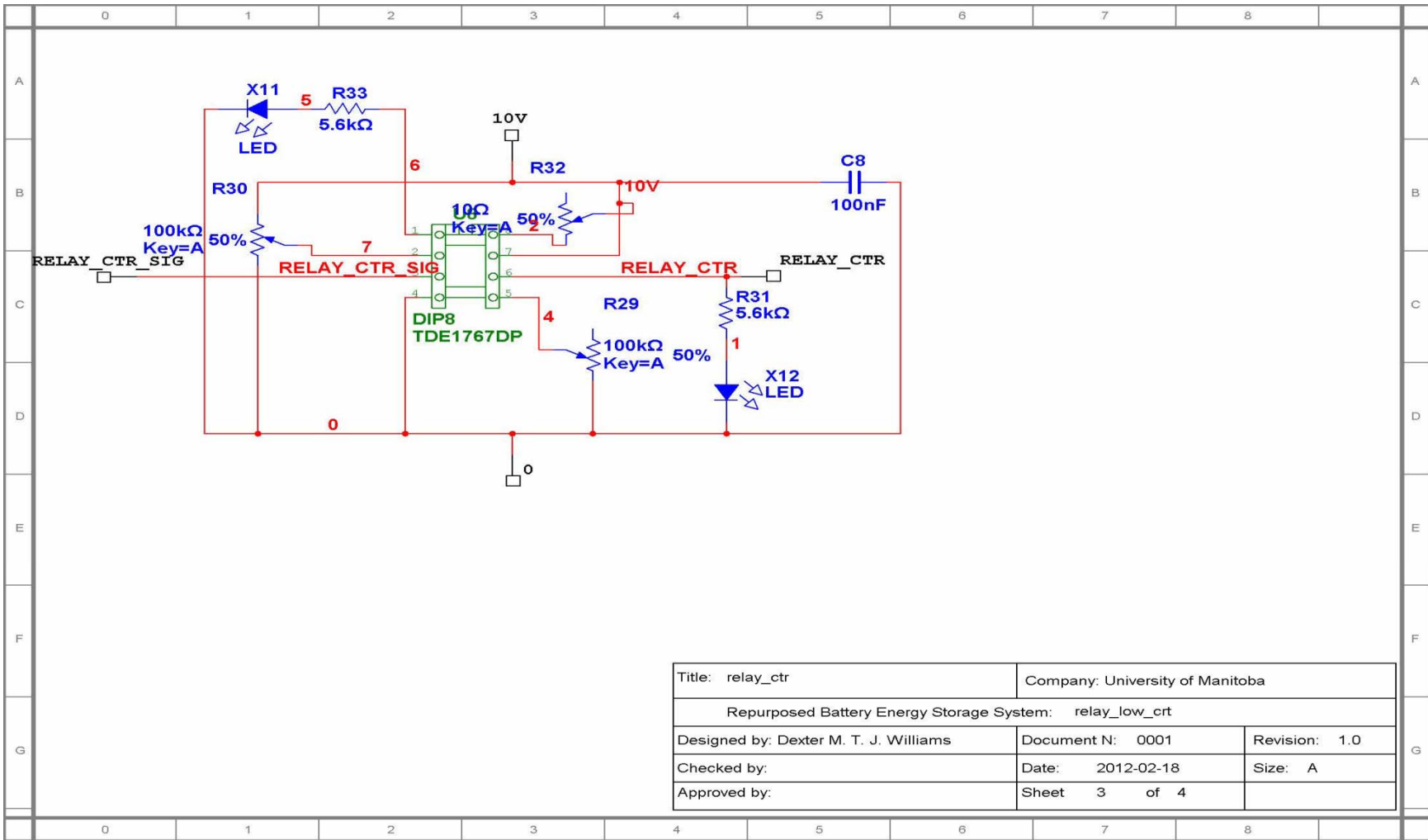
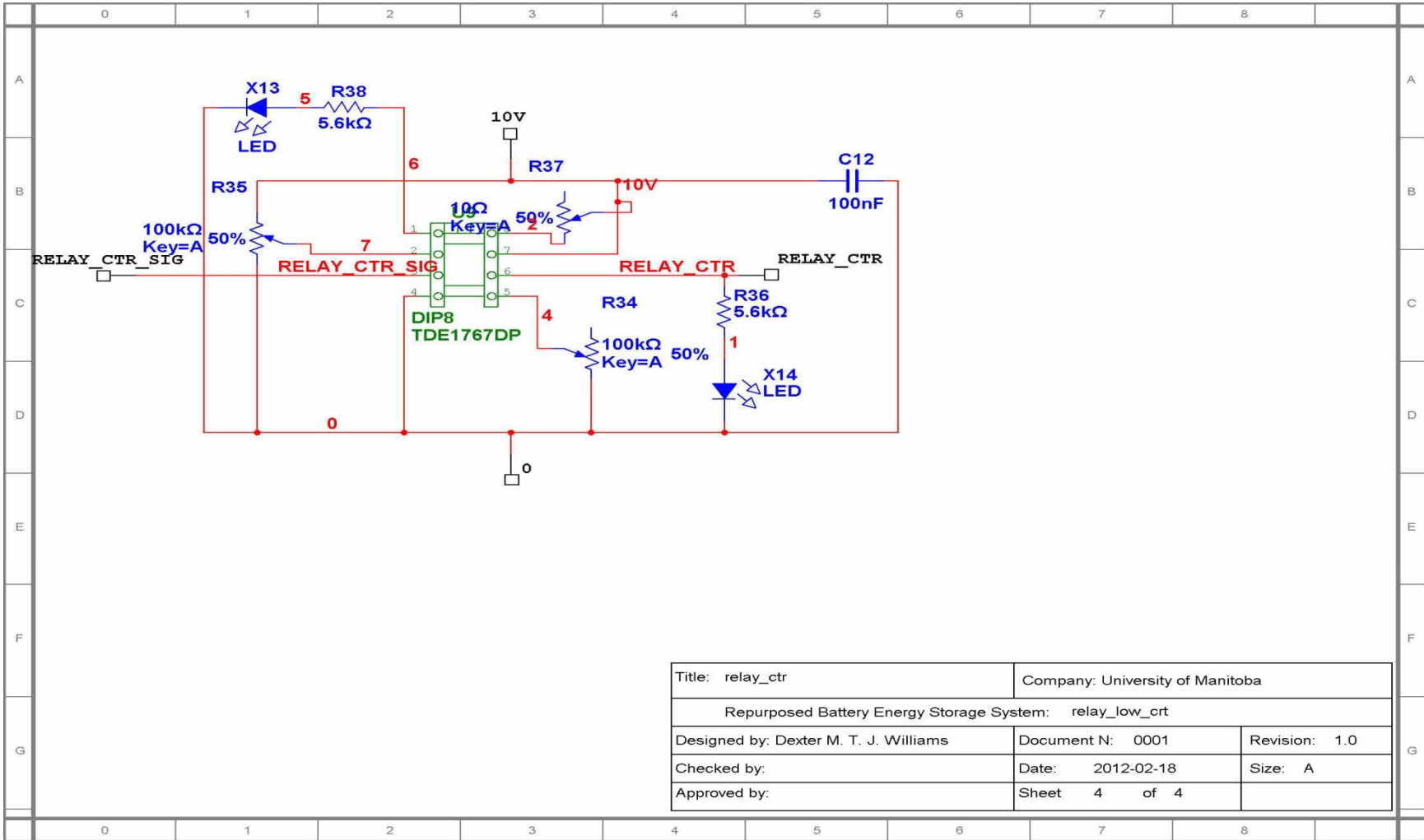


Figure A-24: Repurposed Battery Energy Storage System Schematic 24 of 25.



Title: relay_ctr		Company: University of Manitoba	
Repurposed Battery Energy Storage System: relay_low_ctr			
Designed by: Dexter M. T. J. Williams	Document N: 0001	Revision: 1.0	
Checked by:	Date: 2012-02-18	Size: A	
Approved by:	Sheet 4 of 4		

Figure A-25: Repurposed Battery Energy Storage System Schematic 25 of 25.

Appendix B Battery Profiling System

The battery profiling system was developed as a means to determine the characteristics of a battery (See Figure B-1 bellow). The battery profiling system can be used to determine the open circuit voltage characteristic of a battery and the discharge and the charge capacities of the battery.

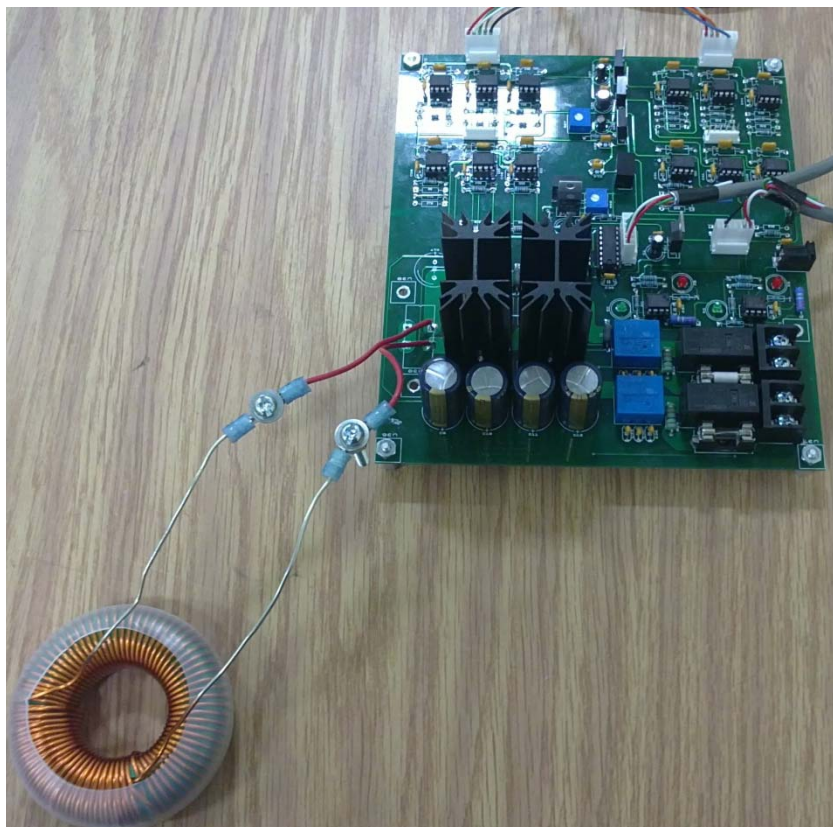


Figure B-1: Battery profiling system board.

The battery profiling system was developed with the same parameters as the stage two converters discussed in this thesis. Thus the battery profiling system was designed as a bidirectional step down and step up converter. The battery profiling system was designed to step up and step down voltages between 8 V and 15 V at the low side voltage

terminals and 25 V to 35 V at the high side voltage terminal. In addition, the battery profiling system is able to handle up to 10 A at the low side voltage terminal and up to 5 A on the high side voltage terminal.

The battery profiling system used the same hardware parameters as the stage two converters. Thus the battery profiling system has 1200 μF capacitors on the high side voltage terminal, 22 μF capacitors on the low voltage terminal and us a 3.3 mH inductor. The battery profiling system utilized a resistor and contactor in parallel to pre-charge (resistor) the system and for continues running of the system (contactor).

Great care was taken in the design of the battery profiling system to prevent noise in the ground distorting the measurements. Thus, two ground plains were created one to for digital signals and power, and one for analog signal. The two ground plains were connected via a 1 Ω resistor and filters. Therefore, this arrangement maintained an equal ground potential in the two circuits and prevented noise migration between the two circuits. The schematics of the battery profiling system are found at the end of this appendix.

In addition, reducing the noise the measurement accuracy was also improved. The voltage measurements were improved by using precision resistors and better tuned filters to measure the voltage. The current measurements were improved by reconfiguring the current sensors for a nominal current range of 5 A to obtain better accuracy.

The battery profiling system utilized similar control algorithms as was used to control the stage 2 converters of the RBESS. In addition, the battery profiling system utilized both a hardware control interface and a software control interface.

The hardware interface of the battery profiling system consists of one LCD, eight slide switches, two push button switches and one rotary dial. The slides switches are used to enable the RBESS, to select the mode of operation and to select the location of the battery that should be on the high or low side of the converter (see control operations in Table B.1). The push button switches work in conjunction with the LCD to scroll through the different pages of the LCD (see Table B.2 for description of pages). Furthermore, the push button switches can also be used to start or stop or reset the RBESS charge converter's controls when they are on the associated LCD page. The rotary dial can be used to increase or decrease the voltage or current depending on the page of the LCD display.

Table B.1: RBESS charge converter switch control interface.

Slide switch	Operation (0/1)
0	Disable/Enable RBESS
1	Step down/Step up control mode
2	Battery low side /battery high side
3-7	Not used

Table B.2: RBESS charge converter display page indexes.

Page index	Page Display
0	Start RBESS
1	Stop RBESS
2	Reset RBESS controls
3	DOD, SOC Capacity
4	High and low side converter voltage and current
5	High and low side bus voltage and current
6	Stage 2 Converter 1 High and low side voltage and current
7	Stage 1 Converter 1 Step down mode: Low side voltage set point, duty cycle, actual voltage Step up mode: High side voltage set point, duty cycle, actual voltage
8	Stage 2 Converter 1 Step down mode: Low side voltage set point, duty cycle, actual voltage Step up mode: High side voltage set point, duty cycle, actual voltage
13	Power on the converter and bus for both the high and low side of the converter

The serial port tab in the GUIs (Figure B-2) is used to initiate serial communication with the board. When the serial port tab is activated it automatically detects any available serial port, and a user can use the interface to connect or to disconnect from a port. All connections and errors are logged in the text box on the serial port tab. The serial port tab also has the ability to enable data logging on connection to the serial port. The logged data is stored in a CSV file that can be used for analysis of the system's operation. (See Table B.3 for data logging format).

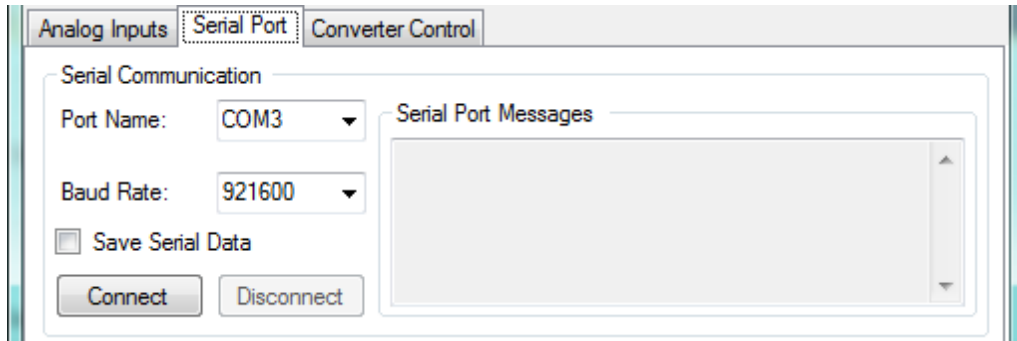


Figure B-2: Serial port tab of GUI.

Table B.3: RBESS charge converter data logging format.

Time			High side Voltage		Low Side Voltage		Current	
Hours	Minutes	Seconds	Bus	Converter	Bus	Converter	High side	Low side
Capacity			Fault		Time			
DOD	SOC		Fault code		Ticks			

The battery profiling system has an additional data logging system that uses the National Instruments USB-6008 Data Acquisition (DAC) board. The USB-6008 has 12bits of pension in comparison to the 10bts of the Cerebot 32MX4 board, thus providing

additional measurement permission. The USB-6008 DAC GUI is seen in Figure B-3. The USB-6008 DAC GUI allows the selection of the channels to measure the type of measurements, the frequency of samples and the number of samples. The USB-6008 DAC GUI (Analog input tab) (see Figure B-3) allows for starting and stopping the data logging process. The data is logged in a CSV file that contains the current time and the selected channels data.

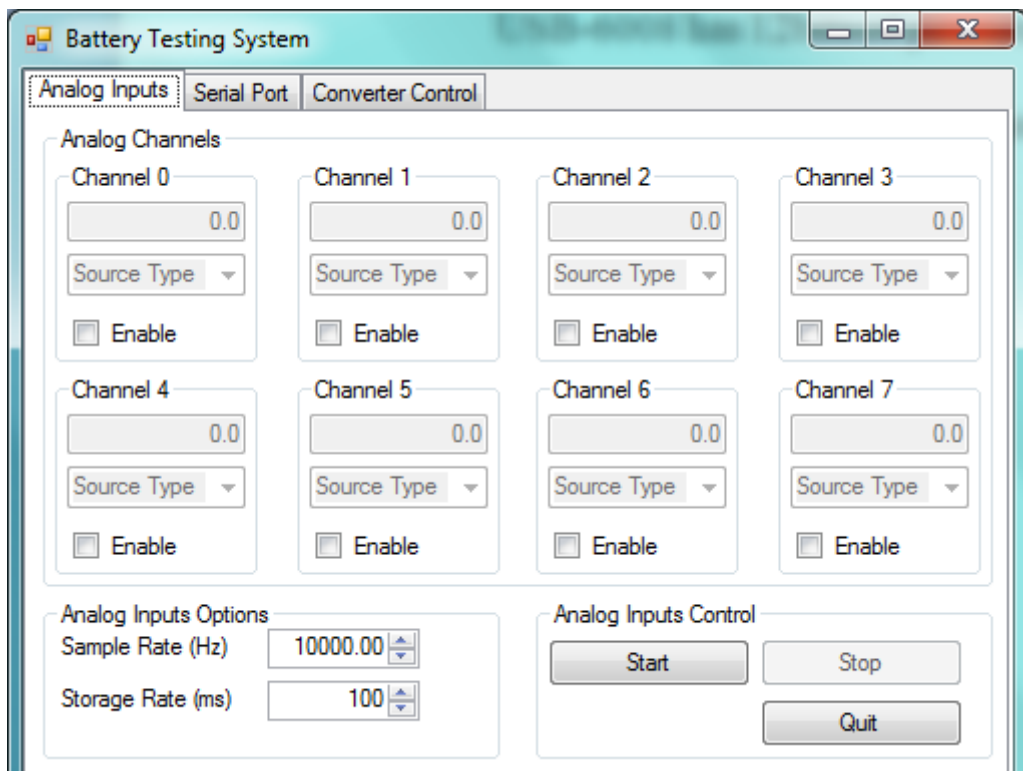


Figure B-3: The USB-6008 DAC GUI interface.

The battery profiling system GUI's converter control tab (Figure B-4) provides online monitoring and control of the battery profiling system. The battery profiling system GUI's converter control tab displays all measured currents and voltages on the high and low sides of the converters. In addition, the battery profiling system GUI's

converter control tab allows the set points for the bus voltages and currents to be changed. Furthermore, battery profiling system GUI's converter control tab permits online tuning of the converter controls. Finally, the battery profiling system GUI's converter control tab allows for the selection of the side the battery is on, for the mode of operation of the converter, for enabling or disabling the converter and for starting or stopping the converter.

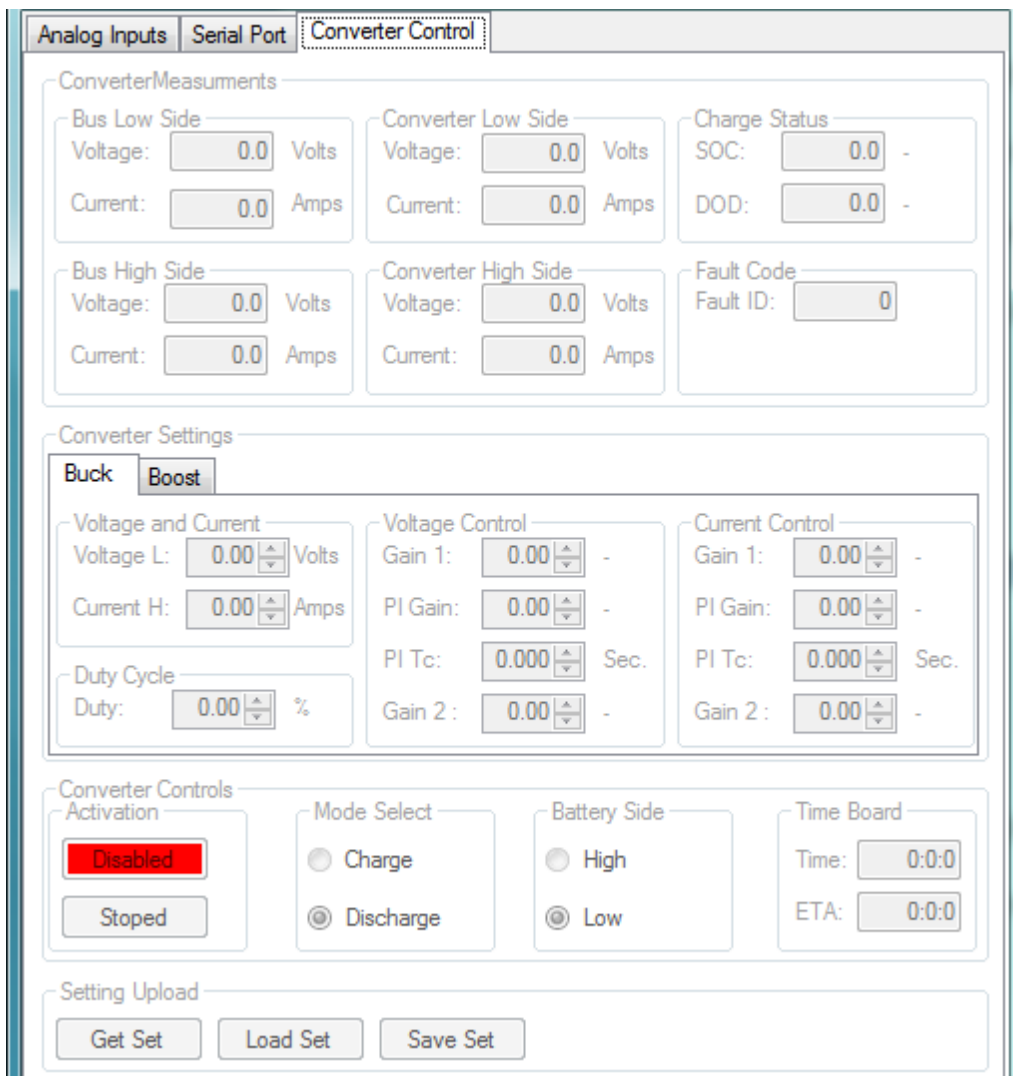


Figure B-4: the battery profiling system GUI's converter control tab.

The K2 battery was profiled to determine its open circuit characteristics. The K2 battery's open circuit characteristic was determined with the battery profiling system for both charging and discharging of the battery. The open circuit test required the running of the battery profiling system at a constant current for a capacity change of 10% followed by a 30 minute rest period for voltage recover. Then the process is repeated until the battery is fully charged or discharged. The results of the open circuit test are seen in Figure B-5 and Figure B-6 and the resulting open circuit characteristic is seen in Figure B-7.

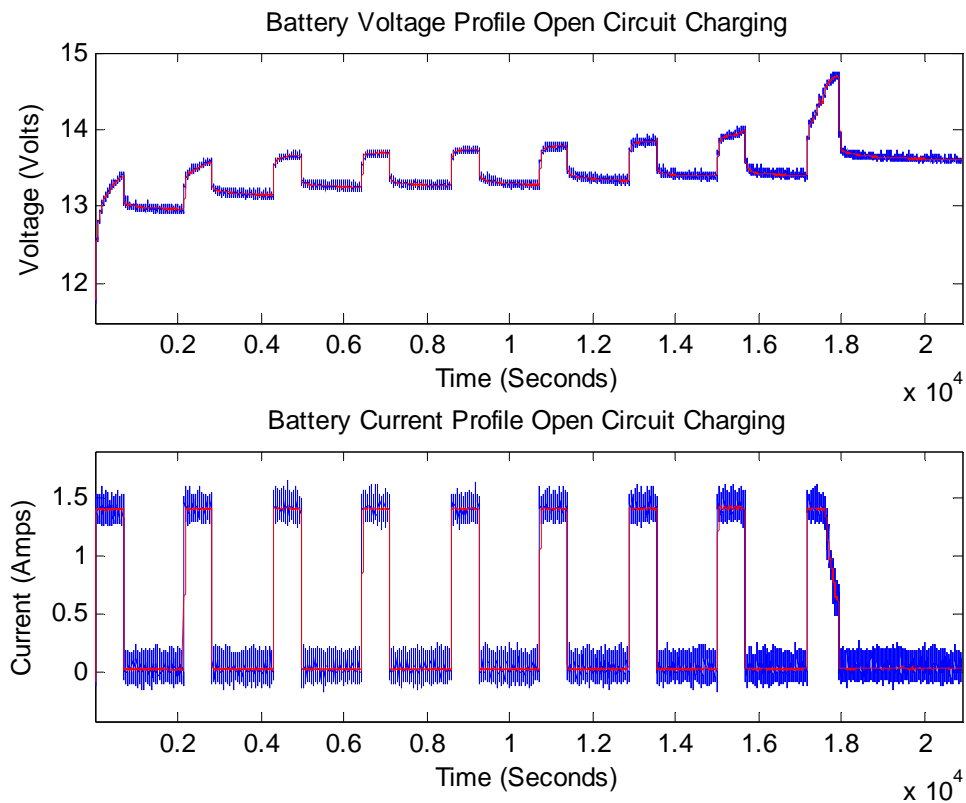


Figure B-5: K2 Battery charging open circuit test.

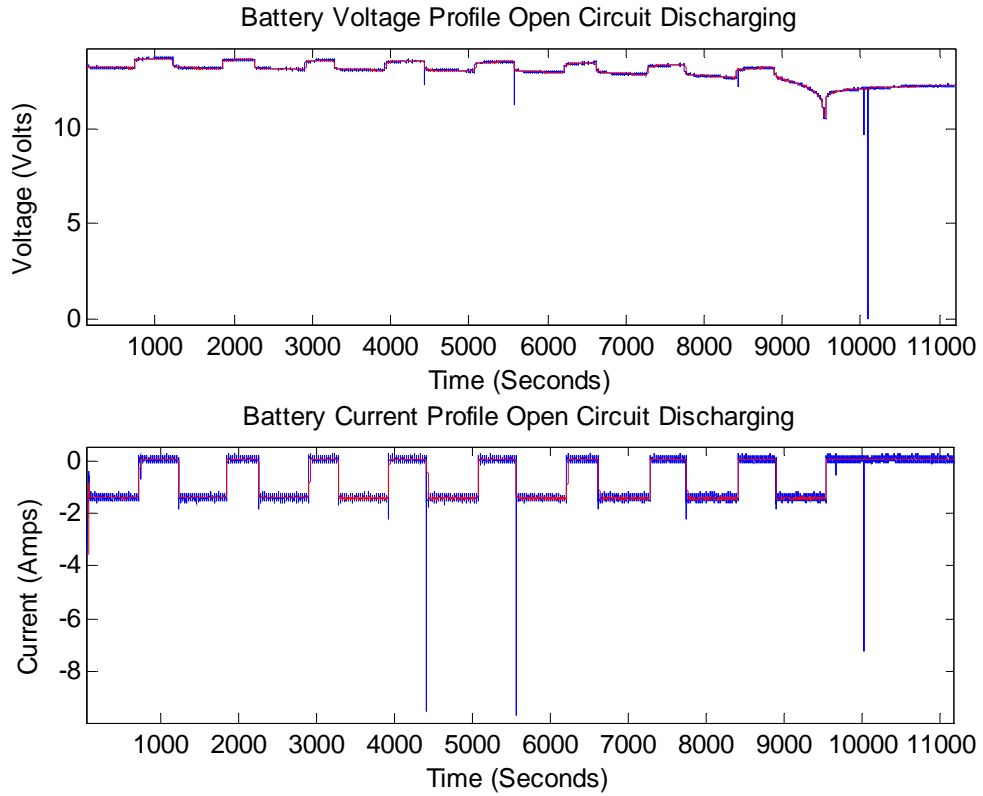


Figure B-6: K2 Battery discharging open circuit test.

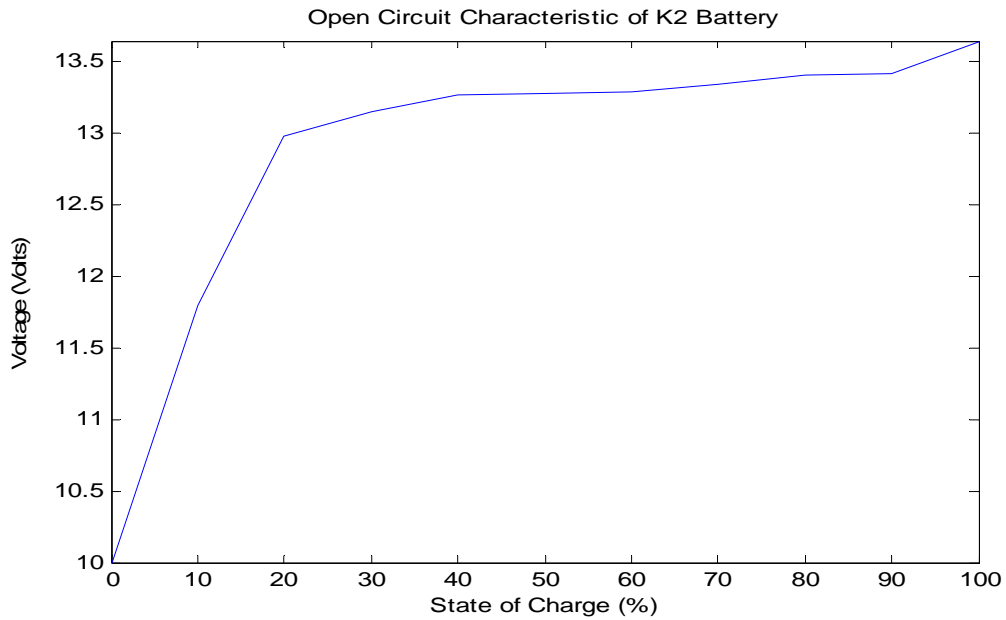


Figure B-7: K2 Battery open circuit voltage SOC characteristic.

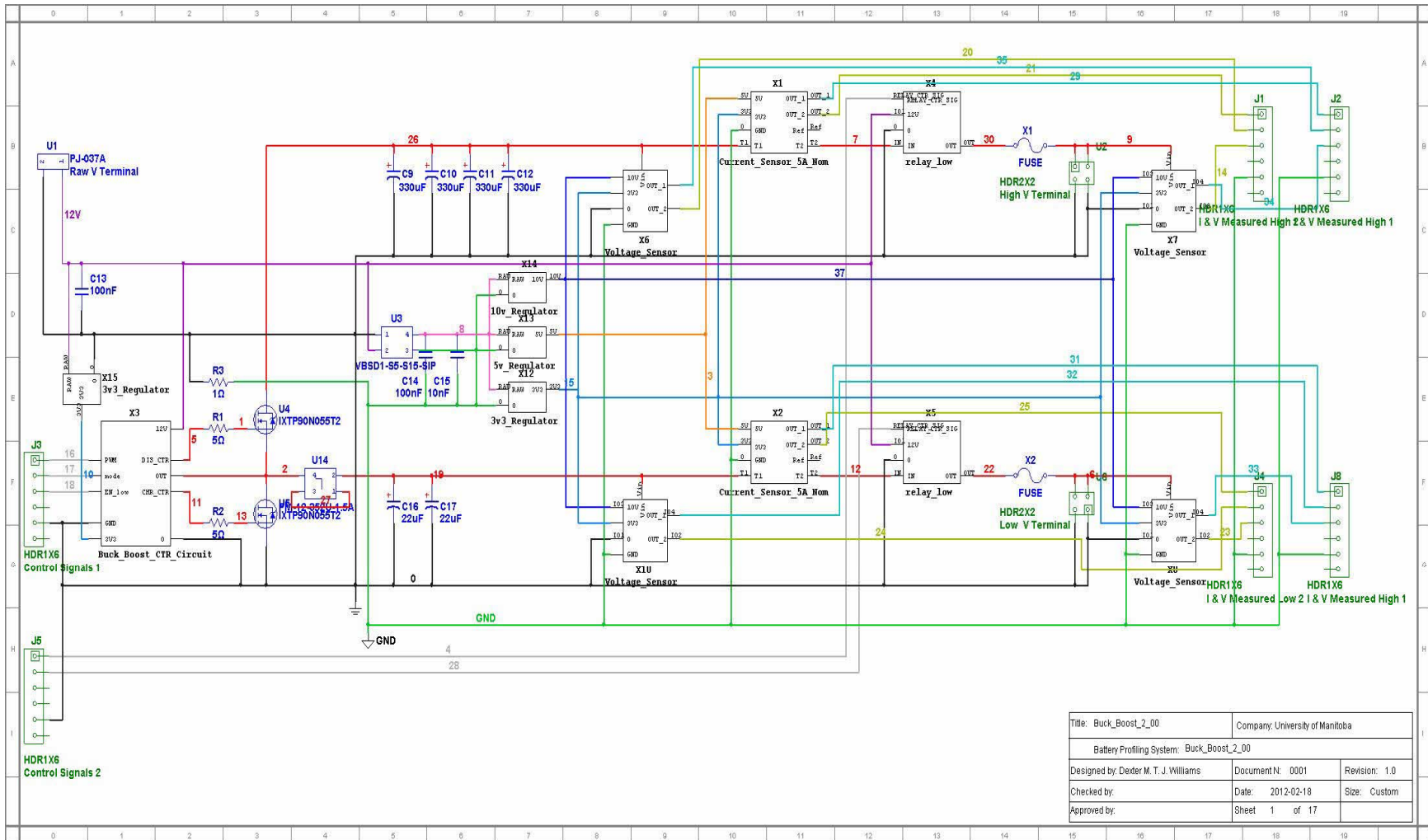


Figure B-8: Battery profiler system schematic 1 of 17.

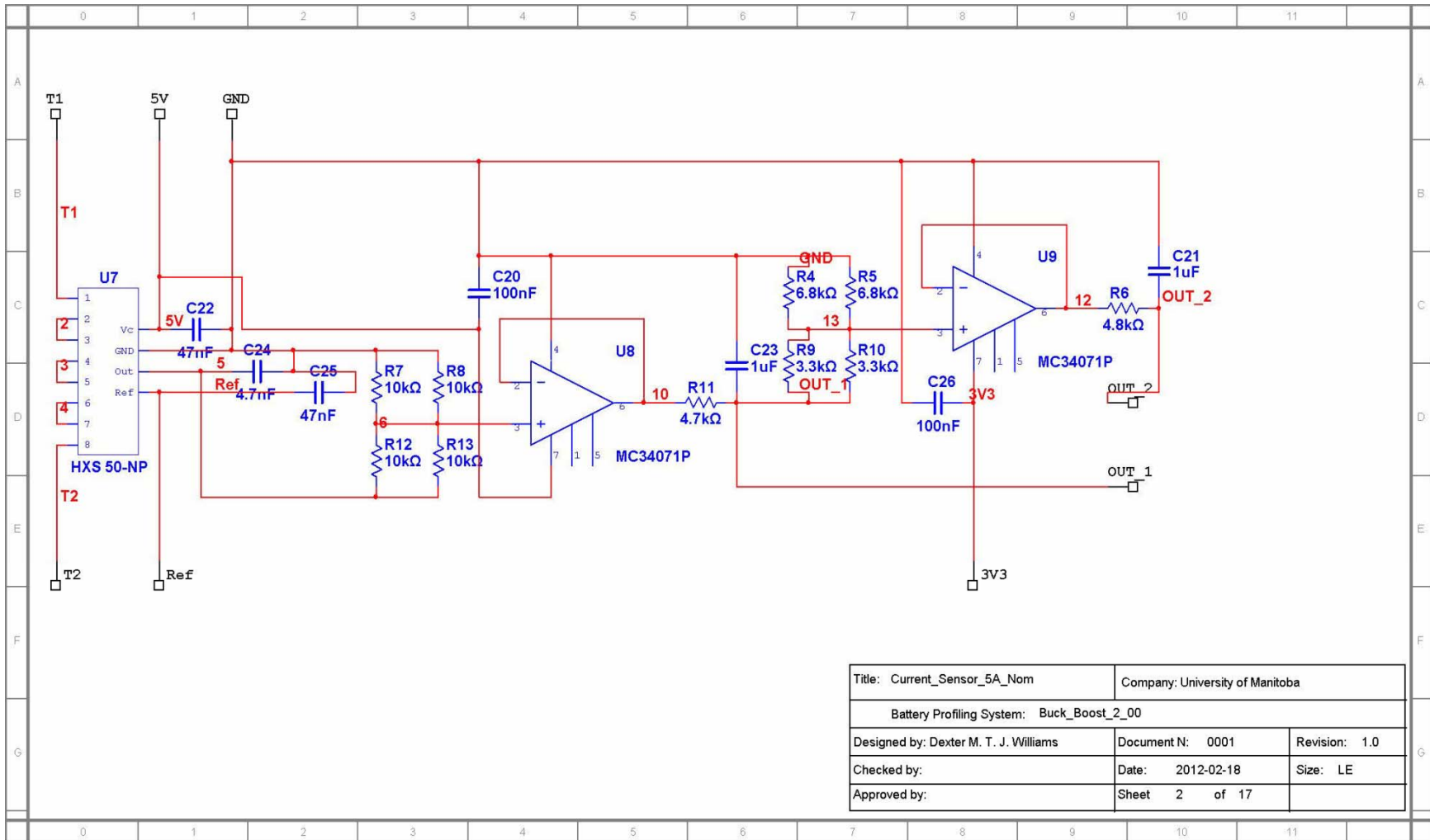


Figure B-9: Battery profiler system schematic 2 of 17.

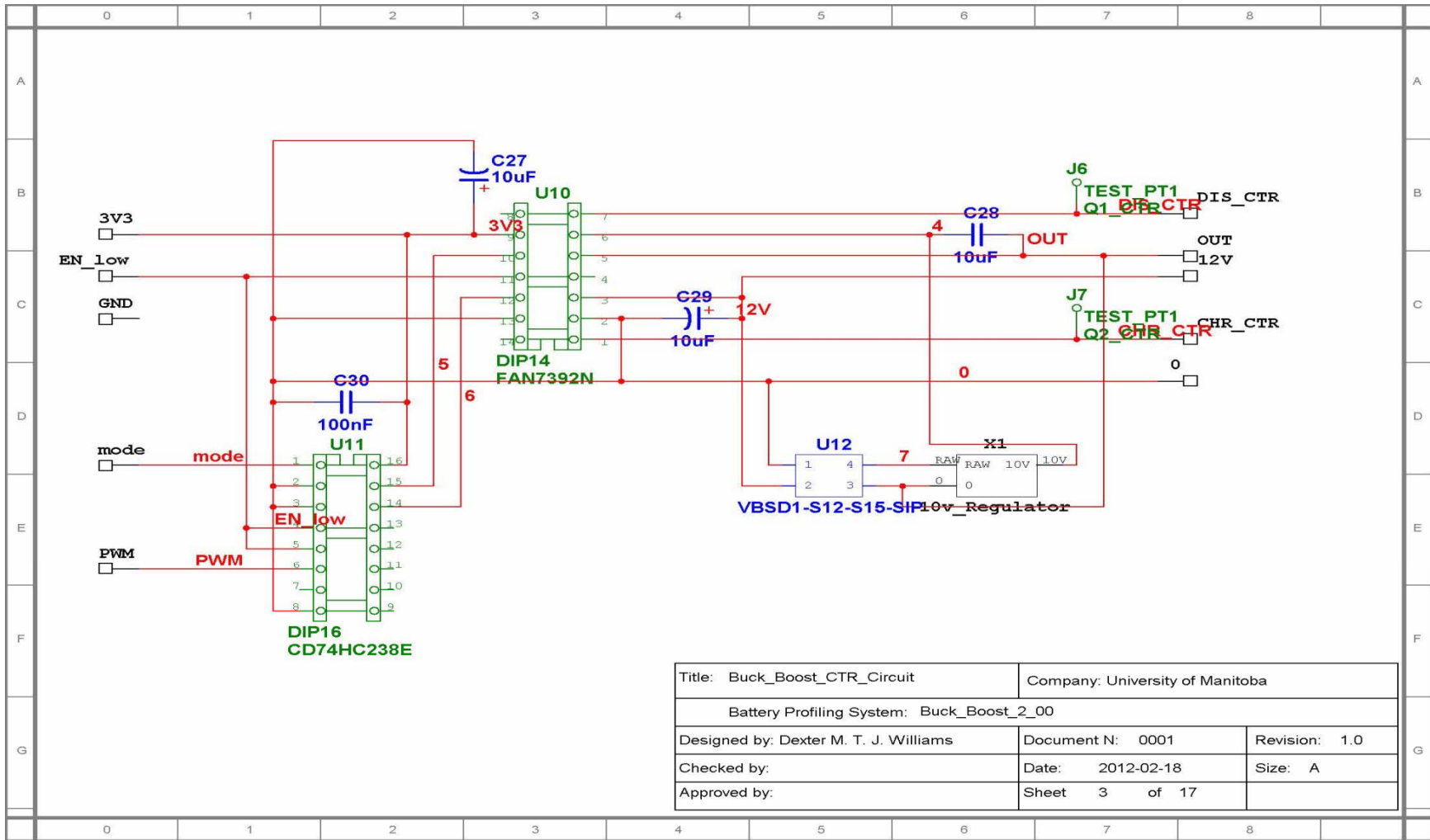


Figure B-10: Battery profiler system schematic 3 of 17.

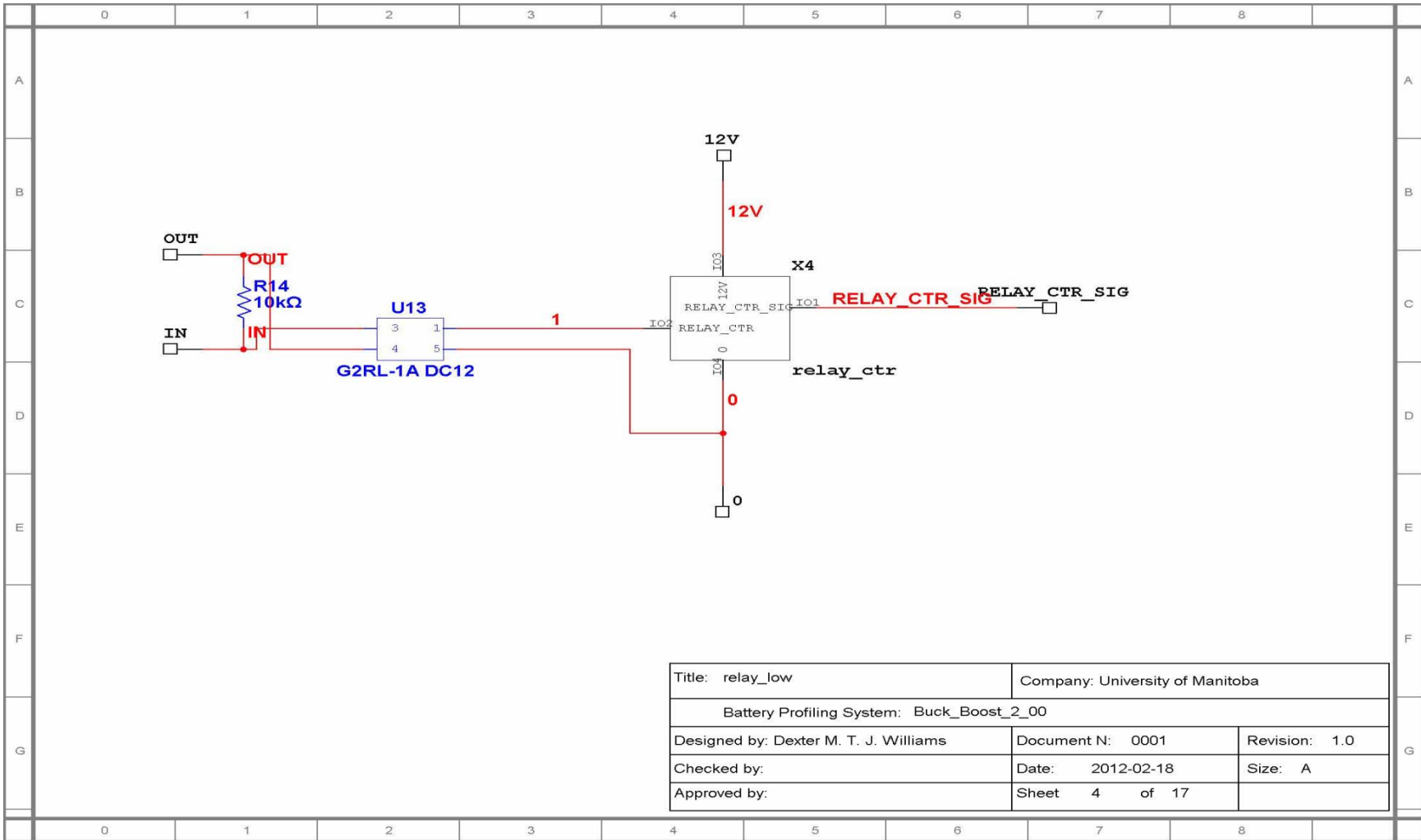


Figure B-11: Battery profiler system schematic 4 of 17.

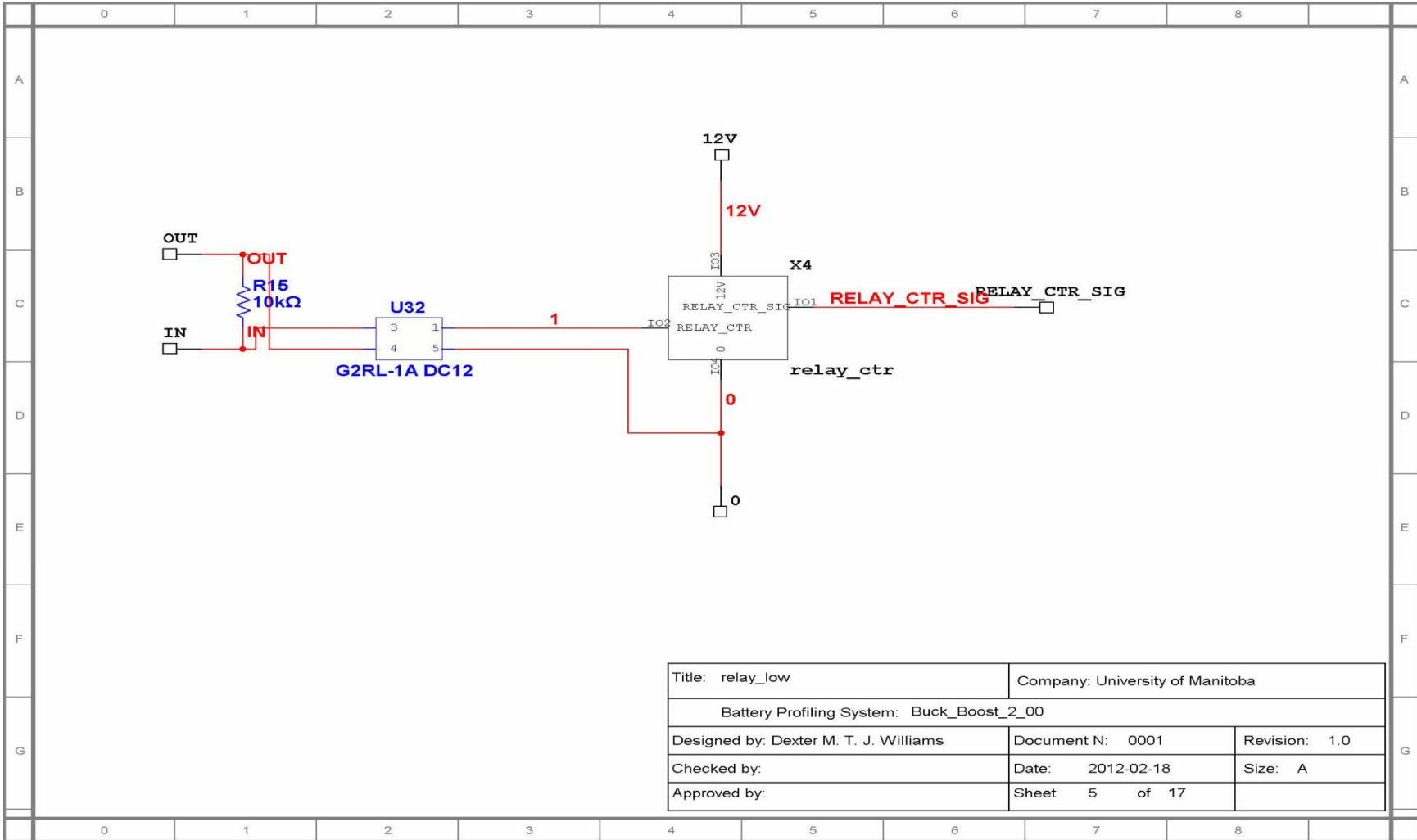


Figure B-12: Battery profiler system schematic 5 of 17.

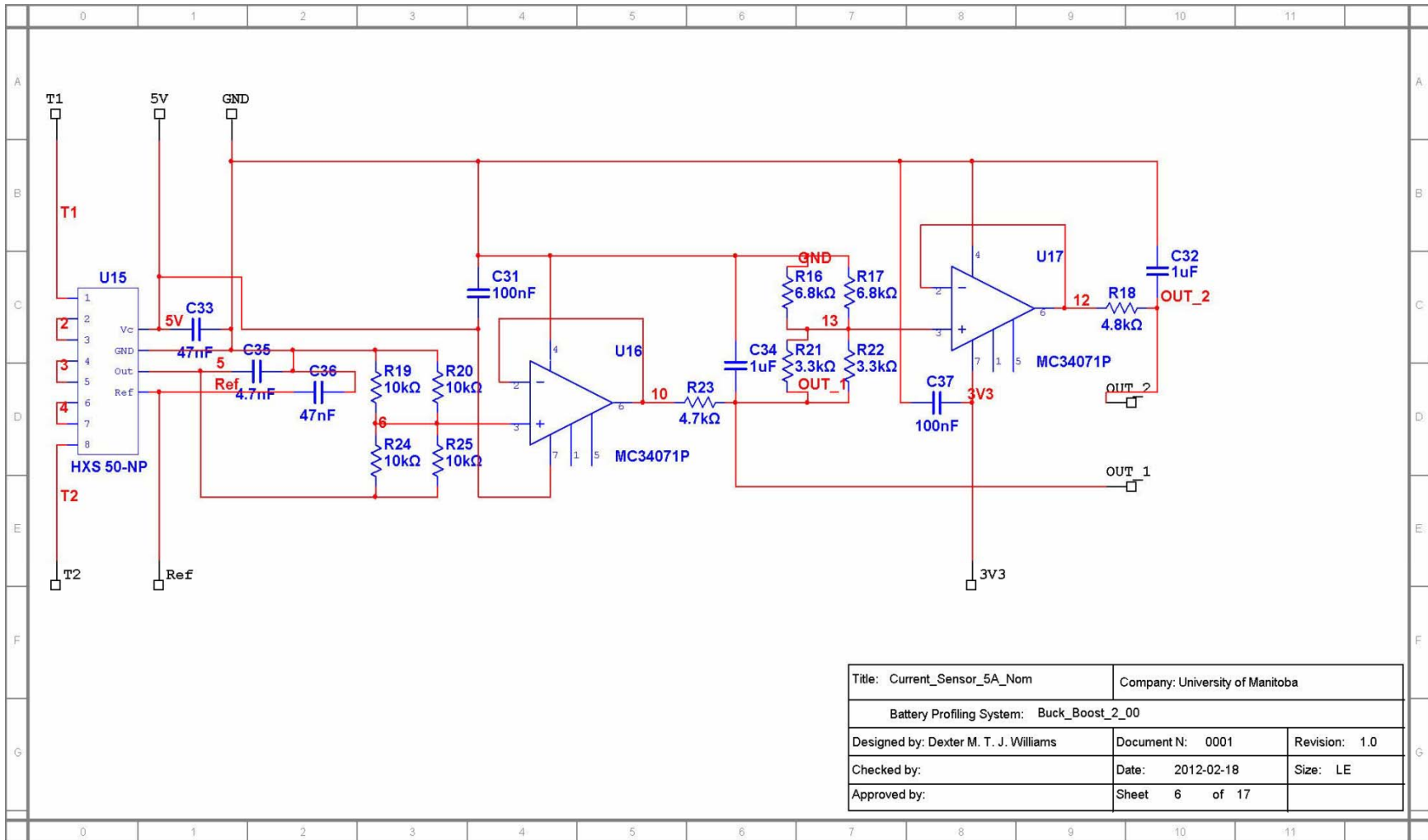


Figure B-13: Battery profiler system schematic 6 of 17.

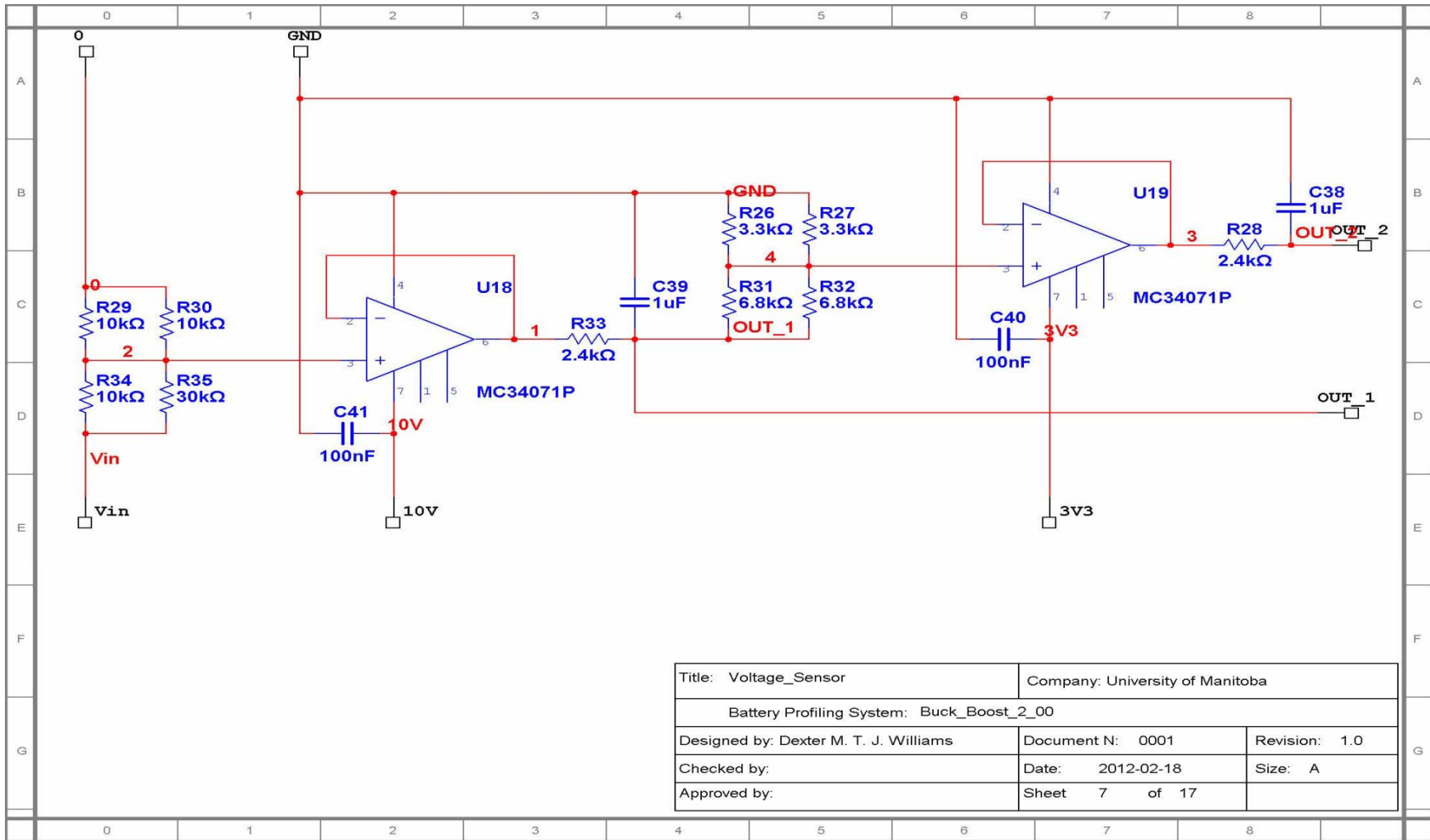


Figure B-14: Battery profiler system schematic 7 of 17.

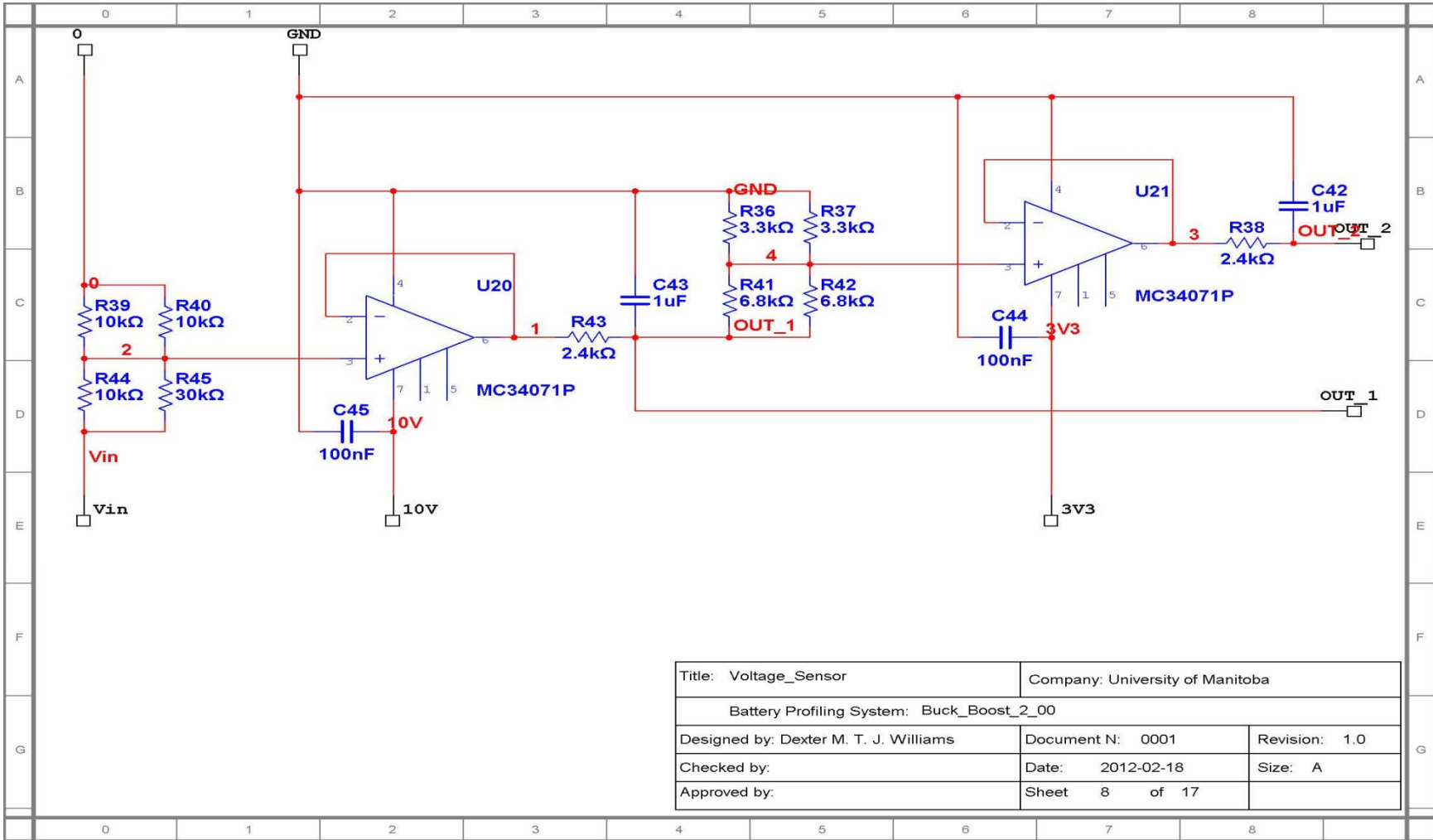


Figure B-15: Battery profiler system schematic 8 of 17.

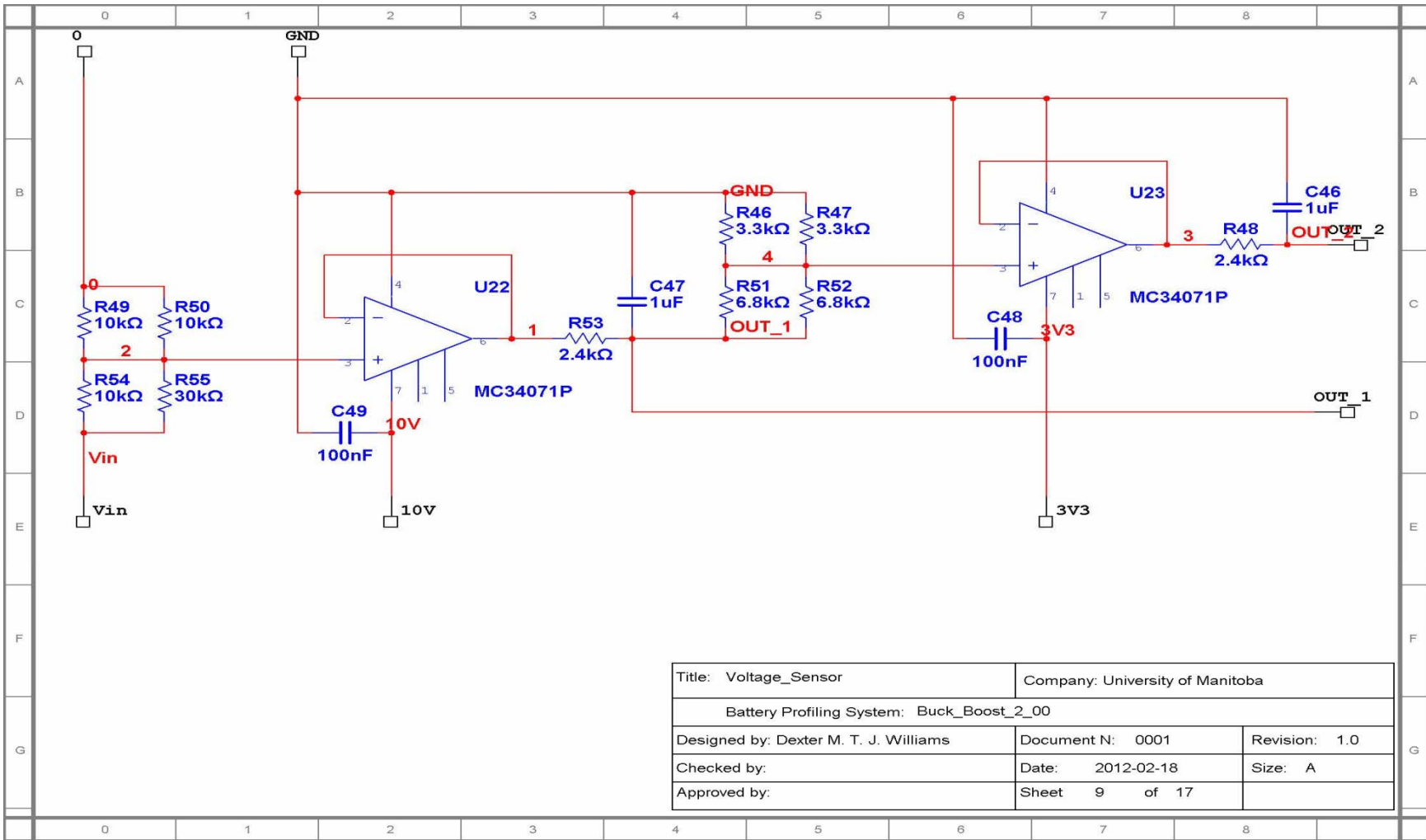


Figure B-16: Battery profiler system schematic 9 of 17.

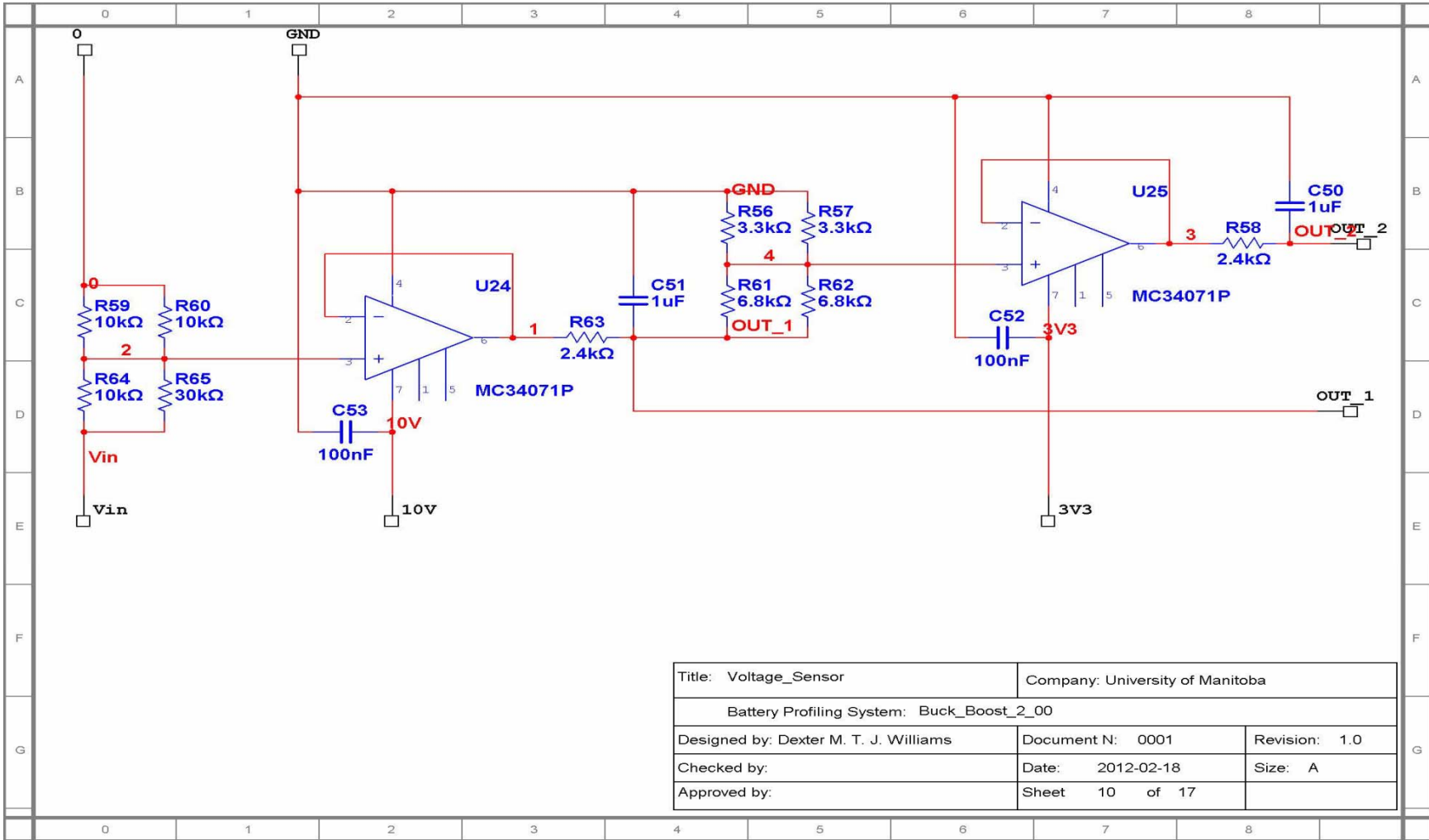


Figure B-17: Battery profiler system schematic 10 of 17.

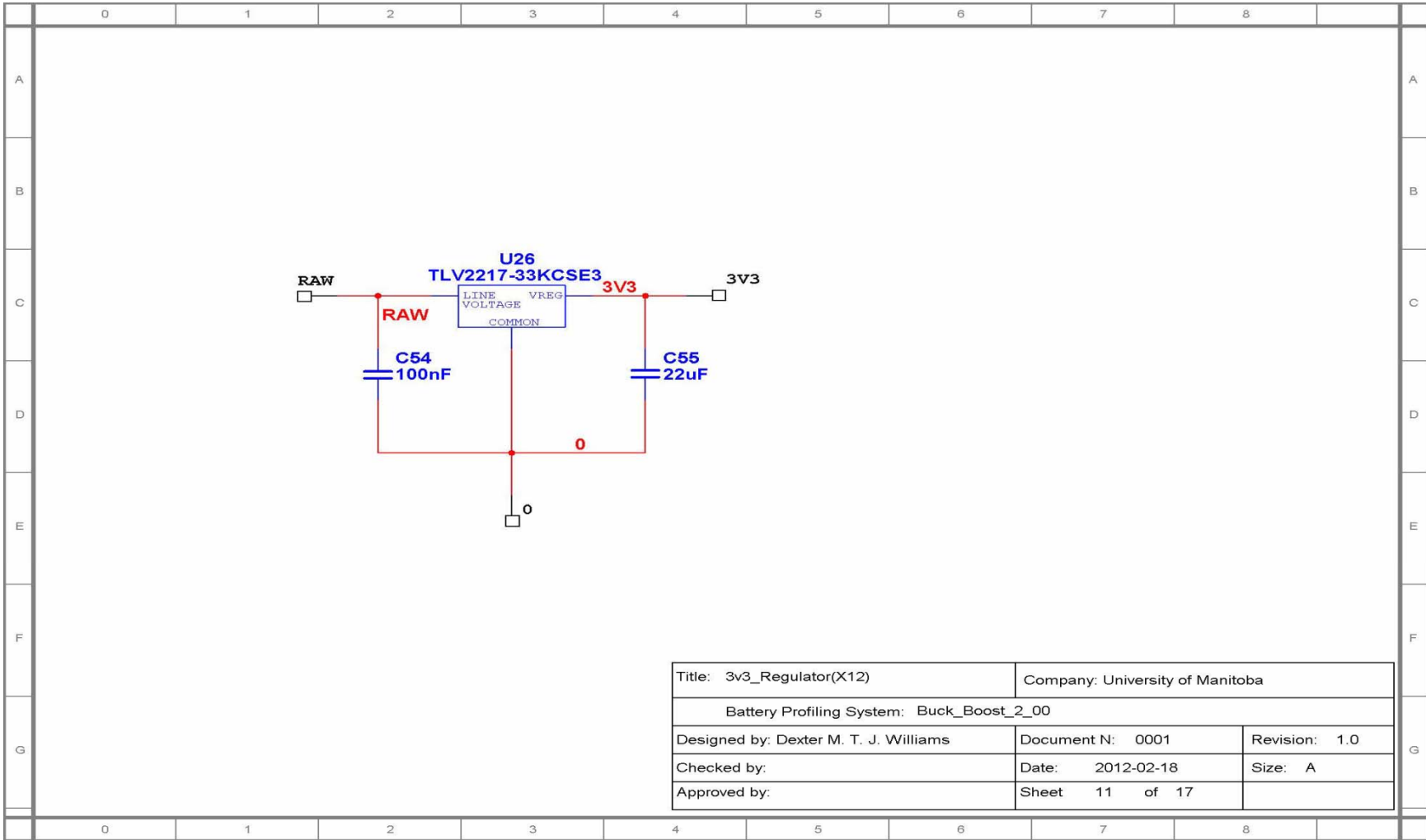


Figure B-18: Battery profiler system schematic 11 of 17.

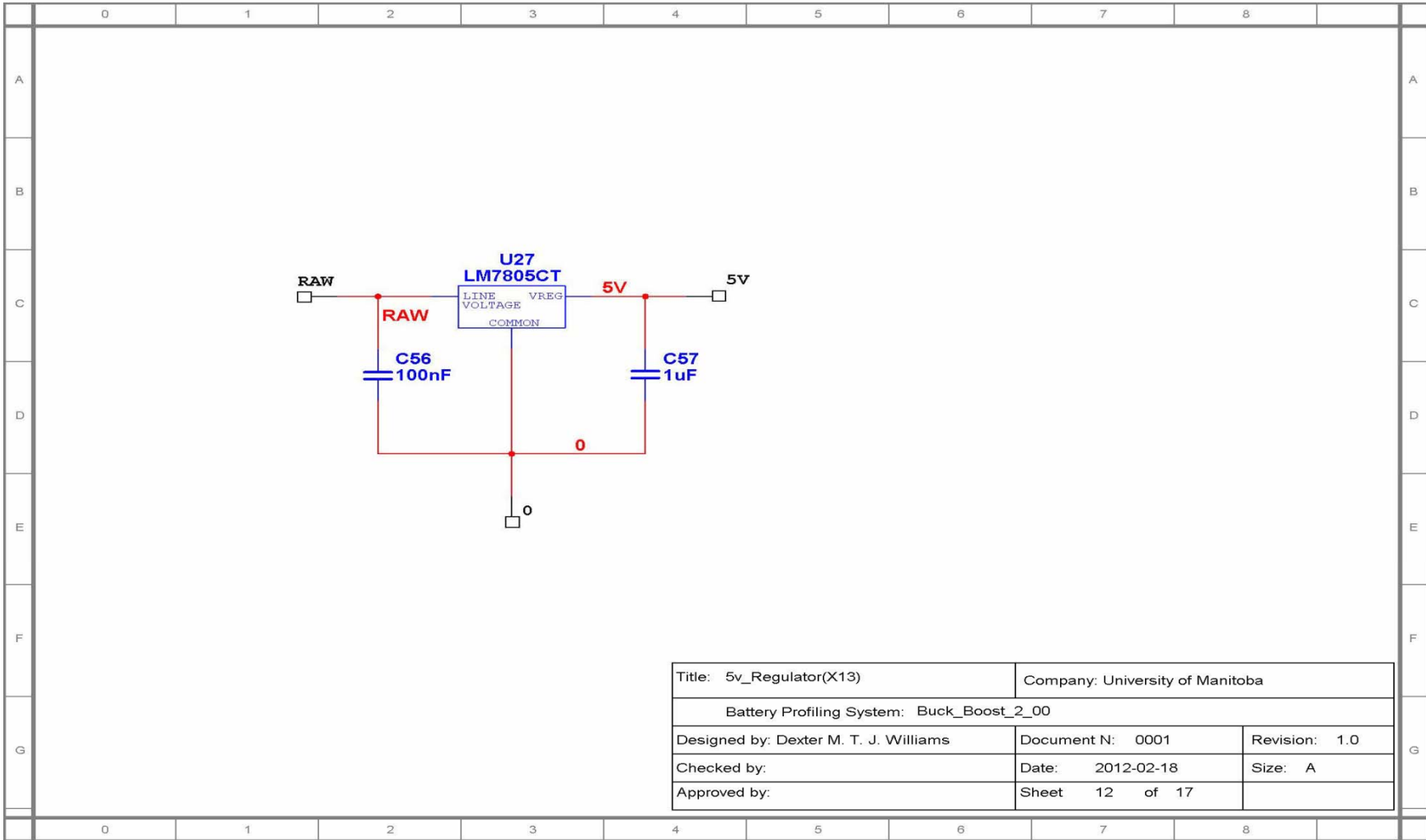


Figure B-19: Battery profiler system schematic 12 of 17.

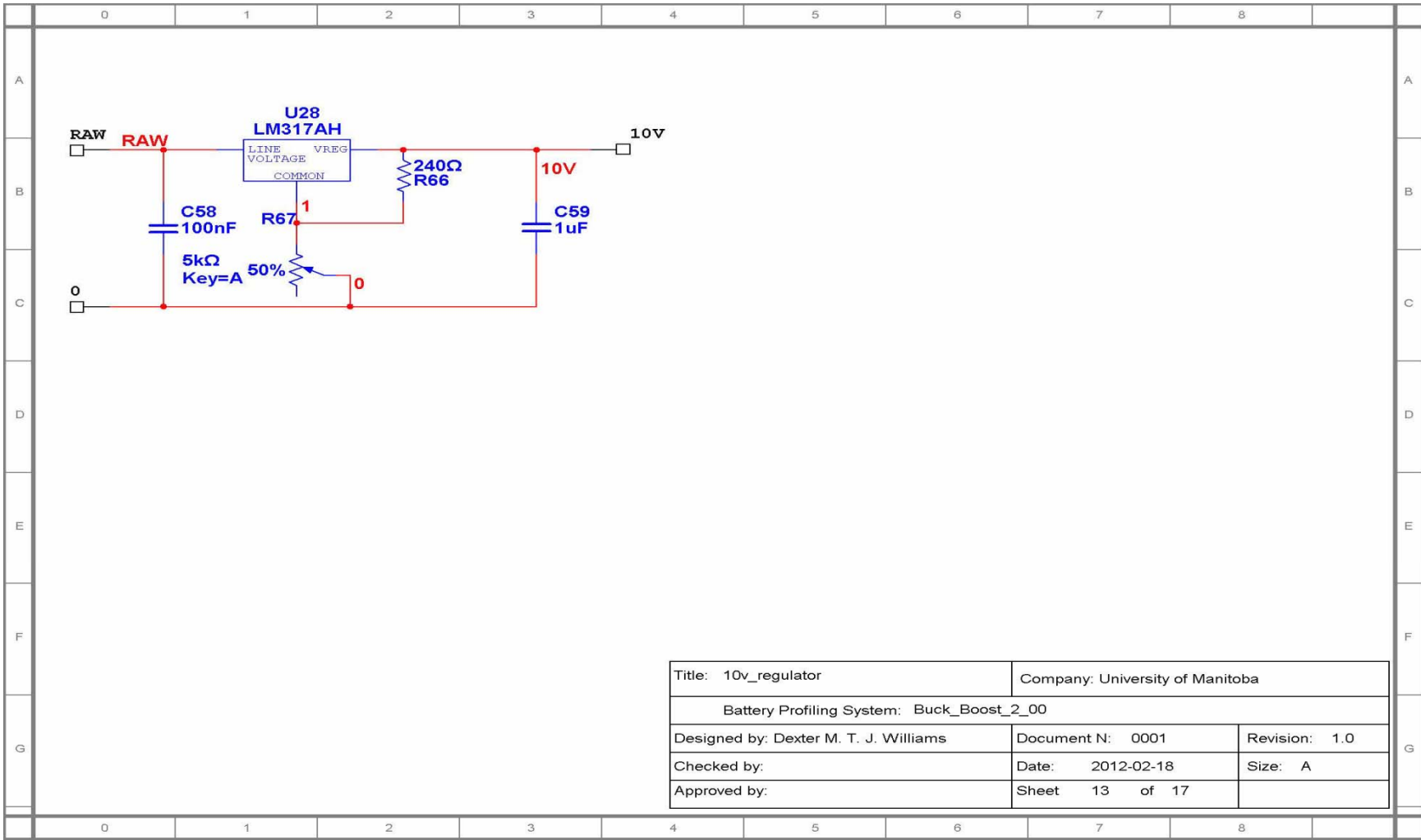


Figure B-20: Battery profiler system schematic 13 of 17.

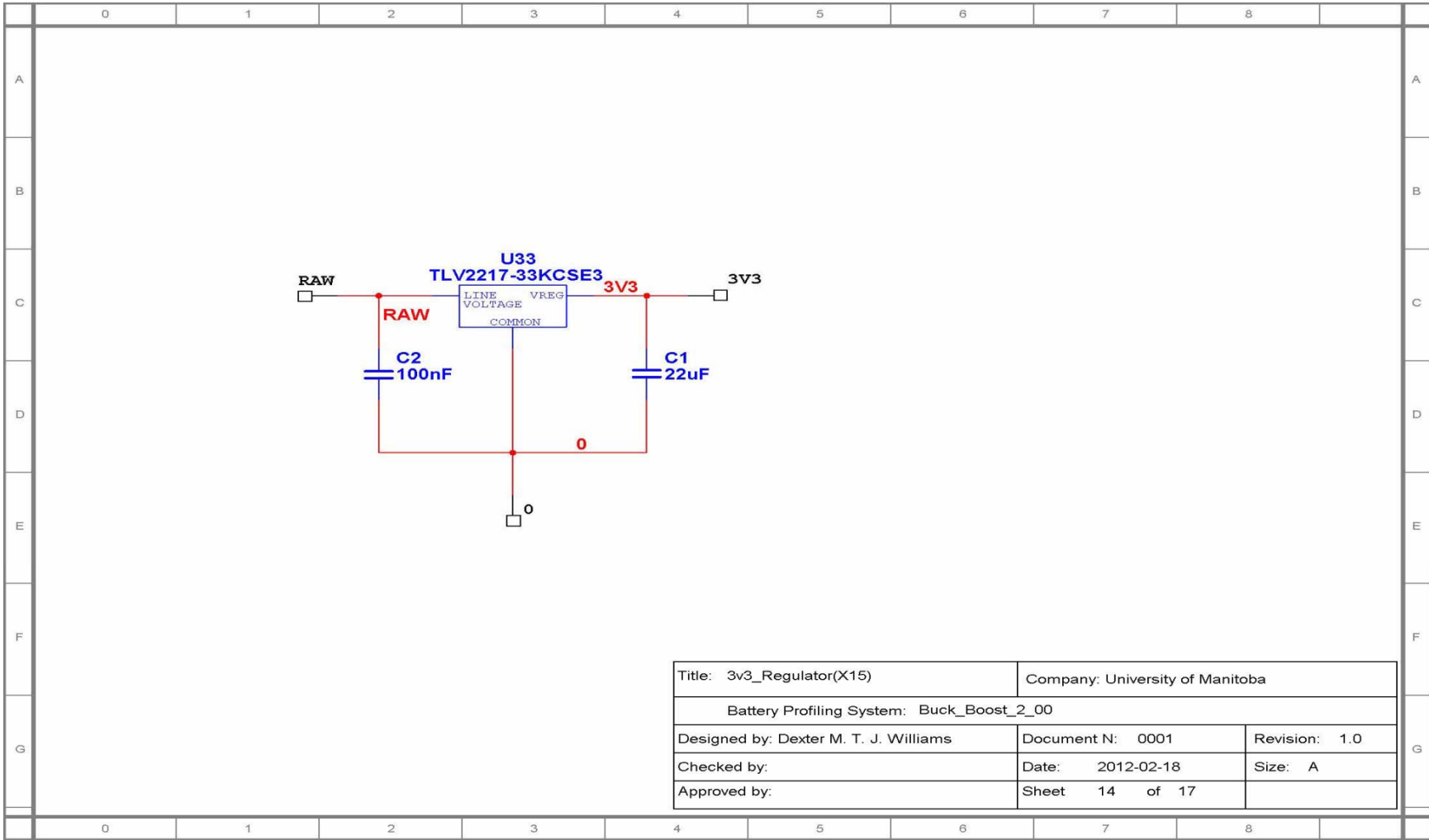
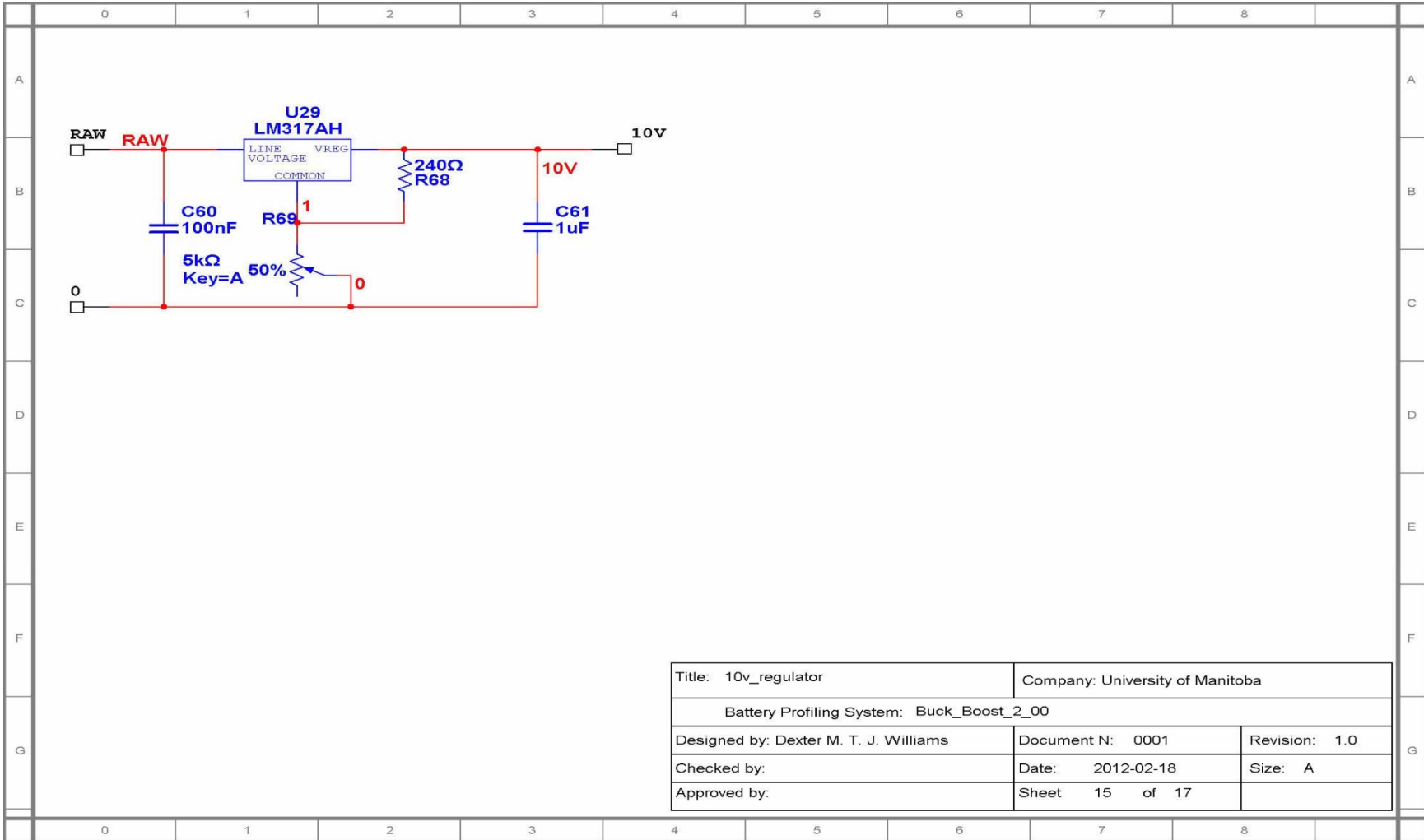


Figure B-21: Battery profiler system schematic 14 of 17.



Title: 10v_regulator		Company: University of Manitoba	
Battery Profiling System: Buck_Boost_2_00			
Designed by: Dexter M. T. J. Williams		Document N: 0001	Revision: 1.0
Checked by:		Date: 2012-02-18	Size: A
Approved by:		Sheet 15 of 17	

Figure B-22: Battery profiler system schematic 15 of 17.

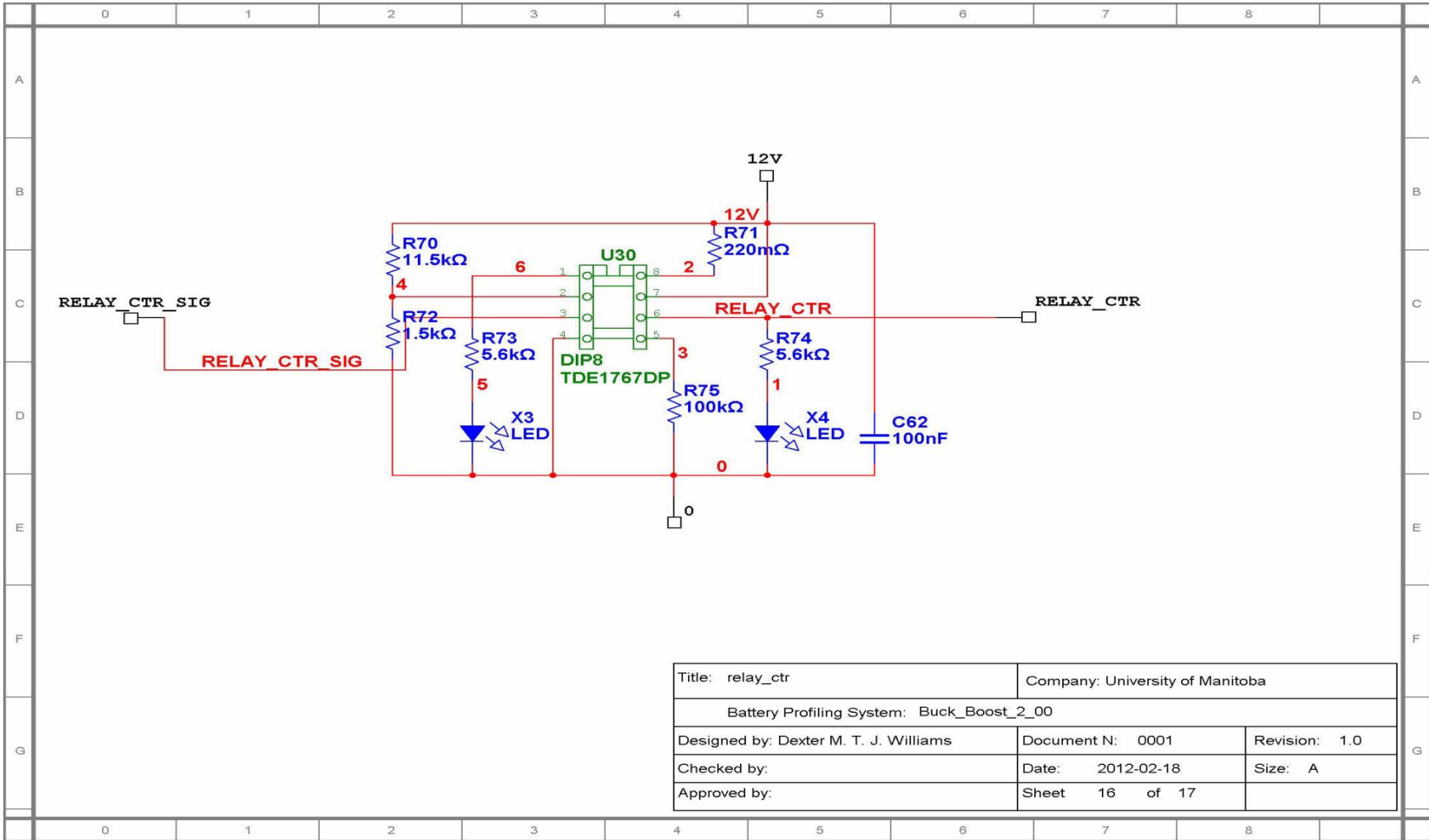


Figure B-23: Battery profiler system schematic 16 of 17.

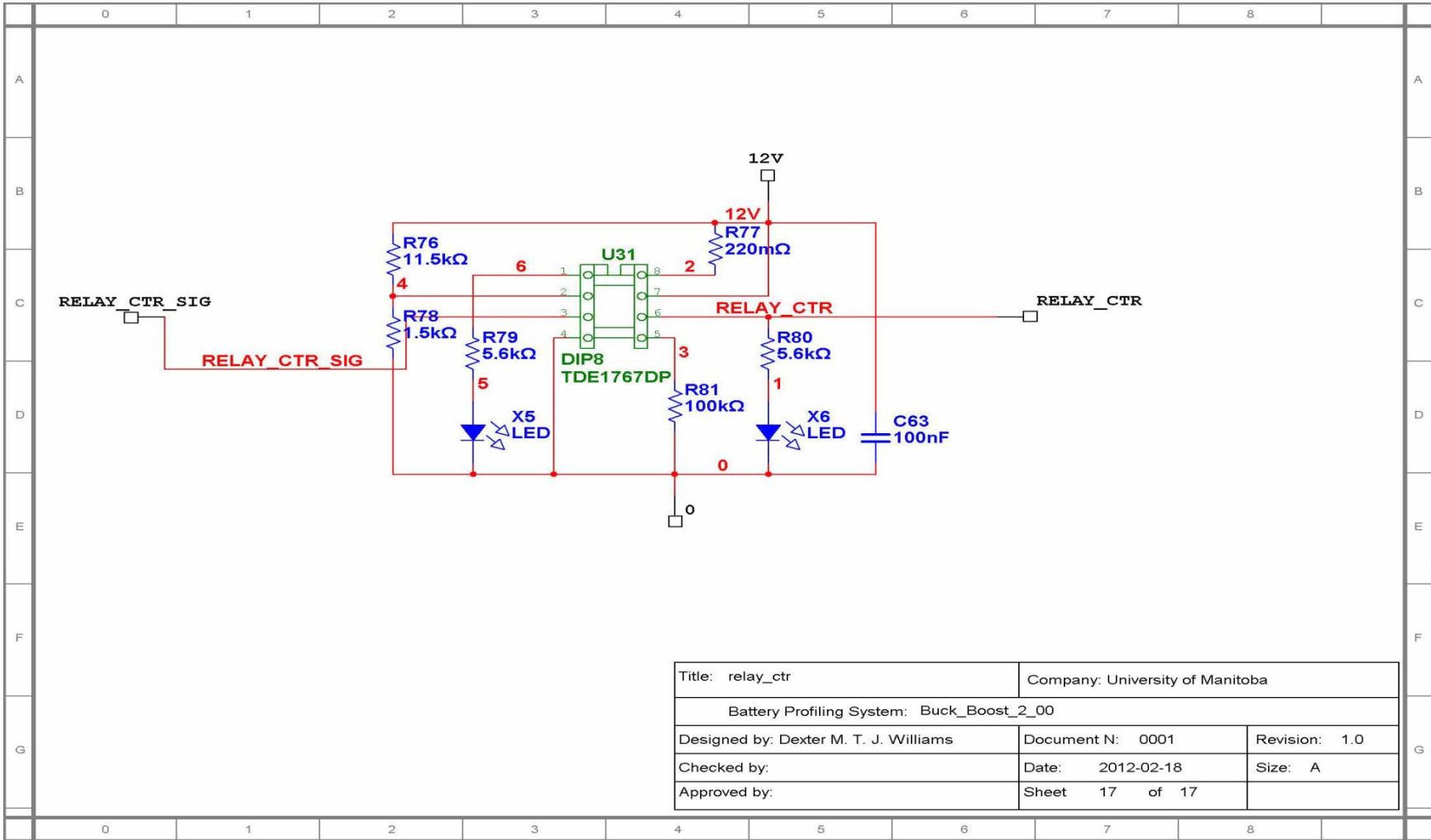


Figure B-24: Battery profiler system schematic 17 of 17.